

*Cardiff University*  
*School of Medicine*  
*Systems Immunity Research Institute*

*Prifysgol Caerdydd*  
*Yr Ysgol Meddygaeth*  
*Sefydliad Ymchwil Systemau Imiwnedd*



# Identifying a novel $\gamma\delta$ T-cell stress ligand: Potential for cancer immunotherapy

Sophie Wheeler

A thesis submitted to Cardiff University

in candidature for the degree of

Doctor of Philosophy

**December 2017**





## **DECLARATION**

This work has not been submitted in substance for any other degree or award at this or any other university or place of learning, nor is being submitted concurrently in candidature for any degree or other award.

Signed ..... (candidate) Date .....

## **STATEMENT 1**

This thesis is being submitted in partial fulfilment of the requirements for the degree of PhD.

Signed ..... (candidate) Date .....

## **STATEMENT 2**

This thesis is the result of my own independent work/investigation, except where otherwise stated, and the thesis has not been edited by a third party beyond what is permitted by Cardiff University's Policy on the Use of Third Party Editors by Research Degree Students. Other sources are acknowledged by explicit references. The views expressed are my own.

Signed ..... (candidate) Date .....

## **STATEMENT 3**

I hereby give consent for my thesis, if accepted, to be available online in the University's Open Access repository and for inter-library loan, and for the title and summary to be made available to outside organisations.

Signed ..... (candidate) Date .....

## **STATEMENT 4: PREVIOUSLY APPROVED BAR ON ACCESS**

I hereby give consent for my thesis, if accepted, to be available online in the University's Open Access repository and for inter-library loans after expiry of a bar on access previously approved by the Academic Standards & Quality Committee.

Signed ..... (candidate) Date .....



## Acknowledgements

The research described in the thesis would not have been possible without the contribution of my supervisory team, my colleagues, my collaborators and my funders. Firstly, a massive thanks to the Medical Research Council and Cardiff University for funding me through a 4 year MRes + PhD programme. Without this funding, I would not have been able to complete such an exciting PhD project, or achieved an MRes qualification.

A massive thank you to my primary supervisor Andrew Sewell for enabling me to undertake this exciting project, as well as for his support throughout the past 3.5 years. A very special thanks to my secondary supervisor, Garry Dolton, for training and fostering my independence as a researcher while providing me with support, inspiration and sometimes motivation whenever I needed it.

I would like to acknowledge all the help I received from my colleagues with methodologies described within this thesis. My greatest thanks goes to Garry Dolton for his help and assistance with cell culture - you are the T-cell clone growing god! Also thanks to Mateusz Legut and Cristina Rius for cell culture help whenever I was away. A massive thanks to Cristina and Mereim Attaf for all help sequencing related. Another thanks to Mateusz for being such a wiz to develop the TCR transduction technology used in my thesis, as well as providing assistance and sequencing of my whole genome CRISPR/Cas9 libraries. Thanks also to Bruce MacLachlan, Alex Greenshields-Watson and Aaron Wall for assistance with MHC class II refolding. Thanks to Thalia for performing all Western Blots for me. All my colleagues from the T-cell modulation group have greatly contributed to my overall experience in Cardiff, both in professional and private life. In particular I would like to thank members of the 2F01 office, Cristina and Mateusz, for coffee breaks and much needed chocolate!

I do not even know where to begin thanking my partner in crime, Glyn. Without him I would not have survived the toughest times, or celebrated the best times quite as well. Glyn, you are my rock! My mum, dad and sister also deserve a special mention for also supporting me in every way possible. Also thanks Dan for the best cakes!

A final thanks to Matthias Eberl, James Matthews and Alan Parker for taking the time to support me during the review processes, to Bernhard Moser and Paul Klennerman for being on my examination panel, and to Anwen Williams, Amanda Tonks, Aled Holt and all others at the PGR office.



## Summary

**Background:**  $\gamma\delta$  T-cells can kill multiple cancer types and virally infected cells independent of human leukocyte antigen (HLA). Targeting is believed to occur via recognition of generic, unidentified, stress signals at the target cell surface via the  $\gamma\delta$  T-cell receptor (TCR). Consequently,  $\gamma\delta$  TCR and its ligands offer potential for pan-population, off-the-shelf immunotherapies for a range of pathologies including cancer. I aimed to identify pan-cancer targeting  $\gamma\delta$  T-cells, describe their TCRs and discover the ligands they use to recognise such a wide range of targets.

**Results:** I used herpesvirus infected cells to prime and isolate rare, tumour reactive  $\gamma\delta$  T-cell lines from three healthy donors. An interesting T-cell clone from each individual was subjected to novel technologies to find the TCR ligand. A whole genome CRISPR/Cas9 library screen determined that tumour recognition by one clone required that transformed cells express SCNN1A, a key component of the major epithelial sodium transporter. Surprisingly, CRISPR gene editing and lentiviral transduction technologies demonstrated that the two other clones recognised allogeneic HLA class II alleles expressed on tumour cells.

**Conclusions:** My results offer opportunities for broad-ranging cancer immunotherapies that are HLA-independent and could be applied in all individuals. My discovery that  $\gamma\delta$  T-cells can recognise allogeneic HLA alleles also serves as a cautionary note to those wishing to apply therapeutic approaches via allogeneic  $\gamma\delta$  T-cells. My results blur the boundaries between conventional  $\alpha\beta$  T-cell recognition of peptide-HLA and the 'unconventional'  $\gamma\delta$  T-cell subset that are often currently believed to be blind to HLA. These findings will be of major interest to the  $\gamma\delta$  T-cell field and should serve as important milestone to future studies of HLA-restricted and non-HLA restricted  $\gamma\delta$  T-cells.





## Abbreviations

Ab- antibody  
ACT – adoptive cell transfer  
AIRE – autoimmune regulator  
APC – antigen presenting cell  
bp – base pair  
BSA- bovine serum albumin  
BTN – butyrophilin  
CVDJ – constant, variable, diversity, joining  
CAR – chimeric antigen receptor  
CD – cluster of differentiation  
cDNA – complementary DNA  
CDR – complementarity-determining region  
CMV – cytomegalovirus  
Cr- chromium  
CRISPR – clustered regularly interspaced short palindromic repeats  
CTLA – cytotoxic T-lymphocyte associated protein  
DMSO – dimethylsulfoxide  
DNA – deoxyribonucleic acid dNTP – deoxynucleotide  
DTT – dithiotreitol  
E:T – effector to target  
EBV – Epstein-Barr virus  
EDTA – ethylenediaminetetraacetic acid  
EF – elongation factor  
ELISA – enzyme-linked immunosorbent assay  
ELISPOT – enzyme-linked immunospot  
EPCR – endothelial protein C receptor  
FACS – fluorescence activated cell sorting  
FDA- food and drug administration  
FITC – fluorescein isothiocyanate  
FPLC- fast protein liquid chromatography  
FSC – forward scatter  
GalCer – galactosylceramide  
GeCKO – genome-wide CRISPR knock-out  
GF- gel filtration  
gRNA – guide RNA  
HeBS – HEPES buffered saline  
HEPES - 4-(2-hydroxyethyl)-1-piperazineethanesulfonic acid  
HLA – human leukocyte antigen  
HMBPP - (E)-4-Hydroxy-3-methyl-but-2-enyl pyrophosphate  
ICS – intracellular cytokine staining  
IFN – interferon  
IL – interleukin  
IPP – isopentenyl pyrophosphate  
IPTG- Isopropyl  $\beta$ -D-1-thiogalactopyranoside  
KO – knock-out  
LB – lysogeny broth  
LCL – lymphoblastoid cell line  
MACS – magnetic activated cell sorting  
MFI – median fluorescence intensity

MHC – major histocompatibility complex  
 MIC – MHC I chain-related polypeptide  
 MIP – macrophage inflammatory protein  
 MOI – multiplicity of infection  
 MR1 – MHC-I related 1  
 MSH – MutS homologue  
 ND – not determined  
 NGS – next generation sequencing  
 NK – natural killer  
 NKG2D – natural killer group 2 member D  
 ns – not significant  
 nt – nucleotide  
 PAg – phosphoantigen  
 PAM – protospacer adjacent motif  
 PBMC- peripheral blood mononuclear cells  
 PBS – phosphate buffered saline  
 PCR – polymerase chain reaction  
 PDB – Protein DataBase  
 PE – phycoerythrin  
 PHA – phytohaemagglutinin  
 PKI – protein kinase inhibitor  
 RACE - rapid amplification of cDNA ends  
 RBC – red blood cell  
 RNA – ribonucleic acid  
 SCNN1A: epithelial sodium channel sub-unit 1  
 SMARTer - switching mechanism at 5' end of RNA transcript  
 SSC – side scatter  
 TAPI – TNF $\alpha$  processing inhibitor  
 TCR – T-cell receptor  
 TE – tris-EDTA  
 TIL – tumour-infiltrating lymphocytes  
 TNF – tumour necrosis factor  
 TNFRSF – TNF $\alpha$  receptor superfamily  
 ULBP – UL16 binding protein  
 $\alpha\beta$ - alpha beta  
 $\beta$ 2m – beta-2-microglobulin  
 $\gamma\delta$ - gamma delta

# Contents

1	Introduction .....	1
1.1	T-cells .....	1
1.1.1	The T-cell receptor .....	2
1.1.2	The generation of T-cell receptor diversity.....	2
1.1.3	Structure of the T-cell receptor .....	7
1.1.4	T-cell development, selection and differentiation.....	7
1.2	The convention of T-cell immunity .....	9
1.2.1	Conventional MHC T-cell ligands .....	10
1.3	Unconventional 'MHC-like' molecules and the unconventional T-cells that recognize them	10
1.4	The $\gamma\delta$ T-cell: Orchestrators of immunosurveillance .....	13
1.5	Mechanisms of $\gamma\delta$ T-cell anti-tumour reactivity .....	15
1.5.1	Sensing of metabolic intermediates .....	16
1.5.2	MICA/B presentation of self-antigens .....	18
1.5.3	Lipid presentation by CD1.....	19
1.5.4	Expression of stress ligands .....	20
1.6	Cancer immunotherapy .....	21
1.6.1	Monoclonal antibodies .....	21
1.6.2	Immune checkpoint inhibitors .....	22
1.6.3	Cancer vaccines.....	23
1.6.4	Adoptive T-cell therapy.....	24
1.7	The $\gamma\delta$ T-cell: Potential for immunotherapy .....	26
1.7.1	Sensitizing tumour to $\gamma\delta$ T-cell killing .....	28
1.7.2	$\gamma\delta$ T-cell based vaccines .....	28
1.7.3	$\gamma\delta$ T-cell adoptive cell therapy .....	29
1.7.4	Using $\gamma\delta$ T-cells to identify stress ligands .....	30
1.8	Aims and Objectives.....	31

2	Materials and Methods .....	33
2.1	Cell Culture .....	33
2.1.1	Cell culture media and buffers .....	33
2.1.2	Immortalised cell culture.....	33
2.1.3	Lymphoblastoid cell line generation .....	33
2.1.4	Primary T-cell culture: maintenance and expansion .....	36
2.1.5	PBMC Isolation .....	36
2.1.6	Cloning by limiting dilution.....	36
2.1.7	Human cytomegalovirus infection.....	36
2.1.8	Cell counting.....	37
2.1.9	Cryo-preservation and thawing of cell lines .....	37
2.1.10	HLA typing.....	37
2.2	Magnetic cell sorting .....	37
2.2.1	Surface marker separation .....	37
2.2.2	TNF/IFN $\gamma$ magnetic pullout.....	38
2.3	Lentiviral transductions.....	38
2.3.1	Lentivirus production.....	38
2.3.2	Lentiviral transduction of immortalised cell lines .....	39
2.3.3	Lentiviral transduction of primary T-cells.....	40
2.3.4	Selection of transduced cells .....	40
2.4	Flow cytometry.....	40
2.4.1	Flow cytometry analysis .....	41
2.4.2	pMHC tetramer staining .....	42
2.5	Functional T-cell assays .....	43
2.5.1	T-cell proliferation assay.....	43
2.5.2	Intracellular-cytokine staining (ICS).....	43
2.5.3	TAPI-0 activation assay .....	44
2.5.4	Long term FACS based killing assay .....	44

2.5.5	Chromium release ( <sup>51</sup> CR) killing assay.....	45
2.5.6	Antibody blocking assays .....	45
2.5.7	Enzyme-Linked ImmunoSpot (ELISpot).....	47
2.6	TCR sequencing and clonotyping .....	47
2.6.1	Total RNA extraction .....	47
2.6.2	SMARTer RACE cDNA amplification .....	48
2.6.3	Analysis and sequencing of human $\gamma\delta$ TCR repertoires.....	52
2.7	Molecular cloning .....	52
2.7.1	Plasmid Design .....	52
2.7.2	Cloning into the pELNS vector.....	53
2.7.3	Cloning into the pLentiCRISPR v2 vector .....	55
2.7.4	Sequencing and analysis .....	57
2.7.5	Plasmid Maxiprep .....	57
2.8	Whole Genome CRISPR/Cas9 Library Screens .....	57
2.8.1	Library setup and screening .....	58
2.8.2	Library Sequencing.....	58
2.9	Western blot protein analysis.....	59
2.9.1	Sample preparation .....	59
2.9.2	Western blot membrane preparation and antibody staining.....	61
2.10	Protein expression, refolding and purification .....	62
2.10.1	Vectors for protein expression .....	62
2.10.2	Transformation of competent <i>E. coli</i> cells .....	62
2.10.3	Expression of inclusion bodies in Rosetta <i>E.coli</i> .....	62
2.10.4	Sodium Dodecyl Sulphate-Polyacrylamide Gel Electrophoresis (SDS-PAGE).....	63
2.10.5	Protein Refolds.....	63
2.10.6	Protein Purification .....	64
2.10.7	Protein Biotinylation .....	65
2.11	Data Analysis.....	65

3	Using herpes virus infected cells to generate cancer-reactive $\gamma\delta$ T-cell clones .....	67
3.1	Introduction .....	67
3.1.1	Aims .....	67
3.2	Results .....	68
3.2.1	CMV-infected cells failed to prime robust $\gamma\delta$ T-cell responses from healthy PBMC 68	
3.2.2	Autologous EBV infected B-cells predominately primed $\alpha\beta$ T-cells .....	70
3.2.3	Purified $\gamma\delta$ T-cells responded to LCL.....	70
3.2.4	LCL-primed $\gamma\delta$ T-cell clones recognized cancer cells .....	72
3.3	Discussion .....	79
4	Whole genome CRISPR/Cas9 gene editing identifies a novel $\gamma\delta$ T-cell ligand .....	81
4.1	Introduction .....	81
4.1.1	The discovery of $\gamma\delta$ T-cell ligands .....	81
4.1.2	The use of whole genome CRISPR/Cas9 technology to identify novel T-cell ligands 82	
4.1.3	Aims and Objectives .....	82
4.2	Results .....	83
4.2.1	SW.3G1 recognised LCL and tumour cells .....	83
4.2.2	Whole genome CRISPR/Cas9 libraries identified a novel $\gamma\delta$ T-cell ligand.....	85
4.2.3	SCNN1A: a $\gamma\delta$ T-cell target.....	89
4.2.4	SW.3G1 did not recognise a splice variant of SCNN1A.....	91
4.2.5	The SW.3G1 TCR mediates recognition of tumour cells.....	92
4.3	Discussion .....	96
4.3.1	Whole genome CRISPR: An efficient method for finding T-cell targets .....	97
4.3.2	The sodium channel: a T-cell target .....	98
4.3.3	The SW.3G1 TCR: A powerful tool for immunotherapy .....	99
4.3.4	Future directions .....	100
5	$\gamma\delta$ T-cell recognition of MHC on tumour cells .....	103

5.1	Background .....	103
5.1.1	Aims and objectives .....	103
5.2	Results.....	104
5.2.1	SW.6B10 recognizes HLA-DR7 <sup>+</sup> targets .....	104
5.2.2	TCR mediated recognition of HLA-DR7 by SW.6B10.....	108
5.2.3	SW.6B10 recognizes tumour cells through HLA-DR7.....	108
5.2.4	SW.6B10 recognition of target cells is peptide specific.....	111
5.2.5	SW.11H7: A second MHC II restricted $\gamma\delta$ T-cell clone .....	114
5.3	Discussion.....	117
5.3.1	MHC restricted $\gamma\delta$ T-cells: Not so unconventional after all? .....	117
6	General discussion and Conclusions .....	119
6.1	The $\gamma\delta$ TCR: Foundations of an off-the-shelf pan-population immunotherapy .....	121
6.2	Concluding remarks .....	124
7	References .....	125
8	Appendix .....	145

## List of Figures:

<b>Figure 1.1:</b> Signal transduction pathways involved in T-cell activation.....	3
<b>Figure 1.2:</b> The genetic basis of the $\alpha\beta$ and $\gamma\delta$ T-cell receptors (TCRs).....	4
<b>Figure 1.3:</b> The mRNA and protein basis of the $\alpha\beta$ and $\gamma\delta$ T-cell receptors (TCRs).....	5
<b>Figure 1.4:</b> T-cell development, differentiation and selection during thymic selection.....	8
<b>Figure 1.5:</b> An overview of known $\gamma\delta$ T-cell receptor (TCR) ligands.....	14
<b>Figure 1.6:</b> An overview of adoptive cell therapy.....	27
<b>Figure 2.1:</b> Gating strategy for FACS phenotypic and/or functional analysis of T-cells.....	42
<b>Figure 2.2:</b> Gating strategy and analysis of long-term killing assays.....	46
<b>Figure 2.3:</b> Agarose gel electrophoresis of PCR products for $\gamma\delta$ T-cell receptor clonotyping.....	50
<b>Figure 2.4:</b> Schematic representation of lentiviral transfer plasmids pLentiCRISPR (A) and pELNS (B).....	53
<b>Figure 2.5:</b> Agarose gel electrophoresis after restriction digestion of lentiviral transfer plasmid pELNS and construct plasmid pUC57 carrying a synthesised T-cell receptor (TCR) of interest.....	54
<b>Figure 3.1:</b> Cytomegalovirus infected fibroblasts failed to prime $\gamma\delta$ T-cells from peripheral blood mononuclear cells (PBMCs).....	69
<b>Figure 3.2:</b> Autologous EBV immortalised B-cells primarily expand $\alpha\beta$ T-cells.....	71
<b>Figure 3.3:</b> Magnetic enrichment of $\gamma\delta$ T-cells from the PBMCs of indicated donors.....	72
<b>Figure 3.4:</b> Epstein-Barr virus immortalised B-cell lines prime purified $\gamma\delta$ T-cells.....	73
<b>Figure 3.5:</b> T-cell receptor sequencing of $\gamma\delta$ T-cells primed with non-autologous EBV immortalised B-cells.....	74
<b>Figure 3.6:</b> The procurement and characterisation of $\gamma\delta$ T-cell clones reactive to EBV immortalised B-cells.....	76
<b>Figure 3.7:</b> EBV immortalised B-cell killing by clones SW.6B10 (A), SW.11H7 (B) and SW.3G1 (C).....	77
<b>Figure 3.8:</b> $\gamma\delta$ T-cell clones generated using EBV immortalised B-cells recognize cancer cells.....	78
<b>Figure 3.9:</b> An optimised protocol for the procurement of tumour-reactive, rare V $\delta$ 2- $\gamma\delta$ T-cells from peripheral blood using EBV immortalised LCL.....	80
<b>Figure 4.1:</b> The use of whole genome CRISPR/Cas9 (GeCKO) libraries to delineate T-cell targets.....	83
<b>Figure 4.2:</b> Clone SW.3G1 recognizes Epstein Barr Virus (EBV) immortalized B-cells but not healthy cells.....	84
<b>Figure 4.3:</b> Clone SW.3G1 kills a wide range of cancer cell types.....	85
<b>Figure 4.4:</b> SW.3G1 did not recognize known $\gamma\delta$ T-cell ligands.....	86
<b>Figure 4.5:</b> Whole genome CRISPR/Cas9 identifies multiple candidate genes involved in the recognition of target cells by SW.3G1.....	87
<b>Figure 4.6:</b> Confirmation that candidate gene SCCN1A is involved in the recognition of LCL by SW.3G1.....	90
<b>Figure 4.7:</b> SCNN1A is required for SW.3G1 recognition of tumours.....	91
<b>Figure 4.8:</b> SCNN1A expression in knockout cell lines restores recognition of target cells by SW.3G1.....	92



<b>Figure 4.9:</b> Healthy, EBV immortalised and tumour cell lines all express isoform 1 SCNN1A.....	93
<b>Figure 4.10:</b> The T-cell receptor gene and protein sequence of clone SW.3G1.....	94
<b>Figure 4.11:</b> Recognition of target cells by clone SW.3G1 is via the TCR.....	95
<b>Figure 4.12:</b> TCR mediated killing of target cells lines via recognition of SCNN1A.....	96
<b>Figure 5.1:</b> Clone SW.6B10 recognized the target cell line 0439 lymphoblastic cell line (LCL) through MHCII rather than established $\gamma\delta$ T-cell ligands.....	105
<b>Figure 5.2:</b> Clone SW.6B10 only recognized HLA-DR7 <sup>+</sup> LCL.....	106
<b>Figure 5.3:</b> SW.6B10 kills MHCII-negative LCL targets that are transduced with HLA DR7.....	107
<b>Figure 5.4:</b> Clone SW.6B10 recognized HLA-DR7 <sup>+</sup> LCL through the TCR.....	109
<b>Figure 5.5:</b> 6B10 TCR transduced T-cells require HLA-DR7 for recognition of 0439 LCL.....	110
<b>Figure 5.6:</b> SW.6B10 kills HLA-DR7 <sup>+</sup> tumours.....	110
<b>Figure 5.7:</b> SW.6B10 targets melanoma cell line MM909.24 through HLA-DR7....	112
<b>Figure 5.8:</b> SW.6B10 TCR recognizes tumour MDA-MB-231 via HLA-DR7.....	113
<b>Figure 5.9:</b> Clone SW.11H7 only lysed HLA-DR15 <sup>+</sup> LCL.....	114
<b>Figure 5.10:</b> Clone SW.11H7 only lysed HLA-DR15 <sup>+</sup> tumours.....	115
<b>Figure 5.11:</b> Clone SW.11H7 recognizes HLA-DR15 <sup>+</sup> LCL via the TCR.....	116
<b>Figure 6.1:</b> An updated overview of known $\gamma\delta$ T-cell receptor (TCR) ligands.....	120
<b>Figure 8.1:</b> Cytomegalovirus infected fibroblasts failed to prime $\gamma\delta$ T-cells from PBMC.....	152
<b>Figure 8.2:</b> EBV transformed B cell lines prime $\gamma\delta$ T-cell lines that exhibit cancer reactivity.....	152
<b>Figure 8.3:</b> SCCN1A expression in knockout and knockin .174 cell lines.....	154
<b>Figure 8.4:</b> The recognition of tumour cell line MM909.24 by clone SW.6B10 does not require $\beta$ 2M.....	154
<b>Figure 8.5:</b> CRISPR/Cas9 targeted knockout of HLA-DR7 in tumour cell line MDA-MB-231.....	155
<b>Figure 8.6:</b> SW.6B10 recognizes a specific peptide bound with HLA-DR7.....	155
<b>Figure 8.7:</b> HLA-DR staining of .174 LCL transduced with HLA-DR15.....	156

## List of Tables:

<b>Table 1.1:</b> A summary of MHC-Ib molecules and the T-cells that recognize them.....	12
<b>Table 1.2:</b> Antigen selectivity of human and mouse $\gamma\delta$ T-cell receptors.....	16
<b>Table 2.1:</b> The composition of cell culture media and buffers used throughout the thesis.....	34
<b>Table 2.2:</b> Cell lines used throughout this thesis.....	35
<b>Table 2.3:</b> Plasmids used for production of 2 <sup>nd</sup> and 3 <sup>rd</sup> generation lentiviruses.....	39
<b>Table 2.4:</b> Antibodies used for flow cytometry staining.....	41
<b>Table 2.5:</b> Buffers and reagents used in western blot analysis.....	60
<b>Table 2.6:</b> Quantities and refold procedure for MHC class I and MHC class II proteins.....	64
<b>Table 3.1:</b> An overview of all clones procured from EBV primed $\gamma\delta$ T-cell lines from donors BB67, 0439 and 9909.....	75
<b>Table 4.1:</b> An overview of genes identified in tumour and LCL GeCKO libraries.....	88
<b>Table 8.1:</b> Primers used for sequencing and PCR.....	145
<b>Table 8.2:</b> Amino acid sequence of $\gamma\delta$ TCRs synthesised and cloned into the lentiviral vector pELNS.....	146
<b>Table 8.3:</b> Amino acid sequences synthesized and cloned into the lentiviral pELNS.....	147
<b>Table 8.4:</b> Primer sequences for HiSeq (Illumina) sequencing of GeCKO libraries.....	148
<b>Table 8.5:</b> Amino acid sequences synthesized and cloned into the expression vector pGMT7	148
<b>Table 8.6:</b> Culture media and buffers used for protein expression, refolding and purification	149
<b>Table 8.7:</b> HLA-typing information for LCL used in the thesis for $\gamma\delta$ T-cell donors and priming donors.....	150
<b>Table 8.8:</b> Sequence alignment of SCCN1A splice isoforms.....	153





# 1 Introduction

The mammalian immune system is highly developed and diverse having evolved over millions of years to protect hosts against exogenous (i.e. infections) and endogenous (i.e. malignantly transformed cells) threats. Most immune cells originate from haematopoietic stem cells (HSCs) and go on to develop into either lymphoid or myeloid progenitor cells to give rise to the adaptive and innate arms of the immune system, respectively (Wu et al. 2009). The cells of the innate system, such as phagocytes and neutrophils, act in a rapid manner to similar signals found on a broad range of pathologies independent of immunological memory. Alternately, cells of the adaptive arm tend to react to pathogen-specific signals via a receptor, either the B-cell receptor (BCR) or T-cell receptor (TCR), and create immunological memory after an initial response to a pathogen. There are three components of the adaptive arm of the immune system: B-cells,  $\alpha\beta$  T-cells and  $\gamma\delta$  T-cells, which have been maintained throughout the entirety of jawed vertebrate evolution. A specific subset of lymphocytes,  $\gamma\delta$  T-cells, have potent anti-tumour reactivity and are the focus of this thesis.

## 1.1 T-cells

T-cells form part of the adaptive immune system involving elements of immunological memory to allow rapid and vigorous responses to infectious pathogens or cellular transformation via the TCR. T-cells are derived from HSCs in bone marrow before undergoing selection and differentiation in the thymus to eliminate self and non-reactive T-cells. Developing T-cells, known as thymocytes, rearrange germline encoded gene segments, coded for by *tra*, *trb*, *trg* and *trd* genes, termed: variable (V), diversity (D) and joining (J) which are fused to a constant (C) domain to form a TCR (Section 1.1.1). T-cells can be broadly separated into two subsets;  $\alpha\beta$  and  $\gamma\delta$  T-cells based on the pairing of either TCR $\alpha$  with TCR $\beta$  chains, or TCR $\gamma$  with TCR $\delta$  chains.

In the human periphery,  $\alpha\beta$  T-cells constitute the major subset forming up to 90% of circulating lymphocytes. 'Conventional'  $\alpha\beta$  T-cells recognise peptide antigens presented by major-histocompatibility complex (MHC) molecules via their clonotypic  $\alpha\beta$  TCR. The  $\gamma\delta$  T-cell compartment, although a minority in the peripheral blood, can constitute up to 50% of lymphocytes found in tissues such as the skin and gut epithelia (Vantourout and Hayday 2013) and can be rapidly increased in the periphery with the onset of infection (Willcox et al. 2012).  $\gamma\delta$  T-cells, as well as some subsets of  $\alpha\beta$  T-cells such as invariant natural killer T cells (iNKTs) (Section 1.3) are deemed 'unconventional' as they are thought not to recognise peptide antigens presented by MHC. Whilst there is some knowledge of the potent anti-stress activity of  $\gamma\delta$  T-cells and the role they play in adaptive immunosurveillance, the mechanisms by which they do

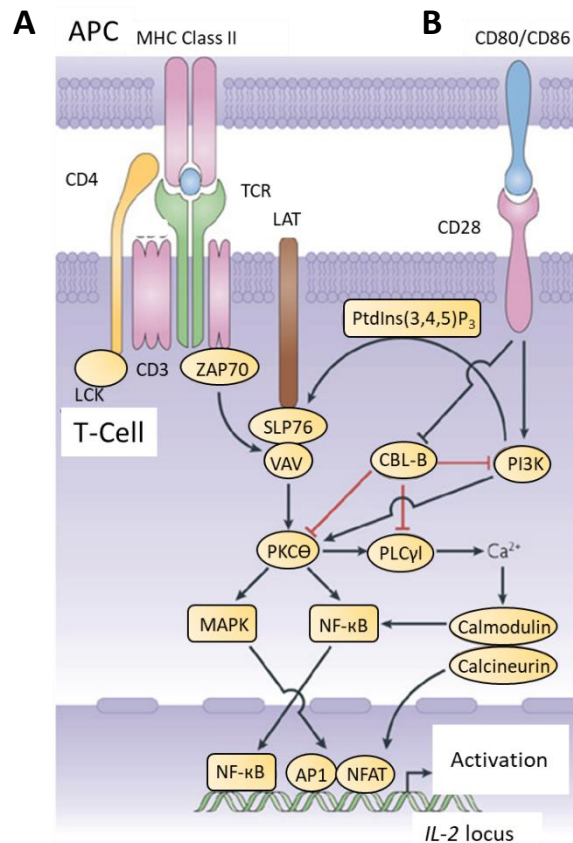
so are not well characterised. This thesis seeks to unravel modes of  $\gamma\delta$  T-cell anti-tumour immunity, and how this can be harnessed for immunotherapies.

### 1.1.1 The T-cell receptor

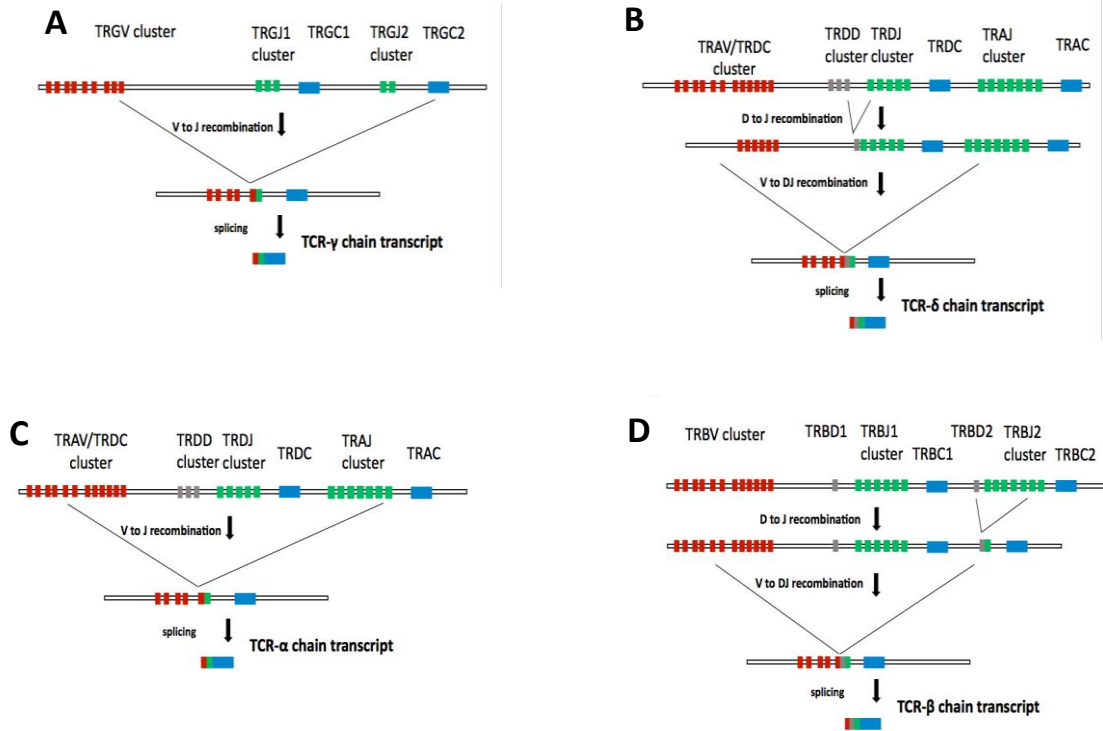
$\alpha\beta$  and  $\gamma\delta$  TCRs are disulphide-linked heterodimeric, cell surface-expressed proteins responsible for the recognition and binding of a ligand, resulting in a signal transduction cascade (Figure 1.1) leading to activation and clonal expansion of the T-cell (Smith-Garvin et al. 2009). TCRs are composed of V and C domains bound by intra-chain disulphide bonds and hinge regions (Figure 1.2 and 1.3). Whilst the C domains are N-terminal to the transmembrane region, variable domains which incorporate loop structures known as complementary determining regions (CDRs), are distal to the cell surface and form the antigen binding site (Wucherpfennig et al. 2010). Once the TCR is bound with a cognate ligand, a naïve T-cell undergoes clonal expansion of between 10-20 rounds of cell division (Obst 2015) following the recruitment and signal propagation of cellular transduction machinery. Upon activation, T-cells release numerous cytokines and chemokines such as interferon- $\gamma$  (IFN- $\gamma$ ), interleukin-2 (IL-2) and  $\beta$ -chemokines that alert other immune cells (Price et al. 1999; Smith-Garvin et al. 2009). CD8<sup>+</sup> cytotoxic T-cells also secrete perforin and granzymes when they activate which allow these cells to lyse their target. The TCR is generated by a genetic recombination event during T-cell development and is responsible for the ability of T-cells to respond to a vast array of targets.

### 1.1.2 The generation of T-cell receptor diversity

To adapt to the changing landscape of pathogens and cellular transformations many different TCRs are generated by the somatic genetic recombination event of the *tra*, *trb*, *trg* and *trd* loci during early T-cell development in the thymus (Davis and Bjorkman 1988; Davis 2004). Each T-cell generated in this way generally expresses a single type of TCR, and is deemed a T-cell clonotype. As illustrated (Figure 1.2) in the case of *tra* and *trg* loci the process involves recombination between one V and one J segment that are juxtaposed by splicing with the respective C domain. In the *trb* and *trd* loci up to three D segments and a J segment recombine, followed by a V domain. Additional levels of diversity are generated due to spontaneous non-homologous end joining or addition of nucleotides at the 3' end of V and 5' end of J segments (Burtrum et al. 1996; Davis 2004).

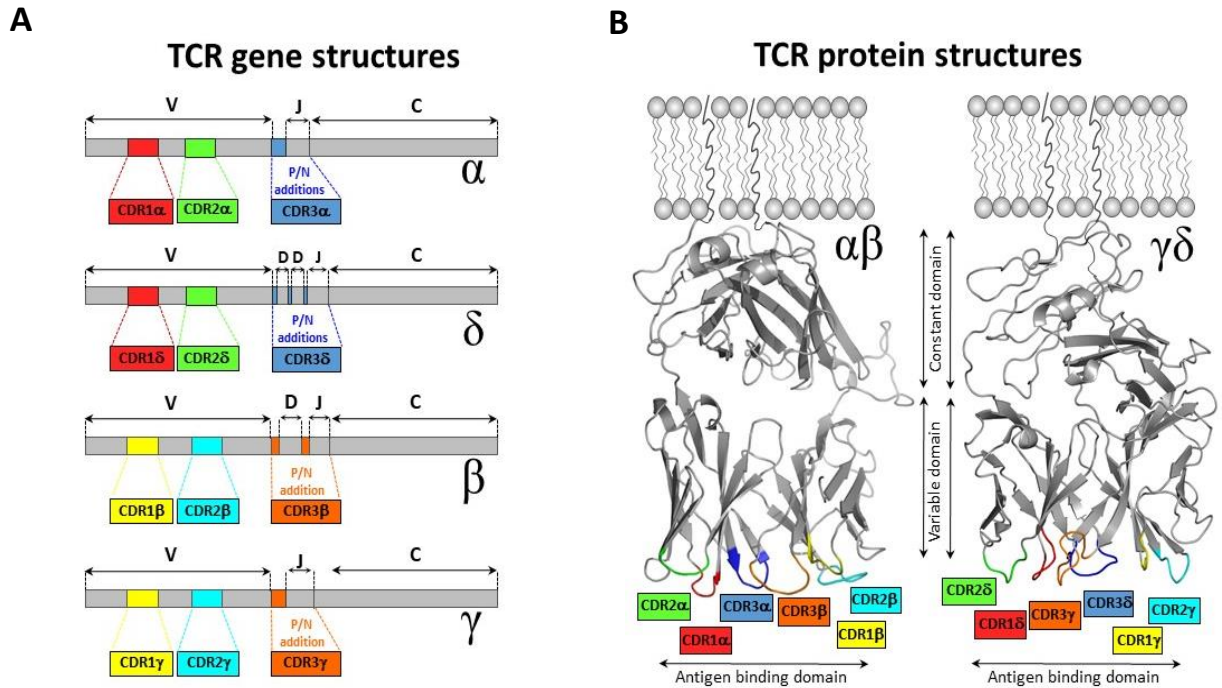


**Figure 1.1: Signal transduction pathways involved in T-cell activation.** Two signals are involved in T-cell activation. Firstly, the signal from the T-cell receptor (TCR) following binding to a peptide presented by major histocompatibility complex (MHC) on an antigen presenting cell (APC) (A). The second signal in T-cell activation comes from co-stimulatory molecules, such as CD28, following binding of molecules CD80/CD86 on the APC (B). The TCR exists in complex with five CD3 subunits ( $\gamma$ ,  $\delta$ ,  $\epsilon$ ,  $\zeta$ , and  $\eta$ ). The TCR molecules must be associated with CD3 molecules to be inserted into the T-cell surface membrane. CD3 molecules mediate T-cell signal transduction once the TCR has bound peptide-MHC. The coreceptor CD4 binds to the MHC class II molecule to stabilise the TCR/antigen complex. Note if peptides are presented by MHC class I CD8 molecules act as the coreceptor. Ligation of the TCR by MHC complexed with antigen results in sequential activation of Lck and zeta-chain associated protein kinase 70 kDa (ZAP70). ZAP70 phosphorylates several downstream targets, including Linker for Activation of T-cells (LAT) and SRC homology 2 domain-containing leukocyte protein of 76 kDa (SLP76). SLP76 is recruited to membrane bound LAT. Together SLP76 and LAT nucleate a multimolecular signalling complex along with the GTP/GDP exchange factor VAV which induces a host of downstream responses via protein kinase C theta (PKC $\theta$ ) including : calcium influx via the activation of phospholipase C1 (PLC1), mitogen-activated protein kinase (MAPK) activation, and cytoskeletal reorganisation. As a result, nuclear factor-B (NF- $\kappa$ B), nuclear factor activated T-cells (NFAT) and activator protein 1 (AP1) pathway are activated and induce a programme of gene expression that leads to interleukin 2 (IL-2) production. Simultaneously to the TCR signal 1, co-stimulation by CD28 results in the activation of phosphoinositide 3-kinase (PI3K), which further enhances the activation of PKC $\theta$  as well as phosphatidylinositol-3,4,5-triphosphate (PtdIns[3,4,5]P<sub>3</sub>) to further indirectly activate PKC $\theta$  . TCR engagement in the absence of co-stimulation results in the induction of NFAT proteins without AP1 activation, resulting in the production of anergy genes such as Casitas B-lineage lymphoma B (CBL-B), which inhibits the aforementioned T-cell activation pathways. (Adapted from (Miller et al. 2007)).



**Figure 1.2: The genetic basis of the  $\alpha\beta$  and  $\gamma\delta$  T-cell receptors (TCRs).** During T-cell development TCR $\alpha$ -,  $\beta$ -,  $\gamma$ - and  $\delta$ -chains undergo variable-diversity-joining (V-[D]-J) recombination to generate a highly diverse T-cell receptor (TCR) repertoire. The *trg* locus (A) is composed of six functional T-cell receptor (TCR) variable gamma (TRGV), five TCR gamma joining (TRGJ), and two TCR gamma constant (TRGC) segments. At the *trg* locus V-J joining joins one TRGV to a TRGJ segment. The intervening regions are spliced, generating a TCR- $\gamma$  transcript in which V, J and C segments are directly adjacent. (B,C) The generation of TCR- $\alpha$  and TCR- $\delta$  occurs at the *tra/trd* locus. The *tra/trd* locus consists of a cluster of 46 functional TCR alpha variable (TRAV) and eight TCR delta variable (TRDV) segments, followed by three segments in the TCR delta diversity (TCDD) cluster and four segments in the TCR delta joining (TRDJ) cluster. In the generation of TCR- $\delta$  V-(D)-J recombination occurs as a two-step process. D-J recombination occurs first, followed by V-DJ recombination. D-J recombination occurs to bring together a TRDD segment with a TRDJ segment. V-DJ recombination then occurs to bring together a TRDV segment with the TRDD/TRDJ transcript. Finally, the intervening segments are spliced, generating a TCR- $\delta$  segments in which V, J and C segments are directly adjacent. The generation of TCR- $\alpha$  also occurs at the *tra/trd* locus, where a total of 46 functional TRAV segments lie between the TRDC and the TCR alpha chain constant (TRAC) region. V-J recombination first bring together one of many TRAV segments and one of many TRAJ segments and the intervening sequences are spliced out to produce a TCR- $\alpha$  transcript in which V, J and C segments are directly adjacent. All V genes in the *tra/trd* locus can recombine with TRAJ, but only a subset can recombine with TRDD. Thus, many V genes are used exclusively for TCR- $\delta$  rearrangement in early thymic precursors, while others are used exclusively for TCR- $\alpha$  rearrangement in double positive thymocytes. Some V chains can be used interchangeably. (D) The *trb* locus comprises 48 functional TCR beta variable (TRBV), two TCR beta diversity (TRBD), 12 TCR beta joining (TRBJ) and two TCR beta constant (TRBC) segments. In TCR- $\beta$  rearrangement V-(D)-J recombination occurs in a two-step process like for TCR- $\delta$ . D-J recombination occurs first to juxtapose TRBD1 to one of many TRBJ1 segments, or TRBD2 to one of many TRBJ2 segments. V-DJ recombination subsequently brings the rearranged DJ to join one of the many TRBV segments. The intervening sequences are spliced out to generate the TCR- $\beta$  transcript in which V, D, J and C segments are directly adjacent. (Adapted from (Attaf et al. 2015b; Legut et al. 2015)).





**Figure 1.3: The mRNA and protein basis of the  $\alpha\beta$  and  $\gamma\delta$  T-cell receptors (TCRs).** (A) The mRNA structure of the  $\alpha\beta$  TCR [Protein Data Bank: 3HG1 (Cole et al. 2009)] and the  $\gamma\delta$  TCR [Protein Data Bank: 1HXM (Allison et al. 2001)] loci show that the complementary determining regions (CDR) one (CDR1) and two (CDR2) are encoded in the germline. CDR3 is the product of junctional diversity at V-J joins of TCR- $\alpha$  and TCR- $\gamma$  chains, and V-D-J joins in the TCR- $\beta$  and TCR- $\delta$  chains, and is thus hypervariable. (B) At the protein level, tertiary structures form that position the CDR regions at the membrane distal end of the molecules. Six CDR loops form the antigen binding site of the TCR. The areas in grey represent constant and variable domains of the TCRs. (Adapted from (Attaf et al. 2015b; Legut et al. 2015)).

In humans there are 46 functional TCR $\alpha$  V (TRAV) and 48 TCR $\beta$  V (TRBV) segments, compared with three TCR $\delta$  (V $\delta$ 1-3) V (TRDV) and seven TCR $\gamma$  (TRGV) segments (V $\gamma$ 2,-3,-4,-5,-8,-9 and -11) (Hinz et al. 1997; Adams et al. 2015). The *trd* locus is present within the *tra* locus, potentially resulting in the expression of up to five V segments that can be used in either TCR $\alpha$  or TCR $\delta$  chains (V $\delta$ 4/TRAV14, V $\delta$ 5/TRAV29, V $\delta$ 6/TRAV23, V $\delta$ 7/TRAV36 and V $\delta$ 8/TRAV38) (Lefranc 2001). The consequence of such genomic recombination is the possibility of generating hybrid TCRs expressing TCR $\delta$ /TCR $\alpha\beta$  chains. One example of such a hybrid TCR was recently identified by Pellicci and colleagues, who postulated that such events are not as rare as are currently perceived (Pellicci et al. 2014). Current tools to examine TCRs such as TCR chain-specific antibodies or specific TCR chain PCR primers fail to detect hybrid TCRs, so it remains possible that such TCRs constitute a significant minority of the overall TCR repertoire.

TCR diversity is a prerequisite of an efficient adaptive immune response to the universe of foreign and stressed-self or altered-self antigens. Generally, TCR diversity is generated in the first two decades of life in the thymus and then shaped via antigen exposure and clonal fitness of naïve T-cells in the periphery. Recent advances in high-throughput sequencing have made it possible to systematically investigate the composition of TCR repertoires in physiological and pathological settings (Robins et al. 2009), providing a potent statistical descriptor of T-cell homeostatic maintenance and response to disease. For example, one study found estimates of 100 million unique TCR $\beta$  sequences in human repertoires (Qi et al. 2014). TCR repertoire analysis can reveal differences in TCR specificities, for example hydrophobic amino acid residues at the tips of the CDR3 are believed to promote the development of self-reactive T-cells (Stadinski et al. 2016). As T-cell clonotypes are expanded when they activate, it has been proposed that T-cell repertoires can act as predictors of health and disease (Attaf et al. 2015a). Whilst the TCR repertoires of  $\alpha\beta$  T-cells have been extensively studied in diverse settings, few comprehensive descriptions of the  $\gamma\delta$  TCR repertoire have been published.

Recent studies indicate that the  $\gamma\delta$  TCR repertoire is highly diverse and contributes to adaptive immunity. Ravens and colleagues recently showed, using high throughput RNA sequencing methods, how the human  $\gamma\delta$  T-cell pool is shaped during ontogeny and regenerated after HSC transplantation. Interestingly in patients with cytomegalovirus (CMV) infection, or a reactivation event occurring as a result of transplantation, the  $\gamma\delta$  TCR repertoire was profoundly altered (Ravens et al. 2017). Furthermore, it was demonstrated that  $\gamma\delta$  TCR repertoires in the peripheral blood of healthy adults were stable over time and contained public *trg* and private *trd* sequences. Another recent study showed that the  $\gamma\delta$  TCR repertoire in the V $\delta$ 1<sup>+</sup> compartment in cord blood is initially private and unfocused, but typically becomes strongly focused on a few high-frequency clonotypes by adulthood, indicating the process of adaptive immunity and clonal expansion in response to antigen exposure (Davey et al. 2017).

The preferential pairing between TRGV9 and TRDV2 segments in  $\gamma\delta$  T-cell repertoire biology is well characterised, and believed to be a consequence of post-natal antigenic exposure (Hayday 2009). However, subsequent studies have shown that the foetal repertoire is dominated by a public, germ-line encoded TRGV9/TRDV2 sequence as early as the 23<sup>rd</sup> week of gestation (Dimova et al. 2015). Such findings were further supported by Davey and colleagues (Davey et al. 2017). Another example of public  $\gamma\delta$  TCR repertoires was found in a study where CMV infection resulted in the striking enrichment of a TRGV8/TRDV1 TCR by 21 weeks of gestation, indicating that the foetal  $\gamma\delta$  TCR is generated during early development (Vermijlen et al. 2010).

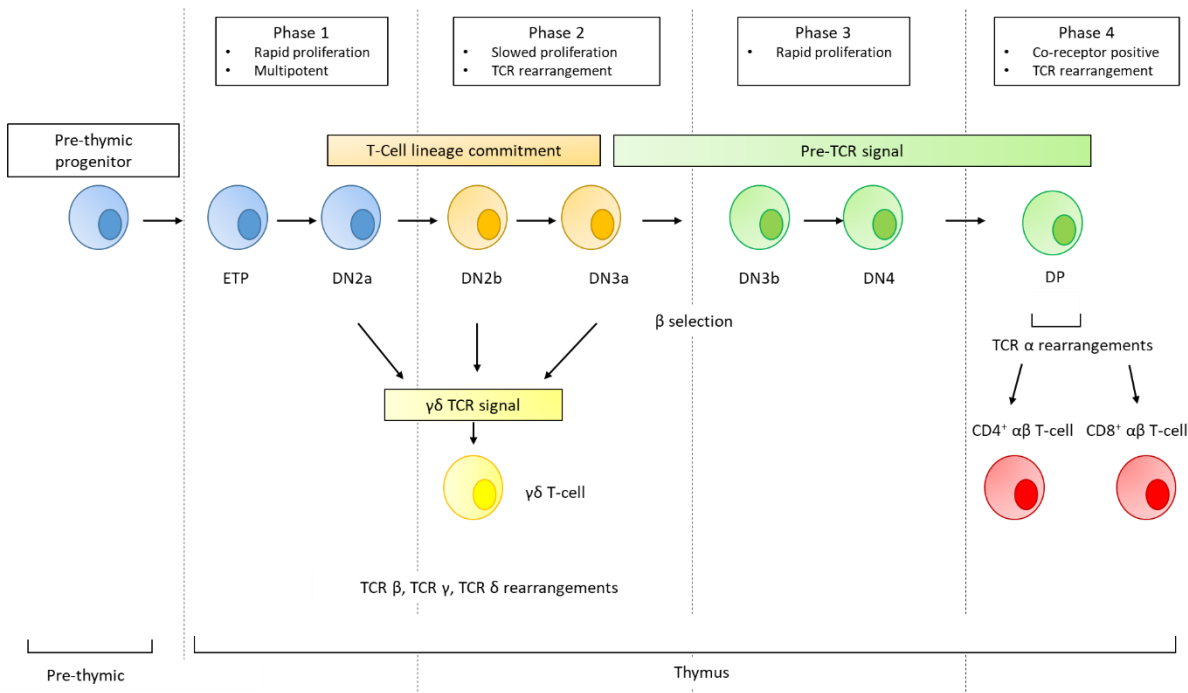
These studies further support the notion that  $\gamma\delta$  T-cells, like  $\alpha\beta$  T-cells, are augmenters of the adaptive immune response.

### 1.1.3 Structure of the T-cell receptor

Theoretically, the genetic recombination of TCR loci and spontaneous addition/deletion of nucleotides results in a potential of up to  $\sim 10^{15}$  and  $10^{18}$  different  $\alpha\beta$  TCR clonotypes in mouse and human respectively (Sewell 2012). In a recent study analysing the TCR $\gamma$  and TCR $\delta$  of 500 adult repertoires, over  $20 \times 10^6$  productively rearranged  $\gamma\delta$  TCR sequences were yielded (Ravens et al. 2017). Such diversity enables host protection against previously un-encountered pathogens and stresses. The genetic variability of TCRs is mainly translated into the membrane-distal CDR domains of the receptors that form the antigen binding site (Figure 1.3). Every TCR chain possesses three CDR hairpin loops (CDR1, CDR2, CDR3), which are responsible for TCR-ligand contact (Davis 2004). Whereas CDR1 and -2 are germline-encoded, CDR3 is produced as a result of VJ or VDJ recombination and is therefore said to be hypervariable (Chien and Konigshofer 2007). For conventional  $\alpha\beta$  TCRs, the amino acid sequence and length of the CDR3 loop tends to define the peptide ligand it binds within the restricting MHC molecule (Cole et al. 2014). In both TCR $\alpha$  and TCR $\beta$  chains CDR3 length is constrained, whereas in the TCR $\delta$  chain it is usually more variable and longer than its TCR $\gamma$  counterpart (Rock et al. 1994). The longer CDR3 regions in TCR  $\delta$  chains, and the ability to incorporate up to three different D regions results in the potential for greater variability in the  $\gamma\delta$  TCR. This greater TCR diversity may indicate that there is a greater diversity in potential ligands (Section 1.5) in comparison to the  $\alpha\beta$  TCR.

### 1.1.4 T-cell development, selection and differentiation

T-cell development, selection and differentiation is a highly controlled and orchestrated process which commences when bone-marrow derived HSCs seed the thymus. There are four main stages of thymic selection (Figure 1.4). During stage one of thymic development, gene rearrangement of the TCR  $\gamma$  and TCR  $\delta$  occurs, resulting in the expression of a  $\gamma\delta$  TCR complex in stage two (Prinz et al. 2006). During the third stage, developing thymocytes commit to either the  $\gamma\delta$  or  $\alpha\beta$  lineage. Thymocytes committed to the  $\alpha\beta$  lineage in stage three of thymus development express rearranged TCR $\beta$  chains which associated with a pre-TCR $\alpha$  molecule to form the pre  $\alpha\beta$  TCR. The pre  $\alpha\beta$  TCR signals to: drive proliferation, silence the TCR $\gamma$  chain and initiate transition to stage four (Ferrero et al. 2006). The fourth stage, known as the double positive stage, is named so due to the expression of T-cell co-receptor molecules CD4 and CD8.



**Figure 1.4: T-cell development, differentiation and selection during thymic selection.** Thymic selection occurs over four main stages and commences as bone marrow pre-thymic progenitors arrive at the thymus and concludes as either differentiated  $\gamma\delta$  or  $\alpha\beta$  T-cells leave the thymus for maturation in the periphery. The Notch signalling pathway plays a key role in T-cell lineage fate, and the thymic environment provides Notch ligands. An absence of Notch ligands in the thymus result in the development of B-cells, dendritic cells, granulocyte, macrophage and natural killer cell development from pre-thymic progenitors, ETPs and DN2a cells. During phase 1 early thymic progenitor (ETP) cells are highly proliferative and have a multipotent capacity. Cells in this stage are double negative (DN), i.e. devoid of CD4 and CD8 co-receptors. The signalling of T-cell factor 1 (TCF1) and GATA-binding protein 3 (GATA3) in stage 1 drives the commitment of thymocytes to T-cell lineage. CD25, also known as the interleukin 2 (IL-2) receptor, is expressed on all developing thymocytes from the end of phase 1 until the end of phase 2. Towards the end of phase 1 DN2a cells begin to undergo T-cell receptor (TCR) gene rearrangement in the *trb*, *trg* and *trd* loci and start to undergo T-cell lineage commitment. During phase 2 of thymic selection proliferation of cells slows whilst TCR gene rearrangement completes and thymocytes become committed to T-cell development. Developing thymocytes start to express the surface molecule CD3. By the end of phase 2  $\gamma\delta$  T-cells have differentiated from DN2a, DN2b or DN3a cells. It is presently unknown how thymocytes commit to  $\gamma\delta$  T-cell lineage but it has been postulated that the signal strength of rearranged TCR- $\gamma$  and TCR- $\delta$  determine T-cell lineage (Hayes et al. 2005). Towards the end of phase 2 T-cells destined for  $\alpha\beta$  T-cell lineage start to express a pre-TCR and  $\beta$  selection occurs. Only cells with a rearranged TCR $\beta$  that can combine with pre-TCR $\alpha$  to form the pre-TCR and transduce a signal can continue through  $\beta$  selection checkpoint into phase 3. During phase 3 cells become highly proliferative again and develop independently of Notch signalling. The pre-TCR signal dominates in phase 3 which eventually results in the co-expression of CD4 and CD8. In phase 4 gene rearrangement occurs in the *tra* locus and cells become double positive (DP) for the coreceptors CD4 and CD8. Following positive and negative selection DP cells commit to either CD4<sup>+</sup> or CD8<sup>+</sup>  $\alpha\beta$  T-cell lineage. A lot of the knowledge on transcription factors involved in thymic selection and T-cell development are based on mouse studies. (Adapted from (Abbey and O'Neill 2008; Zarin et al. 2014)).

As a prerequisite of  $\alpha\beta$  T-cell lineage commitment, thymocytes must express CD4 and CD8 (hence double positive) to drive the rearrangement of the TCR $\alpha$  gene (and subsequent deletion of the TCR $\delta$  chain) (Abbey and O'Neill 2008). Following the fourth stage of development both positive and negative selection occurs to ensure that thymocytes expressing a non-functional or autoreactive TCR are deleted. For example, TCRs that recognize self-antigens with too high an affinity are deemed inappropriate as they could cause autoimmunity. A consequence of such selection is that differentiated TCRs have much lower affinities for self-antigens compared with exogenously-derived antigens (Cole et al. 2007). T-cells surviving this selection then populate the periphery. Interestingly, it has been found that some T-cells exhibit evidence of extra-thymic selection. Ziegler and colleagues found that a small population of human peripheral blood V $\delta$ 1  $\gamma\delta$  T-cells simultaneously expressed CD4 and differentiated into  $\alpha\beta$  T-cells *ex vivo* in a process called transdifferentiation, which involved the rearrangement as a consequence of TCR- $\gamma$  chain downregulation and the expression of surface V $\delta$ 1V $\beta$  components (Ziegler et al. 2014).

Initial experiments have demonstrated that TCR signal strength is critical for  $\alpha\beta$  or  $\gamma\delta$  T-cell lineage selection. Work by Hayes and colleagues showed that lineage fate was exclusively controlled by the  $\gamma\delta$  TCR, whereby increasing the signal strength of the  $\gamma\delta$  TCR signal favoured  $\gamma\delta$  lineage and weakening it favoured  $\alpha\beta$  lineage (Hayes et al. 2005). This was further supported by Haks *et al.* (2005) when they showed that attenuation of  $\gamma\delta$  TCR signalling diverts thymocytes to  $\alpha\beta$  lineage (Haks et al. 2005). It was also shown that high levels of Notch signalling in the thymus also promotes  $\gamma\delta$  T-cell development (Van de Walle et al. 2013). This strength of signal model implies that  $\gamma\delta$  T-cells require an encounter with a cognate ligand in the thymus. To date the molecule Skint-1 has been identified in a mouse model (Turchinovich and Hayday 2011), however its exact role in thymic selection remains unresolved.

## 1.2 The convention of T-cell immunity

Conventional T-cell immunity refers to  $\alpha\beta$  TCR mediated recognition of peptides antigens, either self or foreign, presented by highly polymorphic classical MHC molecules on target cells. MHC restriction is a critical characteristic of conventional  $\alpha\beta$  T-cell immunity. Human MHC molecules are encoded within the human leukocyte antigen (HLA) locus located on the short arm of chromosome 6. The HLA locus is one of the most polymorphic regions of the human genome, encoding more than 17,000 allelic variants across the human population (Robinson et al. 2016). The *mhc* genes encode two homologous classes of conventional MHC: MHC class I (MHC I) and MHC class II (MHC II). MHC I (comprising HLA-A, -B and -C) and MHC II (HLA-DR, -DP, -DQ) have

the capability of presenting peptide antigens to different cell types. Whilst MHC I accommodates shorter peptides, usually of 9 or 10 amino acids in length, MHC II binds peptides with a 9 mer core that can extend to over 20 amino acids in length by protruding beyond the MHC binding groove. Professional antigens presenting cells (APCs), such as dendritic cells, express MHC II, whilst MHC I is expressed by most nucleated cells and platelets. Broadly speaking,  $\alpha\beta$  T-cells are separated into either helper or cytotoxic T-cells based on the expression of the TCR coreceptor they express, with the former expressing CD4 and the latter expressing CD8. The CD4 and CD8 T-cell coreceptors bind to invariant parts of MHC II and MHC I respectively at sites distinct from the TCR docking platform. CD4<sup>+</sup> helper T-cells are involved in the recognition of peptides from exogenous proteins presented by MHC II molecules, which results in the recruitment of B-cells and cytotoxic T-cells. CD8<sup>+</sup> cytotoxic T-cells recognise peptides from endogenous proteins expressed by MHC I molecules and directly lyse target cells (Pellicci et al. 2014; Attaf et al. 2015b).

#### 1.2.1 Conventional MHC T-cell ligands

MHC I molecules consist of two polypeptide chains: a highly variable 44 kDa membrane-spanning heavy  $\alpha$  chain associated with a conserved 12 kDa  $\beta$ 2 microglobulin ( $\beta$ 2M) domain. The heavy chain is composed of three domains, two of which ( $\alpha$ 1 and  $\alpha$ 2) are polymorphic and form the antigen binding groove, whilst the third domain ( $\alpha$ 3) is a constant domain and does not contact the peptide but instead engages  $\beta$ 2M and the CD8 co-receptor. MHC II molecules are comprised of two polymorphic chains;  $\alpha$  and  $\beta$  which fold into a membrane-distal polymorphic domain followed by an Ig-like domain. The  $\alpha$ 1 $\alpha$ 2 binding groove of MHC-II molecules is characterised by an open-end conformation, allowing for longer peptides to bind. The 9mer core peptide contains the motif for binding to the particular MHC II heterodimer, with peptide flanking regions outside of this core influencing peptide stability. Interestingly, my laboratory have demonstrated that these peptide flanking regions also influence TCR binding and the TCR repertoire (Cole et al. 2012; Holland et al. 2013; Holland et al. 2015).

### 1.3 Unconventional 'MHC-like' molecules and the unconventional T-cells that recognize them

Along with the classical, conventional MHCI and MHC II molecules there are a wide variety of non-classical 'MHC-like' molecules which collectively can present a diverse range of antigens including lipids and metabolites to cognate T-cells. These MHC-like molecules are deemed MHC Ib to differentiate them from the classical MHC molecules that are called MHCIa. Human MHC Ib molecules include HLA-E, MHC-I related protein 1 (MR1), and the cluster of

differentiation 1 (CD1) family of molecules, among others (a full summary can be seen in Table 1.1). MHC Ib molecules can become upregulated during cellular stress and tumorigenesis. The T-cells that are restricted by such MHC like molecules are termed 'unconventional' T-cells and include: mucosal associated invariant T-cells (MAIT), germline-encoded mycolyl reactive (GEM) T-cells, natural killer (NK) T-cells, invariant NK (iNK) T-cells, and  $\gamma\delta$  T-cells.

CD1 molecules, which have been shown to activate both  $\alpha\beta$  and  $\gamma\delta$  T-cells (Paget et al. 2012; Uldrich et al. 2013; Le Nours et al. 2016) present lipid antigens and play non-redundant functions in the tissue surveillance and anti-microbial defence (Adams 2014). CD1 molecules, present in all jawed vertebrates, are grouped into 5 isoforms (CD1a-e), where the first four isoforms (CD1a-d) are capable of presenting lipid antigens to T-cells in association with  $\beta 2M$  (Dascher 2007). The fifth isoform, CD1e, is expressed intracellularly and plays a role in loading of lipids onto other CD1 isoforms, thus does not present lipids at the cell surface (de la Salle et al. 2005; Facciotti et al. 2011). CD1 molecules are not ubiquitously expressed but rather restricted to professional APCs or epithelial cells. Although deemed unconventional, up to 10% of all  $\alpha\beta$  T-cells are thought to recognize lipid antigens in the context of CD1 molecules (Adams 2014; Attaf et al. 2015b).

The most well characterised examples of T-cell interactions with CD1 involve the presentation of self-derived lipids such as sulphatides or  $\alpha$ -galactosylceramide ( $\alpha$ -GalCer) by CD1d to both  $\alpha\beta$  (Le Nours et al. 2016) and  $\gamma\delta$  T-cells (Paget et al. 2012; Uldrich et al. 2013). Interestingly the  $\delta/\alpha\beta$  T-cell clone previously mentioned was shown to recognize peptide- and lipid-based antigens presented by HLA and CD1d, respectively (Pellicci et al. 2014). These cells are deemed unconventional, however the hybrid  $\delta/\alpha\beta$  TCR was shown to represent around 50% of all V $\delta 1$  T-cells which bound CD1d in freshly isolated PBMCs. Importantly, many  $\gamma\delta$  T-cells respond to CD1 molecules presenting endogenous lipids, suggesting that these cells exhibit high levels of autoreactivity: a characteristic central to immunosurveillance of cellular stress.

MR-1 is another MHC-Ib molecule shown to bind both  $\alpha\beta$  T-cells. MR1 presents small bacterially-derived intermediates generated in the riboflavin (vitamin B2) metabolic pathway (Kjer-Nielsen et al. 2012). Unconventional  $\alpha\beta$  MAIT T-cells, constituting up to 10% of the lymphocyte compartment, have been shown to recognize MR1 molecules in the context of *Mycobacterium* infection (Salio et al. 2014; Kurioka et al. 2015).

**Table 1.1: A summary of MHC-Ib molecules, the ligands they present and the T-cells that recognize them.**

MHC-Ib molecule	Ligand	Binds $\alpha\beta$ TCRs?	Binds $\gamma\delta$ TCRs?	T-Cell	Example	
					Ligand	Ref
CD1a	Lipid	Yes#	ND	$\alpha\beta$	Self	(Birkinshaw et al. 2015)
CD1b	Lipid	Yes	ND	GEMs	Glucose monomycolate	(Moody et al. 1999)
CD1c	Lipid	Yes	Yes	$\alpha\beta$	Phosphomycoketide	(Roy et al. 2014)
CD1d	Lipid	Yes#	Yes#	$\gamma\delta$	Sulfatide	(Luoma et al. 2013)
				NKT	$\alpha$ -GalCer	(Le Nours et al. 2016)
MR1	Metabolite	Yes#	ND	MAITs	Riboflavin derivative	(Patel et al. 2013)
HLA-E	Peptide	Yes#	ND	$\alpha\beta$		(Hoare et al. 2006)
HLA-F	Peptide	ND	ND			(Dulberger et al. 2017)
HLA-G	Peptide	ND	ND			
MICA/B	-	ND	Yes#	$\gamma\delta$	Undefined	(Xu et al. 2011)
ULBP	-	ND	Yes	$\gamma\delta$	NKG2D	(Wrobel et al. 2007)
EPCR	Stress ligand	ND	Yes	$\gamma\delta$	Undefined self	(Willcox et al. 2012)

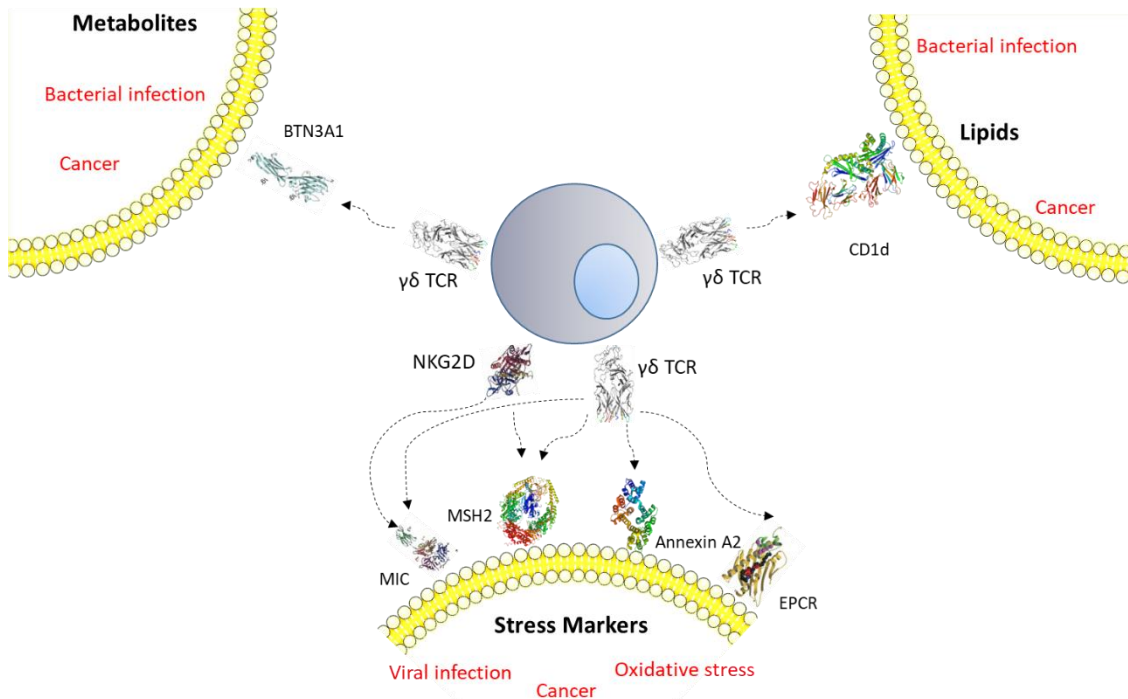
#, structure defined; ND, not defined; TCR, T-cell receptor; GEM, germline encoded mycolyl-reactive; NKT, natural killer T-cell; MR1, major histocompatibility complex class I-related; MAIT, mucosal associated invariant T-cell; MIC, major histocompatibility complex class-I related A/B; ULBP, UL16 binding protein; EPCR, endothelial protein C receptor.



## 1.4 The $\gamma\delta$ T-cell: Orchestrators of immunosurveillance

$\gamma\delta$  T-cells can sense stress ligands by patrolling for stress-induced surface molecules and metabolic intermediates that are frequently dysregulated in infections and cellular transformations  $\gamma\delta$  T-cells. Initial studies in mice indicated the role of  $\gamma\delta$  T-cells in immune surveillance (Vilmer et al. 1988), however progress in our understanding of the role of  $\gamma\delta$  T-cells in the immune system has been hampered by the considerable lack of knowledge regarding the molecular basis of  $\gamma\delta$  T-cell ligand recognition despite extensive efforts by numerous laboratories.  $\gamma\delta$  T-cells are central in the clearance of infection and cancerous cells, tissue homeostasis and repair, and host defence of epithelial surfaces (Hayday 2009; Nielsen et al. 2017).  $\gamma\delta$  T-cells possess a broad range of effector functions, such as the release of IFN $\gamma$  and TNF $\alpha$  (Halary et al. 2005; Vantourout and Hayday 2013). Previously,  $\gamma\delta$  T-cells have been deemed 'innate-like' as they were not believed to require pathogen-specific antigen or TCR activation to develop effector function (Hayday 2009). However, much evidence has come to light, reviewed in this section, to show that  $\gamma\delta$  T-cells behave in a TCR-dependent and adaptive manner.

$\gamma\delta$  T-cells are in the minority in the periphery, forming around 10% of blood lymphocytes, but they can constitute up to 50% of tissue specific T-cells in the skin and gut (Attaf et al. 2015b). Currently human  $\gamma\delta$  T-cells are broadly categorised into two sub-types depending on V $\delta$  chain expression: V $\delta$ 2<sup>+</sup> and V $\delta$ 2<sup>-</sup> T-cells. Around 90% of circulating  $\gamma\delta$  T-cells fall within the V $\delta$ 2<sup>+</sup> subset, preferentially pairing with a V $\gamma$ 9 chain, whereas in tissues the majority of  $\gamma\delta$  T-cells express V $\delta$ 1 and V $\delta$ 3 chains paired with a diverse range of V $\gamma$  chains (Thedrez et al. 2007; Donia et al. 2012; Roy et al. 2016b). Whilst the mechanism of V $\delta$ 2<sup>+</sup> T-cell activity is well characterised, the recognition of target cells by V $\delta$ 2<sup>-</sup>  $\gamma\delta$  T-cells is poorly understood. A summary of known human  $\gamma\delta$  TCR ligands can be found in Figure 1.5. Generally it is accepted that  $\gamma\delta$  T-cells do not require MHC for the recognition of target cells (Vantourout and Hayday 2013; Attaf et al. 2015b; Marlin et al. 2017) despite murine studies suggesting binding between  $\gamma\delta$  TCR and MHC class II molecules (Matis et al. 1989; Rellahan et al. 1991).



**Figure 1.5: An overview of known  $\gamma\delta$  T-cell receptor (TCR) ligands.** The  $\gamma\delta$  TCR is known to recognize lipids, metabolites and stress markers in different disease contexts (red) as confirmed by structural/biophysical studies. The  $\gamma\delta$  TCR recognises MHCIIb molecules CD1d, EPCR and MICA/B as well as the MHC-like molecule BTN3A1. The  $\gamma\delta$  TCR can also recognise non-MHC ligands such as MSH2 and annexin A2. CD1 can present diverse lipids to  $\gamma\delta$  T-cells including self-derived cancer specific lipids and bacterially derived. Similarly, BTN3A1 can present self- and bacterially derived metabolites to the  $\gamma\delta$  TCR. Cellular stress, such as viral infection, leads to an upregulation of stress markers such as EPCR, MIC, MSH2, annexin A2 and EPCR that can be recognized by  $\gamma\delta$  TCRs. Some of the stress markers (MICA/B and MSH2) are also ligands for another immunoreceptor, NKG2D, which is commonly expressed on  $\gamma\delta$  T-cells. NKG2D contributes to  $\gamma\delta$  TCR-mediated stress sensing by providing a co-stimulatory signal. Detailed descriptions can be found in the main body of the text. BTN3A1, butyrophilin 3A1; EPCR, endothelial protein C receptor; MIC, major histocompatibility complex class I-related chain; MSH2, MutS homologue 2; NKG2D, natural-killer group 2, member D.

The V $\gamma$ 9V $\delta$ 2 T-cell subset have been described as providing a bridge between innate and adaptive immunity by responding to the same related set of non-peptidic, phosphorylated compounds known as phosphoantigens(PAGs) (Tyler et al. 2015). Such PAGs include self-derived products of the mevalonate pathway which become dysregulated during viral infection (Poccia et al. 2002) and cellular transformation (Gober et al. 2003), as-well as microbial derived products from the non-mevalonate pathway (Constant et al. 1994; Kistowska et al. 2008). Foetal blood V $\gamma$ 9V $\delta$ 2 T-cells display very little CDR3 diversity and have been shown to be functionally pre-programmed to secrete effector compounds, such as granulysin and perforins, prior to antigenic exposure - a key characteristic of innate-like immunity (Farouk et al. 2004; Dimova et al. 2015). Interestingly, V $\gamma$ 9V $\delta$ 2 T-cells can express MHCII and professionally present protein antigens to both CD4 and CD8  $\alpha\beta$  T-cells, resulting in naïve T-cell differentiation and maturation (Brandes et al. 2005; Tyler et al. 2017). Specific anti-tumour properties of V $\gamma$ 9V $\delta$ 2 T-cells will be covered in Section 1.5.

Previously, the stress surveillance response of  $\gamma\delta$  T-cells have been described as rapid, weakly specific and resulting from activation of large numbers of pre-activated or preprogramed  $\gamma\delta$  T-cells without clonal expansion (Hayday 2009). A recent burst in the research field, however, has shown that V $\delta$ 2<sup>+</sup>  $\gamma\delta$  T-cells undergo genetic rearrangement of the TCR during thymic selection to generate a lifelong, adaptive, antigen-specific immune response. Kallemijn and colleagues found that in CMV infected individuals the  $\gamma\delta$  T-cell compartment shifted from naïve to more effector phenotypes with age and infection (Kallemijn et al. 2017). Others have shown that there is clonal selection in the  $\gamma\delta$  T-cell repertoire (Davey et al. 2017) and observed adaptive clonal expansion in response to viral infection (Ravens et al. 2017). Most importantly, V $\delta$ 2<sup>+</sup>  $\gamma\delta$  T-cells have been shown to recognise moieties that are upregulated on the surface of stressed cells independent of classical MHC presentation (O'Brien and Born 1991; Vantourout and Hayday 2013) and play key roles in TCR dependent anti-viral and anti-tumour immunity.

## 1.5 Mechanisms of $\gamma\delta$ T-cell anti-tumour reactivity

In recent decades  $\gamma\delta$  T-cells have been shown to recognize and kill a variety of solid tumours and leukaemias/lymphomas via the release of cytokines such as TNF $\alpha$  and IFN $\gamma$  (Donia et al. 2012). The delineation of exact mechanisms of cancer cell recognition by  $\gamma\delta$  T-cells, in particular the structural and molecular level of TCR ligand interactions, has only recently begun to emerge.

The majority of  $\gamma\delta$  T-cell cancer-associated targets identified to date rely on presentation by unconventional MHC-Ib molecules such as CD1. A growing body of evidence also suggests that non-MHC molecules become upregulated or translocated to the cell surface upon cellular stress and are important targets for immunosurveillance by  $\gamma\delta$  T-cells. Intriguingly, most of these self-antigens are constitutively expressed on healthy cells and tissues, implying that there must be mechanisms to control the  $\gamma\delta$  T-cell response in appropriate situations to avoid autoimmunity. This section focuses on the evidence indicating that  $\gamma\delta$  T-cells are capable of targeting transformed cells through a number of different antigens (Table 1.2).

**Table 1.2: Antigen selectivity of human and mouse  $\gamma\delta$  T-cell receptors**

<i>Species</i> <i>Origin</i>	<i>TCR</i>	<i>Antigen</i>	<i>Presenting Molecule</i>	<i>Reference</i>
Mouse	V $\gamma$ 2V $\delta$ 5	-	MHC I-E <sup>k</sup>	(Matis et al. 1989)
	G8	-	T20/22	(Adams et al. 2005)
Human	V $\gamma$ 9V $\delta$ 2	IPP, HMBPP	BTN3A1	(Vavassori et al. 2013)
	V $\gamma$ 8V $\delta$ 3	Annexin A2	-	(Marlin et al. 2017)
	V $\gamma$ 4V $\delta$ 5	EPCR	ND	(Willcox et al. 2012)
	V $\gamma$ 5V $\delta$ 1	$\alpha$ GalCer#	-	(Uldrich et al. 2013)
	V $\gamma$ 4V $\delta$ 1	Sulfatide#	-	(Luoma et al. 2013)
	V $\gamma$ 4V $\delta$ 1	-	MICA#	(Xu et al. 2011)
	V $\delta$ 1	Phosphomycoketide	-	(Roy et al. 2016)

#, structure defined; ND, not defined; -, not required; TCR, T-cell receptor; MIC, major histocompatibility complex class-I related A/B; EPCR, endothelial protein C receptor; IPP, isopentenyl pyrophosphate; HMBPP, (E)-4-Hydroxy-3-methyl-but-2-enyl pyrophosphate; BTN3A1, butyrophilin subfamily 3 member A1;  $\alpha$ GalCer,  $\alpha$ -Galactosylceramide.

### 1.5.1 Sensing of metabolic intermediates

One of the earliest identified activators of human  $\gamma\delta$  T-cells were small molecular weight compounds derived from bacterial lysates (Munk et al. 1990). Subsequent studies demonstrated that V $\gamma$ 9V $\delta$ 2 T-cell clones reactive to mycobacterial lysates were cross-reactive to some cancer cell lines, such as the Burkitt's lymphoma Daudi, thus indicating that the mechanism of recognition was similar in both cases (Marx et al. 1997). After further investigation, the molecules responsible for V $\gamma$ 9V $\delta$ 2 T-cell activation were shown to be metabolic intermediates of polyisoprenoid synthesis pathways (Tanaka et al. 1994). The identified V $\gamma$ 9V $\delta$ 2 T-cell ligand in transformed cells is a substrate of the mevalonate pathway: isopentenyl pyrophosphate (IPP).

The microbial derived antigen is an intermediate the non-mevalonate pathway: (E)-4-hydroxy-3-methyl-but-2-enyl pyrophosphate (HMBPP) (Hintz et al. 2001).

Whilst HMBPP is an essential metabolite in most pathogenic bacteria and is absent from the human host (Eisenreich et al. 2004), IPP is a host molecule that can become excessively accumulated intracellularly as a result of tumorigenesis (Gober et al. 2003). The foreign antigen HMBPP is 10,000 times more potent a V $\gamma$ 9V $\delta$ 2 T-cell ligand than the self-derived compound IPP (Rhodes et al. 2015), allowing V $\gamma$ 9V $\delta$ 2 to perform immunosurveillance in cases of significant metabolic dysregulation whilst preventing harmful autoreactivity to normal levels of IPP production. It has been shown that virtually any nucleated cells can present pAgs to V $\gamma$ 9V $\delta$ 2 T-cells (Vavassori et al. 2013), however the mechanism by which it is done is yet to be fully elucidated.

Early studies on the nature of pAg recognition by human V $\gamma$ 9V $\delta$ 2 T-cells showed that these antigens needed to be 'presented' by a cell of human origin and suggested that there was either a species-specific presentation platform or co-receptor (Green et al. 2004). Later studies showed that a butyrophilin (BTN) family member, BTN3A1, is crucial for pAg presentation to human V $\gamma$ 9V $\delta$ 2 T-cells (Harly et al. 2012). Butyrophilins are single-pass transmembrane proteins composed of two Ig-like extracellular domains V and C, and in some cases an intracellular domain called B30.2. Butyrophilin genes are located next to the MHC-I locus on human chromosome 6 and belong to the B7 superfamily of receptors, many of which play important roles in co-stimulating or co-inhibiting T-cell responses (Chen and Flies 2013). The exact mechanism of V $\gamma$ 9V $\delta$ 2 T-cell activation by pAg presented via BTN3A1 remains controversial. Whilst a study proposed that pAgs bind in a shallow pocket within the extracellular domain of BTN3A1 and are thus presented to  $\gamma\delta$  T-cells in a manner similar to MHC presentation of peptide (Vavassori et al. 2013), other groups have postulated that pAgs are bound to the intracellular B30.2 domain, and that the binding event translates into an extracellular conformational change and subsequent T-cell stimulation (Rhodes et al. 2015). What is confirmed, however, is the necessity of the presence of BTN3A1 in the activation of  $\gamma\delta$  T-cells by microbial or endogenous pAg (Harly et al. 2012).

BTN3A1 alone is insufficient for inducing pAg-mediated activation of T-cells. Herrmann and colleagues used rodent cells for antigen presentation and demonstrated that additional genes located on human chromosome 6 were required for efficient T-cell activation (Riano et al. 2014). The exact TCR ligand of V $\gamma$ 9V $\delta$ 2 pAg mediated activation is yet to be elucidated, with molecules

such as the cytoskeletal adapter periplakin (Rhodes et al. 2015) and the small GTPase RhoB (Sebestyen et al. 2016) being uncovered as a range of components necessary.

### 1.5.2 MICA/B presentation of self-antigens

In the context of cellular stress, such as viral infection, oxidative stress and cellular transformation, human  $V\delta 1^+$  T-cells recognise MHC class I related A and –B (MICA/MICB) (Groh et al. 1998; Xu et al. 2011). MICA/MICB molecules are highly polymorphic in the membrane distal interface and show high structural similarities with MHC I (Jinushi et al. 2003). Despite structural similarities with MHC I, MICA/MICB molecules do not present peptides in the binding groove or associate with  $\beta 2M$  (Xu et al. 2011). Instead MICA/B are thought to represent a ubiquitous marker of cellular stress that can become ectopically expressed upon viral infection, cancerous transformation or oxidative stress (Shafi et al. 2011). MICA/B molecules serve as ligands for the activating immunoreceptor natural killer group 2 (NKG2D) expressed on  $\gamma\delta$  T-cells. The MIC/NKG2D interaction serves as a costimulatory signal for some  $\gamma\delta$  T-cells as it facilitates the binding of the TCR with a cognate ligand (Wrobel et al. 2007).

MICA, expressed by epithelial tumours, was one of the first known targets of  $V\delta 1^+$  T-cells (Wrobel et al. 2007). Subsequently, the human tumour biomarker human MutS homologue 2 (hMSH2) was identified as the TCR antigen involved in  $\gamma\delta$  T-cell activation in association with MICA/NKG2D (Dai et al. 2012). hMSH2 is a nuclear protein critical in elements of the DNA mismatch repair system that is ectopically expressed on a large panel of epithelial tumours and EBV immortalised B-cells (Dai et al. 2012). It is generally thought that both hMSH2 and MICA become upregulated in response to cell stress stimuli and that initial contact is provided by NKG2D/MICA interaction followed by the formation of a stable, low affinity TCR-hMSH2 complex (Legut et al. 2015).

#### 1.5.2.1 *NKG2D as a co-stimulator molecule for $\gamma\delta$ T-cell anti-tumour immunity*

The presence of co-receptors and co-stimulatory molecules has long been established as a requirement for effective engagement of ligands by T-cells. For example the co-receptors CD4 and CD8 are required for the engagement of conventional MHC ligands by  $\alpha\beta$  T-cells as described above. The majority of  $\gamma\delta$  T-cells, however, are CD4/CD8 co-receptor negative. Even in  $\gamma\delta$  T-cells expressing either (or both) CD4 and CD8, the physiological relevance of these glycoproteins remains unclear. It is therefore possible that other molecules act as co-receptors, or provide co-stimulatory signals for  $\gamma\delta$  TCRs.

NKG2D is expressed on innate natural killer (NK) cells, invariant natural killer T-cells (iNKT), some CD8 and CD4 T-cells, and all  $\gamma\delta$  T-cells. The expression of NKG2D has been indicated in the lysis

of different melanomas, pancreatic adenocarcinomas, squamous cell carcinomas of the head and neck, and lung carcinoma (Wrobel et al. 2007). NKG2D is a receptor for multiple stress-induced MHC class I related molecules including MICA/B and six members of the UL16 binding protein family (ULBP1-6) (Lanier 2015). For example, it was shown in leukemia/lymphoma expression levels of ULBP1 correlated with sensitivity to  $\gamma\delta$  T-cell induced recognition, which could be blocked with NKG2D blockade (Lanca et al. 2010). Generally, healthy adult tissues do not express NKG2D ligands on the cell surface, but these ligands can be induced by hyperproliferation and transformation, as well as when cells are infected by pathogens. Thus the NKG2D pathway serves as a mechanism for the immune system to detect and eliminate cells that have undergone “stress”. Apart from NKG2D not much is known about  $\gamma\delta$  T-cell co-stimulatory molecules except that they are essential in some instances of  $\gamma\delta$  T-cell recognition of target cells. Molecules such as CD40, CD80, CD86 and adhesion molecule such as CD11a-c, CD18, CD50 and CD54 have all been found on freshly isolated  $\gamma\delta$  T-cells (Chen and Flies 2013) and may play key role in  $\gamma\delta$  T-cell co-stimulation.

### 1.5.3 Lipid presentation by CD1

CD1 isoforms a-d bind and present natural or synthetic lipid-based antigens to  $\gamma\delta$  T-cells, playing non redundant functions in tissue surveillance and anti-microbial defence (Adams 2014). Recent studies have shown that  $\gamma\delta$  T-cells survey both CD1 and the presented lipid, and in some cases are highly lipid specific.

CD1c, a non-polymorphic molecule expressed on human dendritic cells and B cells, binds and displays a diverse range of lipid antigens and induces TCR mediated, lipid-specific  $\gamma\delta$  T-cell activation. Interestingly CD1c has even been demonstrated as a ligand for the V $\delta$ 1 TCR, independent of the presence of a lipid antigen (Spada et al. 2000). In another study, there was a differential pattern of lipids recognised by V $\delta$ 1 T-cells depending on the TCR $\gamma$  chain, indicating a mechanism of ligand discrimination by  $\gamma\delta$  TCRs (Roy et al. 2016a). Furthermore, this study demonstrated the variety of self and foreign lipid antigens that were recognised in the context of CD1c by  $\gamma\delta$  T-cells, such as bacterial phosphomycoketide.

CD1d has also been shown to present a range of lipid antigens to  $\gamma\delta$  T-cells in a range of pathological conditions, such as the allergic response to pollen antigens (Russano et al. 2006), microbial infection (Roy et al. 2016a) and dysregulated self-antigens in tumour cells (Luoma et al. 2013; Uldrich et al. 2013). Sulfatide, an abundant myelin glycosphingolipid, has been reported as a lipid antigen presented by CD1d and it was shown that the majority of CD1d-sulfatide specific T-cells in human blood use a semi-invariant V $\delta$ 1 chain (Bai et al. 2012). Adams *et al*, have

recently solved the crystal structure of CD1d-sulphatide bound by a V $\gamma$ 4V $\delta$ 1 TCR (Luoma et al. 2013). Uldrich and colleagues further described the complex between CD1d- $\alpha$ GalCer and a V $\gamma$ 5V $\delta$ 1 TCR (Uldrich et al. 2013). These two models of CD1d-lipid recognition by  $\gamma\delta$  TCRs highlighted the importance of the V $\delta$ 1 chain in binding the antigen presenting molecule CD1 and may offer insight into the general antigen binding mechanism of  $\gamma\delta$  TCRs. Furthermore, these binding modes allow speculation that  $\gamma\delta$  TCRs could potentially discriminate between different lipid antigens and that the mode of target recognition is adaptive, rather than semi-invariant and innate-like. Human V $\delta$ 3 T-cells have also been implicated in CD1 lipid presentation (Mangan et al. 2013).

#### 1.5.4 Expression of stress ligands

It has been shown that V $\delta$ 1  $\gamma\delta$  T-cells can expand as a result of CMV infection (Halary et al. 2005). In a subsequent study CMV reactive  $\gamma\delta$  T-cells also had potential to recognise and lyse cancer cells *in vitro* and *in vivo* (Willcox et al. 2012). Such findings suggest that CMV infection and malignant transformation could activate an overlapping population of  $\gamma\delta$  T-cells, possibly through the expression of a generic stress signature by target cells. One such cellular stress ligand activator of  $\gamma\delta$  T-cells has been found to date, endothelial cell protein C receptor (EPCR), which acts as a binding partner for a V $\gamma$ 4V $\delta$ 1 TCR (Willcox et al. 2012). EPCR is a multi-liganded and multifunctional receptor involved in the anticoagulant pathway (Mohan Rao et al. 2014) and shows high sequence and structural similarity to CD1 molecules with a capability of presenting phospholipid in its antigen binding groove (Oganesyan et al. 2002). EPCR is considered a stress molecule as it is associated with a higher metastatic potential and resistance to apoptosis in different cancer types (Ruf and Schaffner 2014). Along with the EPCR/TCR interaction, co-stimulation was provided by binding of the adhesion molecules LFA-1 and CD2 to their ligands CD54 and CD58, respectively, on the target cell (Willcox et al. 2012). Another unknown co-stimulatory molecule is required for EPCR recognition by V $\delta$ 1 T-cells. Full understanding of how EPCR is recognised by  $\gamma\delta$  T-cells awaits structural information.

Annexin A2 recognition by  $\gamma\delta$  T-cells provides a further example of the recognition of a stress induced self-antigen. Exposure of cells to various stress situations resulted in targeting by a V $\gamma$ 8V $\delta$ 3 TCR, from which annexin A2 was identified as the direct ligand (Marlin et al. 2017). Purified annexin A2 could stimulate the proliferation of a V $\delta$ 2-  $\gamma\delta$  T-cell subset within PBMCs and other annexin A2 specific cells were subsequently isolated from these PBMC. (Marlin et al. 2017). Annexin A2 is in the family of Ca<sup>2+</sup> regulated phospholipid-binding annexin proteins and is present in the cytoplasm where it is associated with intracellular membranes of different organelles and with the internal or extracellular face of the plasma membrane with roles in many



cellular processes (Benaud et al. 2015). Annexin A2 is overexpressed by many tumour cells, can translocate to the cell surface upon stress signals and plays a key role in membrane repair and wound healing (Deng et al. 2015; Onishi et al. 2015). The diversity and low frequency of annexin A2-specific  $\gamma\delta$  T cells that are described in the Marlin *et al* study suggest that response to annexin A2 may rather represent an adaptive response requiring clonal expansion in specific situations.

## 1.6 Cancer immunotherapy

Cancer immunotherapy was named breakthrough of the year by Science magazine in 2013 (Couzin-Frankel 2013). Immunotherapies harness the power of the immune system to target cancer cells. Antibodies, vaccines and adoptive cell transfer techniques have all been used to yield exciting, positive results. Initially one of the cruder immunotherapies was the use of immune-stimulants such as interleukin-2 (IL-2) and alpha-interferon (IFN- $\alpha$ ) in the treatment of diverse types of cancers including metastatic melanoma (Kirkwood et al. 2001), however now more specific treatments are being investigated.

Cancer is a major health burden worldwide causing up to 8.2 million deaths worldwide annually (Siegel et al. 2014). With many different types and sub-types of different molecular profiles, pathologies and prognostic outcomes finding effective cancer treatments is a main priority in biomedical research. Current systemic approaches, such as radiotherapy and chemotherapy, have varying response rates due to individual genetic variability and the heterogeneous nature of tumours. These broad-brush treatments also kill healthy dividing cells causing side effects that range from hair loss and immune dysfunction through to cardio-toxicity (Malhotra and Perry 2003). There is an urgent need for more targeted approaches, which has seen a major shift towards exploiting the immune system for cancer immunotherapy.

### 1.6.1 Monoclonal antibodies

The use of monoclonal antibodies (mAbs) in cancer treatment aims to direct and enhance the activity of effector immune cells to slow tumour growth and deliver a range of different reagents such as: radioactive isotopes, toxins and chemotherapeutic agents to tumour cells [reviewed in (Weiner et al. 2009)]. There are two main classes of antibody-induced immunotherapy: antibody-dependent cellular cytotoxicity (ADCC) and complement dependent cytotoxicity (CDC). Whereas ADCC tends to involve components of the adaptive immune system, CDC activates the complement system resulting in the formation of multiple pores in target cancer cells, ultimately resulting in cancer cell death (Weiner et al. 2009). The most recent advances in mAb technology are the; development of checkpoint inhibitors, bispecific T-cell engagers (BiTEs) and immune-mobilising monoclonal TCRs against cancer (ImmTACs).

### 1.6.2 Immune checkpoint inhibitors

Checkpoint inhibitors (such as cytotoxic T-lymphocyte antigen 4 [CTLA4], programmed death 1 [PD-1], T-cell immunoglobulin 3 [TIM-3] and lymphocyte-activation gene 3 [LAG-3]) exist on the T-cell surface to act as a naturally occurring negative feedback mechanism to act as the 'brakes' on T-cell activation to prevent harmful autoreactivity. The T-cell negative regulatory signals can be initiated following the binding of cognate ligands to the membrane receptors which all act as 'brakes' on T-cell activation (reviewed in (Pardoll 2012)). Cancer cells have evolved to evade the immune system by exploiting the immune checkpoint pathways (Drake et al. 2006). In patients with advanced cancers the ligands of the immune checkpoint receptors (for example programmed death ligand 1 [PD-L1] is the ligand for PD-1) are upregulated on tumour cells, or non-malignant cells in the tumour microenvironment, causing the development of tumour resistance and immune escape. Immune checkpoint inhibitors have thus been developed to block tumour cell induced immune inhibitor activation.

Three mAbs, Pembrolizumab (Reck et al. 2016), Nivolumab (Sznol et al. 2017) and Atezolizumab are currently approved for the immune blockade of PD-1 having shown successful anti-tumour effects in clinical trials. The combination of checkpoint inhibitors has also proved effective, for example the joint blockade of PD-1 and CTLA-4 using nivolumab plus anti-CTLA-4 inhibitor Ipilimumab, respectively, in advanced stage melanoma and renal cell carcinoma has resulted in significant gains (Callahan and Wolchok 2013). Furthermore, immune checkpoint targeting can be combined with other types of immunotherapy, such as adoptive cell therapy (ACT).

However, treatment with checkpoint inhibitors has drawbacks with severe side effects and toxicities being noted (Hassel et al. 2017; Sznol et al. 2017). The regulatory role of the immune checkpoint molecules is an essential part of avoiding tissue damage and hyper immunity. Turning the 'brakes' off T-cell activation can lead to autoreactivity and adverse effects which can affect multiple organs of the body including skin, GI tract, kidneys, peripheral and central nervous system, liver, lymph nodes, eyes, pancreas and the endocrine system (Abdel-Wahab et al. 2016). Increasingly events of inflammatory or autoimmunity are being seen and, in some cases, have been fatal.

#### 1.6.2.1 Bispecific T-cell engagers BiTEs

BiTEs are a class of artificial bispecific mAb that direct T-cells to tumour cells. For example blinatumomab (MT103), an antiCD19/CD3 bispecific, engages CD19 on haematological malignancies and redirects T-cells to kill target cells via CD3 (Nagorsen et al. 2009). Another

example is solitomab (MT110) in the treatment of gastrointestinal and lung cancers, directed against the EpCAM antigen (Amann et al. 2009).

#### 1.6.2.2 *Immune-mobilising monoclonal TCRs against cancer (ImmTACs)*

ImmTACs are a recently developed development of the BiTE technology where the non-CD3 binding site is replaced by an enhanced-affinity, cancer-specific TCR. Once bound to tumour cells the anti-CD3 effector end of the ImmTAC drives the recruitment of polyclonal T-cells to the tumour site, leading to a potent redirected T-cell response and tumour cell destruction (Oates et al. 2015). For example, the ImmTAC targeting NY-ESO-1 and LAGE-1 positive tumours (McCormack et al. 2013).

### 1.6.3 Cancer vaccines

Cancer vaccines can be virus, peptide, protein, tumour cell, dendritic cell, gene therapy or immunoglobulin-based in either a preventative, prophylactic or treatment setting. One of the first examples of prophylactic successes was the hepatitis B virus (HBV) vaccine approved by the FDA in 1981 as a cancer preventative. The HBV vaccine not only dramatically reduced the rates of HBV infections but also reduced the number of incidences of hepatocellular carcinoma (Chang et al. 2016). A second prophylactic vaccine was developed to target human papilloma virus (HPV), known to be the main cause of cervical cancer. The HPV-16/18 AS04-adjuvanted vaccine was shown to reduce HPV infection and resulting cases of cervical cancer (Skinner et al. 2016). Prophylactic herd immunity offers an attractive solution to viral induced malignancies.

Peptide or protein based vaccines use tumour cell-specific antigens for immunization to activate an adaptive immune response to a specific cancer moiety. Following the molecular identification of a large collection of tumour-associated antigens, several peptide vaccines have been used in clinical settings. Effective peptide vaccines deliver targets to both MHCI and MHCII molecules to promote both CD4 and CD8 T-cell expansions. The advantages of using peptide-based vaccines compared to other immunotherapy approaches include low production costs of synthetic peptides and the easy administration in a clinical setting as an 'off-shelf' reagent.

Even though there is some potential in the future for peptide or protein based vaccines the results with this approach to date have been disappointing. Vitespen is a vaccine that uses a tumour-derived, stress-induced heat shock protein-peptide complex (HSPPC), glycoprotein (gp) 96 as an antigen to protect against malignancies. Vitespen made it to Phase III clinical trials but unfortunately failed to provide a significant increase in overall survival rates and showed no overall benefit in recurrence-free survival (Jonasch et al. 2008). Short and free peptides are likely to be excreted rather quickly from the body without having the chance to associate with a

dendritic cell to evoke an immune response. Furthermore, tumours may elicit escape mechanisms such as immune checkpoint induction or MHC downregulation, which may be largely accountable for the disappointing success of peptide based vaccines in the clinic.

#### 1.6.4 Adoptive T-cell therapy

Adoptive T-cell therapy (ACT) is a new and promising immunotherapy that has been shown to be highly effective against metastatic melanoma (Phan and Rosenberg 2013). This cell-based approach uses autologous T-cells which are expanded, manipulated *ex vivo*, and then re-infused into the patient to exert an anti-tumour response. ACT is traditionally carried out with autologous tumour infiltrating lymphocytes (TILs), however recent advances in ACT research is exploring the possibilities of also using engineered TCRs or chimeric antigen receptors (CARs) on peripheral blood T-cells (Figure 1.6).

##### 1.6.4.1 TIL Therapy

TILs represent a heterogeneous population of T-cells within a tumour microenvironment that include anti-tumour T-cells. The rationale of TIL-based therapy is to enhance the natural anti-tumour immune response by removing cells with anti-tumour potential from an immunosuppressive microenvironment and expanding them with the pro-inflammatory cytokine IL-2 before reintroducing them to the patient. TILs should be returned in high enough numbers to allow trafficking to tumour sights and selective killing of tumour targets. In 1988 Rosenberg and colleagues pioneered this new approach by publishing the first human study that showed how TILs could induce cancer regression when administered to patients with metastatic melanoma (Rosenberg et al. 1988). Since the 1980's the field has expanded to improve these first results by modifying the TIL generation and selection protocols and better preparing the patient to receive and engraft TIL. In this respect, the addition of a lymphodepleting conditioning resulted in considerable improvements of TIL-based ACT by providing a physical and biological 'space' for TILs and other potential effectors to proliferate and survive. Dudley *et al.* showed that the overall response rates and complete response rates were progressively higher in patients receiving greater levels of lymphodepletion (Dudley et al. 2008). TIL therapy has been extremely successful in tumours that are easy to dissect, for example melanoma, however for some tumours it is too difficult or even impossible to access the tumour, for example many bowel cancers. TCR gene transfer and CAR therapy can offer a solution to this by enhancing the cancer targeting capabilities of peripheral blood T-cells, rather than requiring TILs.

#### 1.6.4.2 TCR manipulation

TCR gene transfer immunotherapy involves the genetic transfer of full-length TCR genes which are introduced to large numbers of autologous T-cells via the use of lentiviral vectors. During the *ex vivo* phase T-cells can be transduced to express TCRs targeting tumour associated antigens (TAAs). Clay and colleagues were the first to show that the transfer of TCR genes via a retroviral vector into human lymphocytes resulted in the gain of stable reactivity to MART-1: a melanoma TAA (Mandelcorn-Monson et al. 2003). In the first clinical trial these modified T-cells were tested and whilst the transduced T-cells persisted *in vivo*, only two of the 17 patients had an objective response to therapy (Morgan et al. 2006). This lack of clinical translation can be attributed to the fact that the TCR-pMHC interaction in the context of TAAs have a relatively low affinity for each other, typically exhibiting a dissociation constant in the range of 1-100  $\mu\text{M}$  (Garcia et al. 1997).

One solution to circumventing the very low affinity of natural anti-cancer TCRs is the use of affinity-enhanced TCRs, where modifications in the TCR can lead to fold increases in affinity. My own research group have shown that the TCR binding affinity governs the profile of cancer-specific CD8+ and CD4+ T-cells (Tan et al. 2015; Tan et al. 2017) and that changes in one amino acid of the CDR3 domain can dramatically enhance TCR binding affinity (Cole et al. 2014).

The use of affinity-enhanced TCRs comes with some inherent risks because these engineered TCRs have not undergone the rigours of thymic selection and therefore have the potential to recognise self-peptides leading to dangerous autoimmunity. In the treatment of metastatic renal cell carcinoma a genetically modified TCR was directed against the TAA carbonic anhydrase. However there was unpredicted hepatic toxicity due to the undetected expression of the target antigen in the biliary tract (Lamers et al. 2006). Another example of toxic cross-reactivity manifest itself as fatal cardiovascular toxicity caused by a TCR targeted to MAGE-A3. The first two patients to receive T-cells expressing enhance MAGE-A3 TCR died within a few days of T-cell transfusion from cardiogenic shock due to cross-reactivity to muscle-specific protein titin found on beating cardiomyocyte cultures (Linette et al. 2013). The safety considerations of using such high-affinity TCRs cannot be ignored, and other solutions to more efficient T-cell based immunotherapies must be found. In a further recent development, my research group have recently introduced methodology allowing simultaneous knockout of introduced TCR chains at the same time as TCR transduction of primary T-cells (Legut et al. 2017). This TCR replacement methodology was shown to substantially improve the sensitivity of engineered T-cells to their cognate antigen.

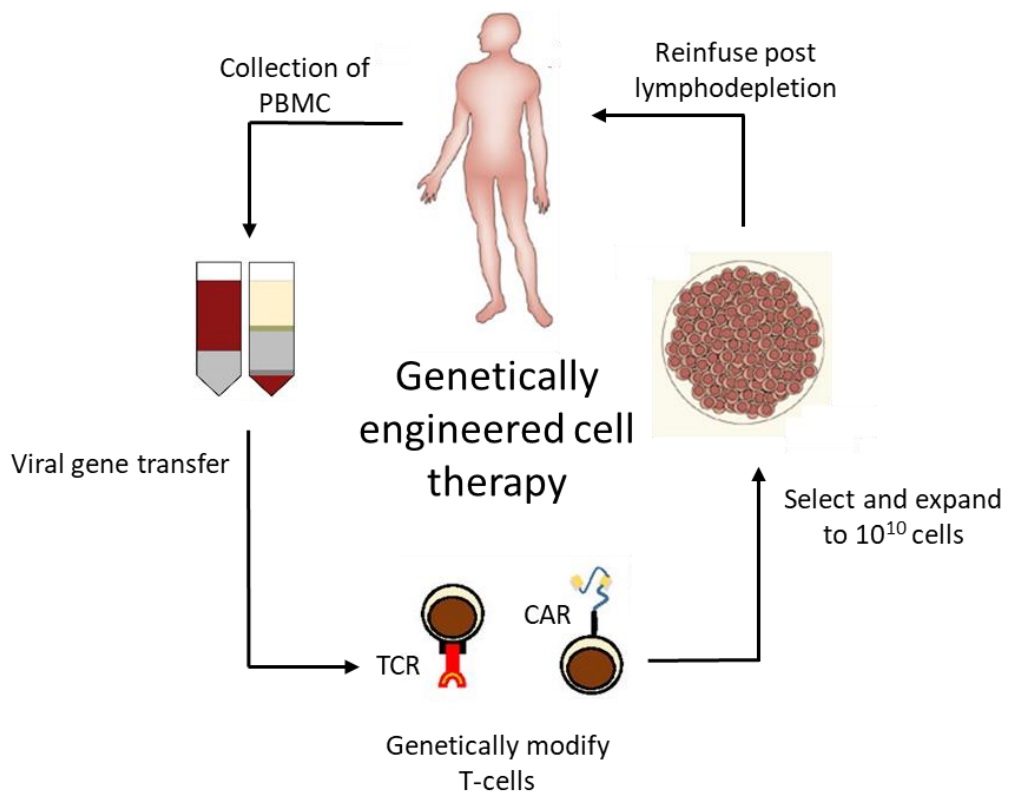
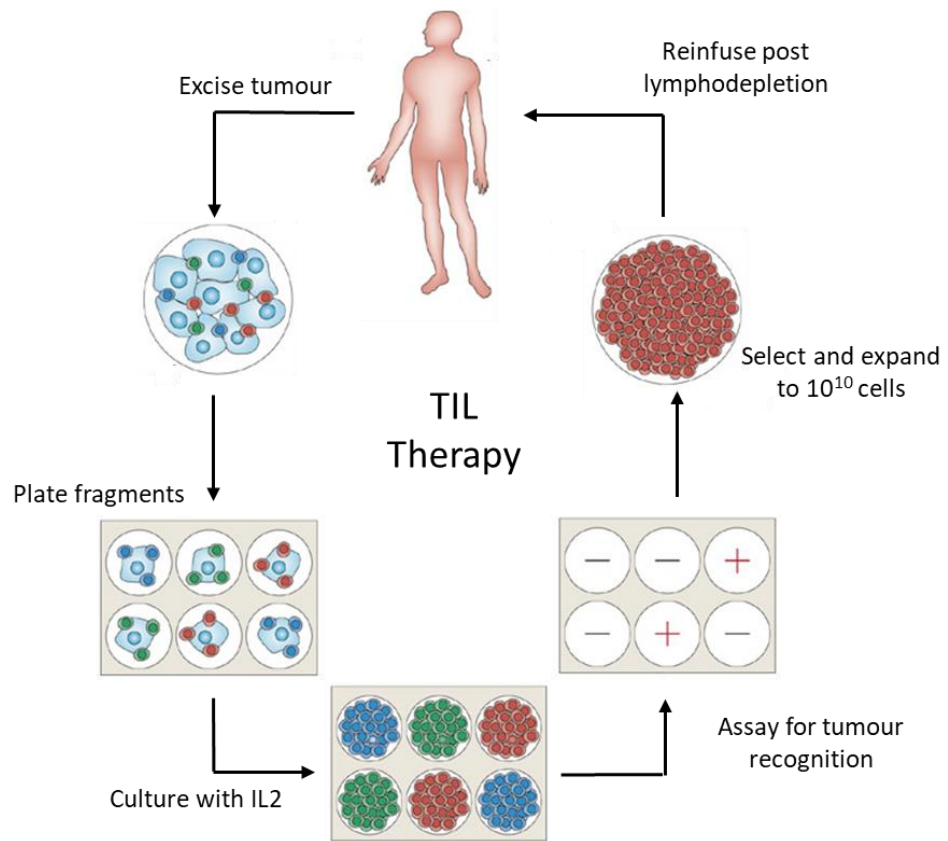
#### 1.6.4.3 *Chimeric antigen receptor therapy*

CAR therapy combines an extracellular single-chain variable fragment of an antibody with intracellular signalling domains required for T-cell activation (Gross et al. 1989). When expressed on T-cells the receptor bypasses the need for antigen presentation on MHC since the surface extracellular domain directly binds to the surface of targets bearing the antigen that the antibody recognises. The high-affinity nature of this extra-cellular domain makes these engineered T-cells highly sensitive to low antigen densities (Jena et al. 2013). Many CARs have been developed, and over four tested in clinical trials. Whilst in the majority of clinical studies poor transgene expression limited CAR efficacy, in one of the trials of metastatic renal cell carcinoma a CAR directed against carbonic anhydrase IX patients PBMCs produced IFN $\gamma$  and developed lytic functions in response to carbonic anhydrase IX expressing targets (Lamers et al. 2006). However, patients in the trial also developed dose-limiting toxicity, again asking serious safety questions.

To date, the biggest successes of CAR ACT therapy have been confined to soluble cancers for the diagnosis and treatment of malignancies. Anti-CD19 CARs have shown great promise for the treatment of B-cell malignancies and two such therapies have recently been licenced by the FDA. My laboratory has recently helped extend this approach by building antibodies and CARs that distinguish between TCRs made with TRBC1 and TRBC2 genes (Maciocia et al. 2017).

### 1.7 The $\gamma\delta$ T-cell: Potential for immunotherapy

Current immunotherapy options have several drawbacks. Autologous cellular therapies are hugely expensive and even successes like those recently described for anti-CD19 CARs are only applicable to a small minority of cancers.  $\alpha\beta$  TCR-based therapeutics of the sort being developed by companies like Adaptimmune and Immuncore are HLA-restricted so any given therapeutic agent is only ever applicable to a minority of patients. The use of  $\gamma\delta$  T-cells and TCR targeting of non-HLA ligands expressed broadly on multiple cancer and infected cells bypasses this obvious problem and is now being viewed as an attractive and promising pathway towards pan-population, pan-pathology therapeutics. To date, the potential of the  $\gamma\delta$  T-cell in anti-tumour immunity has inspired the development of two commercial entities in this field, such as Gadeta (Utecht) and Gamma Delta Therapeutics (London). This section reviews the potential for  $\gamma\delta$  T-cells in immunotherapy.



**Figure 1.6: An overview of adoptive cell therapy.** There has been a burst in the development of adoptive cell therapies over the last few decades, including the use of tumour infiltrating lymphocytes [TIL] (A) and genetically engineered cells (B). (A) In TIL therapy a tumour is excised from a patient and TIL are cultured with interleukin-2 (IL-2) to promote activation and proliferation.  $>10^{10}$  cells are reinfused into the cancer patient following the administration of a conditioning lymphodepleting chemotherapy. (B) Engineered cell therapy involves the use of genetically modified high-affinity T-cell receptors (TCRs) or chimeric antigen-receptors (CARs). TCR gene therapy and CAR therapy aim to equip modified T-cells with a cancer-specific receptor. In TCR therapy gene sequences are transferred to the T-cell to encode new TCR $\alpha$  and TCR $\beta$  chains with a high affinity cancer antigen specificity. In CAR therapy an antibody derived single chain variable fragment, a transmembrane element and an intracellular signalling CD3 domain form a receptor complex which automatically activate a T-cell once the variable chain is bound with antigen. T-cells are harvested from the peripheral blood mononuclear cells (PBMC) of patients and undergo viral gene transfer to induce the expression of a specific cancer reactive TCR or CAR. After a brief selection and expansion period modified T-cells are reinfused back into the patient, following a lymphodepleting chemotherapy. The complexity of engineered T-cell therapy is the multi-step process involved in the manufacture and delivery of viral gene editing methods. Recent advances in TCR transfer in my laboratory (unpublished) may aid in making genetic engineering strategies easier. Figure adapted from (Phan and Rosenberg 2013; Fesnak et al. 2016).

### 1.7.1 Sensitizing tumour to $\gamma\delta$ T-cell killing

Tumours can be sensitized to killing by some  $\gamma\delta$  T-cells using pharmaceutical agents such as the aminobisphosphonates zoledronate, risedronate and pamidronate (Kondo et al. 2011). Such pharmacological agents have been shown to inhibit with the mevalonate pathway by blocking an enzyme downstream of IPP synthesis. This blocking of farnesyl pyrophosphate synthase ultimately results in an accumulation of IPP which makes cells targets for V $\gamma$ V $\delta$ 2 T-cells (Roelofs et al. 2009), and combination with cytokines such as IL-2 further increases  $\gamma\delta$  T-cell tumour cell lysis (Dieli et al. 2007).

Another example of sensitizing tumours to  $\gamma\delta$  T-cell recognition is the use of retinoic (Jinushi et al. 2003) or valproic acid (Wu et al. 2012b) to upregulate MICA/B on cancer cells. Treatment with valproic acid was shown to sensitize pancreatic cancer cells to natural killer cell mediated lysis via the NKG2D/MIC pathway (Shi et al. 2014). Benefits of this type of treatment lie in the use of FDA approved pharmacological agents. Drawbacks include only activating particular subsets of  $\gamma\delta$  T-cells.

### 1.7.2 $\gamma\delta$ T-cell based vaccines

Bernhard Moser's group showed that activated V $\gamma$ 9V $\delta$ 2 T-cells can act as very efficient APCs that rival dendritic cells for function but that are relatively easy to culture *in vitro*. These  $\gamma\delta$  APCs can present specific antigens via MHC or MHC-related molecules to induce primary CD4+ and CD8+



T-cell responses (Brandes et al. 2005; Brandes et al. 2009). CXCR5 expressing  $\gamma\delta$  T-cells can also recruit antibody-producing helper cells for example by the production of the inflammatory cytokines IL-4 and IL-10 (Caccamo et al. 2006). This antigen-presenting and immune orchestrating capacity may help to initiate subsequent tumour antigen-specific  $\alpha\beta$  T-cell responses (Himoudi et al. 2012) to give an enhanced anti-tumour therapy. Furthermore, as discussed by Khan *et al.*, the ease at which V $\gamma$ 9V $\delta$ 2 T-cells can be expanded into large numbers *in vitro* offers an innovative strategy for the development of  $\gamma\delta$  T-cell based vaccines (Khan et al. 2014). The benefits of this method is the activation of multiple cell types which may result in a more effective and robust anti-cancer immune response being elicited and the lack of MHC-restriction.

### 1.7.3 $\gamma\delta$ T-cell adoptive cell therapy

Research done in various laboratories, including my own, demonstrates the importance of  $\gamma\delta$  T-cells in the success of ACT. Significant proportions of  $\gamma\delta$  T-cells have been documented in the TIL products of breast cancer (Hidalgo et al. 2014), colorectal cancer (Galon et al. 2006) and melanoma (Legut *et al.*, unpublished). Importantly in each of these studies there is a correlation between higher numbers of  $\gamma\delta$  TIL and a better prognosis. Furthermore, it should be noted that a recent global analysis indicated that of all lymphocyte subsets present within 39 different cancer types (~18,000 individual human tumour samples) found that the presence of  $\gamma\delta$  T-cells was the strongest positive correlate of a favourable clinical outcome (Gentles et al. 2015).

Specifically isolating and using  $\gamma\delta$  T-cells for ACT has been trialled in over 10 studies involving patients with metastatic cancer. Importantly  $\gamma\delta$  T-cell ACT has been shown to be well tolerated, with mild adverse events such as fatigue and fever being (Kobayashi et al. 2007). Meta-analysis of these trials showed that ACT of V $\gamma$ 9V $\delta$ 2 T-cells improved overall survival rates without compromising on safety and that tumour-reactive  $\gamma\delta$  T-cells were found in the peripheral blood of complete remission patients (Buccheri et al. 2014). This is extremely significant as taking tumour reactive cells from peripheral blood is a less invasive, readily available option as a source of effector T-cells when tumour dissection is not possible.

A current drawback of the above methods for utilizing  $\gamma\delta$  T-cells for immunotherapy is that only a small quantity of tumour reactive  $\gamma\delta$  T-cells are found within a patient, and there is currently no established reliable method of expanding such cells. Importantly, binding affinities for robust pathogen-specific ligands of the  $\alpha\beta$  TCR fall in the  $K_D=0.1-10\ \mu\text{M}$  range whereas for self-cancer specific ligands this value is in the range of  $K_D= > 20\ \mu\text{M}$  [reviewed in (Aleksic et al. 2012). The

weak affinity of  $\alpha\beta$  TCRs for ligands has resulted in the need to develop high affinity options such as TCR and CAR therapy. The use of  $\gamma\delta$  TCRs, however, may avoid this issue if  $\gamma\delta$  TCRs are shown to have a much higher affinity for self-cancer ligands than  $\alpha\beta$  TCRs. For example, the affinity of the  $\gamma\delta$  T-cell expressed NKG2D receptor to the virus/cancer ligand hMSH2 is relatively high for receptor/ligand interactions ( $K_D = 0.132 \mu\text{M}$ ) (Dai et al. 2012). Similarly the affinity of the NKG2D receptor for MICA falls within a similar, high affinity range ( $K_D = 0.3\text{-}21 \mu\text{M}$ ) (Xu et al. 2011). The affinity of V $\delta$ 1 TCRs to CD1d presented lipid also ranges from  $K_D = 0.066\text{-}16 \mu\text{M}$  (Luoma et al. 2013; Uldrich et al. 2013; Pellicci et al. 2014). Specifically, the identification of a high affinity  $\gamma\delta$  TCR broadly reactive to cancer cells via recognition of a ubiquitous stress ligand would revolutionize the potential of  $\gamma\delta$  T-cells for use in immunotherapies.

#### 1.7.4 Using $\gamma\delta$ T-cells to identify stress ligands

My work focussed on the possibilities of using  $\gamma\delta$  T-cells for cancer immunotherapy. Using tumour reactive  $\gamma\delta$  T-cell clones it is possible to identify broadly expressed tumour stress antigens, for example in the cases of EPCR and annexin A2. Once a pan-cancer stress ligand has been identified it can either be targeted by already approved pharmacological agents, or new agents can be developed based on the  $\gamma\delta$  TCR being used in the study. Here, I present a compelling example of using a  $\gamma\delta$  T-cell clone that recognizes multiple tumours to identify a novel  $\gamma\delta$  T-cell stress ligand.

## 1.8 Aims and Objectives

It is generally acknowledged that  $\gamma\delta$  T-cells play a vital role in stress and cancer surveillance, predominantly via cognate TCR-ligand interactions. However, the exact identity of the cognate ligands and the molecular mechanisms of recognition remain poorly defined, especially as the rules learned from extensive  $\alpha\beta$  TCR recognition cannot be automatically applied to the  $\gamma\delta$  TCR. Furthermore, the identification and isolation of rare tumour reactive  $\gamma\delta$  T-cells from the peripheral blood remains a challenge.

$\gamma\delta$  T-cells that recognize stress ligands broadly expressed on cancer cells provide potential for pan-tumour, pan-population immunotherapy. Stress ligand reactive  $\gamma\delta$  T-cells have been shown to be  $V\delta 2^{\text{neg}}$  T-cells cross-reactive to virally infected and tumour cells. Therefore my work focussed on two research objectives:

1. Generating an optimized method for the procurement of rare viral and tumour reactive  $\gamma\delta$  T-cells from the peripheral blood of healthy donors (Chapter 3)
2. Using methodologies such as whole genome CRISPR (Chapter 4) and HLA mapping (Chapter 5) to identify novel ligands involved in tumour recognition by  $\gamma\delta$  T-cells.



## 2 Materials and Methods

### 2.1 Cell Culture

#### 2.1.1 Cell culture media and buffers

All reagents and buffers, with the exception of those supplied as part of commercial kits, used for cell culture are listed below (Table 2.1). All tissue culture plasticware used was sourced from VWR (Pennsylvania, US) and sterile pipette tips were supplied by Greiner Bio One (Kremsmunster, Austria). All buffers and media were sterile filtered through 0.22 µm filter using either syringes or stericup filter bottles (Merck, New Jersey, US), stored at 4°C and used within 30 days after preparation. All media reagents were purchased from Gibco (Paisley, UK) and chemicals from Sigma Aldrich (Missouri, USA), unless specified otherwise.

Cell lines (Table 2.2) were regularly screened for Mycoplasma infection (MycoAlert Kit, Lonza), following manufacturer's instruction. Cells were washed in serum free media (R0) and adherent cells were detached with D-PBS-EDTA (2 mM). R5 medium was used to rest T cells overnight and to perform most of the *in vitro* assays to eliminate spontaneous release of cytokines.

#### 2.1.2 Immortalised cell culture

Tumour cell lines and lymphoblastoid cell lines (LCLs) were cultured in D10 or R10 media. All LCLs were either created for this study (Section 2.1.3) or obtained from laboratory stocks. All tumour lines were acquired from collaborators or laboratory stocks. All cells were incubated at 37 °C in 5% CO<sub>2</sub> and were routinely passaged when confluency reached 70-80%.

#### 2.1.3 Lymphoblastoid cell line generation

LCLs were created from whole blood of either local donors or anonymised healthy buffy coats obtained from the Welsh Blood Service (WBS). Following isolation (Section 2.1.5), 10 million PBMCs were incubated with 1 mL of culture supernatant containing Epstein-Barr virus (EBV) (B95-8 strain, Advanced Biotechnologies) particles, as previously described (Adhikary et al. 2008; Hui-Yuen et al. 2011). To eradicate T-cells, 20 nM of Cyclosporin A (Life Technologies, Paisy, UK) was added along with the culture supernatant in a total of 2 mL R10 media. After two weeks incubation LCL generation was analysed using flow cytometry analysis, to confirm the purity of B-cells (Section 2.4) with an anti-CD19 antibody (Table 2.4).

**Table 2.1: The composition of cell culture media and buffers used throughout the thesis.**

<b>Media</b>	<b>Composition</b>
R0	RPMI 1640 supplemented with 100 U/mL penicillin, 100 µg/mL streptomycin and 2 mM L-glutamine
R5	R0 supplemented with 5% v/v heat-inactivated fetal bovine serum (FBS)
R10	R0 supplemented with 10% v/v FBS
D10/F12	DMEM/F12 supplemented with 100 U/mL penicillin, 100 µg/mL streptomycin and 1mM sodium pyruvate
T-cell priming media	R10 supplemented with 10 mM HEPES, 1 mM sodium pyruvate, 1X non-essential amino acids and 20 IU IL-2 (Proleukin, San Diego, US)
T-cell expansion media	T-cell priming media supplemented with 25 ng/µL IL-15 (Peprotech, Rocky Hill, US)
T-cell culture media	T-cell expansion media supplemented with 200 IU final IL-2
T-cell transduction media	T-cell culture media supplemented with 20% v/v final FBS
<b>Buffers and reagents</b>	
Freezing buffer	90% v/v FBS, 10% dimethyl sulfoxide (DMSO)
Red blood cell (RBC) lysis buffer	155 mM NH <sub>4</sub> Cl, 10 mM KHCO <sub>3</sub> , 0.1 mM EDTA (pH 7.2-7.4)
PBS-EDTA	PBS, 2 mM EDTA
FACS buffer	PBS, 2% v/v FBS
MACS buffer	D-PBS, 2 mM EDTA, 0.5% bovine serum albumin (BSA)
Fixing buffer	4% paraformaldehyde (PFA)
Wash buffer	0.05% Tween-20 in PBS
Reagent Diluent	1% BSA in PBS
Tris-EDTA (TE) buffer	10 mM Tris, 1 mM EDTA in ddH <sub>2</sub> O (pH=8.0)
Buffered water	2.5 mM HEPES in ddH <sub>2</sub> O (pH=7.3)
2XHEPES-buffered saline (HeBS)	0.28 M NaCl, 0.05 M HEPES, 1.5 mM Na <sub>2</sub> HPO <sub>4</sub> in ddH <sub>2</sub> O

**Table 2.2: Cell lines used throughout this thesis**

<i>Cell line</i>	<i>Origin</i>	<i>Culture method</i> <i>Media</i>
MM909.12,-15,-24,-46 Mel526, -624	Malignant melanoma	Adherent, R10
Caki-1	Kidney (carcinoma)	Adherent, D10
HEK 293T	Kidney (embryonic)	Adherent, D10
Colo205, HCT116	Colon (carcinoma)	Adherent, D10
MCF7, MDA-MB231, SKBR3	Breast (adenocarcinoma)	Adherent, R10
Molt3, Jurkat	T-cell (leukaemia)	Suspension, R10
KBM7, K562	Chronic myelogenous leukaemia (CML)	Suspension, R10
THP-1	Acute monocytic leukaemia	Suspension, R10
T2, C1R	Lymphoblast	Suspension, R10
LCL: 0439,Pt146,HOM2,174,5959, 7729, 866x,AP,CH,BB67,D14, D480, MH, MO FB117,-446,-449,-464,-467,-469,- 577,-578,-579,	B-cell lymphoblastoid	Suspension, R10
U266	Multiple myeloma	Suspension, R10
A549	Lung (carcinoma)	Adherent, R10
LnCAP	Prostate (carcinoma)	Adherent, D10
SIHA, MS751	Cervix (carcinoma)	Adherent, D10
TK143, U2OS	Bone (osteosarcoma)	Adherent, D10
Hep2	Normal hepatocyte	Adherent, HCM
SM3	Normal smooth muscle	Adherent, SMCM
CIL1	Normal ciliary epithelium	Adherent, EpiCM
MRC5	Normal fibroblast	Adherent, D10

#### 2.1.4 Primary T-cell culture: maintenance and expansion

Primary T-cells were either obtained from the PBMCs of WBS buffy coats or local donors. Two local donors (0439 and 9909) and one WBS buffy coat (BB67) were used throughout this thesis. T-cells were cultured in T-cell culture media and incubated at 37 °C in 5% CO<sub>2</sub> in a 48 or 24 multi-well plate at densities of 1-2x10<sup>6</sup> or 4-6x10<sup>6</sup> T-cells per well, respectively. Every 2-4 weeks T-cells were subjected to an expansion protocol to ensure optimum activity. During T-cell expansions 1x10<sup>6</sup> T-cells were incubated with 1.5x10<sup>7</sup> 'feeders' (an equimolar mix of irradiated PBMCs from three different donors) in 15 mL of T-cell expansion media with 1 µg/mL of phytohaemagglutinin (Sigma Aldrich) for 7 days in a T25 flask tilted at a 45° angle, before being transferred into T-cell culture media and seeded on 48/24 multi-well plates.

#### 2.1.5 PBMC Isolation

PBMCs were obtained from WBS buffy coats in accordance with appropriate ethical approval. Samples were confirmed seronegative for HIV-1, HBV and CMV. PBMCs were isolated from whole blood using Lymphoprep™ (Stemcell Technologies, Vancouver, Canada) density gradient centrifugation. Up to 50 mL of concentrated whole blood was layered over 130 mL of Lymphoprep™ across three 50 mL falcon tubes. Samples were centrifuged at 900 g for 20 min without braking at room temperature. Using a sterile Pasteur pipette the mononuclear interface layer was removed, transferred into a new 50 mL tube and washed in R10 (700 g for 10 min). The pellet was resuspended in 25 mL red blood cell lysis buffer and incubated at 37 °C for 10 min. A further wash was performed at 200 g for 10 min to remove platelets. PBMCs were finally re-suspended in R10 medium, counted and kept at 4 °C until further processing. PBMCs to be used as feeders were γ irradiated with a dosage of 3000 Gy (Gammacell 1000 elite, Nordion International Industries) before use.

#### 2.1.6 Cloning by limiting dilution

T-cell clones were procured from polyclonal T-cell lines by limiting dilution. Briefly, 0.5 T-cells/well were plated in a 96 U-bottom multi-well plate and subjected to the T-cell expansion protocol using 50,000 feeders/well. At least 10 cloning plates were set up for each polyclonal T-cell line. After 14 days culturing wells were tested by FACS based phenotyping for clonality and were subjected to functional assays. Clonality was confirmed by TCR sequencing.

#### 2.1.7 Human cytomegalovirus infection

Human cytomegalovirus (hCMV) Merlin-GFP strain was used to infect MRC5 fibroblasts. CMV infections were kindly carried out by Dr. Ceri Fielding, Cardiff University. Briefly 250,000 target cells were plated in a 48 multi-well plate in 1 mL total culture media and left to attach overnight.



On the day of infection cell media was replaced with 500  $\mu$ L fresh media and 500  $\mu$ L concentrated Merlin-GFP strain hCMV virus. Cells were rocked at 10 RPM in an incubator for 3 days and then tested for viral uptake using a microscopy to visualize green fluorescent protein (GFP) expression. Cells exhibiting over 90% infection were used for studies in this thesis. Alongside hCMV infection 'mock' infected fibroblasts were set up, which underwent the same treatment as the hCMV infected cells.

#### 2.1.8 Cell counting

Equal quantities of single cell suspensions and Trypan Blue 0.4 % Solution (Sigma-Aldrich) were mixed. 10  $\mu$ L of this mixture was loaded onto a haemocytometer and live cells were counted based on trypan blue exclusion according to the following formula: (number of cells in one section of 16 squares) x (trypan blue dilution factor)  $\times 10^4$  = number cells/ mL. All cells that were counted were first washed (via centrifugation at 500 g for 5 min) and re-suspended in fresh medium.

#### 2.1.9 Cyro-preservation and thawing of cell lines

Cells were centrifuged at 500 g for 5 min to remove culture media, and resuspended in 500  $\mu$ L of freezing buffer. Cells were frozen in internal thread cryovials (Nunc) at  $-80^{\circ}\text{C}$  using a controlled-rate freezing device (CoolCell, Biocision) following manufacturer's instructions, and transferred to liquid nitrogen for long term storage. For defrosting, vials of cryopreserved cells were removed from liquid nitrogen and thawed at  $37^{\circ}\text{C}$ . Immediately upon thawing cells were washed with 10 mL pre-warmed R10 medium. Cells were centrifuged at 500 g for 5 min and resuspended in the appropriate medium prior to counting and transfer to culture flasks or plates.

#### 2.1.10 HLA typing

HLA typing of cells was performed either by Pure Transplant Solutions, LLC (Oklahoma) or Welsh Transplantation and Immunogenetics Laboratory (UK).

### 2.2 Magnetic cell sorting

#### 2.2.1 Surface marker separation

$\text{CD4}^{+}$  and  $\text{CD8}^{+}$  T-cell subsets were isolated from freshly prepared or defrosted PBMC using  $\text{CD4}$  or  $\text{CD8}$  MicroBeads, respectively (all Miltenyi Biotech). TCR  $\gamma/\delta^{+}$  T-cell and anti- $\delta 2$  TCR isolation kit (MACS Miltenyi Biotech, Surrey, UK) were used, according to manufacturer's protocol, to generate T-cell lines enriched for  $\text{V}\delta 2^{\text{neg}}$  T-cells. Briefly 100 million PBMCs were isolated from donors, washed with MACS buffer and then resuspended in 80  $\mu$ L MACS buffer and 20  $\mu$ L Microbeads per  $10^7$  cells. Cells and beads were mixed gently and incubated at  $4^{\circ}\text{C}$  for 15 min.

Following a further wash the cells were applied onto an MS or LS column (depending on cell number). MACS buffer was kept at 4°C at all times, and centrifugation carried out at 4°C to prevent bead internalisation. Potential cell clumps were removed by passing the cell suspension through a 0.4 µm filter. Cells transduced with a particular gene of interest also co-expressed rat CD2 (rCD2) as a marker that allowed magnetic selection of transduced cells by staining with a PE-conjugated anti-rCD2 antibody for 20 min on ice prior to co-incubation with anti-PE MicroBeads (Miltenyi Biotec).

### 2.2.2 TNF/IFN $\gamma$ magnetic pullout

TNF $\alpha$ /IFN $\gamma$  magnetic pullout was used to enrich activated T-cells from polyclonal lines, according to manufacturer's instructions (TNF $\alpha$ /IFN $\gamma$  Secretion Assays, Miltenyi Biotec). Briefly, one day prior to separation T-cells were washed with R0 before being plated in R5 (to minimise spontaneous cytokine release). The following day T-cells were co-incubated with target cells at effector (E) to target (T) ratio of 1:1 for 4 h before being harvested and washed in MACS buffer. Following resuspension in MACS buffer, cells were labelled with IFN $\gamma$  and TNF Catch Reagents (all reagents from Miltenyi Biotec) for 5 min on ice before being diluted in warm R5 media and incubated at 37°C for 45 min under slow continuous rotation. Cells were washed before being incubated with PE-conjugated IFN $\gamma$ /TNF $\alpha$  detection antibodies for 10 min on ice. Cells were washed before being a labelled with anti-PE MicroBeads for 15 min at 4°C followed by washing and application to a magnetic separation column. On the following day the isolated T-cells were either expanded as line or cloned by limiting dilution (Section 2.1.6). MACS buffer was kept at 4°C at all times, and centrifugation carried out at 4°C to prevent cells internalising the beads.

## 2.3 Lentiviral transductions

### 2.3.1 Lentivirus production

HEK-293T cells were transfected using CaCl<sub>2</sub> to create lentivirus particles (Jordan and Wurm 2004). Prior to transfection 2x10<sup>7</sup> HEK-293T cells (ATCC® CRL-1573) were plated in a T175 flask in 50 mL D10 medium and incubated overnight in routine cell culture conditions until cells were 80% confluent. Lentivirus particles were generated using either a 2<sup>nd</sup> or 3<sup>rd</sup> generation plasmid system at the appropriate quantities (Table 2.3). The 2<sup>nd</sup> generation transfer plasmid pLentiCRISPR v2 (kindly provided by Dr. Feng Zhang, Addgene, plasmid #52961) was co-transfected with packaging plasmid psPAX2 (addgene plasmid #12260) and envelope plasmid pMD2.G (Addgene, plasmid #12259). The 3<sup>rd</sup> generation transfer plasmid pELNS (kindly provided by Dr. James Riley, University of Pennsylvania, US) was co-transfected with packaging plasmids pRSV-Rev (Addgene plasmid #12253) and pMDLg/pRRE (Addgene plasmid #12251), and

envelope plasmid pMD2.G. The quantities of plasmids used for transfection are listed in Table 3. The cloning of constructs into plasmids are outlined in Section 2.7.

Plasmids were prepared in up to 250  $\mu$ L TE buffer before adding 1 mL of HEPES buffered water. 125  $\mu$ L of 2.5 M CaCl<sub>2</sub> was added and thoroughly mixed before 1.375 mL of Hepes buffered saline was added in dropwise fashion whilst being vortexed. The transfection mixture was left at room temperature for 15-20 min to precipitate before being added to the HEK-293T cells in a dropwise fashion. After overnight incubation in normal cell culture conditions fresh D10 media was applied to the cells. Supernatant was collected at 24 and 48 h, pooled, and filtered through a 0.45  $\mu$ m filter. The supernatant was ultra-centrifuged (150,000 g, 2 h, 4°C) using an Optima L-100XP ultracentrifuge (Beckman Coulter, California, USA) in sterile polyallomer ultracentrifuge tubes (Beckham Coulter) to produce a lentiviral pellet. The medium was discarded and the lentiviral pellet resuspended in up to 1 mL of media, snap frozen, and stored at -80 °C until use. When thawing lenti-virus was thawed as slow as possible (usually at 4 °C in a fridge overnight).

**Table 2.3: Plasmids used for production of 2<sup>nd</sup> and 3<sup>rd</sup> generation lentiviruses**

<i>Transfer plasmid</i>	<i>Envelope plasmid</i>	<i>Packaging plasmids</i>
pLentiCRISPR v2 (16 $\mu$ g)	pMRD.G (8 $\mu$ g)	psPAX2 (12 $\mu$ g)
pELNS (15 $\mu$ g)	pMRD.G (7 $\mu$ g)	pMDLg/pRRE (18 $\mu$ g) pRSVRev (18 $\mu$ g)

Numbers in brackets indicate the quantity of each plasmid to be added.

### 2.3.2 Lentiviral transduction of immortalised cell lines

Prior to lentiviral transduction 0.5 X10<sup>6</sup> cells were plated in a 48 well plate in 1 mL total media. On the day of transduction half the media was removed and replaced with 500  $\mu$ L of media containing concentrated virus together with 8  $\mu$ g/mL polybrene (Santa Cruz Biotechnology) before being spininfected at 500 g for 2 h. The addition of polybrene increases gene transfer efficient by enhancing virus adsorption on target cell membranes (Davis et al. 2002). Following overnight incubation at 37 °C the lenti-virus containing media was replaced with fresh media.

### 2.3.3 Lentiviral transduction of primary T-cells

Primary T-cells were freshly isolated from PBMC using CD4 and CD8 MicroBeads (**Section 1.5;2.1**) and were plated at  $0.5 \times 10^6$  cells/well in 1 mL T-cell culture media. Cells were activated overnight with anti-CD3/CD28 human T-cell activator Dynabeads (Invitrogen) at a bead to cell ratio of 3:1 to maximise cell viability and proliferation (Neurauter et al. 2007). The following day 900  $\mu$ L of media was removed from the wells, to be replaced with 400  $\mu$ L media containing lentivirus. Polybrene was added at 5  $\mu$ g/mL final concentration. On the following day 500  $\mu$ L T-cell transfection media was added to each well, and was subsequently replaced three times weekly for 14 days post transduction. Transduced T-cells underwent selection before being expanded with allogeneic feeder and PHA (Section 2.1.4).

### 2.3.4 Selection of transduced cells

Cells transduced with the pLentiCRISPR v2 plasmid were subjected to puromycin selection from 3 days post lentiviral transduction at an optimised concentration determined by performing antibiotic titrations. Generally, cell lines were subjected to 1  $\mu$ g/mL puromycin treatment for 7 days to eradicate cells that were not successfully transduced. Cells could be checked for down-regulation of the gene of interest after day 10. Cells transduced with pELNS vector containing the rCD2 marker were either subjected to magnetic sorting (Section 2.2) or FACS based sorting (Section 2.4).

## 2.4 Flow cytometry

Generally, unless otherwise stated, the following protocol was used for cell staining and flow cytometry. 20,000-50,000 cells were stained in a FACS tube or U-bottom 96 well plate. All centrifugation steps were conducted at 700 g for 3 min. Following two washes in PBS (to remove residual proteins from the media) cells were stained in the dark with LIVE/DEAD® Fixable Violet Dead Stain Kit (Thermo Fisher; referred to as Vivid from hereon) for 5 min at room temperature. Without washing primary fluorochrome-conjugated- or unconjugated antibodies were added at a desired concentration according to manufacturer's protocol (Table 2.4) followed by 20 min incubation on ice in the dark. Cells were then washed twice in FACS buffer and were either ready for analysis (in the case of those stained with fluorochrome-conjugated antibodies) or were further stained with a fluorochrome-conjugated secondary antibody for 20 min on ice. Subsequently, the cells were washed twice and, if required, incubated in fixing buffer for 20 mins on ice, followed by two washes with FACS buffer before being analysed. Live cells were sorted by Dr Catherine Nyserian, Cardiff Biotechnology Services, and collected into either R10 for culturing or lysis buffer for DNA/RNA extraction using FACS ARIA.

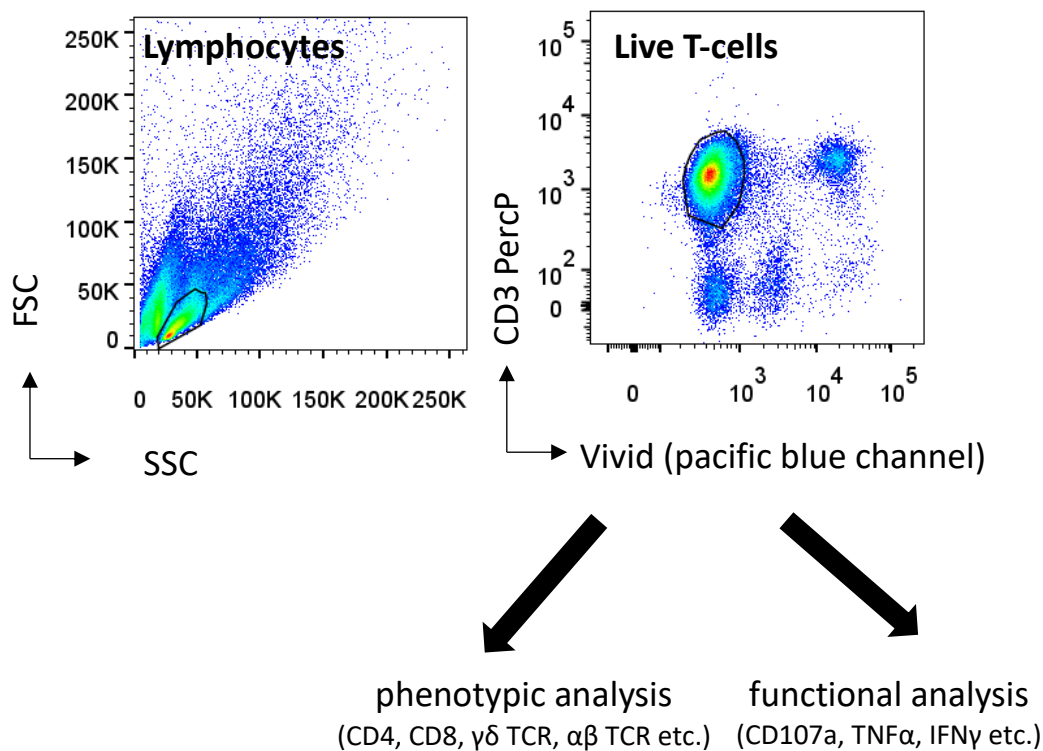
**Table 2.4: Antibodies used for flow cytometry staining**

<b>Antibody Target</b>	<b>Clone</b>	<b>Fluorochrome(s)</b>	<b>Manufacturer</b>
(Rat) CD2	OX-34	FITC, PE	Biologend
CD107a	H4A3	PE	Biologend
CD19	HIB19	Pacific Blue, PE	Miltenyi Biotech
CD3	BW264/56	PerCP	Miltenyi Biotech
CD4	M-T466	PE, PE-Vio770, APC, APC-Vio770	Miltenyi Biotech
CD8	BW135/80	PE, PE-Vio770, APC, APC-Vio770	Miltenyi Biotech
V $\delta$ 1 TCR	REA173	FITC	Miltenyi Biotech
V $\delta$ 2 TCR	123R3	FITC, PE	Miltenyi Biotech
Donkey anti-rabbit	Polyclonal	PE	Thermo
Goat anti-mouse	Polyclonal	PE, APC, FITC	Abcam
HLA ABC	W6/32	PE	Biologend
HLA DR,DP,DQ	Tu39	Unconjugated	Biologend
HLA DR	L243	PE	Biologend
IFN $\gamma$	45-15	APC	Miltenyi Biotech
Mouse Ig	Polyclonal	PE	BD Biosciences
Pan- $\alpha\beta$ TCR	BW242/41 2	FITC, PE	Miltenyi Biotech
Pan- $\gamma\delta$ TCR	11F2	FITC, APC	Miltenyi Biotech
PE	PE001	Unconjugated	Biologend
SCNN1A	Polyclonal	Unconjugated	Thermo
TNF $\alpha$	cA2	PE-Vio77	Miltenyi Biotech

#### 2.4.1 Flow cytometry analysis

Samples were acquired on a BD FACSCanto II flow cytometer using FACSDiva software (both BD Dickinson). Data analysis was performed on FlowJo version 7.6.4 (TreeStar Inc, US). Anti-mouse IgG antibody capture beads (BD Biosciences) were used to prepare individual compensation tubes for each monoclonal antibody used in experiments.

Cells were gated using a typical lymphocyte gate based on forward and side scatters, followed by exclusion of dead cells (Vivid<sup>neg</sup>). T-cells were then gated based on expression of the surface marker CD3. All gates were set based on appropriate biological and fluorescence minus one controls. Typically, at least 1,000 live events were acquired per clonal population and 10,000 per polyclonal sample. A representative gating strategy is shown in Figure 2.1.



**Figure 2.1: Gating strategy for FACS phenotypic and/or functional analysis of T-cells.** Cells were first gated on characteristic forward scatter (FSC) and side scatter (SSC) and displayed as Vivid versus CD3. Viable (Vivid<sup>neg</sup>) T-cells (CD3<sup>+</sup>) cells were gated and then further displayed to analyse phenotypic or functional markers. Representative plots for T-cells co-incubated with B-cells.

#### 2.4.2 pMHC tetramer staining

Biotinylated peptide-MHC (pMHC) monomers, produced in house, were assembled by co-incubation with streptavidin-PE (Biolegend) at the molar ratio of 4:1 (pMHC to streptavidin) in five separate steps interspersed with 20 min on ice as previously described (Dolton et al. 2015). For staining, cells were washed with FACS buffer before being resuspended in 50  $\mu$ L of FACS buffer with 50  $\mu$ L of 100 nM protein kinase inhibitor (PKI; Dasatinib, Axon Medchem, Reston) for incubation at 37 °C for 30 min. PKI prevents signal transduction that would result from TCR engagement, and subsequent TCR-pMHC internalisation (Lissina et al. 2009). Without washing, 0.5  $\mu$ g (with respect to pMHC concentration) tetramer was added to cells for incubation on ice for 30 min. The cells were then washed twice with PBS prior to staining with Vivid, primary fluorochrome-conjugated antibody staining and/or secondary anti-PE antibody staining. After 20 min incubation on ice the cells were washed twice in FACS buffer and acquired on FACS Canto II. Appropriate biological controls, including fluorescence minus one and irrelevant tetramers, were used. This ‘boosted’ protocol enhances tetramer staining intensity and was developed in my laboratory (Dolton et al. 2015).

## 2.5 Functional T-cell assays

Generally, T-cells were used for functional assays either immediately from isolation or at least 14 days after expansion, to ensure cells were at their optimum reactivity (San Jose et al. 2000). Initially CFSE and intra-cellular staining (ICS) assays were used, however my laboratory used a TNF $\alpha$  processing inhibitor (TAPI)-0 based assay, which was adopted half way through my studies. The benefit of TAPI-0 activation assays over ICS was that cells remained viable allowing sorting and culturing of lines or clones (Haney et al. 2011).

### 2.5.1 T-cell proliferation assay

The CellTrace™ CFSE kit (ThermoFisher) was used to monitor distinct generations of proliferating cells by dye dilution, according to manufacturer's protocol. Briefly, PBMC were acquired from local donors or laboratory stocks and washed twice in R0 medium to remove residual proteins. All work was carried out as quickly as possible and in the dark, as CFSE is very sensitive to light. Up to  $1 \times 10^6$  PBMCs were resuspended in 25 mL R0 media and CFSE was added to a final concentration of 2  $\mu$ M and incubated at 37 °C for 10 min in the dark after mixing. Following incubation, 10 mL of FBS was added to quench excess CFSE, then cells were washed and resuspended in T-cell priming media for target cell co-incubation at an E:T ratio of 4:1. Cells were shielded from the light during a 14 day co-incubation period by loosely wrapping the cell culture plate in foil in the incubator. Following 14 days co-incubation cells were phenotypically assessed by flow cytometry to analysed proliferating (CFSE<sup>low</sup>) populations.

### 2.5.2 Intracellular-cytokine staining (ICS)

ICS was used to detect and characterise the functional reactivity of T-cell clones and lines against a range of targets. T-cells were rested overnight in R5 media to minimise spontaneous cytokine release. On the day of assay, T-cells were washed twice in R0 before being added to target cells at an E:T of 1:1, together with protein transport inhibitors brefeldin A and monensin (GolgiPlug™, and GolgiStop™, respectively; BD Biosciences) and anti-CD107a antibody. The protein transport inhibitors stopped cytokines from being released from the T-cells, and kept them internalised so they could be stained later in the protocol (O'Neil-Andersen and Lawrence 2002). CD107a is a lysosomal membrane protein that is transiently expressed at the T-cell surface as secretory lysosomes called lytic granules are released (Zaritskaya et al. 2010). Addition of anti-CD107a antibody at the start of the protocol ensures CD107a is stained before it is recycled into the cell. CD107a staining thereby serves as a marker of cellular degranulation (Betts et al. 2003). Following 4 h (for T-cell clones) and up to 6 h (for T-cell lines) co-incubation with target cells, samples were washed with PBS and stained with Vivid and surface antibodies before being fixed and permeabilised using Cytofix/Cytoperm™ reagent (BD Biosciences)

according to manufacturer's instructions. Following permeabilisation the cells were stained intracellularly with anti-cytokine antibodies such as anti-TNF $\alpha$  and anti-IFN $\gamma$  for 20 min on ice before being washed in FACS buffer and acquired on the FACS Canto II. Typically, at least 1,000 and 10,000 live CD3<sup>+</sup> events were acquired for monoclonal and polyclonal T-cell populations, respectively, using the same gating strategy as described in Section 2.4. PHA stimulation was used as a biological positive control, and negative controls included T-cells alone and target cells alone.

### 2.5.3 TAPI-0 activation assay

A downside of ICS is that cells are permeabilised and fixed so they are not viable. The TAPI-0 protocol was developed to keep activated T-cells intact so they could be used for cell sorting experiments. TAPI-0 is a selective inhibitor of TNF $\alpha$  converting enzyme, thus inhibiting the cleavage of TNF $\alpha$  from the plasma membrane (Balakrishnan et al. 2006). TNF $\alpha$ /TAPI-0 staining was used in conjunction with CD107a as markers of T-cell activation. As in the case of ICS, T-cells were rested overnight in R5 medium followed by co-incubation with target cells at E:T of 1:1 in a 96 U-bottom well plate. At the start of the co-incubation, anti-CD107a and anti-TNF $\alpha$  antibodies were added to the well, together with 30  $\mu$ M TAPI-0 (Sigma Aldrich). Following 4 h co-incubation (for monoclonal T-cells) and up to 6 h (polyclonal T-cell lines) cells were washed with PBS before Vivid and conjugated-antibody surface staining, and subsequent acquisition on FACS Canto II. Typically, at least 1,000 and 10,000 live CD3<sup>+</sup> events were acquired for monoclonal and polyclonal T-cell populations, respectively, using the same gating strategy as described in Section 2.4. PHA stimulation was used as a biological positive control, and negative controls included T-cells alone and target cells alone. Cells prepared with this protocol could be live sorted on FACS Aria for cell culture, RNA extraction and TCR clonotyping.

### 2.5.4 Long term FACS based killing assay

Long term killing assays were used as a methodology to detect target cell killing by T-cells. This method could be used for up to 3 day's co-incubation. Target cells were plated at 10,000 cells/well either on their own (to serve as 100% survival control) or with 10,000 T-cells in a total volume of 100  $\mu$ L priming or R5 medium. Triplicates for each condition were set up. Following 1-3 days co-incubation, target cell lines were harvested and counted on FACS Canto II to assess T-cell killing. Importantly as an internal control CountBright™ Absolute Counting Beads (Life Technologies) were added to each well prior to harvesting/washing (1,000-10,000 beads/well). Target cells and/or T-cells were stained to distinguish between different cell populations and to gate on the target cells depending on the availability of antibodies. The samples were then acquired on FACS Canto II, following Vivid and surface staining. Acquisition of each sample was



standardised based on the number of beads acquired. The representative gating strategy is shown in Figure 2.2. The survival of target cells was calculated according to the following formula:

$$\%survival = \frac{\text{number of experimental cell events/number of experiment bead events}}{\text{number of control cell events/number of control bead events}} \times 100\%$$

Survival of target cells was used to calculate the killing of target cells, which was displayed graphically as an average over the triplicates.

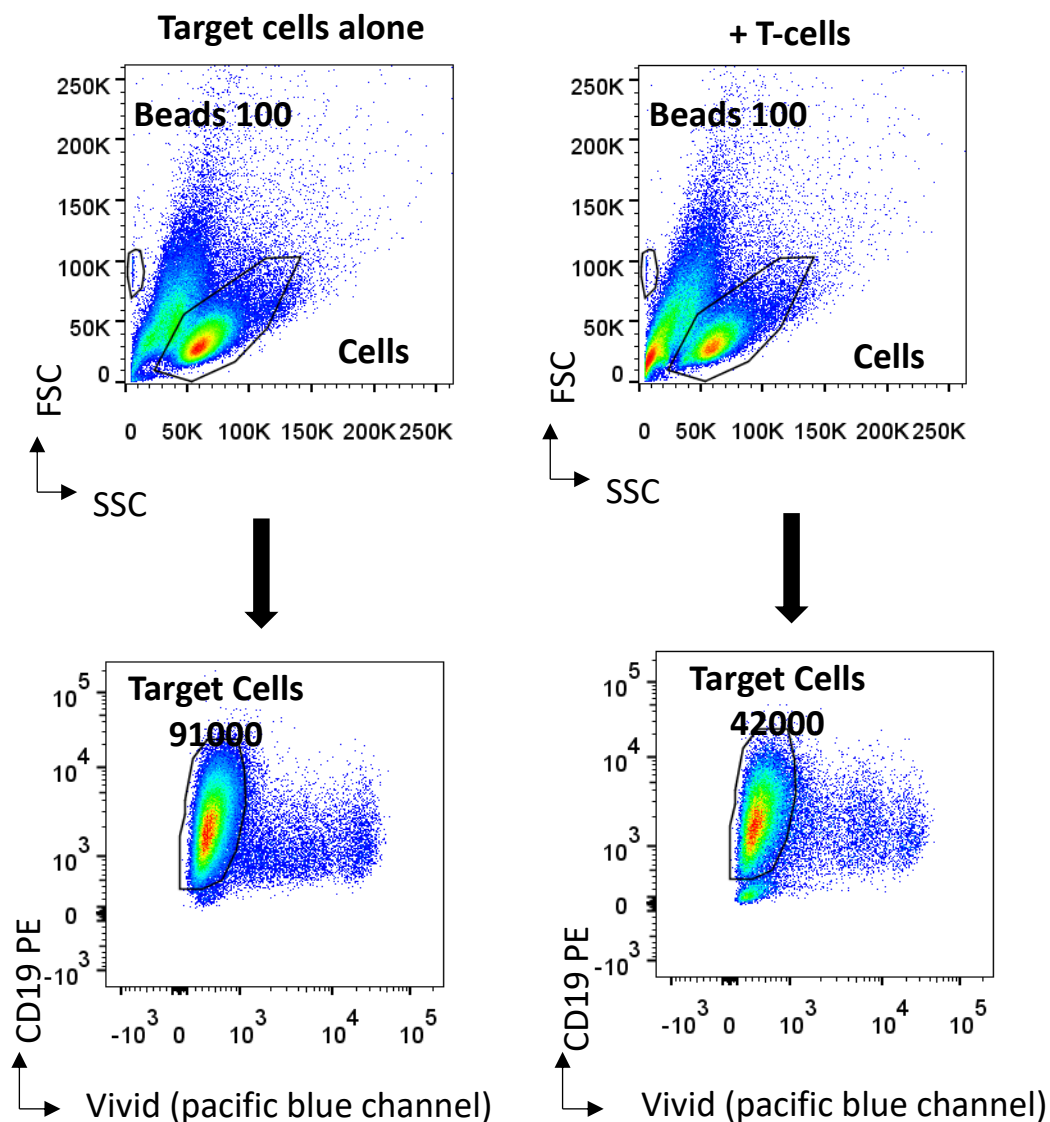
#### 2.5.5 Chromium release (<sup>51</sup>CR) killing assay

Target cells were labelled with 30 µCi <sup>51</sup>Cr (sodium chromate; Perkin Elmer, Waltham, MA) per 1X10<sup>6</sup> cells. After labelling with chromium, target cells were plated in 96 U-bottom well plates at a density of 2,000 cells per well. T-cells were added at a desired E:T and were co-incubated for up to 18 h. Controls were created by incubating target cells either in media alone or with 1% Triton to determine the spontaneous and maximum <sup>51</sup>CR release, respectively. Following co-incubation, 15 µL of the supernatant was harvested and mixed with 150 µL of Optiphase Supermix (Perkin Elmer). The amount of chromium was measured indirectly on a 1450 Microbeta counter (Perkin Elmer). Cytotoxicity was calculated according to the below formula:

$$\%lysis = \frac{\text{experimental } ^{51}\text{Cr release} - \text{spontaneous } ^{51}\text{Cr release}}{\text{total } ^{51}\text{Cr release} - \text{spontaneous } ^{51}\text{Cr release}} \times 100\%$$

#### 2.5.6 Antibody blocking assays

HLA-restriction of T-cell mediated killing was achieved by pre-incubating target cells with HLA specific antibodies for 1 h at 37 °C before the addition of effector cells. The following monoclonal antibodies were used for blocking assays: anti-HLA, B, C (clone W6/32, Biolegend), anti-HLADR, DP, DQ (clone Tu39, Biolegend), anti-EPCR (polyclonal, R&D systems), anti-MICA/MICB (clone 6D4, Biolegend), anti-CD1d (clone 51.1, Miltenyi Biotec) and anti-SCNN1A (polyclonal, Thermo) at a final concentration of 10 µg/mL, unless otherwise stated.



**Figure 2.2: Gating strategy and analysis of long-term killing assays.** In long term killing assays target cells were co-incubated with T-cells for up to 3 days. Prior to FACS analysis the same quantity of control beads were added to each sample. Acquisition of each sample was standardised to the number of beads. Cells were first gated on forward scatter (FSC) and side scatter (SSC) and displayed as Vivid versus CD19 (or CD3). The number of surviving target cells was measured by gating on CD19<sup>+</sup> cells (if B-cells were used as the target cells), or CD3<sup>neg</sup> (if tumour cells were used as target cells). Representative plot of target B-cell line + and – T-cells. The % survival of target cells was calculated as described in the main text, which was used to work out % T-cell killing. Number of cells in each gate is shown.

### 2.5.7 Enzyme-Linked ImmunoSpot (ELISpot)

In instances when T- cell number was limited, IFN $\gamma$  ELISpot was used to screen T-cell reactivity to target cell lines. T-cells were washed in R0 and rested in R5 overnight before co-incubation with target cells. MultiScreen™ 96-well plates (EMD Millipore) were coated with 50  $\mu$ L of 10  $\mu$ g/mL mouse anti-human IFN $\gamma$  capture antibody (mAB 1-D1K, MabTech) at 4 °C for 18 h. The plate was washed four times with 200  $\mu$ L PBS and blocked with 200  $\mu$ L R10 at room temperature for 1 h. As few as 2,000 T-cells were co-incubated with up to 30,000 target cells following blocking for 18 h at 37 °C in a total of 100  $\mu$ L R0 media. After washing four times with PBS, and incubated with 150  $\mu$ L ddH $_2$ O for 10 min at room temperature followed by a further wash with PBS. 50  $\mu$ L of 1  $\mu$ g/mL biotinylated anti-IFN $\gamma$  antibody (mAB7-B6-1, Mabtech) was added to each well and incubated for 2 h at room temperature followed by four further washes with PBS. Finally, 50  $\mu$ L of streptavidin-alkaline phosphatase was added to each well and incubated at room temperature for 2 h in the dark followed by four washes with PBS and incubation with 50  $\mu$ L of detection reagent (Alkaline Phosphatase Conjugate Substrate Kit, Bio-Rad). Once the sports were developed the reaction was stopped by washing the plate several times with tap water and the plate was dried overnight. Spots were imaged and counted using the ImmunoSpot® S6 Analyser.

## 2.6 TCR sequencing and clonotyping

With assistance from Dr. Mereim Attaf and PhD student Cristina Rius-Rafael from my laboratory, TCR sequencing and clonotyping experiments were carried out on  $\gamma\delta$  T-cell lines and clones described in this thesis as follows. All primers used for PCR and sequencing are listed in Appendix Table 8.1.

### 2.6.1 Total RNA extraction

RNA from  $\gamma\delta$  T-cell clones and lines was extracted using the RNeasy Micro Kit (Qiagen), according to manufacturer's protocol. Briefly, samples were lysed and homogenised before ethanol was added to provide ideal binding conditions. The lysates were loaded onto an RNeasy silica membrane, to which RNA binds whilst contaminants are efficiently washed away. Pure, concentrated RNA were eluted in 14  $\mu$ L water. To minimize the loss of RNA, extraction was carried out shortly after cell sorting and standard RNA handling precautions (such as filter tips and RNA free reagents) were used. All RNA isolation, cDNA synthesis and PCR preparation steps were carried out in a clean RNase free room to prevent contamination. RNA samples were stored at -80 °C.

## 2.6.2 SMARTer RACE cDNA amplification

SMARTer™ (Switching Mechanism At 5' end of RNA Transcript) RACE (Rapid Amplification of cDNA Ends) kit (Clontech) was used for the generation of full-length cDNAs from TCR- $\gamma$  and TCR- $\delta$  RNA according to manufacturer's instructions. Samples and reagents were kept on ice at all times and RNA samples were thawed at room temperature.

### 2.6.2.1 First strand cDNA synthesis

The following mix was prepared for each sample:

<b>Reagent</b>	<b>Amount</b>
RNA	10 $\mu$ L
Oligo-dT	1 $\mu$ L
Final volume	11 $\mu$ L

In a thermos cycler the reaction tubes were incubated at 72 °C for 3 min, then at 42 °C for 2 min to anneal the oligo-dT, which binds to poly(A) tail of mRNA. 8  $\mu$ L of the following master mix was then added to each sample:

<b>Reagent</b>	<b>Amount</b>
5X First Strand buffer	4 $\mu$ L
DTT (100 mM)	0.5 $\mu$ L
dNTP (20 mM)	1 $\mu$ L
RNase inhibitor (20 U)	0.5 $\mu$ L
SMARTScribe RT (100 U)	2 $\mu$ L
Final volume	8 $\mu$ L

The SMARTScribe reverse transcriptase adds non-template residues to the first strand of cDNA as it reaches the end of mRNA transcript. 1  $\mu$ L of SMARTer II oligo A was added to each tube, which annealed to the non-template residues on cDNA to act as a template for the extension of cDNA. Thus generated cDNA molecules contain a universal anchor at the 3' end. In a thermos cycler the tubes were incubated at 42 °C for 90 min, then at 70 °C for 10 min. cDNA samples were directly stored at -20 °C or used immediately for the following PCR amplifications step.

#### 2.6.2.2 PCR amplification

PCR was designed to capture the whole variable region of the TCR $\gamma$  or  $\delta$  chain by using a set of forward primers binding to the universal anchor on every cDNA molecule, and a set of gene specific reverse primers binding to the constant regions of the TCR, thus allowing unbiased amplification of the TCRs in the sample, regardless of the variable region. Template controls were set up alongside the samples to test for the presence of contaminations.

The composition of the 1<sup>st</sup> PCR reaction for TCR cDNA amplification were as follows:

<b>Reagent</b>	<b>Amount</b>
Phusion® 5X green buffer	10 $\mu$ L
DMSO (100 mM)	0.5 $\mu$ L
dNTPs (20 mM)	1 $\mu$ L
10x universal primer A (F)	5 $\mu$ L
Gene specific primer (R) (10 $\mu$ M)	1 $\mu$ L
Phusion® HF DNA polymerase	0.5 $\mu$ L
Nuclease free H <sub>2</sub> O	30 $\mu$ L
cDNA template	2 $\mu$ L
Final volume	50 $\mu$ L

The composition of the 2<sup>nd</sup> PCR reaction for TCR cDNA amplification were as follows:

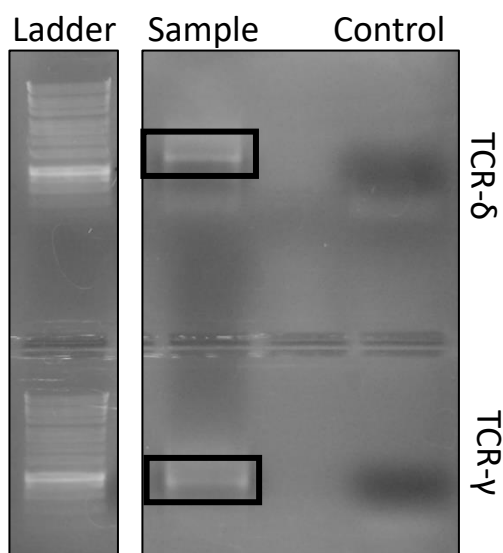
<b>Reagent</b>	<b>Amount</b>
Phusion® 5X HF buffer	10 $\mu$ L
DMSO (100 mM)	0.5 $\mu$ L
dNTPs (20 mM)	1 $\mu$ L
10x short universal primer (F)	1 $\mu$ L
Gene specific primer (R) (10 $\mu$ M)	1 $\mu$ L
Phusion® HF DNA polymerase	0.5 $\mu$ L
Nuclease free H <sub>2</sub> O	34 $\mu$ L
Sample after 1 <sup>st</sup> PCR	2 $\mu$ L
Final volume	50 $\mu$ L

The following cycling parameters were used for the 1<sup>st</sup> and 2<sup>nd</sup> PCR:

Initial denaturation	94 °C 5 min	
Denaturation	94 °C 30 s	
Annealing	60 °C 30 s	30 cycles
Extension	72 °C 45 s	
Final extension	72 °C 5 min	

#### 2.6.2.3 Agarose gel electrophoresis

To check for PCR product and a lack of contamination electrophoresis gels were prepared with 1% agarose powder (Invitrogen) dissolved in Tris-acetate EDTA (TAE) buffer. Midori Green nucleic acid staining solution (GeneFlow) was used for DNA visualisation, added before the gel was set. Samples were run for 45 min at 80 V, alongside 5 µL of 1 Kb DNA Hyperladder™(Bioline). Gels were visualised under an LED-based illuminator (FastGene) and bands cut out using a disposable scalpel. A representative gel for TCR clonotyping is shown in Figure 2.3. DNA was purified from the agarose slices using the NucleoSpin® Gel and PCR Clean-Up Kit (Clontech), following manufacturer's instructions.



**Figure 2.3: Agarose gel electrophoresis of PCR products for  $\gamma\delta$  T-cell receptor clonotyping.** PCR products for TCR- $\delta$  and TCR- $\gamma$  chains were electrophoresed on a 1% agarose gel at 80 V for 45 min. Gel products were visualised, as shown, and TCR bands of around 1kb in size, were cut out (as shown in boxes). A negative control was included in the PCR, which contained no DNA template, but all the PCR reagents.

#### 2.6.2.4 TOP® cloning and colony PCR

Blunt end PCR products were cloned into pCR™-Blunt-II-TOPO® vector (Invitrogen), according to the manufacturer's instructions. Briefly, 2 µL of purified PCR product were combined with 0.5 µL salt solution and 0.5 µL of the vector, followed by 5 min of incubation at room temperature to allow the topoisomerase-I mediated ligation to take place. The ligation mixture was added to OneShot™ TOP10 chemically competent *E.coli* (Invitrogen) and incubated for 30 min on ice. Following 30 s heat shock at 42 °C and a further 2 min on ice pre-warmed Super Optimal Broth (SOC, Clontech) was added and the cells were incubated in the orbital shaker (37 °C, 200 rpm) for 1 h. Finally the cells were plated on LB-agar plates containing 50 µg/mL kanamycin and incubated overnight at 37°C.

Bacterial colonies were screened for the presence of insert by colony PCR. The following master mix was prepared:

<b>Reagent</b>	<b>Amount</b>
GreenTaq MasterMix (2X)	12.5 µL
M13 primer (F) (10 µM)	1 µL
M13 primer (R) (10 µM)	1 µL
H2O	10.5 µL
1 Bacterial colony	
Final volume	25 µL

The following cycling programme was used:

Initial denaturation	94 °C 10 min	
Denaturation	94 °C 20 s	
Annealing	57 °C 20 s	30 cycles
Extension	72 °C 45 s	
Final extension	72 °C 5 min	

The PCR reactions were run on a 1% agarose gel for 45 min at 80 V in TAE buffer. The colonies containing an insert were sequenced using the PlateSeq Kit Clone service (Eurofins Genomics), where at least 8 colonies were sequenced per TCR chain for TCR clonotyping.

### 2.6.3 Analysis and sequencing of human $\gamma\delta$ TCR repertoires

Cells were first sorted viably using a combination of TAPI-0 assay followed by FACS Aria sorting. Cells from each experimental condition were washed and sorted directly into microfuge tubes containing 350  $\mu$ L lysis buffer (Qiagen) and stored at  $-80^{\circ}\text{C}$  until RNA extraction. PCR products amplified from sorted T-cell population were prepared for next generation sequencing using NEBNext Ultra Library Preparation kit (NEB) to attach Illumina adaptors and sample specific barcodes to the PCR products. Prepared libraries were multiplexed and run on Illumina MiSeq using MiSeq v2 kit (Illumina), with 2x250 bp paired end reads. Library preparation, MiSeq sequencing and analysis was performed in house by Cristina Rius-Rafael and Dr. Mereim Attaf (Cardiff University). TCR repertoire analysis was carried out using MiXCR software (Bolotin et al. 2015). The TCR repertoire data were filtered to remove the reads fulfilling the following quality criteria: low quality of read (lower than Q30), TCRs represented by five reads or less, and TCRs containing CDR3 sequences shorter than 21 nucleotides.

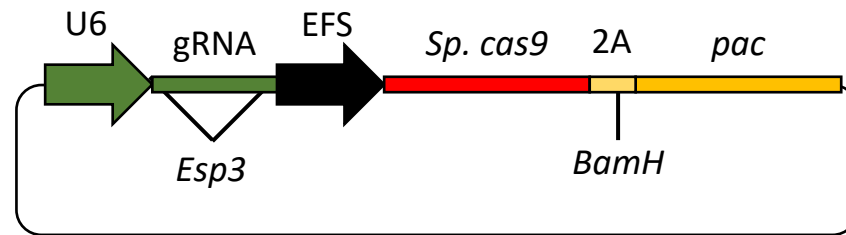
## 2.7 Molecular cloning

### 2.7.1 Plasmid Design

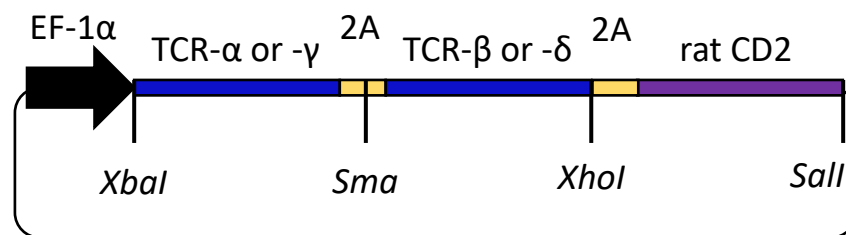
Genes to be expressed were cloned into the 3<sup>rd</sup> generation pELNs vector using XbaI and XhoI restriction sites, whereas those to be knocked out were targeted by cloning into the 2<sup>nd</sup> generation lentiviral vector pLentiCRISPR v2 using an Esp3I restriction site (Figure 2.4). In the case of pELNs the expression of transgenes was driven by the elongation factor (EF)-1 $\alpha$  promoter. The pELNs vector also contains the rCD2 marker gene, separated from the transgene of interest by a self-cleaving 2A sequence, flanked by XhoI and SalI restriction sites, thus facilitating removal if needed. In the case of TCR transgenes the individual chains (TCR $\gamma$  or  $-\delta$ ) were separated by another 2A sequence containing a unique SmaI restriction site, thus ensuring stoichiometric expression of both TCR chains, and enabling rapid exchange of individual TCR chains if required. In the pLentiCRISPR v2 vectors, gRNA template oligonucleotides were cloned into the vector. gRNA transcription occurred from a U6 RNA polymerase III promoter while the *S. pyogenes cas9* gene, linked as a 2A sequence with the *pac* marker gene, was transcribed from the short EF promoter. *Pac* gene encodes puromycin N-acetyltransferase, which confers resistance to puromycin antibiotic.



## A pLentiCRISPR v2



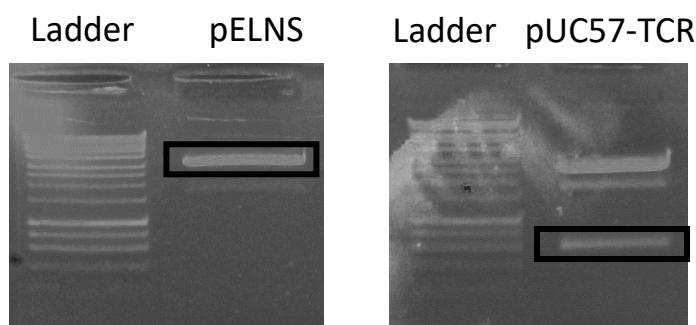
## B pELNS



**Figure 2.4: Schematic representation of lentiviral transfer plasmids pLentiCRISPR (A) and pELNS (B).** Promoters are shown as arrows, transgenes are shown as bars and unique restriction sites are marked with the restriction enzyme name. EF-1 $\alpha$ , elongation factor 1 $\alpha$ ; EFS, short elongation factor; pac, puromycin N-acetyltransferase.

### 2.7.2 Cloning into the pELNS vector

All expression constructs were designed by Dr. Mateusz Legut and built to be codon optimised for *H.sapiens* expression in the pUC57 vector (Genewiz). The sequences of the T-cell receptor constructs are listed in Appendix Table 8.2. Sequences of other proteins of interest cloned into the pELNs vector can be found in Appendix Table 8.3. The vectors were digested for at least 1 h at 37 °C, with 1  $\mu$ L of each of the restriction enzyme XbaI and XhoI, with 2  $\mu$ L 10x FastDigest Buffer (all Thermo), 2 $\mu$ L plasmid DNA and up to 20  $\mu$ L with nuclease free water. Digested plasmids were electrophoresed in a 1 % agarose gel for 1 h at 80 V. The appropriate bands (~9 kb for pELNS backbone and ~2 kb for the insert, Figure 2.5) were cut from the gel and DNA extracted using the Wizard® SV Gel and PCR Cleanup System (Promega) according to manufacturer's instructions. The DNA was eluted into 20  $\mu$ L nuclease-free water and concentration measured using a NanoDrop™ device (Thermo).



**Figure 2.5: Agarose gel electrophoresis after restriction digestion of lentiviral transfer plasmid pELNS and construct plasmid pUC57 carrying a synthesised T-cell receptor (TCR) of interest.** Plasmids were digested for 1 h using XbaI and XhoI restriction enzymes before being electrophoresed at 80 V for 45 min. Products were visualized, as shown, and pELNS vector (9kb band) and pUC57-TCR vector (800bp if singular TCR chain, 2kb if double TCR chain) were cut out of the gel, purified and used for ligation.

The following formula was used to set up an appropriate ligation mixture:

$$\text{amount of insert (ng)} = \frac{\text{Amount of vector (ng)} \times \text{size of insert (bp)}}{\text{Size of vector (bp)}} \times n$$

Where n is the desired ratio of insert to each backbone. Typically, a 5:1 ratio of insert to backbone was used. Appropriate quantities of digested backbone and insert were mixed with 2 µL 10X T4 DNA Ligase Buffer (Thermo), 1 µL T4 Ligase (Thermo) and up to 20 µL nuclease-free water. Ligation was carried out either at 37 °C for 4 h, or overnight at room temperature. The ligation mixture was then used to transform chemically competent XL10-Gold® cells (Agilent Technologies). In brief, 5 µL of ligation mixture was combined with 50 µL of bacteria. After gentle shaking cells were incubated on ice for 30 min followed by a 30 s heat shock at 42 °C and a second incubation of 5 min on ice. Cells were incubated with pre-warmed SOC media for 1 h in an orbital shaker (37 °C, 220 rpm) before being plated on ampicillin containing (100 µg/mL) LB agar plates. Plates were incubated overnight at 37 °C.

Bacterial colonies were screened for the presence of the insert using colony PCR. For PCR reactions the following mastermix was prepared:

<b>Reagent</b>	<b>Amount</b>
GreenTaq MasterMix (2X)	12.5 µL
pELNS F1 primer (10 µM)	1 µL
pELNS R2 primer (10 µM)	1 µL
H2O	10.5 µL
1 Bacterial colony	
Final volume	25 µL

The following cycling programme was used:

Initial denaturation	94 °C 10 min	
Denaturation	94 °C 20 s	
Annealing	60 °C 20 s	30 cycles
Extension	72 °C 2 min	
Final extension	72 °C 5 min	

The PCR reactions were run on a 1% agarose gel for 45 min at 80 V. Colonies containing the insert were transferred into 5 mL of LB media supplemented with 100 µg/mL ampicillin and incubated overnight at 37 °C, 220 rpm in an orbital shaker. Using the PureLink® Quick Miniprep Kit (Invitrogen) the plasmids were extracted from overnight bacterial cultures, according to manufacturer's protocol. Using the pELNS F2 and R3 primers (Eurofins Genomics) the plasmids were sequenced.

### 2.7.3 Cloning into the pLentiCRISPR v2 vector

gRNA sequences were designed using a free web tool (crispr.mit.edu). The 20nt gRNA sequences (without PAM) were ordered as a pair of nucleotides (Eurofins Genomics) with the help of Mateusz Legut with Esp3I-compatible overhangs, as shown below where N in Oligo F indicate nucleotides identical to the target sequence, and N in Oligo R are complementary to corresponding nucleotides in Oligo F:

*Oligo F*     5'     -     CACCGNNNNNNNNNNNNNNNNNNNNNN     -     3'

*Oligo R*     3'     -     CNNNNNNNNNNNNNNNNNNNNNNCAAA     -     5'

Three gRNAs were used throughout this thesis; SCNN1A gRNA1 (CACTTCCACCAACCGATGTA), SCNN1A gRNA2 (CCCGATGTATGGAACTGCT) and HLA-DR7 (CTGCCACAGGAAACGTGCTG).

The oligo pair was set up in the following reaction mixture:

<b>Reagent</b>	<b>Amount</b>
Forward oligo (10 $\mu$ M)	1 $\mu$ L
Reverse oligo (10 $\mu$ M)	1 $\mu$ L
10x T4 ligation buffer (NEB)	1 $\mu$ L
T4 polynucleotide kinase (NEB)	0.5 $\mu$ L
H <sub>2</sub> O	6.5 $\mu$ L
Final volume	10 $\mu$ L

The following cycling parameters were used for oligo phosphorylation and annealing:

Phosphorylation	37 °C 30 min
Annealing	95 °C 5 min
	Ramp down to 25 °C at 5 °C /min

5  $\mu$ g of the transfer vector (lentiCRISPR v2) was digested and phosphorylated for 1 h at 37 °C in a digestion mixture containing 6  $\mu$ L 10x FastDigest buffer, 3  $\mu$ L FastDigest Esp3I, 3  $\mu$ L FastAP (all thermo), 0.6  $\mu$ L 100 mM DTT and up to 60  $\mu$ L with nuclease-free water. The digested plasmid was run on 1% agarose gel at 80 V for 45 min.

Ligation of the digested transfer vector and annealed oligos was performed for 30 min at room temperature by combining the following reagents:

<b>Reagent</b>	<b>Amount</b>
Digest vector	50 ng
Annealed oligo pair (diluted 1:200)	1 $\mu$ L
2x Quick Ligase Buffer (NEB)	5 $\mu$ L
Quick Ligase (NEB)	1 $\mu$ L
H <sub>2</sub> O	Up to 10 $\mu$ L

The ligation mixture was transformed into XL10-Gold® bacteria as described previously.

The size of the insert (~20bp) is too small to visualise by colony PCR, therefore colonies were grown overnight in 5 mL LB media with 100 µg/mL ampicillin, followed by plasmid purification (Purelink® Quick Miniprep Kit) and sequenced using GeCKO F1 primer (Genewiz).

#### 2.7.4 Sequencing and analysis

Sequencing was either carried out by Eurofins Genomics, ESources Biosciences, or Central Biotechnology Services at Cardiff University. The sequencing results were aligned to a reference sequence in the plasmid editor software ApE.

#### 2.7.5 Plasmid Maxiprep

Plasmids containing correct inserts were transformed into XL10-Gold® bacteria and inoculated into 200 mL LB media containing 100 µg/mL ampicillin to be cultured overnight at 37 °C at 220 rpm. Subsequently, bacterial cultures were centrifuged at 4,000 g for 10 min to generate a bacterial pellet. R3 buffer containing RNase A (PureLink® HiPure Plasmid Filter Maxiprep Kit, Invitrogen) was used to resuspend the bacterial pellet before being neutralised with N4 buffer and applied onto an equilibrated HiPure Filter column. The column-bound plasmid was eluted and precipitated using isopropanol following centrifugation at 4,000 g for 1 h at 4 °C. After one wash with ethanol the purified plasmid was air-dried and resuspended in nuclease free water. All maxipreps were sequenced to ensure the presence of the correct insert, and were stored at -20 °C.

### 2.8 Whole Genome CRISPR/Cas9 Library Screens

With assistance from Dr. Mateusz Legut human whole genome CRISPR/Cas9 library, termed GeCKO v2 (Genome-scale CRISPR Knock-Out, Addgene plasmid #1000000048, kindly provided by Feng Zhang) was used in this study. Dr. Mereim Attaf and Cristina Rius-Rafael also provided help with NGS sequencing. Dr. Barbara Szomolay helped analyse the data using a bespoke web tool. The GeCKO library, divided into the sub-libraries A and B, targets every coding gene in the human genome with 6 independent gRNAs and every mRNA with 4 gRNAs (Shalem et al. 2014; Zotova et al. 2016). An additional 1,000 gRNAs that do not target any region in human genome were used as controls for non-specific cell survival. We were kindly provided lentivirus containing the GeCKo v2 libraries A and B courtesy of Prof. John Phillips, University of Utah. The following methods are based on guidance provided by Feng Xhang and colleagues on <http://www.genome-engineering.org/> website. Primer sequences used for HiSeq (Illumina) PCR and sequencing of GeCKo libraries can be found in Appendix Table 8.4.

### 2.8.1 Library setup and screening

Each GeCKO v2 sub-library was transduced into at least  $20^5$  target cells (thus giving >100X coverage of each sub-library with a transduction  $MOI \sim 0.4$ ). Target cells were transduced in 24 well plates, at  $40^4$  cells per well. Lentivirus was added along with 8  $\mu\text{g}/\text{mL}$  polybrene, and the cells were spininfected at 500 g for 2 h. After 2 days the transduced cells were split into two wells, with one being subjected to puromycin selection at a concentration of 1  $\mu\text{g}/\text{mL}$ . After 3 days under these conditions the MOI was calculated according to the formula below:

$$MOI = \frac{\text{number of viable cells treated with puromycin}}{\text{number of viable cells not treated with puromycin}}$$

Transduced cells were cultured for 14 days before co-incubation with T-cells. A minimum of  $6^6$  transduced target cells per sub-library were subjected to T-cell co-incubation, again ensuring >100X coverage of the library. 25,000 transduced target cells were co-incubated with 25,000 T-cells in a 96 U-bottom plate in T-cell priming media. In parallel wells of transduced target cells without T-cells were plated up, as well as untransduced target cells with and without T-cells. Such controls were used to monitor the killing of target cells in the designated conditions. After 14 days co-incubation, with regular replacement of T-cell priming media, surviving target cells were pulled together and replaced with 50,000 T-cells to 25,000 target cells for a further 14 days. Following the second round of T-cell selection target cells were cultured to ensure sufficient cell number for sequencing and functional assays.

### 2.8.2 Library Sequencing

Following successful T-cell selection, genomic DNA was extracted from at least  $5^6$  of the transduced target cells, barcoded and prepared for sequencing. The following reaction components were used for the 1<sup>st</sup> PCR, with a sufficient number of separate reactions set up to ensure adequate coverage:

<b>Reagent</b>	<b>Amount</b>
NEBNext High Fidelity PCR Master Mix 2X (NEB)	25 $\mu\text{L}$
Adaptor F (10 $\mu\text{M}$ )	2.5 $\mu\text{L}$
Adaptor R (10 $\mu\text{M}$ )	2.5 $\mu\text{L}$
Genomic DNA	2.5 $\mu\text{g}$
H <sub>2</sub> O	Up to 50 $\mu\text{L}$

All the reactions set up in the 1<sup>st</sup> PCR were pooled and used as a template for the 2<sup>nd</sup> PCR. The primers used for the 2<sup>nd</sup> PCR contained Illumina chip binding adaptors. The following reaction components were used for the 2<sup>nd</sup> PCR:

<b>Reagent</b>	<b>Amount</b>
NEBNext High Fidelity PCR Master Mix 2X (NEB)	25 µL
Illumina F01-04 (10 µM)	2.5 µL
Illumina R, barcoded (10 µM)	2.5 µL
PCR product	2.5 µL
H <sub>2</sub> O	Up to 50 µL

The following cycling parameters were used for both PCR rounds:

Initial denaturation	98 °C 30 s
Denaturation	98 °C 10 s
Annealing	60 °C 10 s
Extension	72 °C 15 s
Final extension	72 °C 2 min

The first PCR was run for 18 cycles, and the 2<sup>nd</sup> PCR for 24 cycles. The resulting PCR products were run on a 2% agarose gel for 45 min at 80 V, and the DNA cut as described before. HiSeq sequencing was performed at the University of Utah, courtesy of Prof. John Phillips. Data were analysed by Dr. Barbara Szomolay.

## 2.9 Western blot protein analysis

Western blot protein analysis was carried out by Dr. Thalia Zervoudi.

### 2.9.1 Sample preparation

Cells and reagents were kept on ice at all times, and all reagents were used chilled. Healthy, log phase growth cells were cultured to a density of 1<sup>6</sup> for large cells, for example melanoma cells, and 30<sup>6</sup> for small cells, for example PBMCs. Cells were pelleted by centrifugations at 300 g for 5 min at room temperature and were washed once with PBS to remove any proteins from the supernatant. PBS was decanted and aspirated and cells were resuspended in either 50 µL or 100 µL radioimmunoprecipitation assay (RIPA) lysis buffer with inhibitors (Table 2.5) for small or large cells, respectively and then incubated on ice for 30 min. The amount of lysis buffer was

determined for each cell type to ensure efficient lysis as well as an optimal final concentration of protein in the lysate.

**Table 2.5: Buffers and reagents used in western blot analysis**

Reagent	Volume	Final
<u>RIPA lysis buffer</u>		
5 M NaCl	3 mL	150 mM
0.5 M EDTA, pH 8.0	1 mL	5 mM
1 M Tris, pH 8.0	5 mL	50 mM
NP-40	1 mL	1%
10% v/v sodium deoxycholate	5 mL	0.5%
10% v/v SDS	1 mL	0.1%
dH <sub>2</sub> O	84 mL	-
<u>RIPA lysis buffer with inhibitors</u>		
Ice cold RIPA lysis buffer	10 mL	-
100X Halt protease phosphatase inhibitor cocktail	0.1 mL	1X
<u>Membrane wash buffer (PBST)</u>		
PBS	990 mL	-
Tween	1 mL	0.1%
<u>Blocking buffer</u>		
Non-fat milk	5 g	-
PBST	95 mL	1X
<u>Transfer Buffer</u>		
Glycine	2.92 g	
Tris base	5.82 g	
SDS	0.38 g	
CH <sub>3</sub> OH	200 mL	1X

RIPA lysis buffer was made and stored at 4°C for up to 1 month, whereas RIPA lysis buffer with inhibitors was made up fresh each time and stored on ice. NP-40: Nonidet-P40 and 100X Halt™ protease and phosphatase inhibitor (both Thermo Scientific).



The lysate was sonicated at 50% amplitude (Branson Digital Sonifier) three times for 25 secs each with at least one-minute rest on ice in between each pulse. If lysate was still viscous the sonication step was repeated. The lysate was incubated on ice for 15 min and then centrifuged at 13,000 g for 5 min at 4 °C. The supernatant (containing proteins) was kept, avoiding contacting the pellet, and run on SDS gel standard protocol (Section 2.10.4). Equal amounts of protein were loaded into polyvinylidene difluoride (PVDF) membrane (Invitrolon, Life Technologies) wells for SDS-PAGE, along with a molecular weight marker. The gel was run for 1-2 h at 100 V, according to the manufacturer's protocol.

### 2.9.2 Western blot membrane preparation and antibody staining

The PVDF membrane was activated for 1 min in methanol and rinsed with membrane wash buffer. The membrane was blocked for 1 h at room temperature or overnight at 4 °C using blocking buffer. The membrane was incubated with appropriate dilutions (typically a dilution of 1:1000) of primary antibody in blocking buffer followed by overnight incubation at 4 °C. The alpha-ENaC polyclonal antibody (#PA1-920A, ThermoFisher) was the only primary antibody used in this thesis and was used at a dilution of 1:100. The membrane was washed 3 times in washing buffer and incubated with the recommended dilution of conjugated secondary antibody in blocking buffer at room temperature for 1 h. The goat anti-rabbit IgG secondary antibody HRP (#31460, Thermofisher) was used at a dilution of 1:10000 for this thesis. The membrane was washed three times in PBST wash ready for signal development. Peirce ECL Plus western blotting substrate kit (#32132, Thermofisher) was used for signal development, according to manufacturer's protocol.

## 2.10 Protein expression, refolding and purification

### 2.10.1 Vectors for protein expression

The expression plasmid pGMT7 was used as a vector for bacterial protein expression of HLA proteins, conferring resistance to carbenicillin. pGMT7 contains a sequence encoding the protein of interest inducible with Isopropyl  $\beta$ -D-1-thiogalactopyranoside (IPTG) under the control of the T7 RNA polymerase promoter, the sequence for expression was cloned using BamHI and EcoRI restriction sites. pGMT7 expression was used to produce the extra-cellular domain of  $\alpha$ -chain and  $\beta$ -chain soluble domains of MHC molecules. The N-terminus of the  $\alpha$ -chain was tagged with a 15 aa biotinylation sequence (GLNIFEAQKIEWHE) (AviTag<sup>TM</sup>, Avidity) allowing tetramerisation of pMHC monomer or adherence to streptavidin BIAcore chips (see section below). Proteins were expressed without the biotinylation tag for crystallisation studies. A cysteine residue was added to the TCR  $\alpha$ -chain and  $\beta$ -chain extracellular domains in order to introduce potential for a non-native disulphide bond to enhance potential for  $\alpha\beta$  chain pairing during the refolding process, as described below. All protein sequences and construct information can be found in Appendix Table 8.5. Culture media and buffers for protein expression, refolding and purification can be found in Appendix Table 8.6.

### 2.10.2 Transformation of competent *E. coli* cells

Competent Rosetta (DE3) pLysS *E. coli* cells (Invitrogen) were used to produce MHC-I  $\alpha$  and  $\beta_2$ M chains, and MHC-II  $\alpha$ - and  $\beta$ -chains in the form of inclusion bodies. Transformation of competent bacteria cells was performed by thawing 50  $\mu$ L of cells on ice for 5 min. Up to 100 ng of plasmid DNA was added to the bacterial cells and incubated for 5 min on ice before being heat shocked at 42 °C for 2 min and then placed back on ice for 5 min. Cells were plated onto a LB agar medium plate and grown overnight at 37 °C.

### 2.10.3 Expression of inclusion bodies in Rosetta *E. coli*

A starter culture was set up by picking and culturing a single bacterial colony in 30 mL of TYP media, and growing the bacteria in 37 °C at 220 rpm in an orbital shaker (Sanyo, Lecis, UK; MIR-222U) until the culture reached an optimum density ( $OD_{600nm}$ ) approx. 0.5. The starting culture was then grown further, under the same conditions, in 1 L TYP medium for 3 h (or until the  $OD_{600nm}$  was approx. 0.5). Protein expression was induced by adding 0.5 mL of 1 M IPTG and incubating at 37 °C for 3 h in the orbital shaker. A sample was collected pre and post IPTG induction and run on a SDS-PAGE gel (Section 2.10.4) to verify the quality and quantity of protein expression. Cells were harvested and centrifuged at 3450 g for 20 min before being suspended in 40 mL lysis buffer and sonicated on ice at 20 % power for 20 min using 2 sec intervals using a

Sonopulse HD 2070 with MS73 probe (Bandelin). The sonicated pellet was incubated with 200  $\mu$ L of 20 mg/mL DNase (Sigma) for 30 min at room temperature before being re-suspended with 100 mL of Triton wash buffer and centrifuged for 20 min at 15, 180 g. The supernatant was discarded and the pellet was re-suspended into 100 mL of triton wash buffer following homogenization (VWR VD25, 17,500/min). Pellets were re-suspended in 10 mL resuspension buffer and centrifuged for 20 min at 15, 1590 g. Class I inclusion bodies were dissolved in 5-10 mL guanidine buffer and stored in -20 °C until use. Class II inclusion bodies were re-suspended in 40 mL urea buffer A, and were subjected to a further step; anion exchange purification.

Urea solubilised inclusion bodies were filtered using a 0.45  $\mu$ m filter and vacuum pump before being purified by anion exchange chromatography (5 mL HiTrap Q HP; GE Healthcare Life Sciences) on an AKTApure FPLC system (GE Healthcare Life Sciences). Protein was eluted into urea buffer B and collected into 1 mL fractions to be analysed by SDS-PAGE (Section 2.10.4). Fractions containing pure protein were used for refolding.

Protein concentration was estimated using the NanoPhotometer spectrophotometer (Geneflow). The machine was blanked using the appropriate buffer (e.g. guanidine buffer for inclusion bodies). Readings at 280 nm wavelength were recorded and the approximate protein concentration was calculated using the dilution factor and extinction co-efficient (calculated using ProtParam <http://web.expasy.org/protparam/>).

#### 2.10.4 Sodium Dodecyl Sulphate-Polyacrylamide Gel Electrophoresis (SDS-PAGE)

SDS-PAGE (Life Technologies X-Cell SureLock system) was used to verify protein quantity and purity of samples. Each sample was diluted 1:4 with 5X non-reducing or reducing (with the addition of 10 % DTT) buffer and then incubated at 90 °C for 5 min. Samples were loaded onto a pre-cast 10 % Bis/Tris gel (NuPAGE, nvitrogen) with 1X running buffer (NuPAGE, Invitrogen). A protein ladder BLUeye, 10-45 kDa range, Geneflow Ltd) was used as a control. Gels were run at 220 V for 22 min at 200mA, and stained with Quick Coomassie™ Stain (Generon) for band visualisation.

#### 2.10.5 Protein Refolds

Proteins were incubated at relevant quantities (Table 2.6) and mixed at 4 °C for >1 h (Class I) or for 3-5 days (Class II). Dialysis was conducted twice against 10 mM Tris pH 8.1 until the conductivity of the refolds was <2mS/cm. All refolds were filtered through a 0.22  $\mu$ m filter before further FPLC purification steps (Class I) or antibody column (Class II).

**Table 2.6: Quantities and refold procedure for MHC class I and MHC class II proteins**

Refold Type	Quantities	Procedure
Class I	30 mg of HLA chain 30 mg of $\beta$ 2M 4mg of synthetic peptide	Separately incubated at 37 °C for 15 min Added to cold refold buffer together
Class II	5 mg HLA-DR $\alpha$ 5 mg HLA-DR $\beta$ 0.5 mg peptide	Refold mixture stirred vigorously for 1 h before being left for 72-96 h at 4 °C

\*all are per 1L refold

### 2.10.6 Protein Purification

Specific purification methods for different types of refolded proteins are outlined below. Following purification, proteins were eluted into 700  $\mu$ L PBS buffer and biotinylated (Section 2.10.7) and either subjected to FPLC based (Class I) or antibody based (Class II) purification.

#### *2.10.6.1 Class I FPLC based*

The refolded proteins were first purified using an anion exchange column (POROS 50HQ, Life Technologies) equilibrated with ion exchange buffer A. Protein samples were loaded at a flow rate of 20 mL/min (5 MPa pressure) and eluted using buffer A into FPLC tubes (Greiner Bio-One). Fractions were analysed for purity by SDS-PAGE, pooled and concentrated at 3000 g until sample volume was <1 mL using a 4 mL Vivaspin (10 kDa, Sartorius).

Buffer exchange and the removal of aggregates was achieved by gel filtrating the sample, using a Superdex HR 200-exclusion column (Amersham Pharmacia), previously equilibrated with the appropriate buffer (crystal or PBS). Samples were eluted into FPLC tubes and analysed via SDS-PAGE, as before. Correctly folded proteins were stored at -20 °C. For BIAcore surface plasmon and tetramer experiments proteins were biotinylated.

#### *2.10.6.2 Class II antibody column based*

Following incubation, refolded MHC class II protein was concentrated using a Vivaflow crossflow concentration cassette (molecular weight cut-off 10 kDa; Sartorius) and peristaltic pump to less than 50 mL prior to the addition of 500 mL PBS buffer. The PBS refold mixture was concentrated to 50 mL in the Vivaflow system before being further concentrated to 10 mL using a 10 kDa MWCO centrifugal filter unit (Millipore).

An immune-affinity column containing the anti-HLA-DR antibody (L243, in house hybridoma) was used to purify the refold solution. Columns were equilibrated with PBS before the addition of 10 mL refold solution. PBS was used to wash the column 3-4 times before 8 mL of CAPS buffer was applied to elute the column into 2 mL fractions containing equal amounts of neutralising buffer. As above a centrifugal filter unit was used to exchange the refold into crystal or PBS buffer, to a final volume of 700  $\mu$ L, depending on intended use; whether crystallisation or tetramer staining, respectively.

#### **2.10.7 Protein Biotinylation**

Biotin was added to refolded proteins containing a biotin tag using a BirA biotinylation kit (Avidity). Refolded proteins were re-suspended in 700  $\mu$ L of the relevant buffer and 100  $\mu$ L of Biomix A, BiomixB and d-Biotin were added along with 2  $\mu$ L BirA enzyme (Avidity) for overnight room temperature incubation

Excess biotin was removed by buffer exchange in a centrifugal filter unit into PBS and a biotin shift assay was carried out by SDS-PAGE. 5  $\mu$ g refolded protein was incubated with 5  $\mu$ g of streptavidin for 20 min at room temperature before being analysed on SDS-PAGE; where protein/biotin multimers were assessed by size in reduced and non-reduced conditions.

#### **2.11 Data Analysis**

Unless specified otherwise, all data were analysed in GraphPad Prism software or Microsoft Excel. Where appropriate 2-sample t-tests were performed to analyse the difference between the means of two samples (for example WT vs knockout). Results are displayed as mean with standard deviation (s.d.).



### 3 Using herpes virus infected cells to generate cancer-reactive $\gamma\delta$ T-cell clones

#### 3.1 Introduction

As reviewed in Chapter 1,  $\gamma\delta$  T-cells have been shown to play pivotal roles in targeting stressed cells, such as pathogen infected and transformed cells (Déchanet et al. 1999; Halary et al. 2005; Willcox et al. 2012). The molecular mechanisms by which  $\gamma\delta$  T-cells recognize stressed cells are poorly understood. The  $V\gamma 9^+V\delta 2^+$  subset, usually comprising 90-99% of peripheral blood  $\gamma\delta$  T-cells, is well characterised and known to recognize non-peptidic phosphorylated antigens displayed by bacterially infected and transformed cells (Marx et al. 1997; Riano et al. 2014). In contrast, less is known about  $V\delta 2^{\text{neg}}$  subset, but studies have shown that these cells have the capacity to recognize target ligands that are displayed following viral infection and cellular transformation.

The most widely studied herpes virus in the context of  $\gamma\delta$  T-cell target recognition is human cytomegalovirus (hCMV; also known as human herpesvirus 5). It has been established that  $V\delta 1^+$  T-cells rapidly expand in response to hCMV infection (Halary et al. 2005) and reactivate following immunosuppression (Puig-Pey et al. 2010), but little is known about the ligands that trigger such expansions. One recent study demonstrated that a  $V\delta 1^+$  TCR clonotype within the peripheral blood of a hCMV infected transplant recipient responded to the stress ligand EPCR (Willcox et al. 2012). Curiously, EPCR is also expressed on the surface of some tumour cell lines (Menschikowski et al. 2011; Willcox et al. 2012) suggesting that  $\gamma\delta$  T-cells may provide a general stress surveillance system that offers the host protection against both viral infection and tumours.

Although less is known about the closely related Epstein-Barr virus (EBV; human herpesvirus 4) with respect to  $\gamma\delta$  T-cell responses, previous studies have shown that EBV immortalised B-cells induced the activation and proliferation of  $V\delta 1^+$   $\gamma\delta$  T-cells from the peripheral blood of transplant recipients (Fujishima et al. 2007; Farnault et al. 2013). Other studies have identified the expression of a surface protein, hMSH2, upregulated on EBV immortalised B-cell lines and tumour cells (Dai et al. 2012), which increased  $\gamma\delta$  T-cell activation. Similarly, Kong and colleagues showed that  $\gamma\delta$  T-cells could recognise UL16-binding protein, ULBP4, on both tumour and EBV immortalised B-cells (Kong et al. 2009).

##### 3.1.1 Aims

Given that  $\gamma\delta$  T-cells can recognize herpes viruses and tumour cells via shared ligands, my research set out to identify other novel stress ligands that could be targeted by  $\gamma\delta$  T-cells. My

approach involved using virally infected targets to generate  $\gamma\delta$  T-cell lines exhibiting reactivity towards both virus and tumour from the peripheral blood of healthy donors. Procurement of such cell types was challenging due to the rarity of  $V\delta 2^- \gamma\delta$  T-cells in blood and the dominance of  $\alpha\beta$  T-cells within antiviral immune responses.

The aim of this chapter was to isolate rare tumour-reactive  $V\delta 2^{\text{neg}} \gamma\delta$  T-cell clones from the peripheral blood of healthy donors, using herpes virus infected cells as a priming mechanism. The approach and initial characterisation of the T-cell clones isolated are described in this chapter. Interesting T-cell clones were further analysed in Chapters 4 and 5.

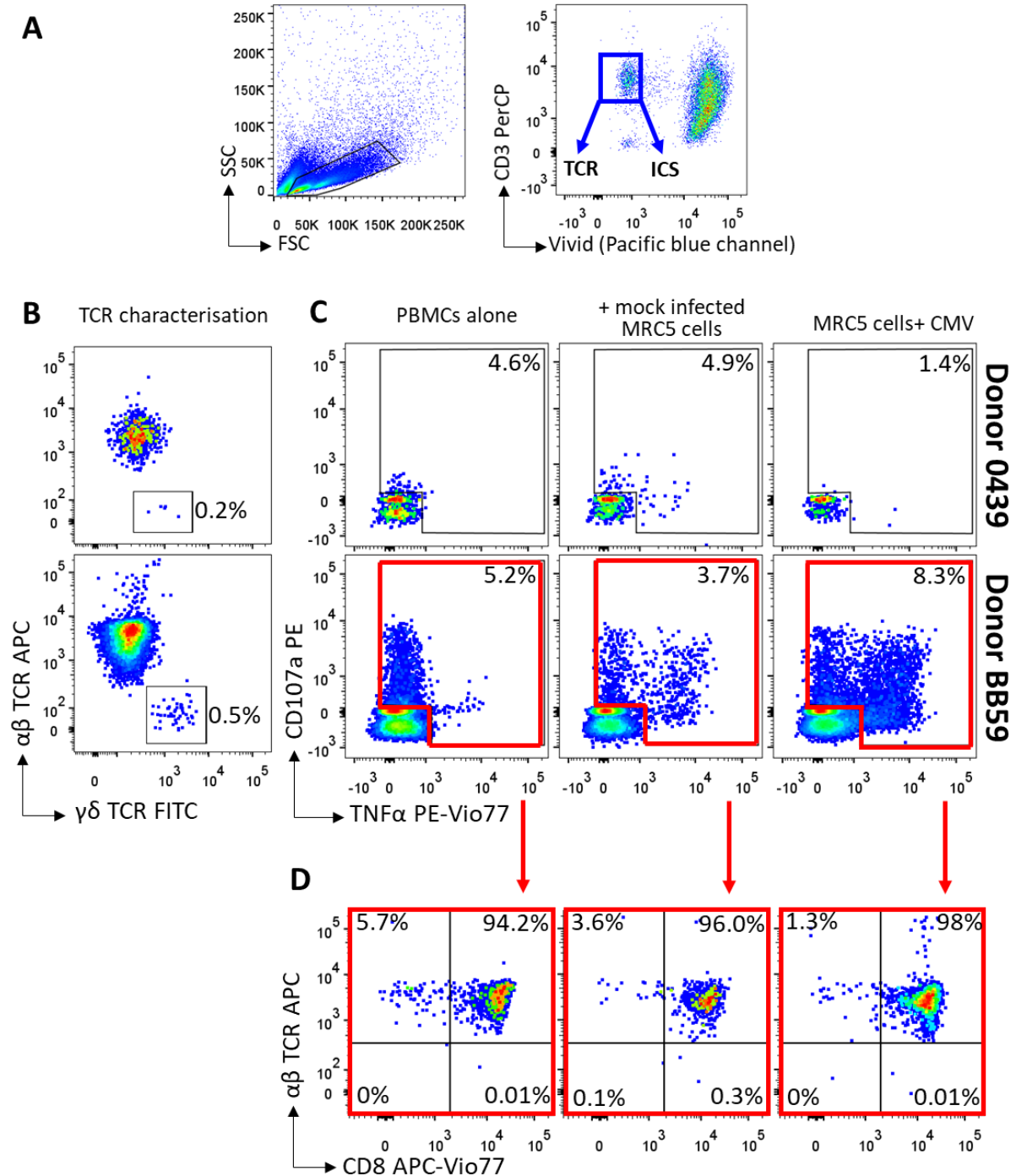
## 3.2 Results

### 3.2.1 CMV-infected cells failed to prime robust $\gamma\delta$ T-cell responses from healthy PBMC

I began my studies looking for hCMV-reactive  $\gamma\delta$  T-cells as previous studies have indicated that hCMV-reactive cells can recognise ligands that are also present on tumour cells. Use of hCMV also allowed me to exploit local expertise on this virus in the laboratory of Professor Gavin Wilkinson. The Wilkinson group recently collaborated to show that CMV infection alters gene expression of thousands of cell surface-expressed proteins (Weekes et al. 2014). I reasoned that if I could generate CMV-reactive  $\gamma\delta$  T-cells then I could make use of the many deletion strains in Prof Wilkinson's laboratory and the proteomic experience within this team to identify ligands.

PBMCs were isolated from donors BB59 and 0439 and co-cultured with CMV strain Merlin (Cunningham et al. 2010) infected MRC5 fibroblast cells for 14 days. Intracellular cytokine staining (ICS) was used to assess the reactivity by measuring TNF $\alpha$  and CD107a expression of the PBMCs to CMV infected MRC5 cells. Briefly, CMV primed PBMCs were either cultured alone or co-incubated with mock-infected or CMV-infected MRC5 cells for 6 h at an E:T cell ratio of 1:1. Surface antibodies including anti-CD3, anti- $\gamma\delta$  TCR, anti- $\alpha\beta$  TCR, and anti-CD8 were used to phenotype the PBMC. Viable CD3 $^+$  cells were gated (Figure 3.1A) and displayed either as anti- $\gamma\delta$  TCR versus anti- $\alpha\beta$  TCR (Figure 3.1B), or anti-TNF $\alpha$  versus CD107a (Figure 3.1C). Characterisation of the TCR distribution amongst the cells showed that in donors 0439 and BB59, 0.2% and 0.5% respectively of CD3 $^+$  cells were  $\gamma\delta$  TCR $^+$ . In donor 0439 no activation was seen when PBMCs were co-incubated with CMV-infected cells (1.4%), indeed the activation was less than that seen for the mock-infected MRC5 cells (4.9%). For donor BB59, 8.3% of viable CD3 $^+$  cells expressed TNF $\alpha$  and CD107a when co-incubated with CMV-infected fibroblasts compared with 3.7% when co-incubated mock-infected MRC5 cells. 98% of responding cells were  $\alpha\beta$  TCR $^+$ CD8 $^+$  (Figure 3.1D). In summary, whole PBMCs from healthy donors primed with CMV strain Merlin failed to elicit  $\gamma\delta$  T-cell responses. Next, I used EBV infected B-cells as another approach to procure  $\gamma\delta$  T-cells.





**Figure 3.1: Cytomegalovirus infected fibroblasts failed to prime  $\gamma\delta$  T-cells from peripheral blood mononuclear cells (PBMCs).** PBMCs from donors 0439 and BB59 were used in an ICS assay to compare reactivity to CMV and mock infected MRC5 cells. (A) Cells were gated on forward scatter (FSC) versus side scatter (SSC), then CD3<sup>+</sup> viable cells (Vivid<sup>neg</sup>) for phenotypic and functional analysis. (B) Staining of cells from A for  $\gamma\delta$  T-cell receptor (TCR) and  $\alpha\beta$  TCR. The percentage of  $\gamma\delta$  TCR<sup>+</sup> cells is shown. (C) Staining of cells from A for effector functions CD107a and TNF $\alpha$  following ICS. The percentage of cells in the activated cell gate is shown. Activated cells (TNF $\alpha$ <sup>+</sup> and/or CD107a<sup>+</sup>) from donor BB59 were gated on and displayed in D as  $\alpha\beta$  TCR versus CD8. The percentage of cells in each quadrant is shown.

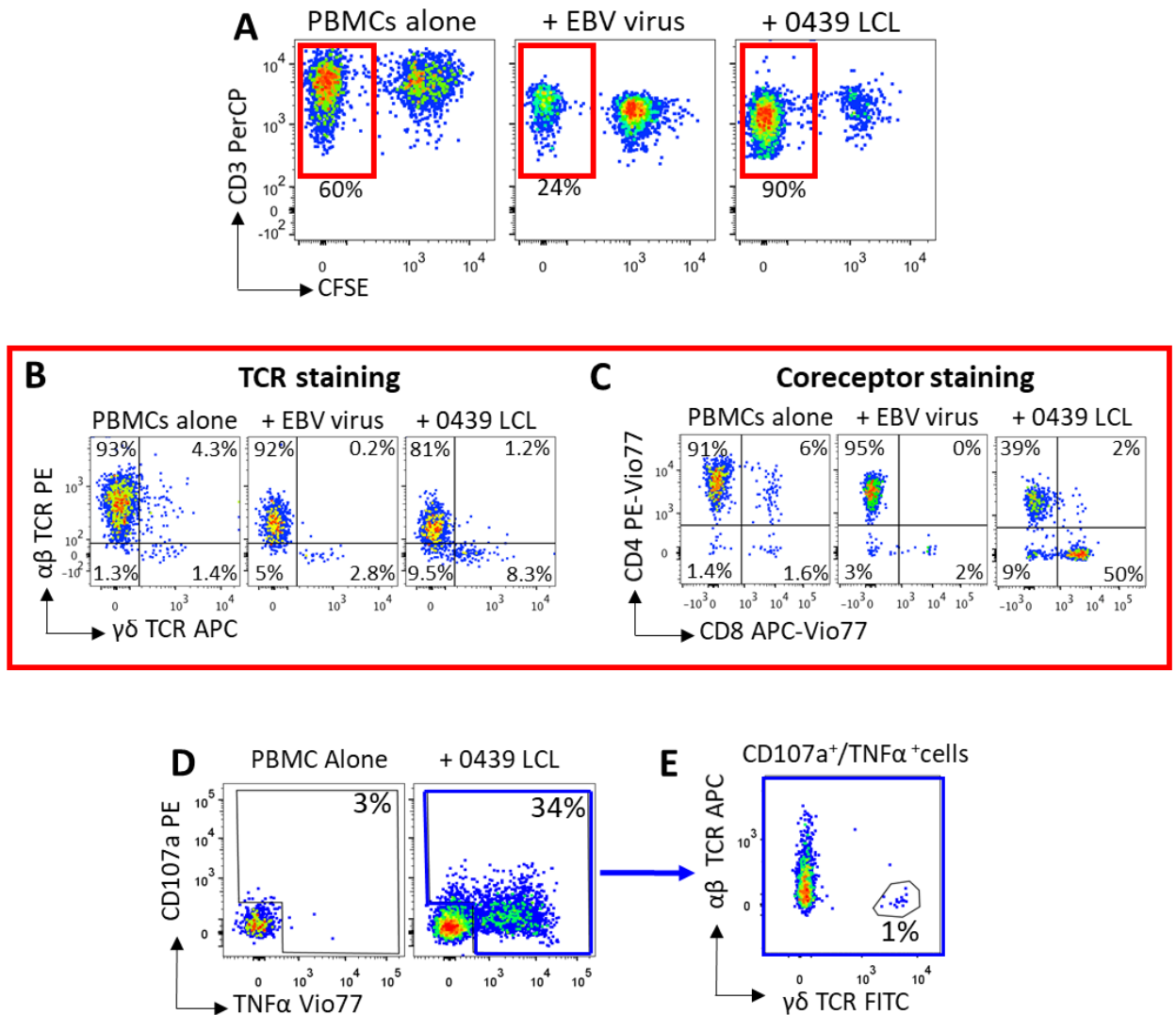
### 3.2.2 Autologous EBV infected B-cells predominately primed $\alpha\beta$ T-cells

PBMC from donor 0439 were labelled with the proliferation dye CFSE then cultured alone or co-incubated for 14 days with either concentrated EBV virus, or irradiated autologous LCLs (Figure 3.2). The use of EBV virus and LCLs allowed priming of T-cells that responded to antigens present during acute and latent stage infection. After 14 days, proliferating cells (CFSE<sup>low</sup>) were phenotyped. Viable, CD3<sup>+</sup> proliferating (CFSE<sup>low</sup>) cells were gated (Figure 3.2A) and stained for  $\alpha\beta$  TCR and  $\gamma\delta$  TCR (Figure 3.2B) or CD4 and CD8 (Figure 3.2C). While there appeared to be a small  $\gamma\delta$  T-cell population expanded in response to LCL, this response was dwarfed by that of  $\alpha\beta$  TCR<sup>+</sup>CD8<sup>+</sup> T-cells. A TAPI-0 assay confirmed the dominant response via  $\alpha\beta$  TCR (Figure 3.2D&E). In order to bypass the dominance of  $\alpha\beta$  T-cells, I next decided to simply use purified  $\gamma\delta$  T-cells as starting material.

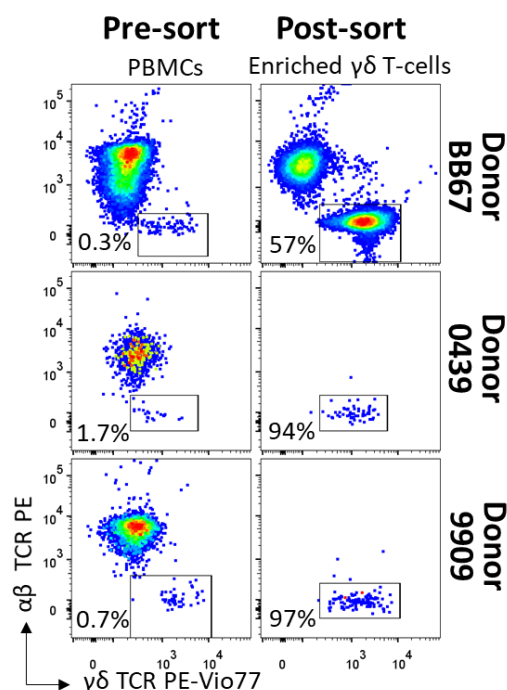
### 3.2.3 Purified $\gamma\delta$ T-cells responded to LCL

Magnetic separation was used to enrich V $\delta$ 2<sup>neg</sup>  $\gamma\delta$  T-cells from the PBMCs of donors BB67 (0.3%  $\gamma\delta$  T-cells), 0439 (1.7%  $\gamma\delta$  T-cells) and 9909 (0.7%  $\gamma\delta$  T-cells) (Figure 3.3). Post magnetic separation  $\gamma\delta$  T-cells constituted 57%, 94% and 97% of total live CD3<sup>+</sup> cells from donor BB67, 0439 and 9909, respectively. The magnetic separation for donor BB67 was less successful as many more cells were used, possibly leading to antibody saturation. Typically, 10<sup>5</sup> V $\delta$ 2<sup>neg</sup>  $\gamma\delta$  T-cells were generated from 10<sup>8</sup> PBMC. I next incubated the V $\delta$ 2<sup>neg</sup>  $\gamma\delta$  T-cells from each donor with irradiated, non-autologous LCLs (HLA information in Appendix Table 8.7). After 14 days incubation with irradiated LCLs, ICS assays showed that each donor line was reactive to the LCLs that they were originally exposed to (Figure 3.4). The line generated from Donor BB67 (Figure 3.4A) showed 18% reactivity to the non-autologous LCL 0439, compared to 1% reactivity towards the autologous LCL. Donor 0439  $\gamma\delta$  T-cells were reactive to both autologous (13%) and non-autologous (14%) LCLs (Figure 3.4B). After 14 days, donor 9909  $\gamma\delta$  T-cell line was 18%, 13% and 7% reactive to LCL 0439, HOM-2 and Pt-146 respectively. A further 14-day incubation with these LCLs increased this reactivity to 67%, 45% and 9% (Figure 3.4C). Similar experiments were undertaken to grow hCMV-reactive  $\gamma\delta$  T-cell lines but were unsuccessful. These experiments are shown in Appendix Figure 8.1 and will not be discussed further.

## Donor 0439 and autologous LCLs



**Figure 3.2: Autologous EBV immortalised B-cells primarily expand  $\alpha\beta$  T-cells.** CFSE labelled PBMCs from donor 0439 were cultured alone or with either concentrated EBV virus or irradiated autologous EBV immortalised LCL. (A) Viable CD3<sup>+</sup> CFSE<sup>low</sup> proliferating cells were gated and stained for  $\gamma\delta$  TCR and  $\alpha\beta$  TCR (B) or CD8 and CD4 co-receptor (C). The percentage of cells in each gate/quadrant is shown. (D) ICS assay with PBMCs cultured alone or with autologous LCL. Viable CD3<sup>+</sup> cells were gated and stained for TNF $\alpha$  and CD107a (D). Activated cells (TNF $\alpha$ <sup>+</sup> and/or CD107a<sup>+</sup>) were further gated on and displayed as  $\gamma\delta$  TCR and  $\alpha\beta$  TCR (E). The percentage of cells in each gate is indicated.

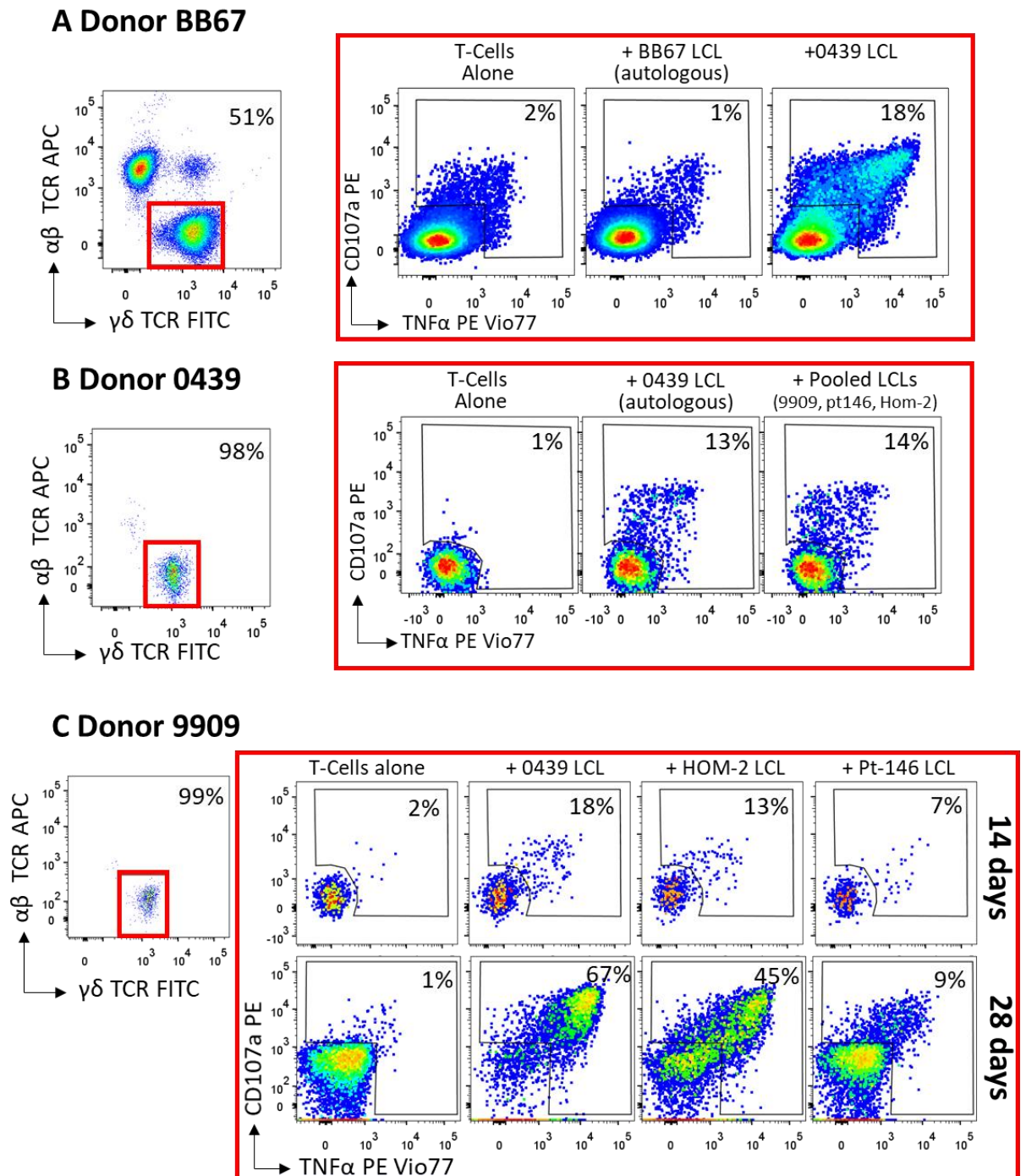


**Figure 3.3: Magnetic enrichment of  $\gamma\delta$  T-cells from the PBMCs of indicated donors.** PBMCs from each donor were enriched for  $V\delta 2^{\text{neg}}$  T-cells. Viable  $CD3^+$  cells were gated and stained for  $\gamma\delta$  TCR and  $\alpha\beta$  TCR in PBMC (left panel) and following enrichment (right panel). The percentage of cells in each gate is shown.

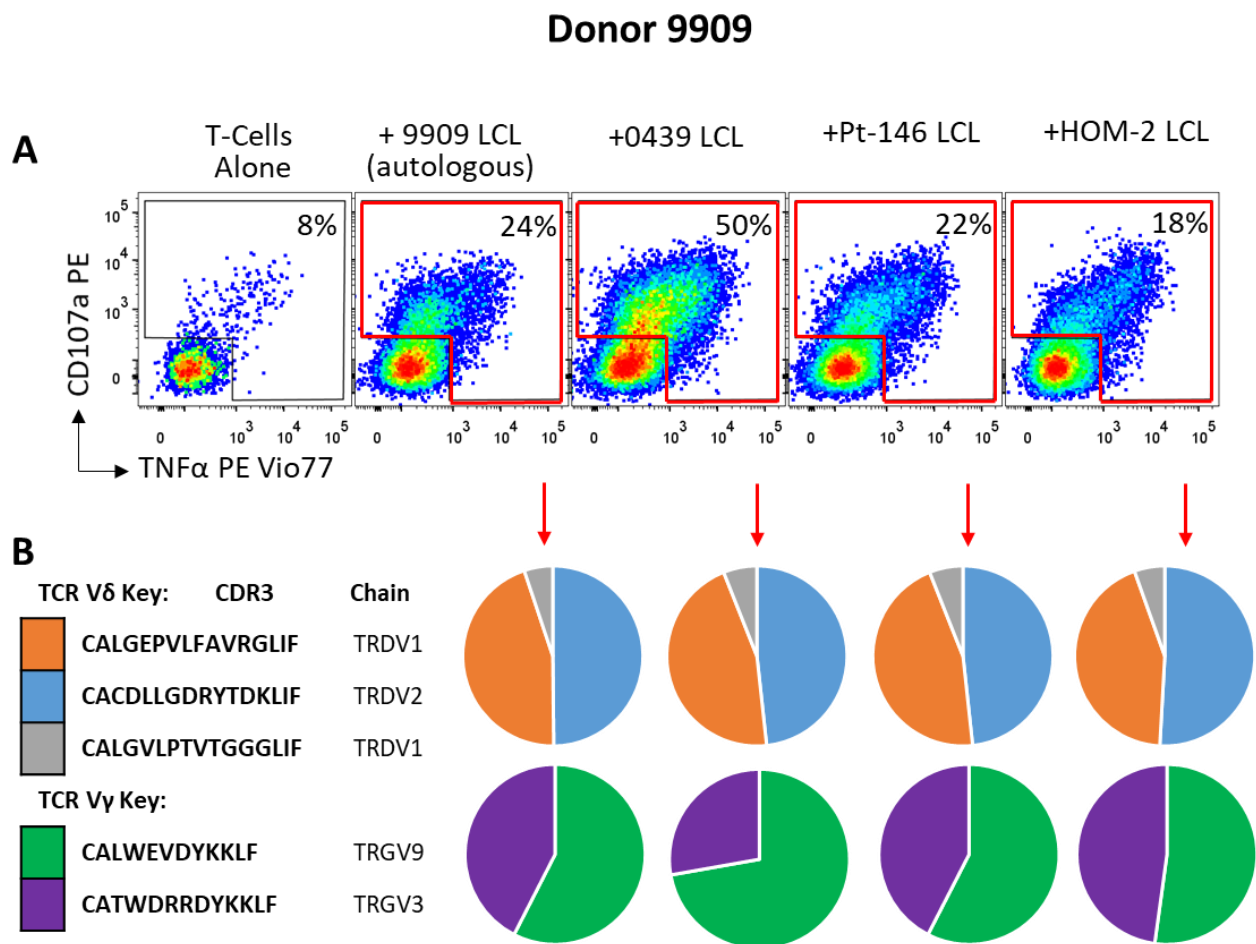
I next proceeded to characterise the  $\gamma\delta$  T-cell lines generated using non-autologous LCL targets. The line from donor 9909 will be used as an exemplar of the approach I undertook. This  $\gamma\delta$  T-cell line was shown to respond to all the LCL lines it was primed on in addition to the autologous LCL (Figure 3.5A). Clonotypic analysis of the responding cells showed that T-cells with the same three  $\delta$ -chains and two  $\gamma$ -chains responded to all LCL (Figure 3.5B). My original aim was to find T-cell clones that cross-reacted with herpesvirus-infected and tumour cells. A preliminary screen showed that the 9909  $\gamma\delta$  T-cell line reacted to the tumour cell line MDA-MB-231 (Appendix Figure 8.2). I next proceeded to generate monoclonal  $\gamma\delta$  T-cells from all three donors mentioned above.

### 3.2.4 LCL-primed $\gamma\delta$ T-cell clones recognized cancer cells

Cloning by limiting dilution was used to derive clones from LCL primed  $\gamma\delta$  T-cell lines from donors BB67, 0439 and 9909. Clones were selected based on  $\gamma\delta$  TCR expression, strong reactivity to LCL and good growth in culture as described in Table 3.1. Three clones were selected for further investigation; SW.6B10 (from donor BB67), SW.11H7 (donor 0439) and SW.3G1 (donor 9909). LCL reactivity, TCR sequence and antibody staining phenotypic analyses for all three clones are shown in Figure 3.6. Each clone expressed a different TCR and exhibited a distinct pattern of LCL-reactivity (Figure 3.7). All three clones showed reactivity towards tumour cells (Figure 3.8).



**Figure 3.4: Epstein-Barr virus immortalised B-cell lines prime purified  $\gamma\delta$  T-cells.**  $\gamma\delta$  T-cells from donors BB67 (A), 0439 (B) and 9909 (C) were tested for reactivity to LCLs in an ICS assay. Viable  $CD3^+ \gamma\delta^+$  cells were gated on (left panel) and displayed as  $TNF\alpha$  versus  $CD107a$  (right panel) for each donor. The percentage of gated cells is shown. Data shown is representative of three independent experiments.



**Figure 3.5: T-cell receptor sequencing of  $\gamma\delta$  T-cells primed with non-autologous EBV immortalised B-cells.** A TAPI-0/CD107a activation assay was carried out on the  $\gamma\delta$  T-cell line from donor 9909. Activated, viable CD3<sup>+</sup> cells were sorted based on TNF $\alpha$  and/or CD107a using the gates indicated in the top panels. Unbiased RACE-based NGS sequencing was used to sequence the TCR variable (V)  $\delta$  (D) and  $\gamma$  (G) chains within the indicated gate. The pie charts show the proportions of V $\delta$  chains and Vy chains within the cells sorted from each gate. The percentage of cells within each gate is shown.

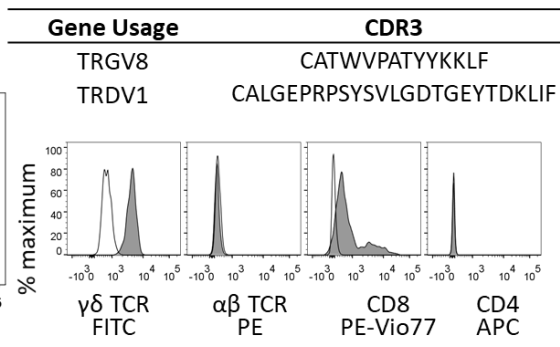
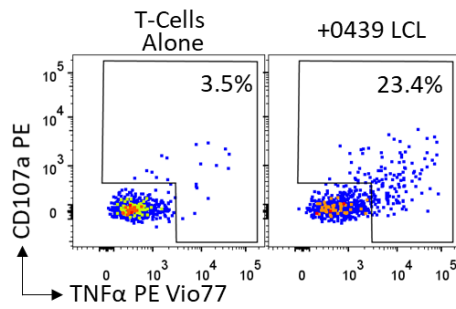
**Table 3.1: An overview of all clones procured from EBV primed  $\gamma\delta$  T-cell lines from donors BB67, 0439 and 9909.**

Clone name	$\alpha\beta$ TCR	$\gamma\delta$ TCR	V $\delta$ 2 <sup>neg</sup>	Reactivity	Growth
<b>Donor BB67</b>					
1A8	✓	✗	-	Green	-
2B8	✓	✗	-	Red	-
2F9	✓	✗	-	Green	-
2F10	✓	✗	-	Red	-
4D11	✓	✗	-	Green	-
7B8	✓	✗	-	Green	-
1H11	✗	✓	✓	Green	Red
6B10	✗	✓	✓	Green	Green
<b>Donor 0439</b>					
2F8	✗	✓	✓	Green	Red
6C3	✗	✓	✓	Green	Red
5D9	✗	✓	✓	Green	Red
5F5	✗	✓	✓	Red	Red
5A9	✗	✓	✓	Green	Red
9H5	✗	✓	✓	Red	Red
11H7	✗	✓	✓	Green	Green
12D1	✗	✓	✓	Green	Red
5G12	✗	✓	✓	Green	Red
<b>Donor 9909</b>					
1E3	✗	✓	✓	Green	Red
2C3	✗	✓	✓	Red	Red
2F2	✗	✓	✓	Green	Red
2H9*	✗	✓	✓	Green	Green
3A4*	✗	✓	✓	Green	Green
3A6*	✗	✓	✓	Green	Green
3A9	✗	✓	✓	Green	Red
3G1*	✗	✓	✓	Green	Green
3H7*	✗	✓	✓	Green	Green
4F8*	✗	✓	✓	Green	Green
4H2	✗	✓	✓	Green	Red
5F12	✗	✓	✓	Green	Red
6H2	✓	✗	-	Green	-
7B8	✗	✓	✓	Green	Red

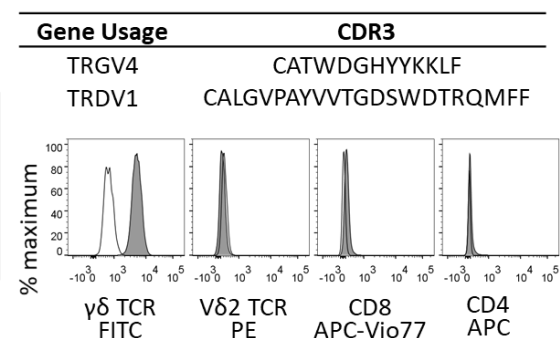
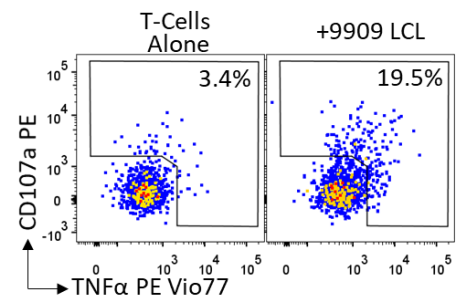
Clones were generated from  $\gamma\delta$  T-cell lines from donor BB67, 0439 and 9909 as described previously. Clones that were  $\alpha\beta$ TCR<sup>+</sup> were not pursued. Three V $\delta$ 2<sup>neg</sup>  $\gamma\delta$  T-cell clones (indicated by boxes and grey shading) were taken forward for further analysis as they exhibited high levels of reactivity and grew well in culture as indicated by colouring. LCL killing data for these three clones is shown in Figure 3.7. Reactivity: **green** and **red** indicate >10% and <10% reactivity. Clones that expanded to > 10<sup>6</sup> cells are shown in **green**. \*Indicates sister clones with identical TCRs.



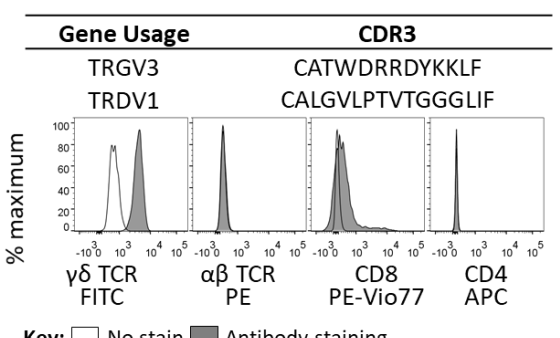
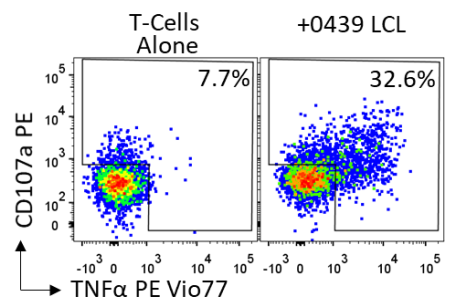
### A Donor BB67 clone SW.6B10



### B Donor 0439 clone SW.11H7



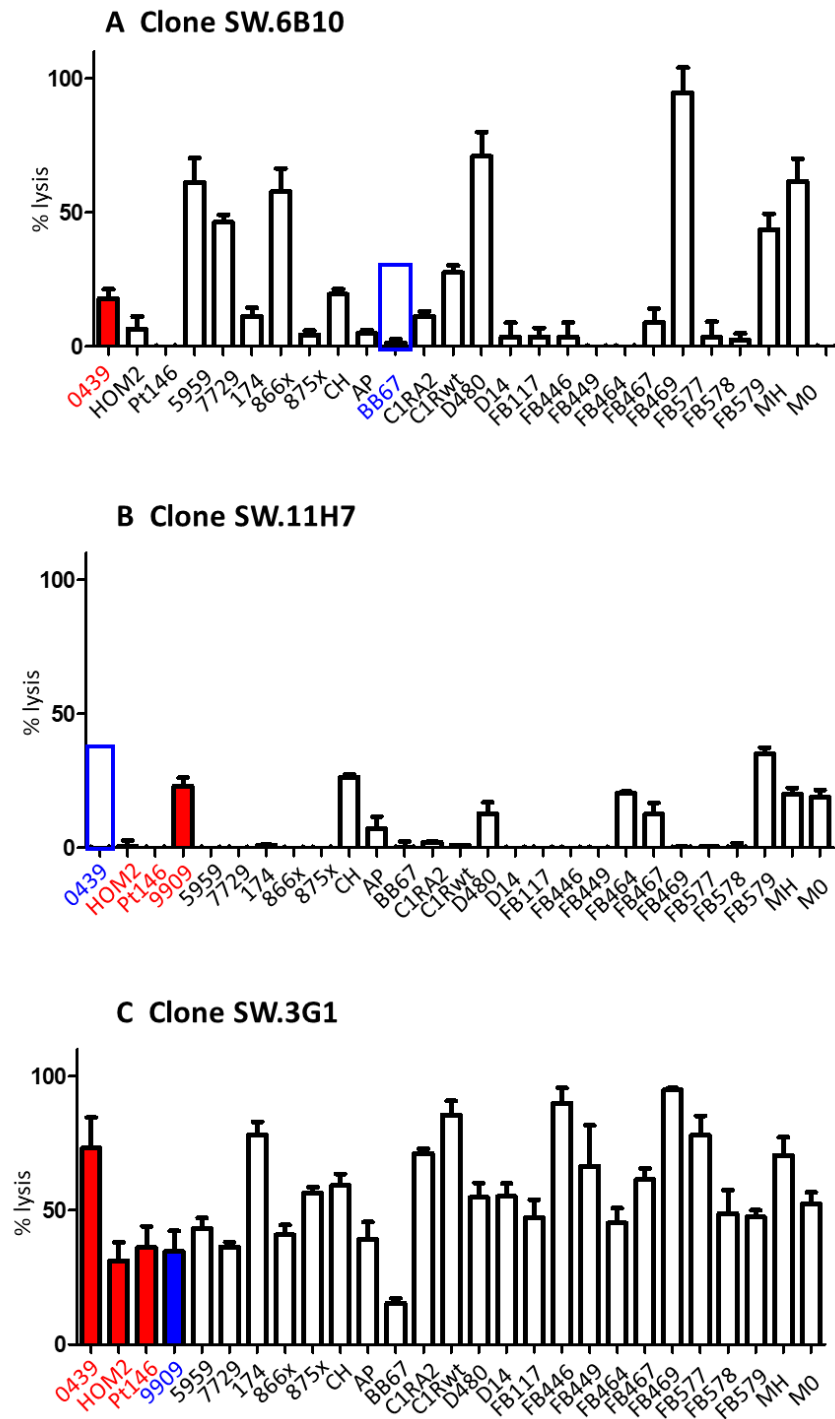
### C Donor 9909 clone SW.3G1



Key:  No stain  Antibody staining

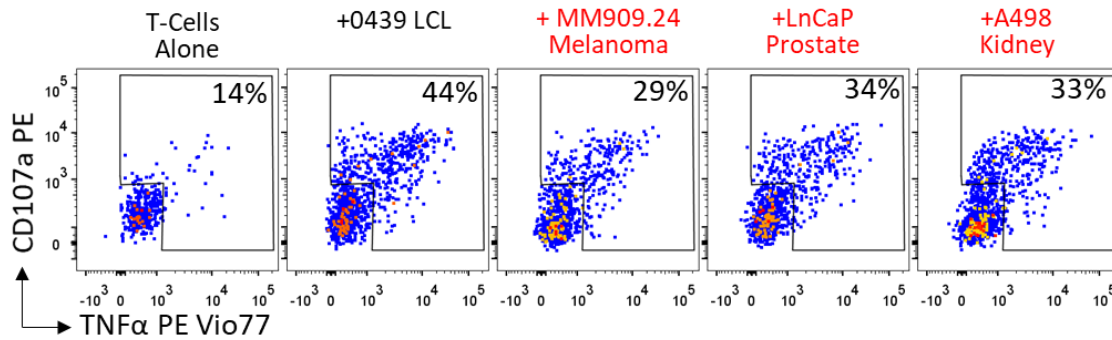
**Figure 3.6: The procurement and characterisation of  $\gamma\delta$  T-cell clones reactive to EBV immortalised B-cells.** Clones SW.6B10 (A), SW.11H7 (B) and SW.3G1 (C) were derived from  $\gamma\delta$  T-cell lines from donors BB67, 0439 and 9909, respectively. Clones were tested for activation in a TAPI-0/CD107 assay (left panel). Viable CD3<sup>+</sup> cells were gated and displayed as TNF $\alpha$  versus CD107a. Percentage of activated cells is displayed. Results displayed are one representative experiment. 10 independent experiments were done. Sequencing of the T-cell receptor (TCR) variable (V)  $\gamma$  (G) and  $\delta$  (D) chains were carried out to confirm clonality (right panel). The amino acid sequence of the complementary determining region (CDR) 3 is displayed for each TCR chain. Phenotypic analysis of each clone was carried out (right panel). Viable CD3<sup>+</sup> cells were gated and displayed as various surface markers against a no stain control.



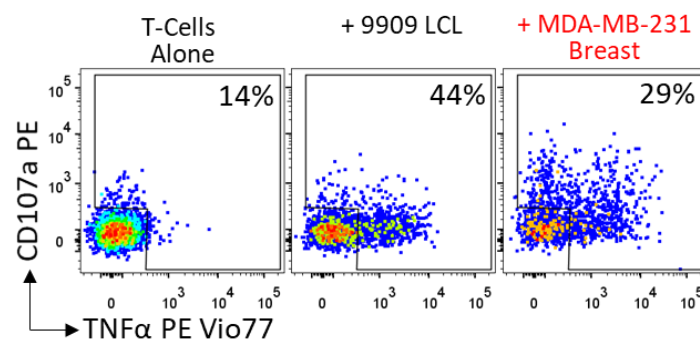


**Figure 3.7: EBV immortalised B-cell killing by clones SW.6B10 (A), SW.11H7 (B) and SW.3G1 (C).** Bar charts show the percentage lysis of indicated EBV immortalised LCL in a 6.5 h chromium release assay at an E:T ratio of 10:1 by each clone. **Red bars** indicate LCL lines the clones were primed on and **blue bars** indicate autologous LCL. Results are displayed as the mean  $\pm$  s.d. of triplicates from one representative experiment. Two independent experiments were done.

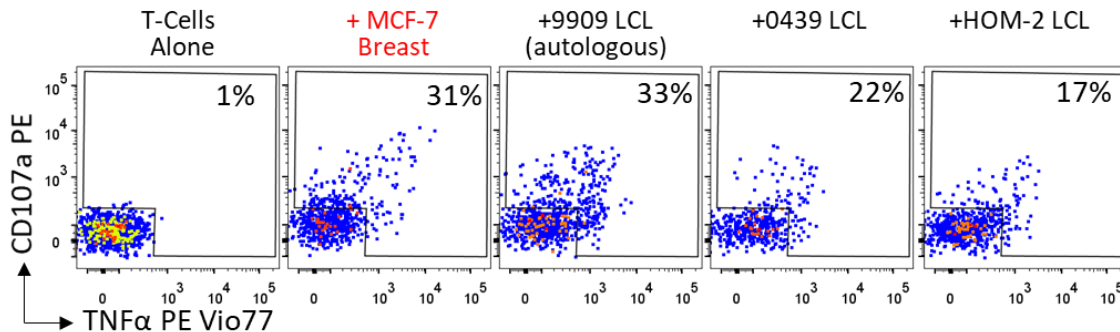
### A Clone SW.6B10 (donor BB67)



### B Clone SW.11H7 (donor 0439)



### C Clone SW.3G1 (donor 9909)

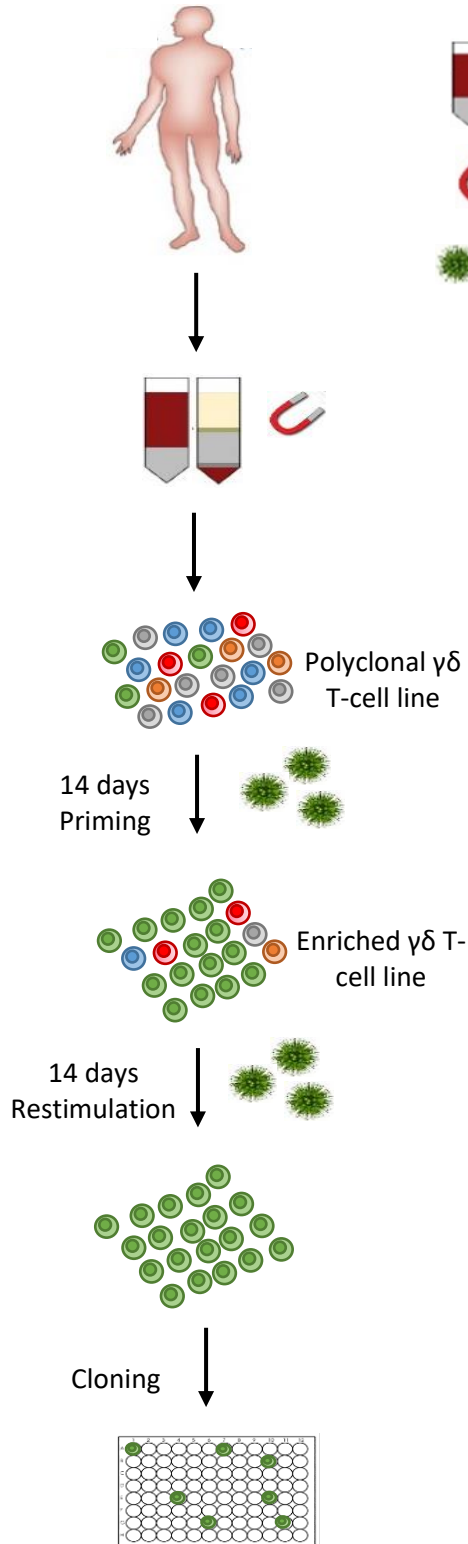


**Figure 3.8:  $\gamma\delta$  T-cell clones generated using EBV immortalised B-cells recognize cancer cells.** Recognition of indicated cancer cell lines by  $\gamma\delta$  T-cell clones SW.6B10 (A), SW.11H7 (B) and SW.3G1 (C) in a TAPI-0/CD107 activation assay. All three clones were tested against the non-autologous LCLs that were used for priming and the cancer cell lines shown (red text). Viable CD3<sup>+</sup> cells were gated and stained for TNFα and CD107a. The percentage of activated cells within the indicated gates is shown. Data displayed as one representative experiment. Three independent experiments were done.

### 3.3 Discussion

I generated an optimised protocol for procuring tumour reactive V $\delta$ 2<sup>neg</sup>  $\gamma\delta$  T-cell clones from peripheral blood of healthy donors using allogenic LCL priming (Figure 3.9). CMV-infected cells failed to elicit robust  $\gamma\delta$  T-cell responses from whole PBMC. This may be due to the varied and well-known capacity of wild type strains CMV to evade T-cell immunity as recently reviewed (Wilkinson et al. 2015). Previous successful attempts to grow hCMV-reactive  $\gamma\delta$  T-cells have used deletion strains that have attenuated ability to evade T-cell responses. By way of example, the studies that characterised EPCR as a  $\gamma\delta$  T-cell ligand used the hCMV strain TB40/E that lacks many genes involved in hCMV immune escape including those that down-regulate MHC (Sinzger et al. 2008). In future studies, it could be advantageous to use hCMV strains such as TB40/E that exhibit attenuated immune suppression capabilities. An alternative approach might involve using patient samples following hCMV-reactivation induced following organ transplantation. Transplant recipient patients can have up to 50% V $\delta$ 2<sup>neg</sup>  $\gamma\delta$  T-cells in peripheral blood, compared with <1% in healthy donors (Déchanet et al. 1999; Halary et al. 2005; Willcox et al. 2012; Farnault et al. 2013). Such a high enrichment of V $\delta$ 2<sup>neg</sup>  $\gamma\delta$  T-cells could enable direct *ex vivo* isolation of viral reactive cells. Due to the failure of the generation of CMV-reactive V $\delta$ 2<sup>neg</sup>  $\gamma\delta$  T-cells I next explored the use of a different herpesvirus; EBV.

PBMC priming with autologous LCL resulted in a large outgrowth of CD8<sup>+</sup> $\alpha\beta$ TCR<sup>+</sup> T-cells, which dwarfed a minor  $\gamma\delta$  T-cell subset. This was unsurprising given the existence of memory populations of  $\alpha\beta$  T-cells reactive to EBV in peripheral blood of EBV<sup>+</sup> donors (Murray et al. 1992; Landais et al. 2005). To increase the chances of procuring viral specific V $\delta$ 2<sup>neg</sup>  $\gamma\delta$  T-cells I next decided to use purified  $\gamma\delta$  T-cell populations *ex vivo* for LCL priming with non-autologous LCL. This approach generated EBV reactive V $\delta$ 2<sup>neg</sup>  $\gamma\delta$  T-cell lines from all three donors. A monoclonal V $\delta$ 2<sup>neg</sup>  $\gamma\delta$  T-cell was grown from each donor, and shown to react to tumour and LCL. These three clones were taken forward for further characterisation. Clone SW.3G1 recognized all LCL tested and forms the basis of Results Chapter 4, whilst clones SW.6B10 and SW.11H7 appeared to recognize a pattern of LCL and are featured in Results Chapter 5.



**Figure 3.9: An optimised protocol for the procurement of tumour-reactive, rare V $\delta$ 2-  $\gamma\delta$  T-cells from peripheral blood using EBV immortalised LCL.** PBMC from healthy donors were magnetically sorted to generate polyclonal  $\gamma\delta$  T-cell lines. Irradiated non-autologous Epstein-Barr Virus (EBV) immortalised B-cells (LCL) were used to prime reactive T-cells for 14 days to generate an T-cell line enriched for LCL-reactive  $\gamma\delta$  T-cells. A further 14 days restimulation with irradiated LCL resulted in a more enriched  $\gamma\delta$  T-cell line. Cloning by limiting dilution was used to generate monoclonal  $\gamma\delta$  T-cell populations prior to confirmation of reactivity, phenotypic, clonotypic and functional characterisation.

## 4 Whole genome CRISPR/Cas9 gene editing identifies a novel $\gamma\delta$ T-cell ligand

### 4.1 Introduction

$\gamma\delta$  T-cells play a key role in immune surveillance by the recognition of ubiquitous stress moieties independent of MHC. Thus,  $\gamma\delta$  T-cells and their T-cell receptors could prove to be the basis of a new generation of pan-population cancer immunotherapies (reviewed in Chapter 1.5). Currently, the application of  $\gamma\delta$  T-cells in immunotherapy is hampered by our lack of understanding of  $\gamma\delta$  T-cell biology, especially in terms of proven  $\gamma\delta$  TCR ligands. Therefore, the identification of  $\gamma\delta$  TCRs with specificities for novel cancer cell-expressed stress ligands is of considerable interest to the field. In this chapter I describe the use of whole genome CRISPR/Cas9 technology to identify a cell surface protein that was required for recognition cancer targets by the V $\delta$ 1<sup>+</sup>  $\gamma\delta$  TCR from the T-cell clone SW.3G1, which I identified in Chapter 3.

#### 4.1.1 The discovery of $\gamma\delta$ T-cell ligands

The characterisation of novel  $\gamma\delta$  TCR ligands has required innovative, complex approaches. Vavassori and colleagues identified BTN3A1 as a necessary component for phosphoantigen recognition by V $\gamma$ 9V $\delta$ 2 T-cells by using simultaneous chromosome gene editing techniques in mouse-human hybrid T-cells (Vavassori et al. 2013). An alternative methodology was developed, whereby laboratory mice were immunized with cancer cells recognized by  $\gamma\delta$  T-cell clones. Antibodies were generated from the immunised mice and were tested for their ability to block the interaction between  $\gamma\delta$  T-cells and cancer cells. If blocking was successful the antibodies were used for immunoprecipitation and identification of the ligands EPCR and annexin A2 (Willcox et al. 2012; Marlin et al. 2017). Although the aforementioned approaches proved successful the advent of CRISPR/Cas9 technology has provided a powerful means of conducting forward genetic screens for ligand identification.

CRISPR/Cas9 technology has resulted from the clever manipulation of a naturally occurring mechanism in archae and bacteria to evade viral infection (Horvath and Barrangou 2010). A short, 20 nucleotide long, guide RNA (gRNA) is designed to be complimentary against a gene to be targeted and inserted into a backbone under the control of the U6 promoter and containing a cas9 gene (Cho et al. 2013). Such gRNAs are transduced into target cells in a 2<sup>nd</sup> generation lenti-virus system, and whenever DNA complimentary to the gRNA is recognised, double stranded breaks are made (Mali et al. 2013). Resulting non-homologous end joining, as well as

random insertions and deletions, results in bi-allelic disruption of the gene targeted by the specific gRNA (Richter et al. 2013). Recent advancements in CRISPR/Cas9 technology have resulted in the development of libraries which target whole genomes (Shalem et al. 2014). With guidance from my supervisor Professor Sewell and collaboration with Doctor John Phillips at the University of Utah I made use of whole genome CRISPR/Cas9 technology to study clone SW.3G1.

#### 4.1.2 The use of whole genome CRISPR/Cas9 technology to identify novel T-cell ligands

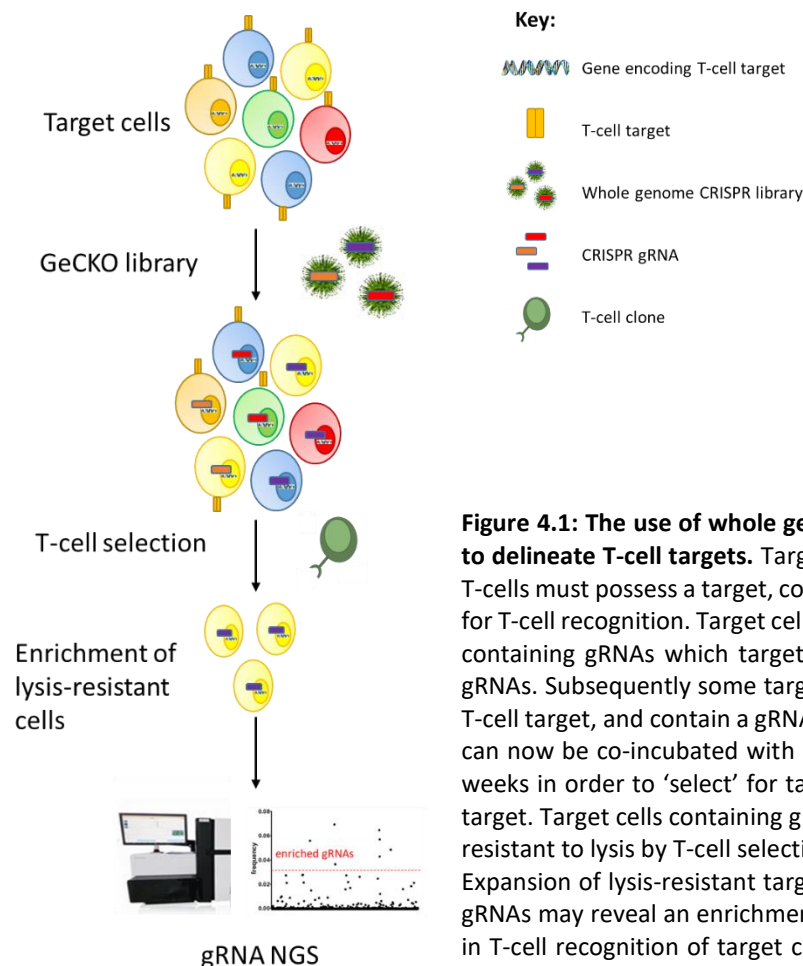
Whole genome CRISPR/Cas9 (GeCKO) technology has revolutionized the use of forward genetic screens to identify novel genes involved in cellular processes and signalling pathways in haploid mammalian cell lines. Forward genetic screens create cellular libraries with a mutation of a single gene per cell, allowing for an unbiased screening of essential genes involved in a particular process (Moresco et al. 2013). Zhang and colleagues initially designed a genome-scale CRISPR/Cas9 knockout (GeCKO) library that targeted 18,080 genes with 64,751 unique guide sequences by lentiviral delivery (Shalem et al. 2014). Such GeCKO libraries have been used to identify known and novel genes involved in viral infection in human cells (Kim et al. 2017), determine antigen specificity of a monoclonal antibody (Zotova et al. 2016), identify proteins in multiple myeloma responsible for drug resistance (Shi et al. 2017a), identify the cellular receptor for *Clostridium difficile* (Yuan et al. 2015), screen for regulators of protein stability (Wu and Kang 2016) identify oncogenic driver mutations (Kiessling et al. 2016), and to highlight key genes involved in CD8 T-cell targeting of melanoma cells (Patel et al. 2017). Due to the targeting of all human genes GeCKO screens have the potential to unveil important genes involved in T-cell immunity (Figure 4.1). Other members of my laboratory, including Dr. Mateusz Legut and Michael Crowther have used the GeCKO screens to reveal genes involved in target cell recognition by HLA and MR1 restricted T-cells (unpublished). I applied this methodology to identify a novel stress ligand of the  $\gamma\delta$  T-cell clone SW.3G1.

#### 4.1.3 Aims and Objectives

The aim of my thesis was to identify ligands for broadly tumoricidal V $\delta$ 2<sup>neg</sup>  $\gamma\delta$  T-cells. In this chapter I describe the initial characterisation of the TCR ligand of the V $\delta$ 2<sup>neg</sup>  $\gamma\delta$  T-cell clone SW.3G1 identified in Chapter 3 using whole genome CRISPR/Cas9 techniques. Specifically, the objectives of this chapter were to:

1. Fully characterise clone SW.3G1
2. Generate GeCKO target cell libraries resistant to SW.3G1 mediated lysis
3. Sequence the above GeCKO libraries to identify gRNA enrichments to identify possible T-cell targets

4. Validate identified genes in knock-out and knock-in experiments
5. Confirm recognition of target ligands is via the TCR using TCR transduction techniques.

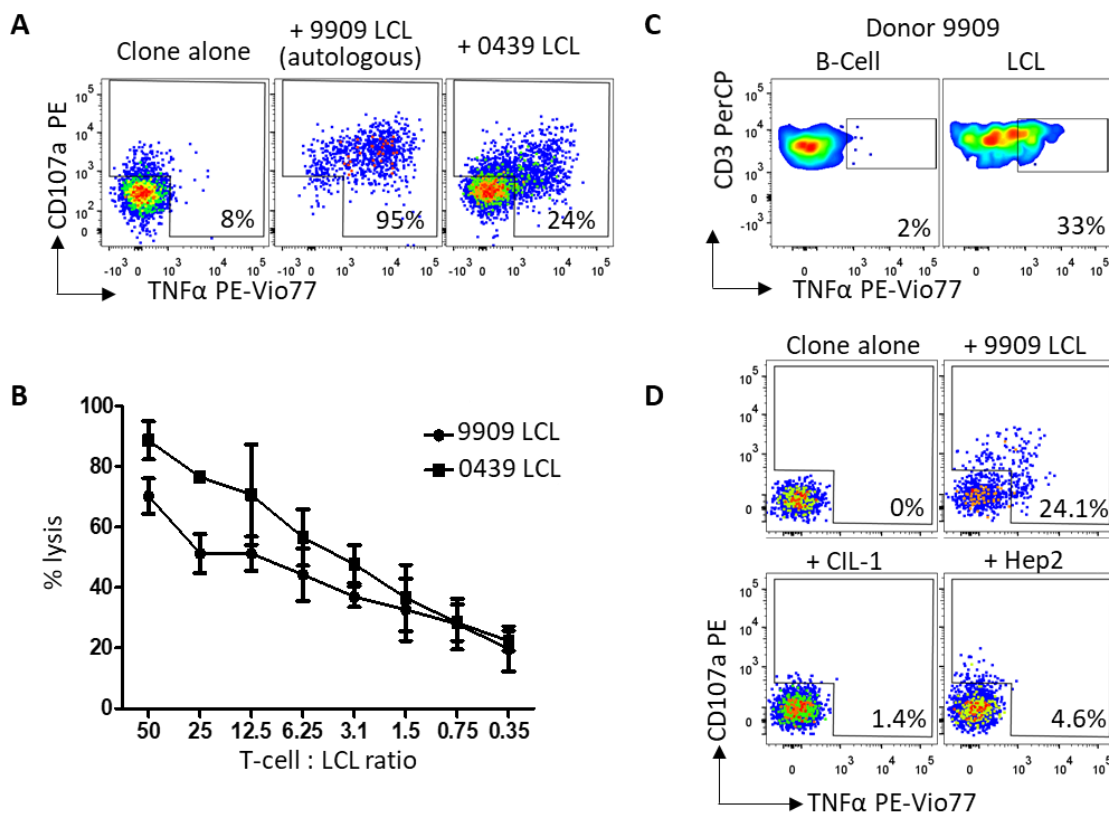


## 4.2 Results

### 4.2.1 SW.3G1 recognised LCL and tumour cells

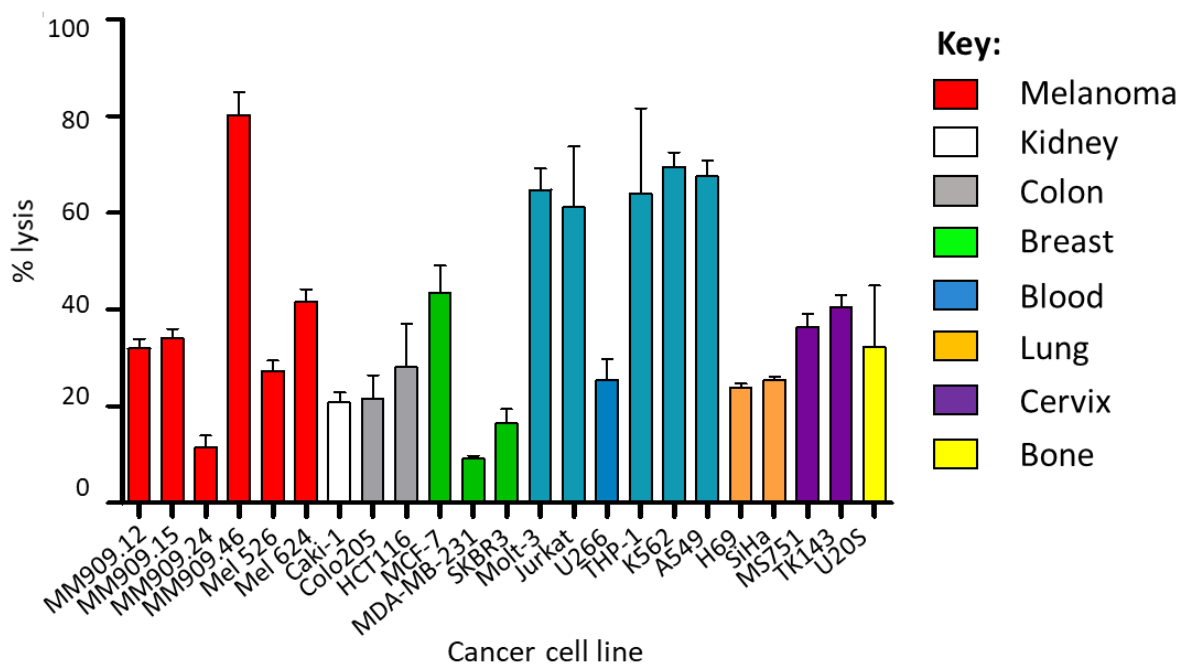
SW.3G1 is a Vy3Vδ1 T-cell clone isolated from an LCL primed line from donor 9909 (Chapter 3.2.2). After SW.3G1 was shown be a pan-LCL killer (Figure 3.8, pg 76), it was postulated that the TCR recognizes a stress ligand found on the surface of all LCL. After confirming the recognition (Figure 4.2A) and lysis (Figure 4.2B) of autologous and non-autologous LCL, I next screened SW.3G1 against healthy cells. Primary, magnetically sorted B-cells were used alongside EBV immortalised LCL in a 4 h TAPI-0 assay at an E:T of 1:1. SW.3G1 was reactive to LCL (33% TNFα<sup>+</sup>) but not to primary B-cells (2% TNFα<sup>+</sup>) (Figure 4.2C), indicating that SW.3G1 preferentially targets

EBV immortalised cells. Furthermore, SW.3G1 did not respond to the healthy cell lines non-pigmented ciliary epithelium (CIL) and hepatocyte 2 (HEP2) (Figure 4.2D). Next a diverse panel of tumour cell lines from different tissue origins was assembled and screened for lysis by SW.3G1 in a cytotoxicity chromium release assay (Figure 4.3). Following 6.5 h co-incubation with cancer cells at an E:T of 1:1, SW.3G1 lysed all cancer cells it was screened against. Such data indicated that SW.3G1 recognised a ligand associated with EBV immortalisation and cellular transformation that is not found on the surface of healthy cells. As no HLA was shared between recognised targets, recognition was deemed to be non-HLA restricted and to occur by a population-conserved, cancer-specific antigen. This finding made SW.3G1 a very interesting T-cell.



**Figure 4.2: Clone SW.3G1 recognizes Epstein Barr Virus (EBV) immortalized B-cells but not healthy cells.** (A) Reactivity of SW.3G1 to LCL as tested by TAPI-0/CD107 assay. Viable CD3<sup>+</sup> cells are gated and displayed as CD107a versus TNFα (n=10). (B) 6.5 h chromium release cytotoxicity assay using the same LCLs as in (A). Results are displayed as the mean ± s.d. of triplicates from one representative experiment (n=2). (C) Autologous healthy B-cells magnetically purified directly *ex-vivo* from donor 9909 were used in activations assays as in A, with 9909 LCL used as a positive control for activation (n=2). (D) Activation assays as in A, using 9909 LCL and the healthy cell lines, CIL-1 (non-pigmented ciliary epithelium) and Hep2 (hepatocyte) (n=2). Percentage of gated cells is shown. Results displayed as one representative example. n=number of independent experiments.



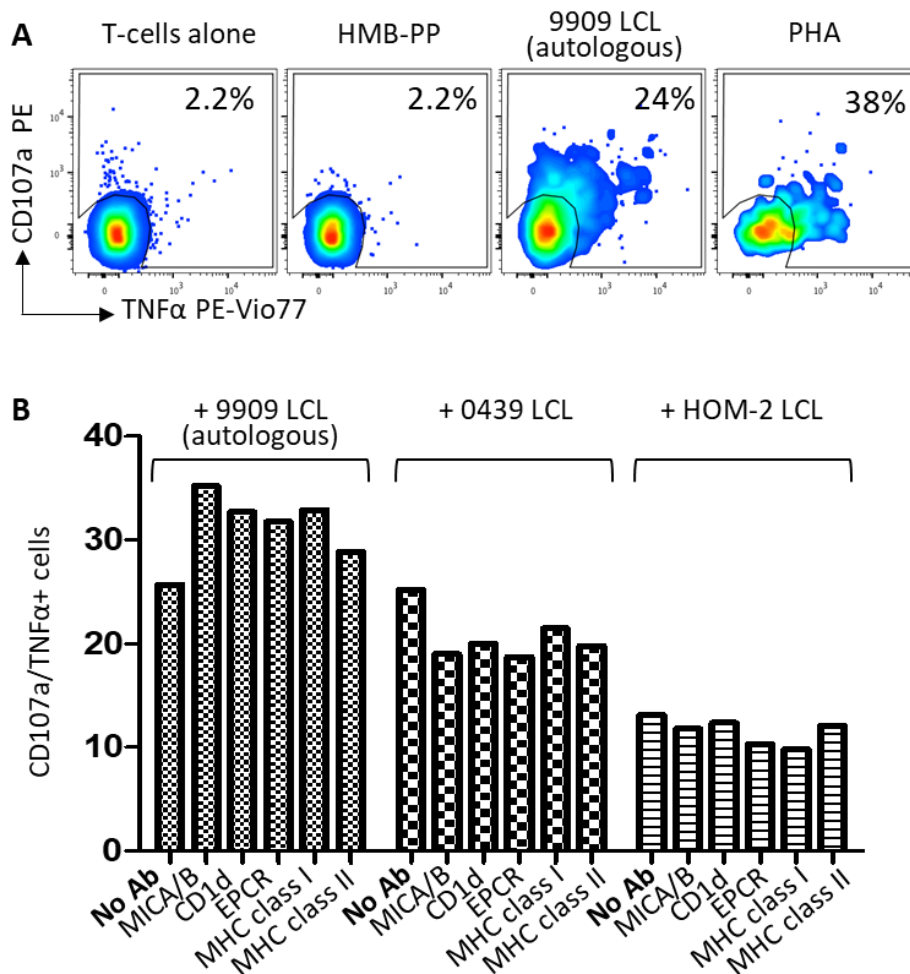


**Figure 4.3: Clone SW.3G1 kills a wide range of cancer cell types.** SW.3G1 was used in 6.5 h chromium release cytotoxicity assays at T-cell to target cell ratio of 1:1. A panel of cancer cell lines (named on the x-axis) of different tissue origin (key). Results are displayed as the mean  $\pm$  s.d. of triplicates from one representative experiment. Six independent experiments were done.

SW.3G1 did not recognise the known V $\gamma$ 9V $\delta$ 2 TCR ligand HMBPP (Figure 4.4A). Furthermore, blocking antibodies included for known  $\gamma\delta$  ligands MICA/B, CD1d and EPCR did not reduce SW.3G1 recognition of target LCLs 9909, 0439 and HOM-2 (Figure 4.4B). Although not an extensive exclusion process of known  $\gamma\delta$  T-cell ligands, these data suggested that SW.3G1 was possibly recognising target cells through a novel ligand.

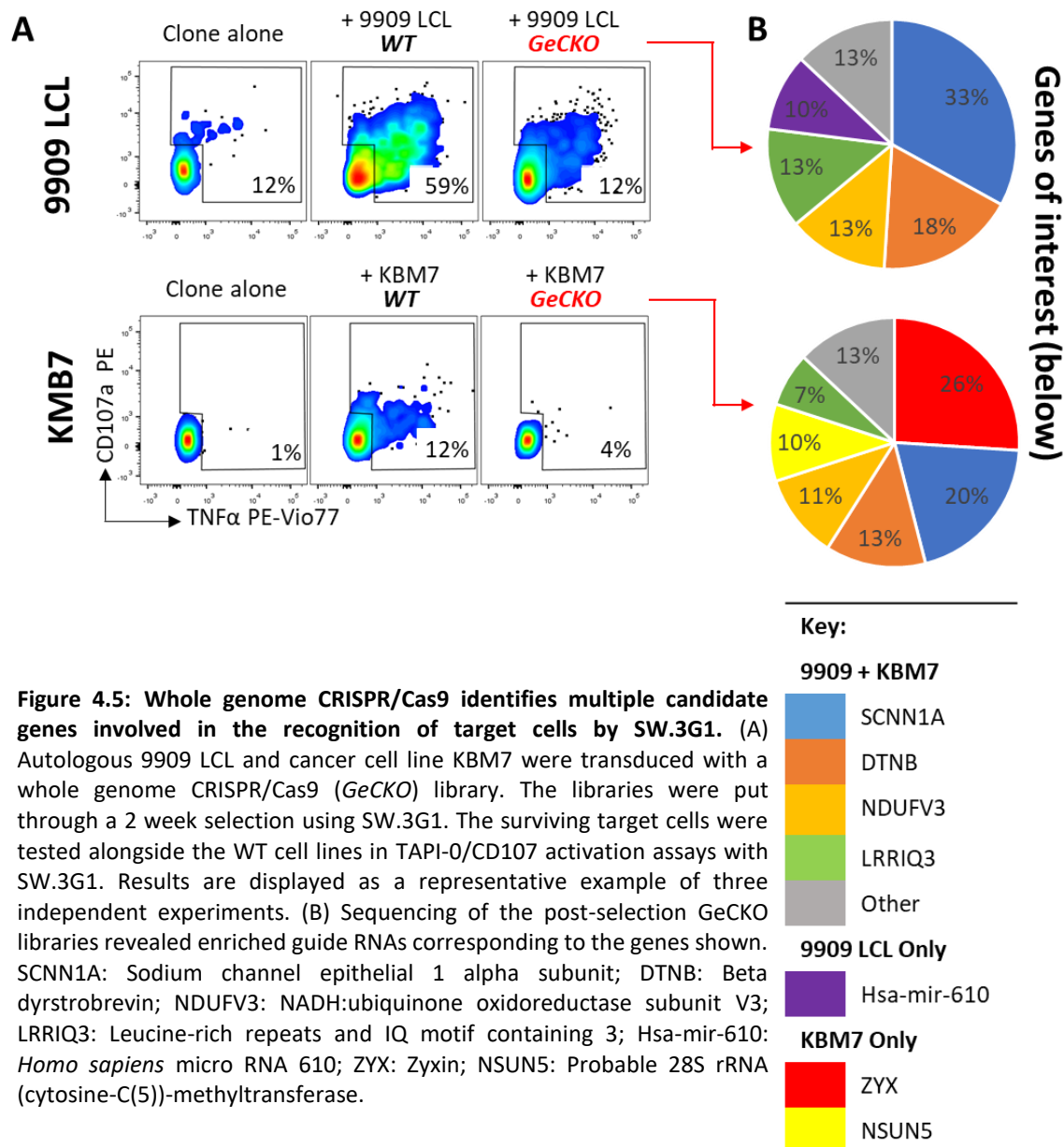
#### 4.2.2 Whole genome CRISPR/Cas9 libraries identified a novel $\gamma\delta$ T-cell ligand

The GeCKO v2 library, pioneered in the Zhang laboratory and kindly provided as validated lentivirus by Professor John Phillips (University of Utah), was used throughout this chapter. The GeCKO library consisted of sub-libraries -A and -B, with each containing three unique gRNAs targeting the 5' regions of conserved, protein-coding exons of all human genes (Shalem et al. 2014). Sub library A also contained four gRNAs targeting micro-RNA (miRNA), and 1,000 gRNAs targeting non-coding genes (acting as internal controls). I used these libraries as lentivirus to transduce target cell lines KBM7 (haploid leukaemia) and the 9909 autologous LCL.



**Figure 4.4: SW.3G1 did not recognize known  $\gamma\delta$  T-cell ligands.** (A)  $\gamma\delta$  SW.3G1 clone was co-incubated for 4 h with HMB-PP, 9909 LCL and phytohaemagglutinin (PHA) and measured for activation by TAPI-0/CD107 assay. The percentage of activated cells shown above the gated cells. Data displayed as one representative example from three independent experiments. (B) Using the same activation assay as in (A), SW.3G1 was incubated with LCLs that had been pre-labelled with antibodies (Abs) that bind the proteins named on the x-axis. The percentage of reactivity is shown graphically (y-axis). MICA/B (Major Histocompatibility Complex (MHC) Class-I related chain A/B) and EPCR (Endothelial protein C receptor). Anti-MHC class I and II Abs were included also included.




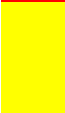
GeCKO transduced target cells were co-incubated with SW.3G1 at an E:T of 0.5 for 14 days. Dead cells and debris were removed and surviving target cells were screened for resistance to SW.3G1 recognition. Only target cells from GeCKO sub-library A survived the screening process. SW.3G1 was 47% and 33% less reactive to GeCKO sub-library A selected 9909 LCL and KBM7 when compared with the untransduced 9909 LCL and KBM7 cells, respectively (Figure 4.5A). Surviving target cells were expanded to a minimum of 30 million and used for genomic DNA extraction and subsequent PCR. The gRNA representation in selected libraries was determined by next generation sequencing courtesy of Dr Meriem Attaf and Cristina Rius from my research group.



**Figure 4.5: Whole genome CRISPR/Cas9 identifies multiple candidate genes involved in the recognition of target cells by SW.3G1.** (A) Autologous 9909 LCL and cancer cell line KMB7 were transduced with a whole genome CRISPR/Cas9 (*GeCKO*) library. The libraries were put through a 2 week selection using SW.3G1. The surviving target cells were tested alongside the WT cell lines in TAPI-0/CD107 activation assays with SW.3G1. Results are displayed as a representative example of three independent experiments. (B) Sequencing of the post-selection *GeCKO* libraries revealed enriched guide RNAs corresponding to the genes shown. *SCNN1A*: Sodium channel epithelial 1 alpha subunit; *DTNB*: Beta dystrobrevin; *NDUFV3*: NADH:ubiquinone oxidoreductase subunit V3; *LRRIQ3*: Leucine-rich repeats and IQ motif containing 3; *Hsa-mir-610*: *Homo sapiens* micro RNA 610; *ZYX*: Zyxin; *NSUN5*: Probable 28S rRNA (cytosine-C(5))-methyltransferase.

Both the KMB7 tumour cell line and 9909 LCL contained gRNA enrichments for the genes *SCNN1A*, *DTNB*, *NDUFV3* and *LRRIQ3* (Figure 4.5B). gRNA enriched for *hsa-mir-610* were only found in the 9909 LCL library, and gRNA enrichments for *ZYX* and *NSUN5* were only found in the KMB7 library. Given that there was a high enrichment for *SCNN1A* gRNA in both 9909 LCL and KMB7 (forming a third and fifth of enriched gRNAs in each library, respectively), and that the *SCNN1A* protein is expressed on the surface and known to be associated with cancer and viral infection (Del Monaco et al. 2009; Kapoor et al. 2009; Steinmann and Pietschmann 2010; Nieto-Torres et al. 2015), the *SCNN1A* gene became the focus of my studies following advice from my supervisory team. A summary of all the genes identified by gRNA enrichments can be found in Table 4.1.

**Table 4.1: An overview of genes identified in tumour and LCL GeCKO libraries**

<b>Key:</b> <b>9909 LCL + KBM7</b>		<b>Role</b>	<b>Cellular location</b>	<b>EBV/cancer association?</b>	<b>Ref</b>
	SCNN1A	Sodium channel regulation	Surface membrane	Yes	(Hanukoglu and Hanukoglu 2016)
	DTNB	Sarcomere: membrane contact	Intracellular	ND	(Blake et al. 1998)
	NDUFV3	Subunit of NADH respiratory complex	Intracellular	ND	(de Coo et al. 1997)
	LRRIQ3	ND	Intracellular	ND	(Watanabe et al. 2014)
<b>9909 LCL Only</b>					
	Hsa-mir-610	ND	Intracellular	Yes	(Wang et al. 2012)
<b>KBM7 Only</b>					
	ZYX	Cytoskeletal organisation	Intracellular	Yes	(van der Gaag et al. 2002)
	NSUN5	Methyltransferase	Intracellular	ND	(Schosserer et al. 2015)

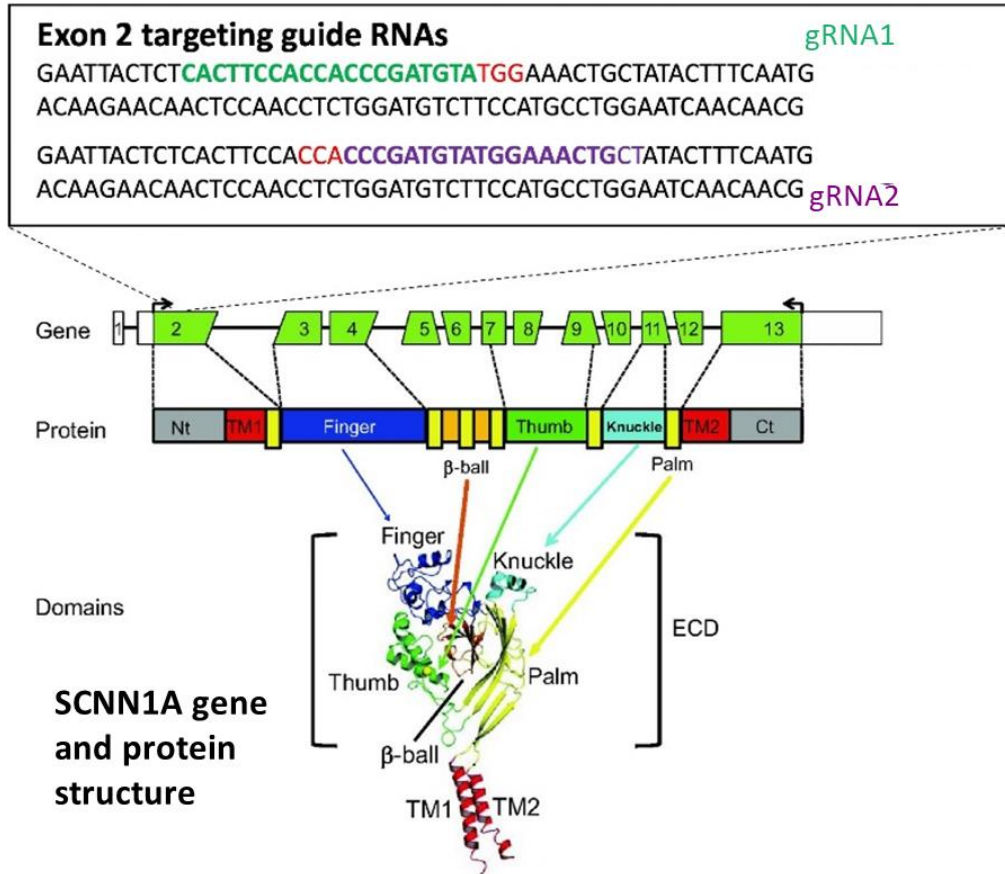
SCNN1A: Sodium channel epithelial 1 alpha subunit; DTNB: Beta dystrobrevin; NDUFV3: NADH:ubiquinone oxidoreductase subunit V3; LRRIQ3: Leucine-rich repeats and IQ motif containing 3; Hsa-mir-610: *Homo sapiens* micro RNA 610; ZYX: Zyxin; NSUN5: Probable 28S rRNA (cytosine-C(5))-methyltransferase; ND: not defined.

#### 4.2.3 SCNN1A: a $\gamma\delta$ T-cell target

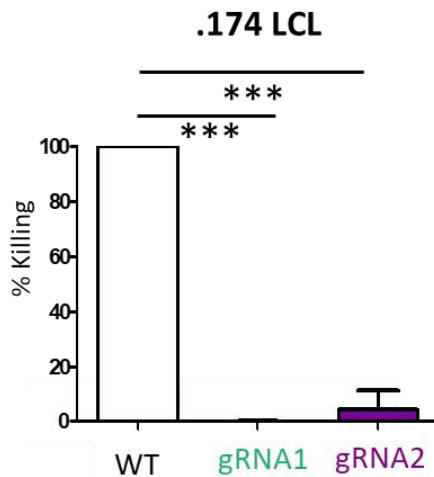
Human SCNN1A protein (protein aliases alpha ENaC-2; Alpha-ENaC;  $\alpha$ ENaC; Alpha-NaCH; amiloride-sensitive epithelial sodium channel alpha subunit; Amiloride-sensitive sodium channel subunit alpha; amiloride-sensitive sodium channel subunit alpha 2; ENaCalpha; Epithelial a (+) channel subunit alpha; Epithelial Na(+) channel subunit alpha; FLJ21883; nasal epithelial sodium channel alpha subunit; Nonvoltage-gated sodium channel 1 subunit alpha; SCNEA; SCNN1; sodium channel, non-voltage gated 1 alpha subunit; sodium channel, non-voltage-gated 1 alpha subunit; sodium channel, nonvoltage-gated 1 alpha) is coded for by the *SCNN1A* gene (gene aliases BESC2; ENaCa; ENaCalpha; SCNEA; SCNN1). The *SCNN1A* gene is composed of 13 exons and codes for 6 splice variants of varying lengths (Appendix Table 8.8). Isoform 1 (669 amino acids in length, 75,704 kDa in size) is considered the canonical sequence and was used in this study (Hanukoglu and Hanukoglu 2016).

There is currently no structure for SCNN1A, but studies comparing it to the structure of closely related ASIC1 have postulated that it consists of a finger, knuckle, palm, thumb, ball and trans-membrane domains (Figure 4.6A) (Hanukoglu 2017). I used two gRNAs targeting the *SCNN1A*; gRNA1 was the same one identified from the GeCKO libraries and gRNA2 was one I designed myself using an optimized CRISPR gRNA design resource (<http://crispr.mit.edu/>). Both gRNAs targeted exon 2 of the *SCNN1A* gene. I transduced the LCL line .174 with each of the gRNAs (Appendix Figure 8.3) and then set up a long term killing assay with SW.3G1 T-cells. Following 1 day co-incubation at an E:T of 1:1, SW.3G1 killed 100% of .174 WT LCL, compared with 0% and less than 5% of gRNA1 and gRNA2 knockout cells, respectively (Figure 4.6B). I next transduced the tumour cells lines MDA-MB-231 and MM909.24 with gRNA2, generating MDA-MB-231<sup>SCNN1A<sup>neg</sup></sup> and MM909.24<sup>SCNN1A<sup>neg</sup></sup>, respectively. In a long term killing assay, as above, SW.3G1 killed 63% of WT MDA-MB-231 which significantly dropped to 8% of MDA-MB-231<sup>SCNN1A<sup>neg</sup></sup> ( $p > 0.001$ , unpaired t-test) (Figure 4.7A). Similarly, SW.3G1 killed 68% of WT MM909.24, which dropped to 0% of MM909.24<sup>SCNN1A<sup>neg</sup></sup> ( $p > 0.0001$ , unpaired t-test) (Figure 4.7B). A Western blot of the MDA-MB-231 SCNN1A protein confirmed the loss of SCNN1A protein from the cells (Figure 4.7C). A protein loading control needed to be carried out alongside the measurement of SCNN1A to truly validate the SCNN1A protein downregulation, but this was a good preliminary check seen as the same number of cells and same procedure was used for all samples.

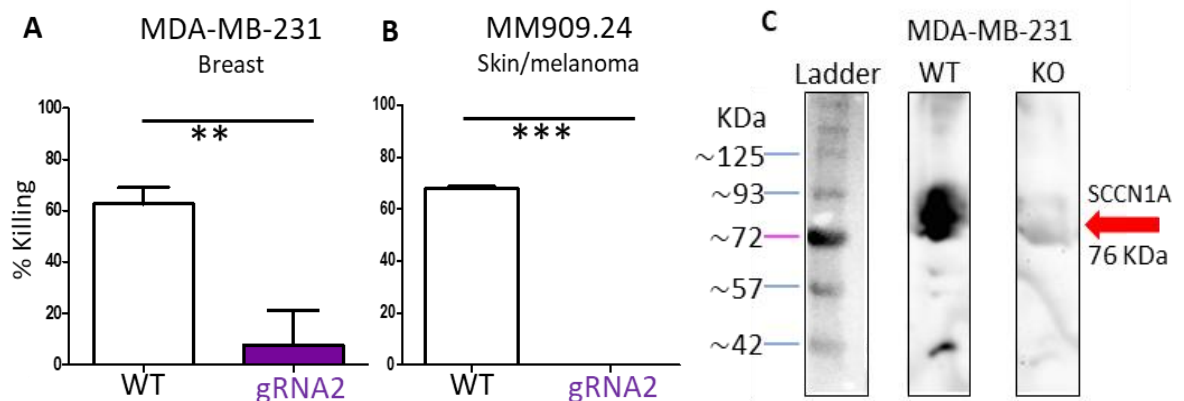
**A**



**B**



**Figure 4.6: Confirmation that candidate gene SCNN1A is involved in the recognition of LCL by SW.3G1.** (A) Schematic of the SCNN1A gene and protein, with guide RNA (gRNA) sites from the whole genome GeCKO library (**gRNA1**) and 'my' designed gRNA (**gRNA2**). (B) Long term killing assay using SW.3G1 with .174 LCL WT, gRNA1 and gRNA2 knockout 174 LCL (n=3). **Green indicates GeCKO gRNA1; purple indicates my own designed gRNA2**. Results are displayed as the mean  $\pm$  s.d. of triplicates from one representative experiment. Three independent experiments were done. \*\*\*=p<0.0005 (2 sample t-test).

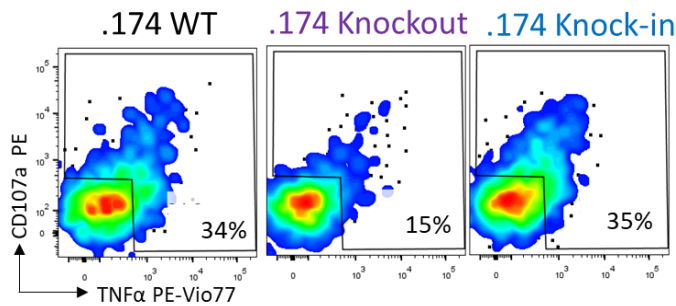


**Figure 4.7: SCNN1A is required for SW.3G1 recognition of tumours.** In long term killing assay clone SW.3G1 was co-incubated with target cell lines at an E:T of 1:1 for 24 h. Target cell lines included wild-type (WT) MDA-MB-231 (A) and MM909.24 (B) and **gRNA2 SCNN1A knockout cells**. Results are displayed as the mean  $\pm$  S.D. of triplicates from one representative experiment. Three independent experiments were done. \*\*= $p < 0.001$ , \*\*\*= $p < 0.0005$  (2 sample t-test). (C) Western blot for SCNN1A protein expression in MDA-MB-231 WT and gRNA2 knockout cells to confirm removal of protein.

#### 4.2.4 SW.3G1 did not recognise a splice variant of SCNN1A

Removal of SCNN1A from .174 cells, MDA-MB-231 and M909.24 cells ablates recognition of these cells by T-cell clone SW.3G1 (Figures 4.6B and 4.7). SCNN1A is known to be expressed by normal healthy cells but these cells are not targets for the SW.3G1 T-cell clone. Collectively, these results suggest that there must be a difference between tumour and healthy cells that is related to SCNN1A. My first hypothesis was that SW.3G1 recognised different splice variants of SCNN1A expressed on healthy versus stressed cells. To test my hypothesis, I designed a codon-optimised plasmid containing isoform 1 SCNN1A gene coding information. This allowed 'knock in' experiments with target cell lines that had been knocked out for the *SCNN1A* gene. Preliminary experiments showed that transduction of isoform 1 SCNN1A into .174 cells that had the *SCNN1A* gene disrupted increased the activation observed with SW.3G1. Unfortunately, these experiments were not the cleanest as it appeared that there was residual expression of SCNN1A in the knockout line (Appendix Figure 8.3). Nevertheless, these preliminary results suggest that isoform 1 of SCNN1A enhances recognition by the SW.3G1 clone (Figure 4.8). Later experiments using  $\alpha\beta$  T-cells transduced with the SW.3G1 TCR, gave much cleaner results with knock-in cells expressing only isoform 1 SCNN1A (see below). Due to the results using  $\alpha\beta$  T-cells transduced with the SW.3G1 TCR described later in this chapter I did not pursue experiments with the SW.3G1 clone further.





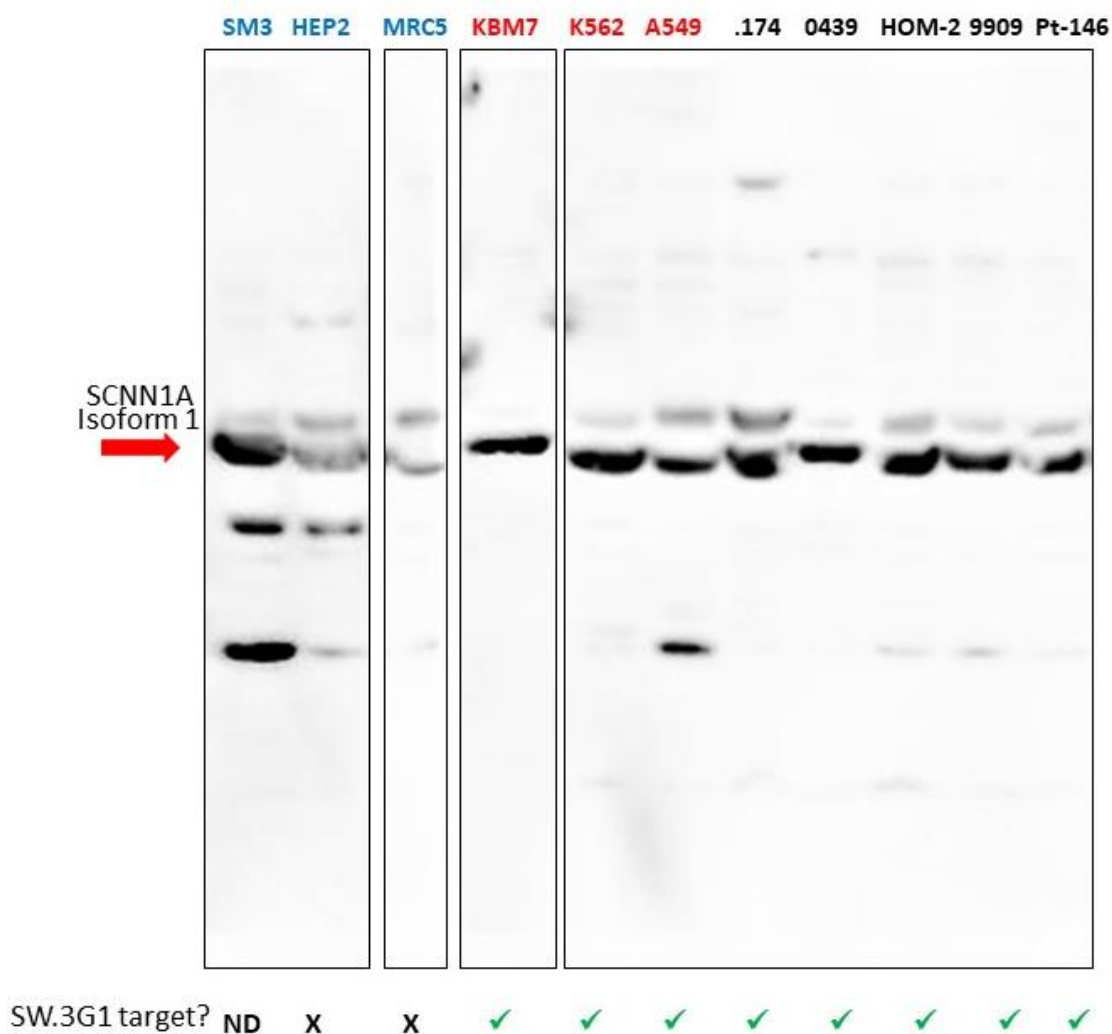
**Figure 4.8: SCNN1A expression in knockout cell lines restores recognition of target cells by SW.3G1.** Activation assay using SW.3G1 with wildtype .174 cells, gRNA2 SCNN1A knockout cells and knock in cells. Activation assessed by inclusion of TAPI-0, anti-CD107a and anti-TNFα antibodies. Percentage of gated cells is shown. Data displayed as representative example from three independent experiments. **Purple indicates gRNA2 SCNN1A knockout cells; blue indicates gRNA2 SCNN1A knockout cells which have been transduced with codon-optimized SCNN1A.**

I next hypothesised that SW.3G1 recognised isoform 1 SCNN1A protein, and not the other isoforms. Therefore I analysed non-target healthy cells (SM3, HEP2 and MRC5 cells), LCL and tumour cells lines by western blot to try and establish a pattern of isoform expression which may have accounted for SW.3G1 recognition. The antibody used in the western blot analysis targeted all six isoforms (Appendix Table 8.8). Results showed that all cell types, independent of whether they were SW.3G1 targets or not, expressed isoform 1 of the SCNN1A protein (Figure 4.9). Thus, the element that confers recognition by SW.3G1 cannot simply be expression of SCNN1A and further work will be required to pinpoint the exact nature of the ligand that it recognised by the SW.3G1 TCR.

#### 4.2.5 The SW.3G1 TCR mediates recognition of tumour cells

γδ T-cells are known to express a variety of activation receptors, such as NKG2D (Kong et al. 2009; Lanier 2015; Ribeiro et al. 2015) so it was important that I established that SW.3G1 recognised target cells via its TCR. I first sequenced the full TCR-γ and TCR-δ chains of the SW.3G1 TCR (Figure 4.10). I next magnetically sorted polyclonal CD8<sup>+</sup> αβ T-cells from donor 1 PBMC, generating 1.WT T-cell line, and co-transduced them with the protein coding regions of the SW.3G1 TCR and a CRISPR/Cas9 gRNA targeting the endogenous TCR-β chain to ablate expression of the endogenous αβ TCR, generating 1.3G1 (Legut et al. 2017). Flow cytometry confirmed that the 1.3G1 line was 93% positive for the SW.3G1 TCR (Figure 4.11A). 1.WT T-cells were set up alongside 1.3G1 TCR transduced T-cells in a TAPI-0 activation assay whereby T-cells were either incubated alone or co-incubated with the LCLs; 9909 (autologous), 0439, and Pt-146 for 5 h at an E:T of 1:1. Whilst 1.WT T-cells were unreactive to all LCL, 1.3G1 T-cells were 12%, 32% and 33% reactive to 9909, 0439 and Pt-146 LCL, respectively (Figure 4.11B). In a similar TAPI-0 activation 1.3G1 TCR transduced T-cells were 51% reactive towards tumour cell line MDA-MB-231 (Figure 4.11C), indicating that recognition of target LCL and tumour cells is via the TCR.





**Figure 4.9: Healthy, EBV immortalised and tumour cell lines all express isoform 1 SCNN1A.** Western blot analysis was carried out to analyse SCNN1A protein expression in healthy cells (blue), tumour cells (red) and LCL (black). Cell lines were defined as targets or non-targets of T-cell line SW.3G1 in TAPI-0, long term killing and cytotoxicity assay. ND= not defined.

**A**

### SW.3G1 clone V $\gamma$ 3 chain protein sequence

CDR regions are shown in bold underlined text and colour coded throughout the figure

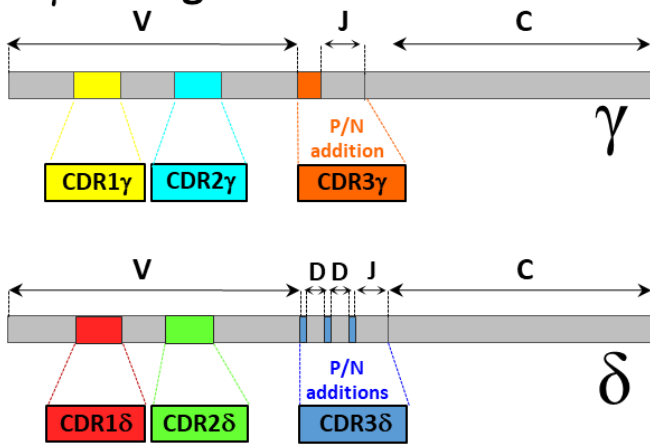
SSNLEGRTKSVTRQTGSSAEITCDLT**VTNTFY**HWYLHQEGKAPQRLLY**YDVSTARD**VLESGLSPGKYTHT  
 PRRWSWILRLQNLIENTSGVYY**CATWDRRDYKKLF**GSGTTLVVTDKQLDADVSPKPTIFLPSIAETKLQKA  
 GTYLCLEKFFPDVIKIHWQEKKSNILGSQEGNTMKTNDTYMKFSWLTVPKSLDKEHRCIVRHENNKNG  
 VDQEIIFFPIKT

### 3G1 clone V $\delta$ 1 chain protein sequence

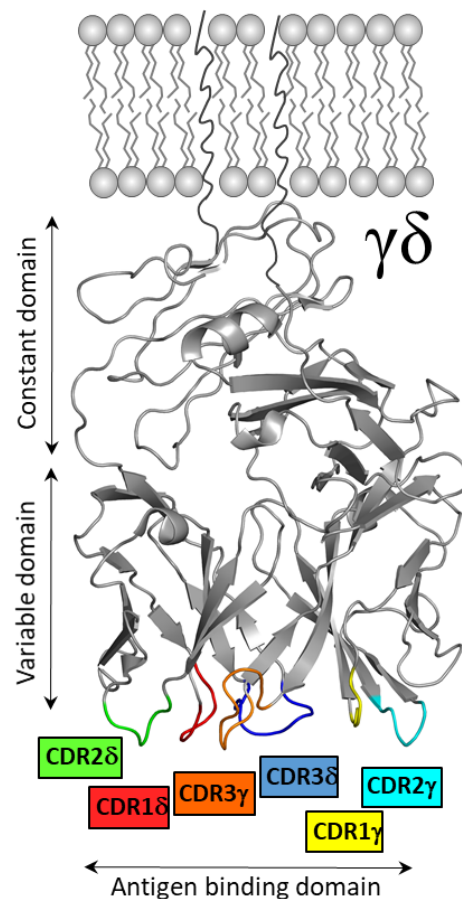
CDR regions are shown in bold underlined text and colour coded throughout the figure

AQKVTQAQSSVSMPVRKAVTLNCLYE**TSWWSYY**IFWYKQLPSKEMIFLIR**QGS**DEQNAKSGRYSVNFKK  
 AAKSVALTISALQLEDSAKYF**CALGVLPTVTGGGLIF**GKGTRVTVEPNSQPHTKPSVFVMKNGTINVACLVK  
 EFYPKDIRINLVSSKKITEFDPAIVISPSGKYNAVKLGKYEDSNSVTCSVQHDNKT VHSTDFEVKT DST

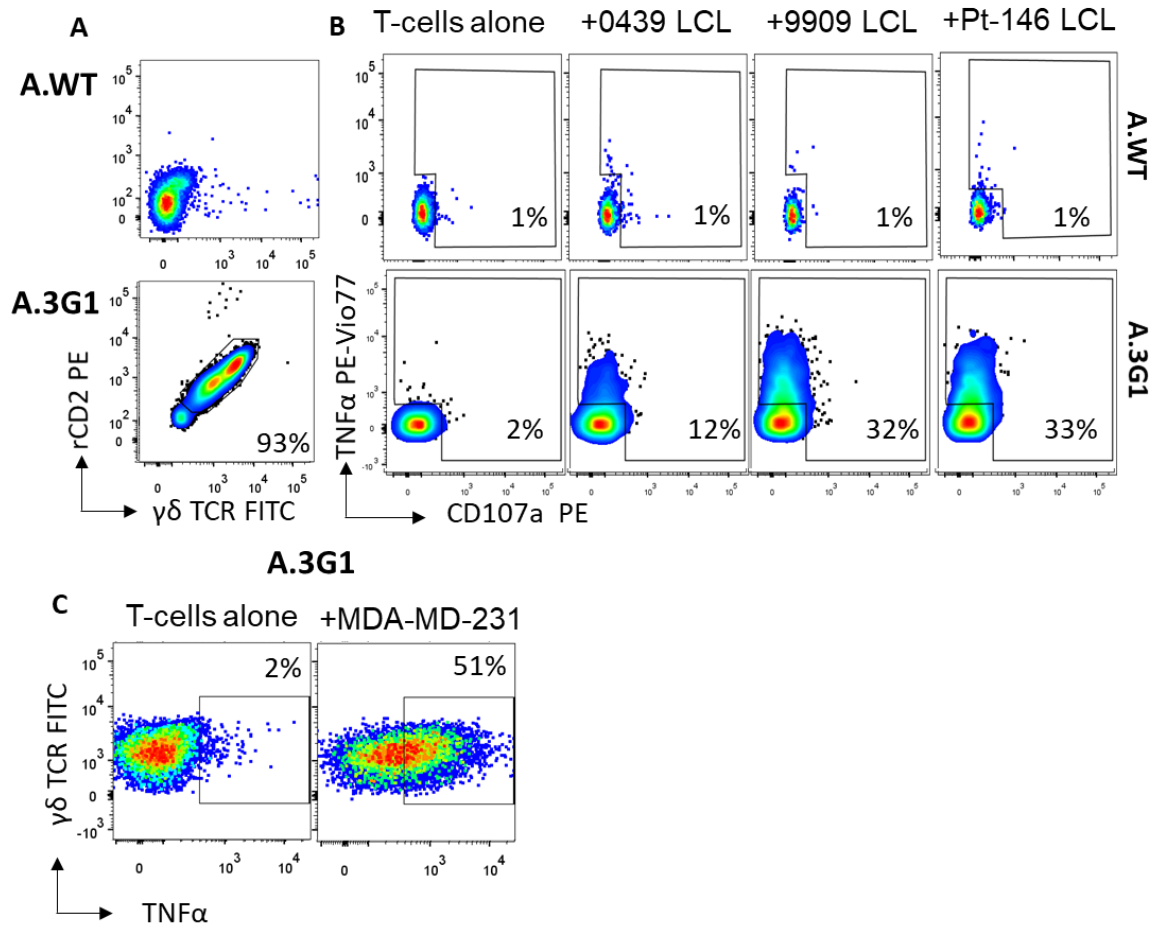
### B $\gamma\delta$ TCR gene structures



### C $\gamma\delta$ TCR protein structure



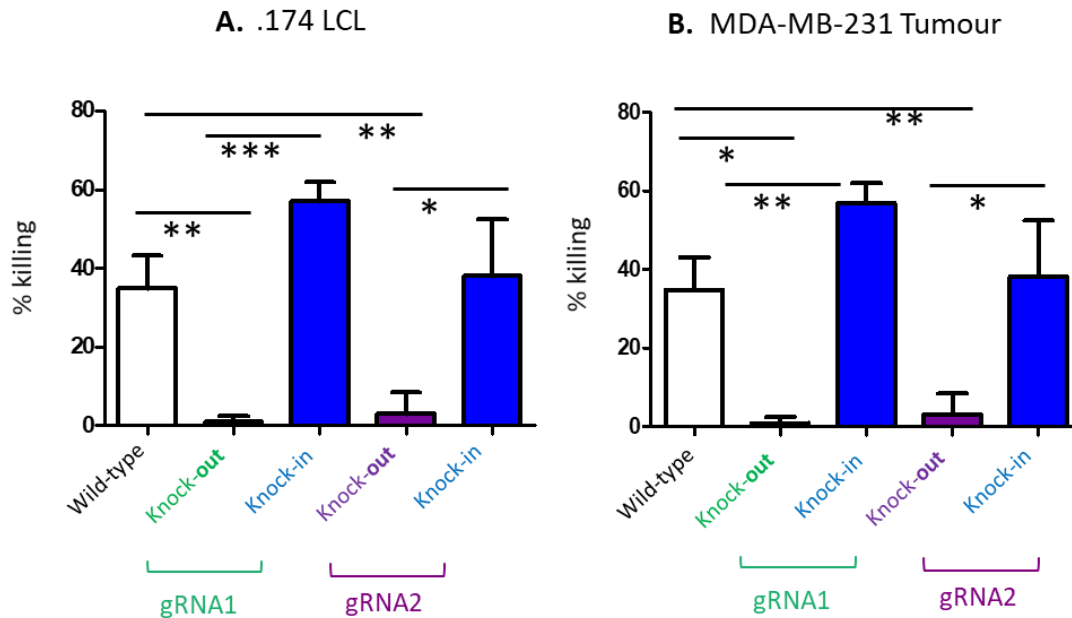
**Figure 4.10: The T-cell receptor gene and protein sequence of clone SW.3G1.** (A) The amino acid sequence of the variable (V) chains of the SW.3G1  $\gamma\delta$  TCR. (B) The mRNA structures show that for each chain complementarity-determining regions (CDR) CDR1 and CDR2 are encoded in the germline. CDR3 is the product of junctional diversity at V–J joins of T cell receptor (TCR)- $\gamma$  chain and V–D–J joins in TCR- $\delta$  chain. CDR3 is consequently hypervariable. The colour code adopted for the CDR loops is maintained throughout the figure. The areas coloured in grey represent the constant and variable domains of the TCRs (not including the hypervariable CDR loops). (C) Expected protein fold. TCRs adopt similar tertiary structures that position the CDR loops at the membrane distal end of the molecules. Together the six CDR loops form the antigen binding site.



**Figure 4.11: Recognition of target cells by clone SW.3G1 is via the TCR.** (A) CD8<sup>+</sup> T-cells 1.WT were transduced with the SW.3G1 TCR chains, generating 1.3G1 polyclonal T-cell line. Purity of the cells was checked by flow cytometry. Viable CD3<sup>+</sup> cells were gated and displayed as rCD2 versus  $\gamma\delta$  TCR. (B) Cell lines from (A) were used in TAPI-0/CD107 activation assays. Viable CD3<sup>+</sup> cells were gated and displayed as TNF $\alpha$  vs CD107a. Data displayed as representative example of nine independent experiments. (C) 1.3G1 T-cells were incubated alone or co-incubated with tumour cell line MDA-MB-231 for 5 h in an activation assay as in (B).

Finally, TCR transduced 1.3G1 T-cells were used in long term killing assay against .174 LCL and MDA-MB-231 tumour cells bearing gRNA1 and gRNA2 SCNN1A knockouts, and subsequent isoform 1 SCNN1A knock-ins. When co-incubated with .174 LCL 1.3G1 killed 35% of WT cells, which dropped to 1% and 3% of SCNN1A gRNA1 and gRNA2, respectively knockout cells. Killing was significantly increased to 57% and 38% in SCNN1A gRNA1 and gRNA2 knock in cells, respectively (Figure 4.12A). The same pattern was observed when 1.3G1 T-cells were co-incubated with tumour cell line MDA-MB-231 (Figure 4.12B). Overall these data confirmed that SW.3G1 recognises LCL and tumour cells lines via the TCR and that recognition requires an intact *SCNN1A* gene.

### 1.3G1



**Figure 4.12: TCR mediated killing of target cells lines via recognition of SCNN1A.** SW.3G1 TCR transduced T-cell line 1.3G1 was co-incubated with .174 LCL (A) and MDA-MB-231 tumour cell line (B) in long term killing assays. Target cells were wild-type, knockout (gRNA1 or gRNA2) or knock-in (gRNA1 or gRNA2 transduced with isoform 1 SCNN1A). Results are displayed as the mean  $\pm$  s.d. of triplicates from one representative experiment. Three independent experiments were done. \*= $p<0.05$ , \*\*= $p<0.001$ , \*\*\*= $p<0.0005$  (2 sample t-test).

## 4.3 Discussion

I identified a  $\gamma\delta$  T-cell clone, SW.3G1 with pan tumour and LCL reactivity in Chapter 3. SW.3G1 was not HLA restricted and recognised a wide range of tumour cell lines (Figure 4.3). Means of targeting many cancer types without the requirement for HLA may open pathways to pan-cancer, pan-population immunotherapies. Such therapies would have multiple advantages. First, the treatment of many tumour types in all individuals would offer considerable economy of scale. Second, the lack of need for a specific HLA unlocks possibilities for non-personalised, off-the-shelf approaches. Subsequent proof of safety would then make extending applications to other tumour types relatively simple.

In order to understand the mechanism by which SW.3G1 recognised tumours I used whole genome CRISPR/Cas9 technology to generate a library of LCL and tumour cell mutants that were deficient for all non-essential genes. The SW.3G1 clone was then turned on these targets and

used to generate lysis-resistant lines. Sequencing of the CRISPR gRNAs that were enriched in these lines showed similar patterns in 9909 LCL and KBM7 cells (Figure 4.5). The dominant gRNA selected in 9909 was specific for the *SCNN1A* gene and constituted a third of all gRNAs in this line. One in five of the gRNAs, and second dominant, enriched in the KBM7 lysis-resistant line also targeted this gene. The selection of gRNA for the same gene, from >19,000 genes targeted by the GeCKO library, in two independent experiments with two different target cell lines was deemed to be extremely significant and highly unlikely to be a chance event. The shared enrichment in two independent libraries, combined with the fact that *SCNN1A* encodes for a protein that is expressed at the cell surface, made the SCNN1A protein an interesting candidate for further exploration.

I next proceeded to show that knockout of the *SCNN1A* gene from tumour cell targets of the SW.3G1 T-cell clone removed recognition. Importantly, I also showed that transfer of the SW.3G1 TCR to CD8<sup>+</sup>  $\alpha\beta$  T-cells conferred recognition. I conclude that the SW.3G1 recognises its targets via its TCR and that recognition requires expression of an intact SCNN1A protein. As SCNN1A is expressed at the target cell surface this opens up the possibility of this protein being a ligand for the SW.3G1 TCR. However, SCNN1A is expressed on normal healthy cells that are not targets for the SW.3G1 T-cell. This suggests that the SW.3G1 T-cell must be recognising differences between healthy and transformed cells and that these differences require expression of SCNN1A to manifest themselves.

#### 4.3.1 Whole genome CRISPR: An efficient method for finding T-cell targets

In this chapter I successfully used a whole genome CRISPR library to identify a gene that was essential for T-cell recognition of target cells. This powerful methodology is ideal for setting up forward genetic screens as it efficiently removes specific genes from diploid mammalian cell lines. The basic premise of these screens is to build a cell line that is knocked out for all non-essential genes individually (Shalem et al. 2014). The GeCKO library I utilized in my screens included 6 guide RNAs for each of >19,000 human genes. Complete coverage of this library required that I screen at least 30 million target cells. Mutant cells can be selected using a number of forward genetic screens. In my case, I wished to screen for genes that were essential for recognition by the SW.3G1 T-cell. As SW.3G1 exhibited efficient target cytotoxicity, screening simply required selection of a target line that became resistant to lysis. I set up screens with 9909 LCL and KBM7 cells that had been transduced with the GeCKO library. The results in these two very different cell lines were remarkably similar (Figure 4.5), with similar enrichments in the majority of gene gRNAs. As described above, I focussed on the *SCNN1A* gene going forward as it exhibited the highest selection in lysis-resistant 9909 LCL and was the second most enriched

gRNA in the KBM7 line that had been subjected to SW.3G1-mediated lysis. The *SCNN1A* gene was also of interest as it expressed a protein that was displayed at the cell surface and thereby a putative ligand for the SW.3G1 TCR. Subsequent experiments showed that the disruption of the *SCNN1A* gene with two different guide RNAs ablated target recognition by T-cells transduced with the SW.3G1 TCR (Figure 4.12). Transduction of these knockout targets with a lentiviral construct expressing a codon-optimised isoform 1 *SCNN1A* open reading frame restored recognition of target cells that had been transduced with gRNA targeting the *SCNN1A* gene. These experiments confirmed that the *SCNN1A* gene is required for target recognition by SW.3G1, and they also demonstrate the power of whole genome CRISPR for the discovery of genes that are essential to T-cell recognition.

#### 4.3.2 The sodium channel: a T-cell target

Results from the GeCKO screens highlighted numerous proteins that may be involved in SW.3G1 targeting of tumour cells and LCL that should be explored in future studies (Table 4.1). It is possible that the proteins encoded for by *ZYX* and *DTNB* play key roles in the APC/T-cell interface by acting upon cytoskeletal remodelling at focal adhesion points (Drees et al. 2000) and subsequent cell signalling. Other identified genes, *NSUN5* and *NDUFV3* may be novel players on the cell stress response by being involved in ribosomal related stress responses (Schosserer et al. 2015) and the creation of reactive oxygen species (Vander Heiden et al. 2009), respectively. Ultimately, I focussed my efforts on the cell surface protein *SCNN1A* as it was highly enriched in both the LCL and tumour GeCKO library screens.

*SCNN1A* is the  $\alpha$  sub-unit of a heterotrimeric epithelial sodium channel (ENaC) formed of  $\alpha$ ,  $\beta$  and  $\gamma$  sub-units (Canessa et al. 1994), which enables the passive flow of sodium ions across epithelial cell surface membranes to maintain body salt and water homeostasis in epithelial cell layers (Shehata 2009). The ENaC subunits are part of the ENaC/Degenerin superfamily, also containing acid sensing ion channels (ASICs). Based on comparisons a molecular model for ENaC was built *in silico* mutagenesis of an ASIC1 structure (Figure 4.6A) (Hanukoglu 2017). *SCNN1A* is considered the most important sub-unit of the ENaC heterotrimer; *SCNN1A*-deficient mice did not live 40 h post birth, however mice with a single knockout in the  $\beta$ - or  $\gamma$ -ENaC chains had low but sufficient levels of sodium ion absorptive capacity (Hummler and Beermann 2000). Importantly, ENaC is expressed in multiple cancers and is involved in cancer development by mediating sodium transport resulting in cell proliferation, invasion and migration (Liu et al. 2016; Xu et al. 2016).

SCNN1A has been explicitly described as an important mediator in the process of cancer cell proliferation. Maryna and colleagues showed that knockdown of SCNN1A using siRNA inhibited cell proliferation by arresting cells in the cell cycle, thus initiating apoptosis (Bondarava et al. 2009). SCNN1A has also been implicated in cell migration; Kotsias and colleagues showed that antisense oligonucleotides directed against SCNN1A decreased the migratory response of cancer cells compared to those untreated (Del Monaco et al. 2009). Furthermore, knockdown of ASIC1 and ENaC subunits inhibits glioblastoma whole cell current and cell migration (Kapoor et al. 2009). In breast cancer SCNN1A has been associated with tumorigenesis (Dressman et al. 2001) and in ovarian cancer has been identified as a biomarker for early detection of neoplastic transformation (Tchagang et al. 2008).

The SW.3G1 T-cell was identified in screens with EBV-immortalised LCL undertaken in Chapter 3. SW.3G1 efficiently targeted LCL but not healthy B-cells. Recognition of LCL was ablated if the *SCNN1A* gene was disrupted using CRISPR/Cas9 technology. The role of SCNN1A in EBV infection has not been documented, however dysregulation of ion channels is a feature of chronic viral infection as viruses exploit and modify host-cell ion homeostasis in favour of viral infection (Nieto-Torres et al. 2015). The next challenge in this project is identifying exact mechanisms of SW.3G1 TCR recognition of SCNN1A.

#### 4.3.3 The SW.3G1 TCR: A powerful tool for immunotherapy

Regardless of the ligand recognised, my work demonstrated that SW.3G1 T-cells target a wide range of tumour cells without the requirement for a specific HLA. This makes the SW.3G1 TCR, and those like it, interesting candidates to explore for immunotherapy. My work suggests that an altered form of SCNN1A might be the target for the SW.3G1 TCR although further studies will be required to confirm this. This discovery is interesting as ENaC, of which the SCNN1A protein is a subunit, is already a promising target for immunotherapy for cancer and viral infection. Antibody targeting of SCNN1A/TNFRSF1A fusions to treat, characterise and diagnose cancer is being developed by Amgen Inc. (Patent number US 8735548). Furthermore, miR-125b has been shown to inhibit hepatitis B virus expression *in vivo* by targeting the *SCNN1A* gene (Zhang et al. 2014). Interestingly, FDA approved drugs such as dexamethasone are known to maximize SCNN1A expression on the cell surface (Edinger et al. 2012) and so might allow manipulation of this target *in vivo*. Future exploitation of the SW.3G1 TCR will require the generation of a full safety profile. In this respect, it will be advantageous to define the precise nature of the SW.3G1 TCR ligand. SCNN1A is expressed very highly in some tissues, especially the kidney (Hanukoglu and Hanukoglu 2016). The SW.3G1 T-cell clone was generated from a healthy individual where it did no obvious damage yet it can kill a wide range of tumour cells including the autologous LCL

(thereby confirming that the donor has capacity to generate the ligand). Understanding how the SW.3G1 TCR is able to target tumour cells without damaging healthy tissue should lead to major breakthroughs.

#### 4.3.4 Future directions

The big challenge now will be to delineate how the SW.3G1 TCR targets transformed cells. The *SCNN1A* gene was present in a read-through fusion transcript with a TNF $\alpha$  receptor (TNFRSF1A) in breast cancer cells (Varley et al. 2014). This provided a very interesting possibility for how the *SCNN1A* gene might be involved in recognition by the SW.3G1 TCR. Unfortunately, no such fusion protein could be detected in our Western Blots for *SCNN1A*. Had the fusion protein been expressed at the levels previously reported in breast cancer cells, I would have expected to see a larger molecular weight band in cell lines that were targets for the SW.3G1 TCR. The lack of *SCNN1A* bands in Western blots that correlated with cell targeting and the observation that expression of isoform 1 of the protein in knockout cells restores recognition would seem to rule out the possibility of recognition occurring via macro-changes in the bulk of *SCNN1A* protein.

It is possible that other, more subtle, posttranslational modifications to *SCNN1A* play a role in tumour recognition. Post-translational modifications of *SCNN1A*, such as hyper-methylation, have been identified in neuroblastoma cells (Caren et al. 2011) and breast cancer cells (Roll et al. 2008). Another possibility is that *SCNN1A* is not the direct ligand of the 3G1 TCR, but it may act as a coreceptor or a regulator of the real ligand. It is possible that one of the other chains of the ENaC channel is the cognate ligand of the SW.3G1 TCR. Disruption of the *SCNN1A* gene in cancer cells could for instance result in lack of surface expression of an altered form of the other ENaC chains  $\beta$ ENaC and  $\gamma$ ENaC, products of *SCNN1B* and *SCNN1G* genes respectively (Hanukoglu and Hanukoglu 2016). A key element going forward will be to demonstrate TCR binding. One way to do this would be to make a TCR tetramer and show that it stains relevant targets. My group has previously shown that tetramers of  $\alpha\beta$  TCRs can be used to stain TCR ligands (Laugel et al. 2005). Such reagents are likely to prove useful when validating ligands for  $\gamma\delta$  TCRs. Unfortunately, my attempts to manufacture soluble SW.3G1 TCR protein were unsuccessful. The other way one could use fluorochrome-conjugated tetramers to demonstrate TCR binding would be to manufacture soluble biotin-tagged ligand as is routinely done for pMHC tetramers (Bai et al. 2012; Dolton et al. 2015). However, the *SCNN1A* protein is both membrane spanning (Figure 4.6A) and part of the wider ENaC pore so does not readily lend itself to such approaches.



In summary, I have made a significant advance by isolating the SW.3G1  $\gamma\delta$  T-cell clone and showing that the SW.3G1 TCR mediates recognition of multiple tumour cell types via an HLA-independent mechanism that requires expression of the SCNN1A gene. Further studies will be required to define the precise molecular nature of the SW.3G1 TCR ligand and how this differs between neoplastic and normal cells. If I had more time then I would like to explore the roles of the other ENaC subunits,  $\beta$  and  $\gamma$ , in recognition by SW.3G1. My studies indicate that tumour cells differ at the cell surface from non-tumour cells and that this difference manifests itself in SCNN1A expression.



## 5 $\gamma\delta$ T-cell recognition of MHC on tumour cells

### 5.1 Background

In Chapter 3, I isolated two further  $V\delta 1^+$   $\gamma\delta$  T-cell clones, SW.6B10 and SW.11H7, which recognized EBV-transformed LCL targets. Unlike the SW.3G1 clone, these  $\gamma\delta$  T-cell clones did not recognise all LCL targets suggesting that the SW.6B10 and SW.11H7 TCRs recognised ligands that were only present on a minority of LCL targets. The aim of this Chapter, as for Chapter 4, was to further characterise these two T-cell clones and to establish how they recognised their targets. One possibility for why SW.6B10 and SW.11H7 only saw some targets and not others was that, like conventional  $\alpha\beta$  T-cells, these clones were HLA-restricted. It is currently believed that  $\gamma\delta$  T-cells do not recognize target cells via MHC (Vantourout and Hayday 2013; Adams et al. 2015; Legut et al. 2015) despite previous efforts to delineate  $\gamma\delta$  T-cell MHC restriction. The hypothesis that  $\gamma\delta$  T-cells can be “conventional” and recognise specific peptides in the context of HLA would be viewed as an absurd suggestion by most immunologists. Nevertheless, there are rare studies in the literature that hint at this possibility as human  $\gamma\delta$  T-cells have been reported to recognise MHC class I (Ciccone et al. 1989) and MHC class II molecules (Flament et al. 1994) on LCL. Indeed, one of the very first co-structures of a  $\gamma\delta$  TCR with a ligand was a mouse  $\gamma\delta$  TCR bound to the MHC molecule I-E (Matis et al. 1989). Previous descriptions of MHC-restriction of  $\gamma\delta$  T-cell recognition have relied on antibody blocking experiments which are not especially ‘clean’. Recent advances in CRISPR/Cas9 gene editing and lentiviral transduction has made the process of identifying MHC restriction easier and more definitive.

#### 5.1.1 Aims and objectives

Despite the current trend in the  $\gamma\delta$  T-cell research field, I postulated that the  $V\delta 1^+$   $\gamma\delta$  T-cell clones SW.6B10 and SW.11H7, isolated in Chapter 3, recognized target cells via specific MHC. Therefore the aim of this chapter was to confirm and validate the HLA restriction of these  $\gamma\delta$  T-cell clones. Specifically my objectives were:

1. Use antibody blocking experiments to confirm MHC restriction
2. Carry out HLA mapping using panels of partially HLA matched target cells to identify potential MHC candidates
3. Conduct knock out and knock in studies to validate the involvement of MHC molecules in the recognition of target cells by  $\gamma\delta$  T-cell clones SW.6B10 and SW.11H7
4. Determine whether MHC recognition was TCR-mediated.

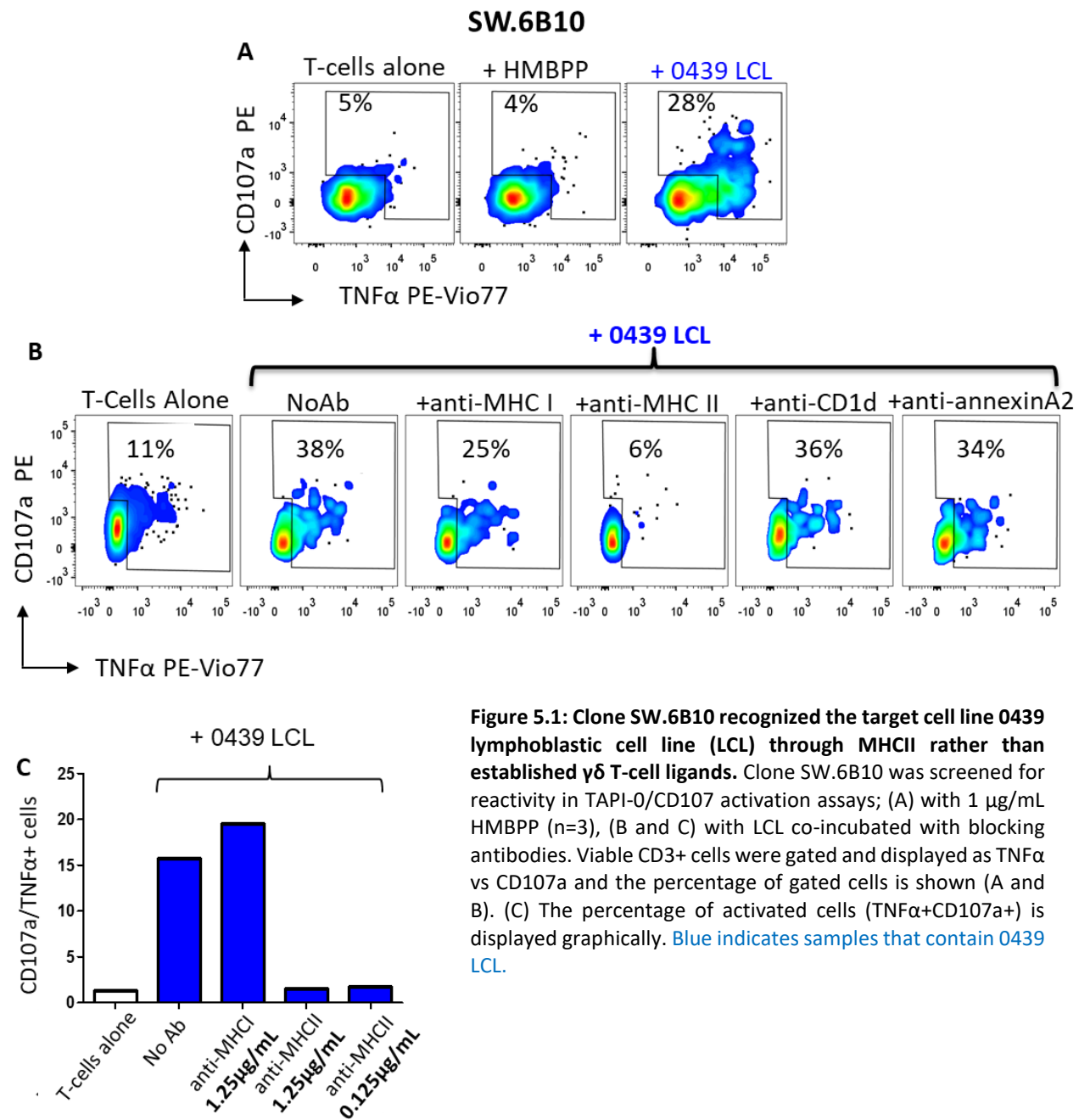
## 5.2 Results

### 5.2.1 SW.6B10 recognizes HLA-DR7<sup>+</sup> targets

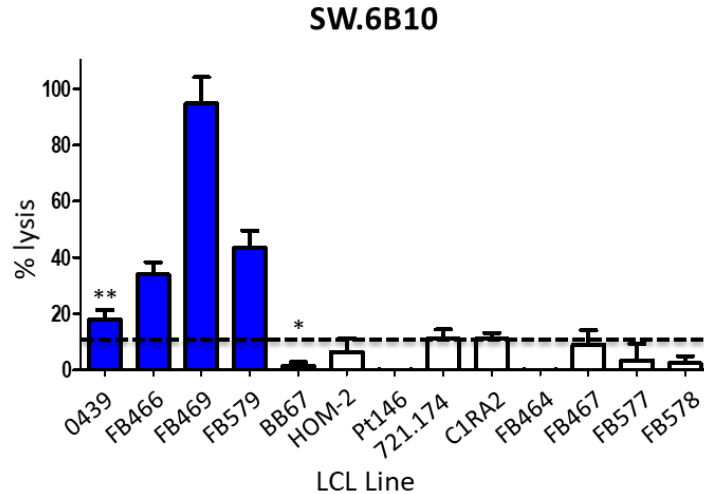
Clone SW.6B10, the V $\gamma$ 8V $\delta$ 1<sup>+</sup>  $\gamma\delta$  T-cell clone isolated from donor BB67 after priming on 0439 LCL (Chapter 3), was shown to recognize a pattern of LCL and some tumours. To delineate the ligand that SW.6B10 was recognizing I first screened for T-cell activation against the known  $\gamma\delta$  T-cell ligand HMBPP. In a 4 h TAPI-0 activation assay, measuring TNF $\alpha$  and CD107a expression, clone SW.6B10 was either incubated alone, with 0439 LCL (positive control), or with 1  $\mu$ g/mL HMBPP. SW.6B10 was 28% reactive to 0439 LCL, but showed no reactivity to HMBPP (Figure 5.1A). I next conducted an TAPI-0 assay in combination with blocking antibodies directed against pan MHC I, pan MHC II and the known  $\gamma\delta$  T-cell ligands CD1d and annexin A2 (Figure 5.1B). SW.6B10 was 38% reactive to 0439 LCL without antibody, which decreased slightly to 25% with the addition of anti-MHC I. Anti-CD1d and anti-annexinA2 had no impact of SW.6B10 activation against 0439 LCL. Interestingly anti-MHC II completely abrogated SW.6B10 reactivity towards 0439 LCL, suggesting that this clone might be MHC II-restricted.

To confirm the role of MHC II in SW.6B10 recognition of target cells I repeated the blocking antibody assay using a 10X lower concentration of anti-MHC II antibody (0.125  $\mu$ g/mL) as well as the original 1X concentration from the assay undertaken in Figure 5.1B (1.25  $\mu$ g/mL). Both concentrations of anti-MHC II blocked SW.6B10 recognition of 0439 LCL (Figure 5.1C). I therefore postulated that SW.6B10 recognized target cells through an MHC II molecule. To delineate the exact MHC II molecule I next carried out HLA mapping of LCL recognized by SW.6B10.

A chromium release cytotoxicity assay was performed to examine SW.6B10-mediated killing of LCL in Chapter 3 (Figure 3.7; pg 75); Half of the 26 LCL had known tissue HLA types. SW.6B10 recognised four LCL lines (0439, FB466, FB469 and FB579) (Figure 5.2). These four LCL shared two MHC II alleles; HLA-DRB1\*07 (HLA-DR7) and HLA-DQB1\*02 (HLA-DQ2). None of the LCL that were unrecognised by SW.6B10 were HLA-DR7<sup>+</sup>. Unrecognised LCL FB577 expressed HLA-DQ2. I therefore concluded that the most likely target for the SW.6B10 T-cell clone was HLA-DR7.



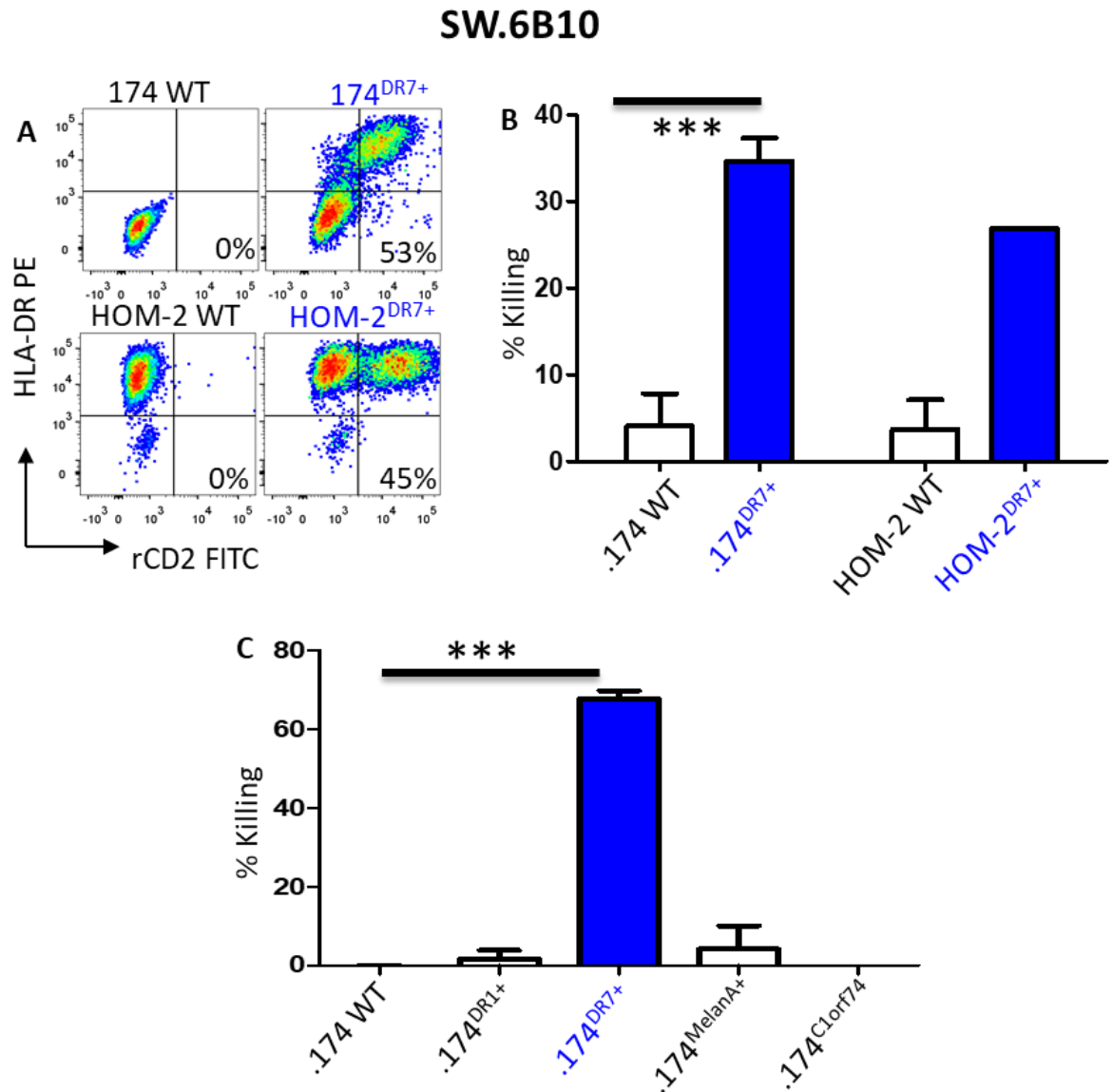
**Figure 5.1: Clone SW.6B10 recognized the target cell line 0439 lymphoblastic cell line (LCL) through MHCII rather than established  $\gamma\delta$  T-cell ligands.** Clone SW.6B10 was screened for reactivity in TAPI-0/CD107 activation assays; (A) with 1  $\mu\text{g/mL}$  HMBPP (n=3), (B and C) with LCL co-incubated with blocking antibodies. Viable CD3+ cells were gated and displayed as TNF $\alpha$  vs CD107a and the percentage of gated cells is shown (A and B). (C) The percentage of activated cells (TNF $\alpha$ +CD107a+) is displayed graphically. Blue indicates samples that contain 0439 LCL.



**Figure 5.2: Clone SW.6B10 only recognized HLA-DR7<sup>+</sup> LCL.** In a 6.5 h chromium release assay at an E:T of 1:1 the percentage lysis of target LCL by T-cell clone SW.6B10 was measured. Dotted line indicates 10% lysis. Results are displayed as the mean  $\pm$  s.d. of triplicates from one representative experiment. Two independent experiments were done. Blue bars indicate HLA-DR7<sup>+</sup> cell lines; \*=autologous LCL; \*\*=LCL used for priming.

To confirm the HLA-DR7 restriction of SW.6B10 I designed a codon-optimised construct to express HLA-DR7 alongside a rCD2 selectable marker. HLA-DR7 was added to MHC II-negative LCL 721.174 (.174) to generate 721.174<sup>DR7+</sup> LCL and HOM-2 to produce HOM-2<sup>DR7+</sup> LCL. Polyclonal 721.174<sup>DR7+</sup> and HOM-2<sup>DR7+</sup> cell lines were confirmed to be 53% and 45% HLA-DR7<sup>+</sup>, respectively (Figure 5.3A). In a 24 h long term killing assay, where 10,000 LCL were set up in triplicate either alone or with 10,000 T-cells, SW.6B10 killed less than 5% of 721.174 and HOM2 wildtype cells, which significantly increased to over 30% killing with 721.174<sup>DR7+</sup> ( $p < 0.0001$ , t-test), and 26% killing of HOM-2<sup>DR7+</sup> (Figure 5.3B).

To confirm increased killing was as a result of HLA-DR7 expression, and not rCD2 upregulation or a result of lentiviral transduction, I generated a wider panel of 721.174 LCL controls which I transduced with an irrelevant protein (Melan A or C1orf74) co-expressed with rCD2. 721.174 transduced with HLA-DR1 (721.174<sup>DR1+</sup>) were used as an MHCII-expressing control. In a 24 h killing assay clone SW.6B10 killed over 60% of 721.174<sup>DR7+</sup> LCL. Wildtype 721.174 cells were not killed ( $p < 0.005$ , t-test) (Figure 5.3C). There was no killing of 721.174<sup>DR1+</sup> or 721.174<sup>C1orf</sup> and less than 5% killing of 721.174<sup>MelanA</sup>. Overall, I concluded that SW.6B10 was restricted by the MHC II allele HLA-DR7, next I tested whether recognition was via the TCR.



**Figure 5.3: SW.6B10 kills MHCII-negative LCL targets that are transduced with HLA DR7.** (A) Viable 721.174 (.174) and HOM-2 LCL transduced with a construct co-expressing HLA-DR7 and a rCD2 marker were gated and displayed as HLA-DR versus rCD2. The percentage of cells in the rCD2<sup>+</sup>HLA-DR<sup>+</sup> gate is shown. (B) Clone SW.6B10 was co-incubated with 721.174 and HOM-2 WT and HLA-DR7 transduced target cells in a 24h killing assay. (C) .174 LCL transduced with Melan A, c1orf74 open reading frame, and HLA-DR1. As in (B) a 24 h long term killing assay was carried out. **Blue bars indicate HLA-DR7<sup>+</sup> LCL.** Results are displayed as the mean  $\pm$  s.d. of triplicates from one representative experiment. Three independent experiments were done. \*\*\*= $p < 0.0005$  (2 sampled t-test).

### 5.2.2 TCR mediated recognition of HLA-DR7 by SW.6B10

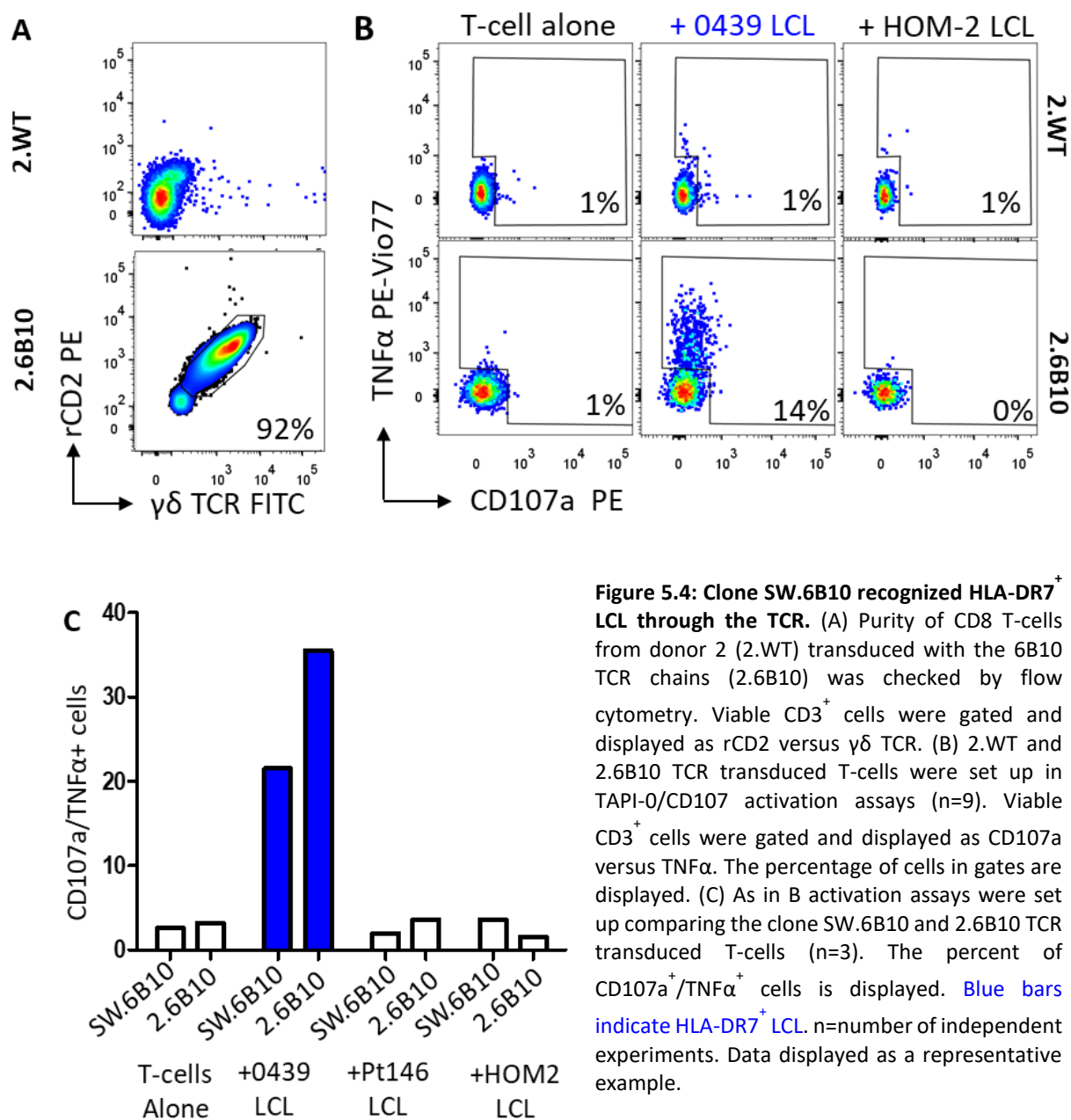
Purified CD8 T-cells from donor 2 were transduced with 6B10 TCR, rCD2 marker and a gRNA to render the endogenous TCR $\beta$  chain negative (2.6B10). Removal of the  $\alpha\beta$  TCR when transducing with  $\gamma\delta$  TCR has been shown to enhance the antigen-sensitivity of the resulting transduced T-cells by over a thousand-fold. The resultant 2.6B10 line was confirmed to be 92% rCD2<sup>+</sup> $\gamma\delta$ TCR<sup>+</sup> (Figure 5.4A). Donor 2 wildtype (2.WT) and 2.6B10 T-cells were either incubated alone or co-incubated with 0439 LCL (HLA-DR7<sup>+</sup>) and HOM-2 LCL (HLA-DR7<sup>neg</sup>) in a 5 h TAPI-0 activation assay at an E:T of 1:1. The untransduced CD8 T-cells did not respond to either target but the line transduced with 6B10 TCR responded to 0439 LCL (Figure 5.4B). This result confirms that the 6B10 TCR confers reactivity to 0439 LCL. I next repeated this experiment including the SW.6B10 clone using a TAPI-0 activation assay. I also included an additional HLA-DR7 negative LCL, Pt146. Both SW.6B10 T-cell clone and 2.6B10 TCR transduced T-cells recognized 0439 LCL (HLA-DR7<sup>+</sup>), but not Pt146 or HOM-2 LCL (both HLA-DR7<sup>neg</sup>) (Figure 5.4C).

Next I designed a CRISPR gRNA, sequence CTGCCACAGGAAACGTGCTG, using a CRISPR gRNA design tool (crispr.mit.edu) to target exon 2 of HLA-DR7. The gRNA was delivered with lentivirus to 0439 LCL, generating 0439<sup>DR7neg</sup>. HLA-DR antibody was a log fold lower for 0439<sup>DR7neg</sup> targets compared to 0439 LCL (Figure 5.5A). The residual HLA-DR staining of 0439<sup>DR7neg</sup> cells is believed to be due to the HLA-DR1 allele in these cells. CD8 2.6B10 T-cells lysed 0439 targets efficiently (84% lysis) but did not kill the 0439<sup>DR7neg</sup> HLA-DR7 CRISPR knockout LCL line (Figure 5.5B). Overall, my data indicated that clone SW.6B10 recognized HLA-DR7 on target LCL in a TCR dependent manner.

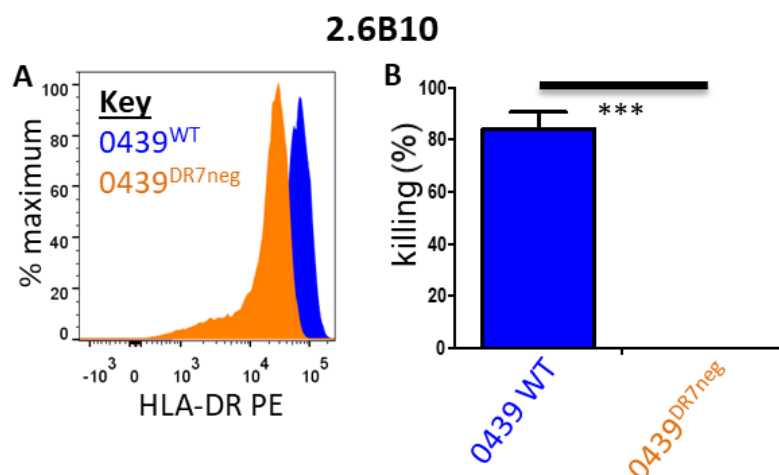
### 5.2.3 SW.6B10 recognizes tumour cells through HLA-DR7

I next examined killing of HLA-DR7<sup>+</sup> tumour cell lines by  $\gamma\delta$  T-cell clone SW.6B10. The SW.6B10 clone efficiently lyses HLA-DR7<sup>+</sup> tumour lines HCT-116, LnCap, MDA-MB-231 and MM909.24 at an E:T ratio as low as 0.375:1 (Figure 5.6). I used MM909.24  $\beta$ 2M knockout cells, generated by Michael Crowther from my laboratory, to show that SW.6B10 did not recognize MM909.24 melanoma cells via MHC Ia molecules, or the MHCIb molecules HLA-E,-F,-G, MR1 and CD1a-d which all require association with  $\beta$ 2M for cell surface presentation (Appendix Figure 8.4).

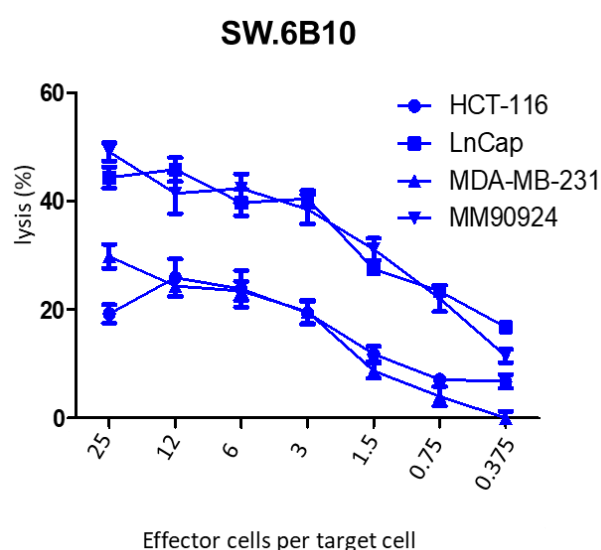




**Figure 5.4: Clone SW.6B10 recognized HLA-DR7<sup>+</sup> LCL through the TCR.** (A) Purity of CD8 T-cells from donor 2 (2.WT) transduced with the 6B10 TCR chains (2.6B10) was checked by flow cytometry. Viable CD3<sup>+</sup> cells were gated and displayed as rCD2 versus γδ TCR. (B) 2.WT and 2.6B10 TCR transduced T-cells were set up in TAPI-0/CD107 activation assays (n=9). Viable CD3<sup>+</sup> cells were gated and displayed as CD107a versus TNFα. The percentage of cells in gates are displayed. (C) As in B activation assays were set up comparing the clone SW.6B10 and 2.6B10 TCR transduced T-cells (n=3). The percent of CD107a<sup>+</sup>/TNFα<sup>+</sup> cells is displayed. Blue bars indicate HLA-DR7<sup>+</sup> LCL. n=number of independent experiments. Data displayed as a representative example.



**Figure 5.5: 6B10 TCR transduced T-cells require HLA-DR7 for recognition of 0439 LCL.** 0439 LCL were transduced with a CRISPR/Cas9 gRNA construct targeting HLA-DR7, generating 0439<sup>DR7neg</sup>. (A) Viable cells were gated on and HLA-DR expression displayed for WT 0439 and 0439<sup>DR7neg</sup>. (B) T-cells transduced with the 6B10 TCR, 2.6B10, were co-incubated with either 0439 or 0439<sup>DR7neg</sup> for 24 h at E:T of 1:1 in a long term killing assay. Results are displayed as the mean  $\pm$  s.d. of triplicates from one representative experiment. Three independent experiments were done. \*\*\*= $p < 0.0005$ , 2 sampled t-test. Blue indicates HLA-DR7<sup>+</sup> LCL, orange indicates CRISPR mediated HLA-DR7<sup>neg</sup> LCL.



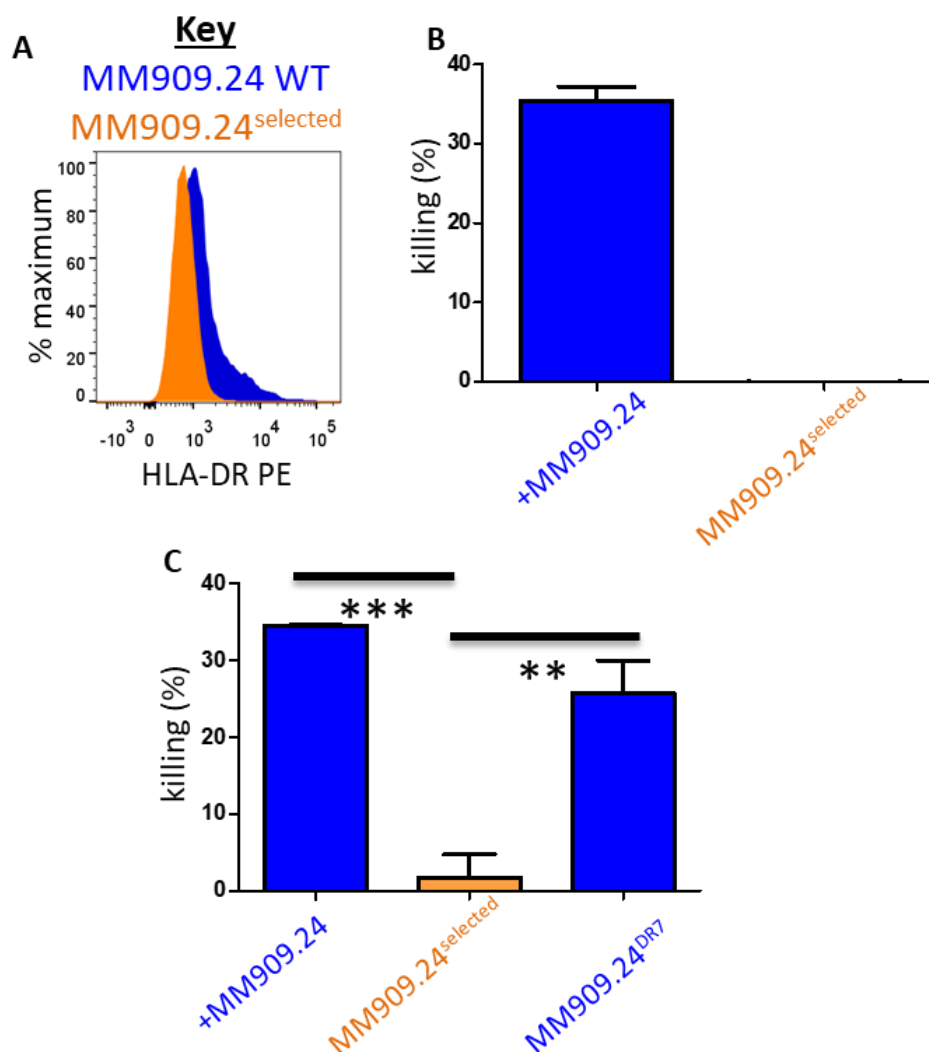
**Figure 5.6: SW.6B10 kills HLA-DR7<sup>+</sup> tumours.** In a cytotoxic chromium release assay clone SW.6B10 was co-incubated with HLA-DR7<sup>+</sup> tumour cell lines for 6.5 h at a range of E:T ratios (shown on x-axis). Results are displayed as the mean  $\pm$  s.d. of triplicates from one representative experiment. Two independent experiments were done.

Following 2 weeks co-incubation of clone SW.6B10 with MM909.24 I generated an MM909.24 line which was negative for HLA-DR staining (MM909.24<sup>DRneg</sup>) (Figure 5.7A). SW.6B10 lysed 35% of wildtype MM909.24 targets in a long-term killing assay. The DR-negative MM909.24<sup>DRneg</sup> line was resistant to lysis by SW.6B10 (Figure 5.7B). It is likely that MM909.24 initiated MHC downregulation as an immune evasive strategy to survive T-cell targeting (Drake et al. 2006). I next transduced the MM909.24<sup>DRneg</sup> with HLA-DR7, generating MM909.24<sup>DR7</sup>. Importantly, SW.6B10 killed 45% of WT MM909.24 and 1.7% of the MM909.24<sup>DRneg</sup> line. Killing was rescued by HLA-DR7 transduction, as SW.6B10 killed 26% of MM909.24<sup>DR7</sup> tumour cell line (Figure 5.7C). The T-cell selection process used to generate the MM909.24<sup>DRneg</sup> line was not targeted at HLA-DR so I undertook CRISPR/Cas9 knockout experiments with an HLA-DR7-specific gRNA in breast cancer cell line MDA-MB-231 that was killed by SW.6B10 (Figure 5.6). The resultant MDA-MB-231<sup>DR7neg</sup> cells (Appendix Figure 8.5) were then used as T-cell targets. A 4h TAPI-0 activation at E:T ratio of 1:1 showed that 38% SW.6B10 reactivity in response to wildtype MDA-MB-231 cells compared with 18% reactivity to DR knockout line MDA-MB-231<sup>DR7neg</sup> (Figure 5.8A). I next co-incubated CD8 2.6B10 TCR transduced T-cells with MDA-MB-231 and MDA-MB-231<sup>DR7neg</sup> targets for 24 h at E:T ratio of 1:1. 6B10 TCR transduced CD8 T-cells killed 65% of MDA-MB-231 but did not kill MDA-MB-231<sup>DR7neg</sup> (Figure 5.8B). These data indicated that recognition of tumour MDA-MB-231 by SW.6B10 was via TCR recognition of HLA-DR7.

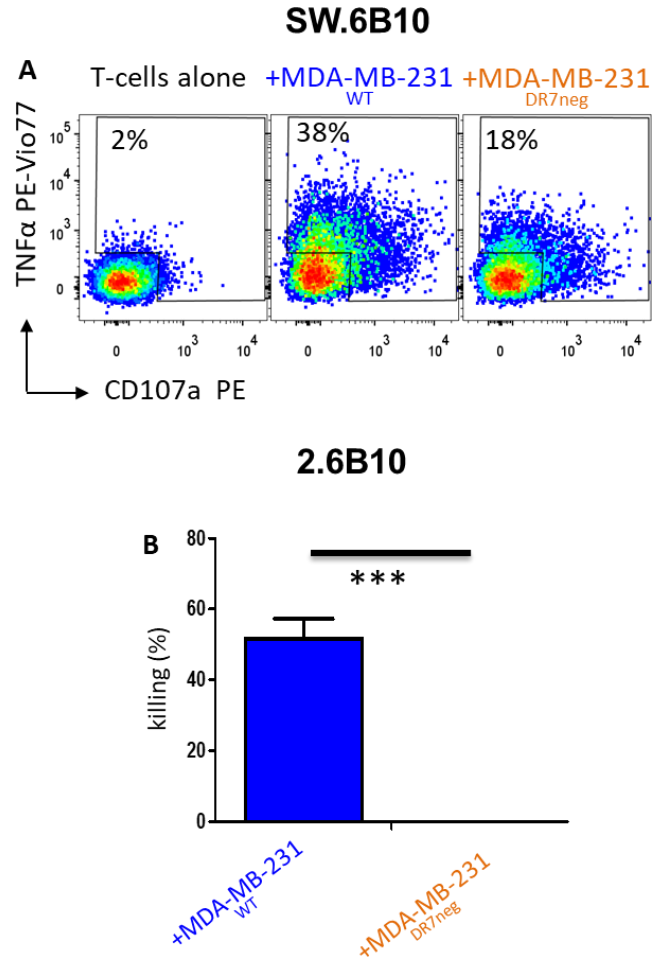
#### 5.2.4 SW.6B10 recognition of target cells is peptide specific

LCL line 721.174 is MHCII null due to a deletion in the MHC locus in the single copy of chromosome 6 that this cell carries (DeMars et al. 1984; Erlich et al. 1986). This deletion means that 721.174 lacks machinery to process and present endogenous antigens. I, therefore, hypothesized that the SW.6B10 TCR recognized HLA-DR7 regardless of the peptide it bound (i.e. that the SW.6B10 T-cell clone was not peptide specific) such as in the case for the previously described mouse  $\gamma\delta$  TCR (Matis et al. 1989). To test this hypothesis I expressed and refolded HLA-DR7 protein bound to the peptide sequence: DPFRLQNSQVFS (DPF). These peptide-MHC (pMHC) monomers were used to generate HLA-DR7-DPF tetramers. The tetramer 'boost' protocol (Dolton et al. 2015), designed to allow tetramer staining even when TCR-pMHC affinity is extremely low ( $KD < 1\text{mM}$ ), was used to stain SW.6B10 T-cells with HLA-DR7/DPF. HLA-DR7-DPF tetramers failed to stain the SW.6B10 T-cell clone suggesting that the 6B10 TCR might only bind to HLA-DR7 presenting a specific peptide in the HLA binding groove, therefore suggesting peptide specificity of SW.6B10 (Appendix Figure 8.6).

## SW.6B10



**Figure 5.7: SW.6B10 targets melanoma cell line MM909.24 through HLA-DR7.** MM909.24 cells were co-incubated with SW.6B10 T-cells at E:T of 1:1 for 2 weeks. (A) HLA-DR staining of MM909.24 and MM909.24 T-cell selected (MM909.24<sup>selected</sup>) cells. (B) SW.6B10 was co-incubated with MM909.24 WT or MM909.24<sup>selected</sup> for 24 h killing assay at E:T of 1:1 (n=3). (C) MM909.24<sup>selected</sup> cells were transduced with a construct expressing HLA-DR7 (MM909.24<sup>DR7</sup>). As in (B) a long term killing assay was set up with the target cells lines MM909.24 WT, MM909.24<sup>selected</sup> and MM909.24<sup>DR7</sup>. Blue indicates HLA-DR7<sup>+</sup>, orange indicates HLA-DR7<sup>neg</sup>. Results are displayed as the mean  $\pm$  s.d. of triplicates from one representative experiment. n= independent experiments done. \*\*= $p < 0.001$ , \*\*\*= $p < 0.0005$  (2 sampled t-test).

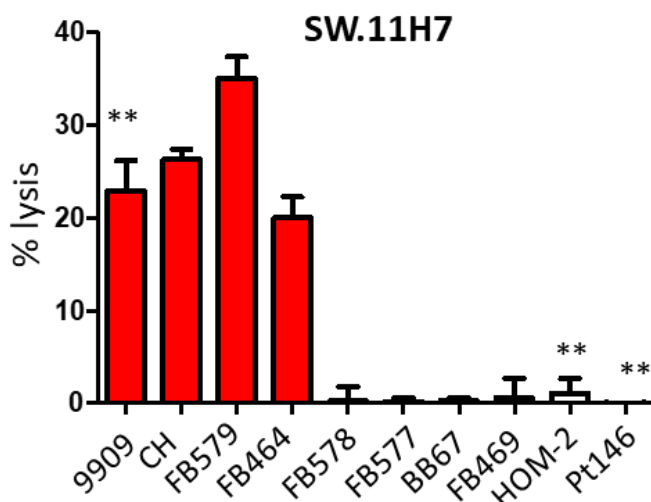


**Figure 5.8: SW.6B10 TCR recognizes tumour MDA-MB-231 via HLA-DR7.** MDA-MB-231 cells were transduced with a CRISPR/Cas9 gRNA targeting HLA-DR7, generating MDA-MB-231<sup>DR7neg</sup>. (A) Clone SW.6B10 was co-incubated with MDA-MB-231 and MDA-MB-231<sup>DR7neg</sup> in a TAPI-0 activation assay (n=3). Viable CD3<sup>+</sup> cells were gated and displayed as TNFα versus CD107a. (C) CD8 T-cells transduced with the 6B10 TCR, 2.6B10, were co-incubated with MDA-MB-231 WT and MDA-MB-231<sup>DR7neg</sup> for 24 h in a at an E:T of 1:1 in a long term killing assay (n=3). Results are displayed as the mean ± s.d. of triplicates from one representative experiment (\*\*p<0.0001, 2 sampled t-test). n=number of independent experiments done. Blue indicates HLA-DR7<sup>+</sup>, orange indicates HLA-DR7<sup>neg</sup>.

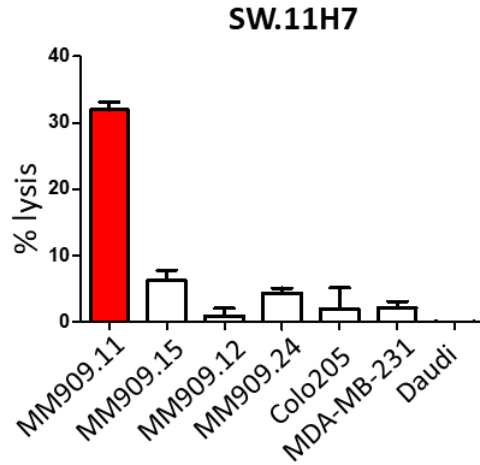
Attempts were made to identify the peptide by combinatorial library screen, however no conclusive results were gained. In summary, my results indicate that the SW.6B10 clone recognises HLA-DR7 via its TCR and that recognition probably involves a specific peptide. The identity of this peptide remains unknown. I next examined the second  $\gamma\delta$  T-cell clone, SW.11H7, which also appeared to be MHC restricted.

### 5.2.5 SW.11H7: A second MHC II restricted $\gamma\delta$ T-cell clone

I conducted similar experiments as with SW.6B10 to delineate SW.11H7 MHC-restriction. A panel of 27 LCLs were used in a chromium cytotoxicity assay with clone SW.11H7 (Figure 3.7; pg 75). Out of the 27 LCL tested, the HLA type was available for 11. I focused on just these targets and plotted these on a new graph (Figure 5.9). Clone SW.11H7 lysed four LCL; 9909, CH, FB579, and FB464, which had the MHC II allele HLA-DRB1\*1501 (HLA-DR15) in common. Clone SW.11H7 was primed on the HLA-DR15<sup>+</sup> LCL 9909, along with HOM-2 (HLA-DR15<sup>neg</sup>) and Pt146 (HLA-DR15<sup>neg</sup>). Whilst 9909 LCL were recognized by SW.11H7, HOM-2 and Pt146 LCL were not. To confirm HLA-DR15 restriction, I next screened SW.11H7 against a panel of tumour cell lines in a chromium release assay. Strikingly, SW.11H7 only lysed one of the lines I tested; melanoma cell line MM909.11 (Figure 5.10). MM909.11 was the only tumour line tested that expressed HLA-DR15. I concluded that it was likely that the SW.11H7 T-cell recognized LCL and tumour lines via HLA-DR15. I next tested whether this reactivity was mediated via the TCR.



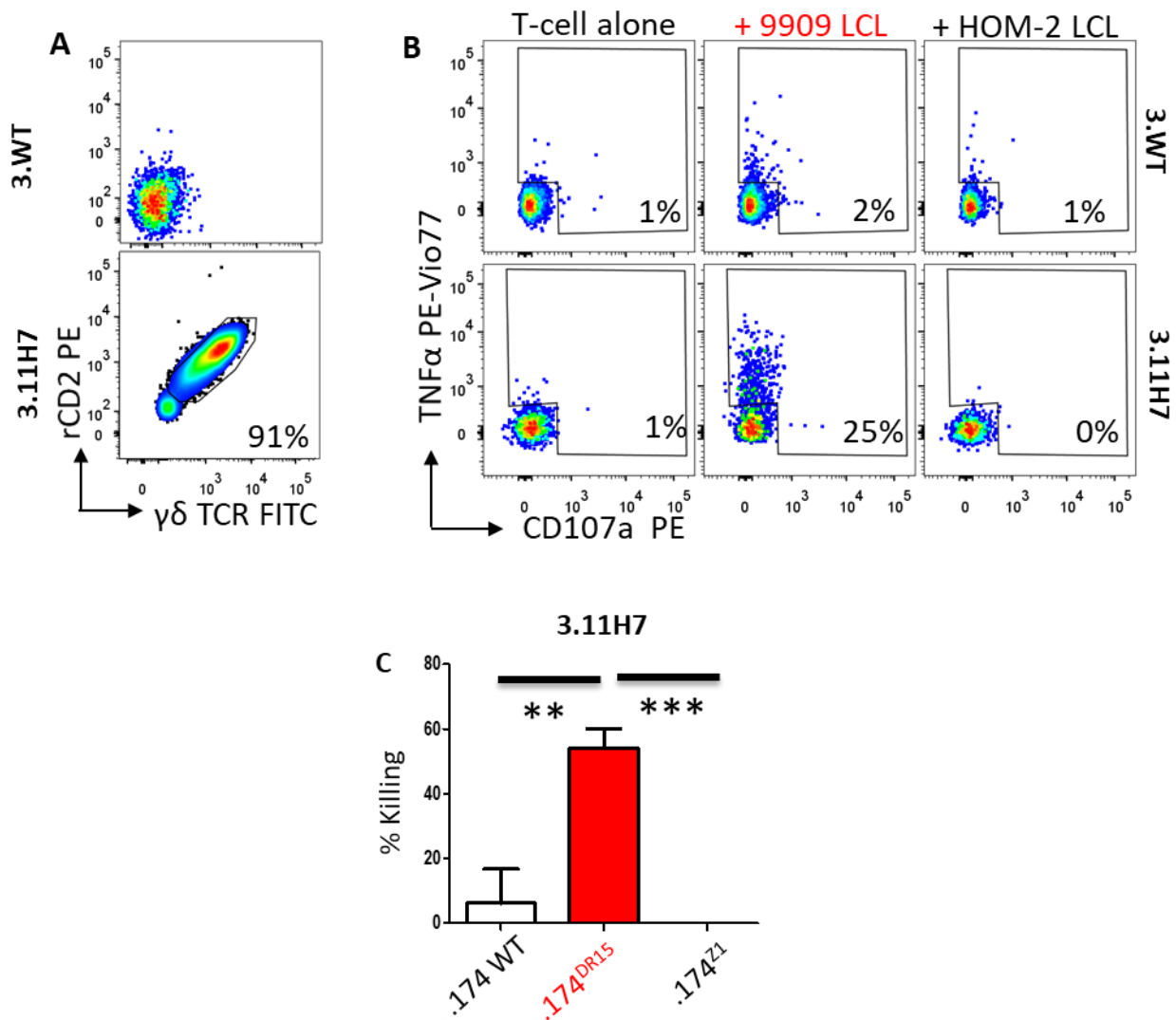
**Figure 5.9: Clone SW.11H7 only lysed HLA-DR15<sup>+</sup> LCL.** SW.11H7 was co-incubated with target LCLs in a cytotoxic chromium release assay. T-cells were co-incubated with target cells at an E:T of 1:1 for 6.5 h before percentage lysis was measured. Red bars indicate HLA-DR15<sup>+</sup> cells; \*\* indicates LCLs primed on. Results are displayed as the mean  $\pm$  s.d. of triplicates from one representative experiment. Two independent experiments done.



**Figure 5.10: Clone SW.11H7 only lysed HLA-DR15<sup>+</sup> tumours.** SW.11H7 was co-incubated with target tumour cell lines in a cytotoxic chromium release assay. T-cells were co-incubated with target cells at an E:T of 1:1 for 6.5 h before percentage lysis was measured. Red bars indicate HLA-DR15<sup>+</sup> cells. Results are displayed as the mean  $\pm$  s.d. of triplicates from one representative experiment. Two independent experiments done.

To determine whether SW.11H7 recognized HLA-DR15 via the TCR, polyclonal CD8<sup>+</sup> T-cells from donor 3 were isolated and transduced with 11H7 TCR chains and TCR $\beta$  targeting CRISPR constructs as was performed for the 6B10 TCR in Figure 5.4, generating the 3.11H7 polyclonal T-cell line. Flow cytometry showed that 3.11H7 TCR transduced line was 91% positive for the 11H7 TCR (Figure 5.11A). A 5 h TAPI-0 activation assay was undertaken with 11H7 TCR transduced and untransduced CD8 T-cells with 9909 (HLA-DR15<sup>+</sup>) and HOM-2 (HLA-DR15<sup>neg</sup>) LCL as targets at an E:T of 1:1. Untransduced CD8 T-cells recognised 9909 LCL poorly (2% CD107a<sup>+</sup>TNF $\alpha$ <sup>+</sup>). Recognition was >10-fold improved for T-cells transduced with the 11H7 TCR (Figure 5.12B). Neither transduced nor untransduced CD8 T-cells recognised HOM-2 LCL (Figure 5.11B).

I next transduced the MHCII-negative LCL 721.174 with a construct containing HLA-DR15 and a rCD2 marker, generating 721.174<sup>DR15</sup> (staining in Appendix 8.7). As a negative control, I also transduced 721.174 LCL with a construct containing an irrelevant protein, Zika virus protein 1 (Z1), with rCD2 to generate 721.174<sup>Z1</sup>. CD8 T-cells transduced with the 11H7 TCR killed 721.174<sup>DR15</sup> but not 721.174 or 721.174<sup>Z1</sup> in a 24 h killing assay at an E:T ratio of 1:1 (Figure 11C). Overall these data were taken as confirmation that SW.11H7 recognized HLA-DR15 through the TCR.



**Figure 5.11: Clone SW.11H7 recognizes HLA-DR15<sup>+</sup> LCL via the TCR.** Purified CD8 T-cells, 3.WT, were transduced with the SW.11H7 TCR chains, generating 3.11H7. (A) Purity of the cells was checked by flow cytometry. Viable CD3<sup>+</sup> cells were gated and displayed as rCD2 versus  $\gamma\delta$  TCR. (B) 3.11H7 TCR transduced and untransduced 3.WT T-cells were set up in TAPI-0 activation assays (n=9). Viable CD3<sup>+</sup> cells were gated and displayed as CD107a versus TNF $\alpha$ . The percentage of cells in the gate is shown. (C) 3.11H7 was used in a 24 h killing assay against 721.174 (.174), 721.174 transduced with HLA-DR15 (.174<sup>DR15</sup>) or 721.174 transduced with irrelevant protein Z1 (.174<sup>Z1</sup>) (n=3). **Red bars indicate HLA-DR15<sup>+</sup> target cells.** Results are displayed as the mean  $\pm$  s.d. of triplicates from one representative experiment. \*\*=p<0.001, \*\*\*=p<0.0005 (2 sampled t-test). n= number of independent experiments done.



## 5.3 Discussion

In this chapter I characterised two  $\gamma\delta$  T-cell clones that target LCL and tumour cells lines via TCR mediated recognition of MHC-II molecules. In each case the recognition I described was allogeneic with the SW.6B10 clone recognising HLA-DR7 and the SW.11H7 targeting HLA-DR15. Allogeneic recognition of non-self MHC by  $\gamma\delta$  T-cells could have profound implications for the use of such TCRs in cellular therapeutics.

### 5.3.1 MHC restricted $\gamma\delta$ T-cells: Not so unconventional after all?

Although it is currently believed that  $\gamma\delta$  T-cells do not recognise target cells via conventional TCR recognition of peptide-MHC pathways, I identified two clones from two different donors that appear to behave in such a way. The expansion of  $\gamma\delta$  T-cells in response to allogeneic transplantation has been documented in bone marrow (Vilmer et al. 1988; van der Harst et al. 1991; Nagai et al. 1998), liver (Puig-Pey et al. 2010), kidney (Willcox et al. 2012) and most recently HSC transplantation (Ravens et al. 2017). Furthermore, researchers have also previously documented  $CD4^{neg}CD8^{neg}$   $\gamma\delta$  T-cell recognition of non-autologous HLA-DR molecules (Flament et al. 1994; Mami-Chouaib et al. 1996). Therefore it is possible that  $\gamma\delta$  T-cells are not so unconventional after all.

Ideally, the next stage of my project would involve identification of the peptides being recognized by the  $\gamma\delta$  TCRs. These could then be refolded in complex with the relevant HLA molecules and used for tetramer staining. Eventually, it would be highly informative to generate  $\gamma\delta$  TCR-pMHC co-crystal structures of these receptors to gain an idea of which CDR loops are involved in peptide contact and of whether  $\gamma\delta$  TCRs use a similar mechanism as  $\alpha\beta$  TCRs for engaging pMHC.  $\alpha\beta$  TCRs generally engage pMHC in conjunction with a coreceptor (Davis and Bjorkman 1988). The coreceptor for  $\alpha\beta$  TCR recognition of peptide-MHCII is the CD4 glycoprotein (Omiya et al. 2002). Neither SW.6B10 nor SW.11H7 clones expressed CD4 (Chapter 3 Figure 6 pg 74). It would be interesting to examine the activity of the 6B10 and 11H7 TCRs in CD4 T-cells in order to test whether CD4 augments recognition of MHCII by the  $\gamma\delta$  TCR.

Unfortunately, my attempts to identify the peptides that were recognised by SW.6B10 and SW.11H7 in the context of HLA-DR7 and HLA-DR15 respectively were unfruitful. My main hope of generating a peptide ligand was to use a combinatorial peptide library approach. This approach has been highly successful for identifying novel peptide ligands that activate T-cells in the context of MHCI (Ekeruche-Makinde et al. 2013; Cole et al. 2016). In future experiments, the use of whole genome CRISPR/Cas9 libraries (as described in Chapter 4) may provide a powerful tool to aid in the identification of the proteins from which the peptide agonists derive from.

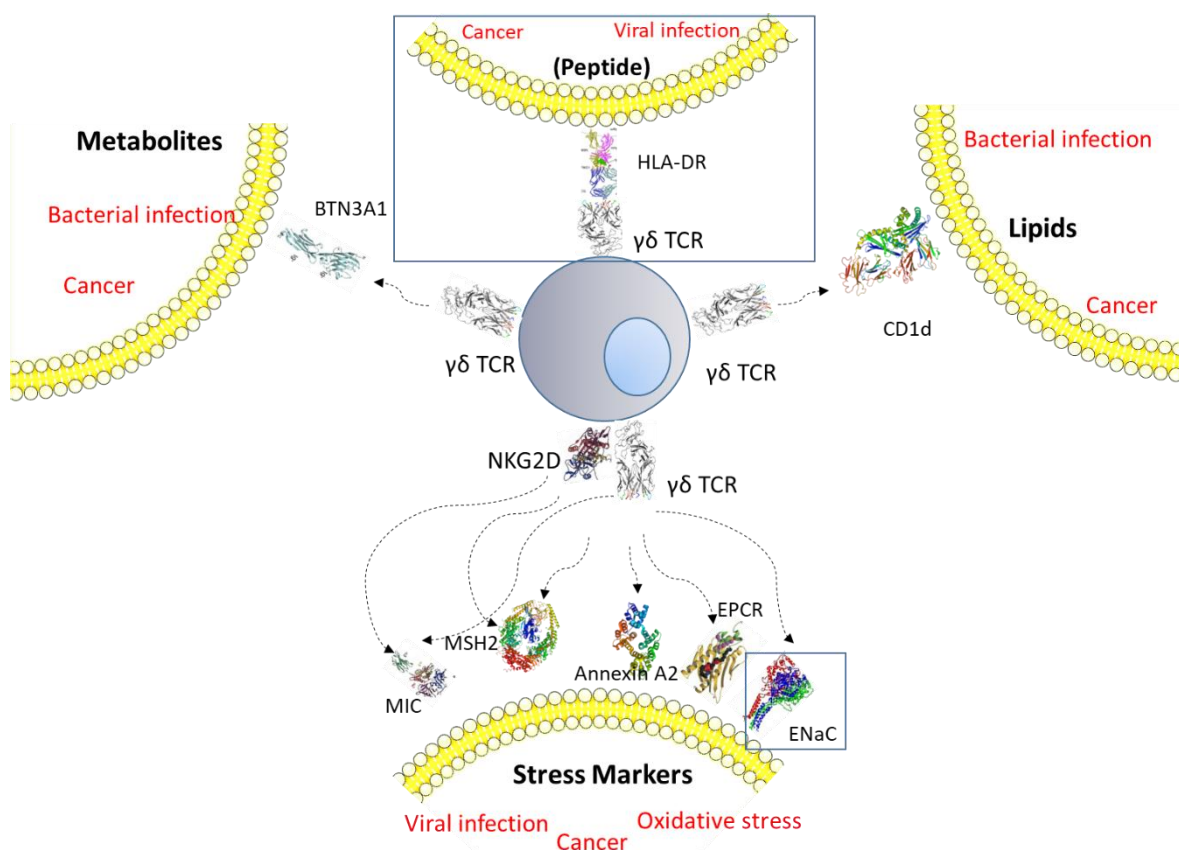
The main T-cells known to recognise peptides in the context of allo-MHC are conventional  $\alpha\beta$  T-cells (Colf et al. 2007; Felix and Allen 2007). The primary role of such cells is to recognise foreign peptides in the context of self-MHC. It is clear that the role of the SW.6B10 and SW.11H7 T-cell clones *in vivo* would not have been to recognise HLA-DR7 and HLA-DR15 respectively. My discovery that these ligands could be functionally recognised by the  $\gamma\delta$  TCR opens up the possibility that like the  $\alpha\beta$  TCR,  $\gamma\delta$  TCR can respond to foreign peptides in the context of self-MHC. If this turns out to be true then it will considerably blur the boundary between conventional and unconventional T-cells and may yet precipitate a whole rethink about the potential role of  $\gamma\delta$  T-cells in immunity.

## 6 General discussion and Conclusions

It is generally acknowledged that  $\gamma\delta$  T-cells play a vital role in stress and cancer surveillance, predominantly via TCR-ligand interactions. However, the exact identity of the cognate ligands and the molecular mechanisms of recognition remain poorly defined, especially as the rules learned from extensive  $\alpha\beta$  TCR recognition cannot be automatically applied to the  $\gamma\delta$  TCR. Furthermore, the identification and isolation of rare tumour reactive  $\gamma\delta$  T-cells from the peripheral blood has been a challenge. My thesis focussed on two important aims: first, generating an optimized method for the procurement of rare tumour reactive  $\gamma\delta$  T-cells from the peripheral blood of healthy donors (Chapter 3), and secondly using methodologies such as whole genome CRISPR (Chapter 4) and HLA mapping (Chapter 5) to identify novel ligands involved in tumour recognition by  $\gamma\delta$  T-cells.

In Chapter 3 I developed a novel methodology for the isolation of rare, tumour reactive  $\gamma\delta$  T-cell clones from peripheral blood of healthy donors. By using magnetic separation techniques I generated enriched polyclonal  $\gamma\delta$  T-cell lines from donors BB67, 0439 and 9909, which I primed on allogeneic LCL. Cloning by limiting dilution allowed me to procure three V $\delta$ 2<sup>neg</sup> monoclonal  $\gamma\delta$  T-cell lines; SW.3G1, SW.6B10 and SW.11H7, which were all shown to be LCL and tumour reactive. Whilst SW.3G1 exhibited pan target reactivity, SW.6B10 and SW.11H7 exerted a pattern of target cell reactivity. I used this information to separate SW.3G1 into Chapter 4 and SW.6B10 and SW.11H7 into Chapter 5 to use different methodologies of delineating exact tumour cell recognition.

In Chapter 4 I focussed on the pan-cancer, pan-LCL reactive clone SW.3G1 and the use of whole genome CRISPR/Cas9 technology to identify novel proteins involved in  $\gamma\delta$  TCR recognition of target cells. I identified a protein, SCNN1A, from the whole genome CRISPR/Cas9 screen. I used knock-in and knock-out methodologies, as-well as TCR transduction techniques to show that SCNN1A was essential for SW.3G1 TCR recognition of both tumour cells and LCL. Thus, in Chapter 4 I identified a novel  $\gamma\delta$  TCR stress ligand. In Chapter 5 I explored the HLA restriction of clones SW.6B10 and SW.11H7 by using antibody blocking, HLA-mapping and single knock-in/knock out methodologies. I showed that both TCRs were able to recognize specific allogeneic MHC Class II molecules (HLA-DR7 and HLA-DR15) found on LCL and tumour. Lastly, I showed that it is likely the  $\gamma\delta$  TCRs required a specific peptide presented by MHC molecules for recognition of tumour cells and LCL. Overall, results from this thesis have identified two novel pathways of  $\gamma\delta$  TCR recognition of target cells in the context of viral infection and cellular transformation (Figure 6.1).



**Figure 6.1: An updated overview of known  $\gamma\delta$  T-cell receptor (TCR) ligands.** The  $\gamma\delta$  TCR recognizes lipids, metabolites, stress markers and MHC in different disease contexts (red). The  $\gamma\delta$  TCR has been shown to recognise the class II MHC molecule HLA-DR on EBV immortalised and tumour cells in an allogeneic setting. The recognition is thought to be dependent on a specific peptide, but further work is needed to confirm this. The  $\gamma\delta$  TCR recognises MHC-1b molecules CD1d, EPCR and MICA/B as well as the MHC-like molecule BTN3A1. The  $\gamma\delta$  TCR can also recognise non-MHC ligands such as SCNN1A, MSH2 and annexin A2. CD1 can present diverse lipids to  $\gamma\delta$  T-cells including self-derived cancer specific lipids and bacterially derived. Similarly BTN3A1 can present self- and bacterially derived metabolites the  $\gamma\delta$  TCR. Cellular stress, such as viral infection, leads to an upregulation/conformational change of stress markers such as EPCR, MIC, MSH2, annexin A2 and EPCR, and thus the cell is recognized by the  $\gamma\delta$  TCR. It is not yet clear how SCNN1A becomes a target for the  $\gamma\delta$  TCR under cancer and viral conditions. Some of the stress markers (MICA/B and MSH2) are also ligands for another  $\gamma\delta$  immunoreceptor, NKG2D. NKG2D contributes to  $\gamma\delta$  TCR-mediated stress sensing by providing a co-stimulatory signal. Detailed descriptions can be found in the main body of the text. BTN3A1, butyrophilin 3A1; EPCR, endothelial protein C receptor; MIC, major histocompatibility complex class I-related chain; MSH2, MutS homologue 2; NKG2D, natural-killer group 2, member D; SCNN1A, sodium channel sub-unit 1.

Collectively the research projects described in my thesis are of great interest to the  $\gamma\delta$  immunology and combines two of the recent 'Breakthroughs of the Year' chosen by the magazine *Science*: immunotherapy (Breakthrough of the Year 2013) and CRISPR/Cas9 mediated genome editing (Breakthrough of the Year 2015). Importantly, the results from my thesis present an interesting avenue for the use of  $\gamma\delta$  TCRs for a pan-population, off-the-shelf immunotherapy. However the ability of  $\gamma\delta$  T-cells to recognise allogeneic MHC molecules presents an added layer of complication, with allogeneic  $\gamma\delta$  T-cell transfusions possibly resulting in harmful graft rejection and graft-versus-host-disease (GvHD).

### 6.1 The $\gamma\delta$ TCR: Foundations of an off-the-shelf pan-population immunotherapy

The development of immunotherapies that are safe, curatively efficient and universal, in terms of pan-tumour and independent of MHC restriction, represents a major challenge in the field. The SW.3G1  $\gamma\delta$  TCR may potentially be one of the first example to solve this challenge; by targeting all tumour types via recognition of a universal stress protein, SCNN1A, via the TCR and independently of MHC restriction. Thus, the use SW.3G1  $\gamma\delta$  TCR and recently enhanced TCR transduction techniques (Legut et al. 2017), could potentially form the foundation of an off-the-shelf pan-population immunotherapy.

The generation of large number of patient-autologous cancer reactive T-cells, as per conventional TIL therapy, can be costly and time consuming (Wu et al. 2012a). Therefore, an off-the-shelf, efficacious, safe allogeneic T-cell product that is readily available in large numbers is highly desirable. I present the case for the production of SW.3G1  $\gamma\delta$  TCR transduced T-cells, in combination with other building blocks (to be discussed below) for successful T-cell therapy, which could be used as an expanded, cryopreserved off-the-shelf method to generate large numbers of allogeneic, cancer specific T-cells. T-cells generated for this purpose must exhibit; functional activity, persistence in the host, immunosuppression escape mechanisms and a safety profile.

In this study I showed that transduction with the SW.3G1 TCR conferred tumour reactivity of polyclonal T-cells (Chapter 4), via recognition of SCNN1A of tumour cells and LCL. Thus, I propose that the SW.3G1 TCR could be transduced into polyclonal T-cell populations, selected for correct TCR expression, and grown up to large numbers to be readily used in immunotherapies. The SW.3G1 TCR is capable of recognizing all tumours expressing SCNN1A in a stress context, which potentially spans across all tumours (Caren et al. 2011; Kohn et al. 2014; Varley et al. 2014; Zhang et al. 2014). As well as SW.3G1 TCR knock-in, it will also be necessary to ensure all of the endogenous TCR is removed, as this has been shown by my laboratory to enhance the anti-

tumour effects of the transduced TCR (Legut et al. 2017). To first use the SW.3G1 TCR in this capacity, however, it is first necessary to understand how the TCR recognition of SCNN1A works, and if SCNN1A is the direct TCR ligand. Future studies should involve biophysical/structural analysis of the TCR bound with SCNN1A.

Next, persistence and survival of the genetically modified T-cells within the patient is considered to be essential to treatment success (Dudley et al. 2008; Pule et al. 2008). One method of improving engraftment and persistence of TCR transferred T-cells is the use of preparative conditioning regimens, such as the use of cyclophosphamide, to deplete the number of host circulating T-cells, otherwise known as lymphodepletion (Wang et al. 2005). Lymphodepletion may promote *in vivo* expansion and survival of TCR transferred T-cells by limiting competition for proliferative cytokines, such as IL-7 and IL-15 (Gattinoni et al. 2005; Paulos et al. 2007). Therefore it would be essential to combine TCR therapy with lymphodepletion techniques.

There are many factors present in the tumour microenvironment affect the efficacy of T-cell based immunotherapies. The tumour microenvironment, consisting of; tumour cells, vasculature and immune cells (Kalluri 2003), is characterised by being highly immune-suppressive. Tumour cells are well known to express ligands, such as PD-L1 and galectin-9, that target and activate immune checkpoint receptors found on the surface of T-cells such as PD-1, TIM-3 and CTLA-4 (Blank and Mackensen 2007; Golden-Mason et al. 2009; Callahan and Wolchok 2013). Such activation of immune checkpoint receptors on T-cells results in T-cell senescence and apoptosis (Schietinger and Greenberg 2014). Current efforts have been focussed on the disruption of immune checkpoint receptor activation, mainly via the use of blocking antibodies (Pardoll 2012; Hassel et al. 2017). When building the SW.3G1 TCR transduction therapy CRISPR/Cas9 technologies could be utilised to target and downregulate immune checkpoint receptors on recipient T-cells. The use of CRISPR/Cas9 to target immune checkpoint receptors has previously been shown to downregulate PD-1 (Su et al. 2016), CTLA-4 (Shi et al. 2017b) and TIM-3 (unpublished data from my laboratory). Importantly, CRISPR/Cas9 targeting of CTLA-4 on cytotoxic T-cells enhanced tumour cell killing by 40% in *in vivo* studies (Shi et al. 2017b) and ablation of PD-1 on TCR transduced T-cells prevented the cells from undergoing tumour induced anergy and exhaustion, as well as promoted their *in situ* anticancer reactivity (Su et al. 2016). Such methodologies should be combined with TCR transduction therapy to significantly improve the anti-tumour activity and survival of TCR transduced T-cells. Furthermore, advancements in CRISPR/Cas9 technology could allow for targeting of all immune checkpoint receptors with a single CRISPR/Cas9 construct (Cong et al. 2013; Jao et al. 2013).

With the removal of checkpoint inhibitors, along with other factors regarding safety of TCR transferred T-cells (discussed below), the use of a genetically engineered safety switch to contain an inducible suicide gene should be used (Gargett and Brown 2014). For example the use of the inducible caspase 9 gene (iCasp9) system together with a small-molecule 'chemical induction of dimerization' (CID) drug AP1903 (Gargett and Brown 2014). The iCasp9 gene contains the intracellular portion of the pro-apoptotic human caspase 9 protein (Straathof et al. 2005) which, with intravenous administration of AP1903, become dimerized causing the activation of downstream executioner caspase 3 and ultimate apoptosis of the cell (Iulucci et al. 2001). The use of iCasp9 system was shown to induce apoptosis in over 99% of targeted T-cells (Marin et al. 2012). Such methodology could be used to eradicate constitutively active TCR transduced T-cells to avoid harmful autoreactivity.

The use of TCR transferred T-cells for immunotherapy has some potential for adverse reactions, such as; on-target off-tumour reactivity [a ligand expressed both on cancer and normal cells], off-target off-tumour reactivity [another ligand is cross-recognised by the receptor, possibly due to an unanticipated structural similarity (Linette et al. 2013)], systemic adverse effects such as cytokine release syndrome (Tanyi et al. 2017) and TCR mis-matching with endogenous TCR. As such a full safety profiling of the SW.3G1 TCR needs to be carried out, both *in vitro* and *in vivo* to check for any unforeseen cross-reactivities to healthy tissue. Furthermore, endogenous TCR should be removed to remove potentially harmful mismatch TCR pairs, which could result in harmful recognition of self antigens (van Loenen et al. 2010). Lastly, in respect to safety MHC should be removed from the surface of TCR transduced T-cells to avoid harmful host allo-reactive immune responses and GvHD in response to the recognition of foreign MHC (Kim et al. 2011). Such methodology has been used previously to show that MHC universal cells can survive in an allogeneic environment following incompatible transplantation (Figueiredo et al. 2013). One could target sequences that have a commonality across all HLA molecules, such as those used in the GeCKO library (Shalem et al. 2014) to achieve MHC knockdown on TCR transfused cells. Another alternative method may involve the targeting of HLA regulators, such as NLRC5 (Meissner et al. 2010; Kobayashi and van den Elsen 2012) and CIITA (Serrat et al. 2010; van den Elsen et al. 2011) which was attempted in my research but was outside the remit of this thesis.

Whilst on the subject of alloreactivity and GvHD it is now necessary to draw attention back to the other two TCRs identified in this thesis; SW.6B10 and SW.11H7, which were shown to recognise and target allogeneic MHC molecules on LCL and tumour cells. Such data will make it absolutely essential for companies, such as Gadeta, that use allogeneic  $\gamma\delta$  T-cell transplants to MHC match donor and host cells prior to transplantation. GvHD, initiated by recognition of

allogeneic MHC molecules, has been shown to be lethal in mouse models (Bendle et al. 2010) and in human patients (Kim et al. 2011). Such data presents a possible implication of using  $\gamma\delta$  T-cells for immunotherapy, and needs to be taken into consideration in the further use of  $\gamma\delta$  TCRs. It would be necessary to fully check whether or not a  $\gamma\delta$  TCR is reactive towards allogeneic MHC before it can be used in the way proposed in this thesis. Finally, the identification of such TCRs as SW.6B10 and SW.11H7 will revolutionize the way that we think  $\gamma\delta$  T-cells work. It is entirely possible that they are not so unconventional after all.

## 6.2 Concluding remarks

Immunotherapy for cancer treatment is a rapidly growing field and has rightly earned its place in *Science's* top scientific breakthrough for 2013, having revolutionised current cancer treatments. In this thesis I focused on investigating the immunotherapeutic potential of  $\gamma\delta$  T-cells. Whilst it is hoped that the future of immunotherapy lies in allogeneic, off-the-shelf cellular products that can target multiple cancers in an efficacious but safe manner, implications from my research add an extra layer of complication when considering the use of  $\gamma\delta$  T-cells. To confirm absolute safety of suggested  $\gamma\delta$  T-cell products full safety profiles must be generated, as well as biophysical and structural analysis of  $\gamma\delta$  TCR/ligand binding to fully understand the mechanisms of reactivity. Overall, it is clear how much potential the  $\gamma\delta$  T-cell has to offer in terms of revolutionizing the field of cancer immunotherapy and this thesis may form the foundation by which future researchers to gain more insight into  $\gamma\delta$  T-cell recognition of cancer cells.



## 7 References

- Abbey, J. L. and O'Neill, H. C. 2008. Expression of T-cell receptor genes during early T-cell development. *Immunol Cell Biol* 86(2), pp. 166-174. doi: 10.1038/sj.icb.7100120
- Abdel-Wahab, N. et al. 2016. Adverse Events Associated with Immune Checkpoint Blockade in Patients with Cancer: A Systematic Review of Case Reports. *PLoS One*. Vol. 11.
- Adams, E. J. 2014. Lipid presentation by human CD1 molecules and the diverse T cell populations that respond to them. *Curr Opin Immunol* 26, pp. 1-6. doi: 10.1016/j.coi.2013.09.005
- Adams, E. J. et al. 2015. Human gamma delta T cells: Evolution and ligand recognition. *Cell Immunol* 296(1), pp. 31-40. doi: 10.1016/j.cellimm.2015.04.008
- Adhikary, D. et al. 2008. Standardized and highly efficient expansion of Epstein-Barr virus-specific CD4+ T cells by using virus-like particles. *J Virol* 82(8), pp. 3903-3911. doi: 10.1128/jvi.02227-07
- Aleksic, M. et al. 2012. Different affinity windows for virus and cancer-specific T-cell receptors: implications for therapeutic strategies. *Eur J Immunol* 42(12), pp. 3174-3179. doi: 10.1002/eji.201242606
- Allison, T. J. et al. 2001. Structure of a human gammadelta T-cell antigen receptor. *Nature* 411(6839), pp. 820-824. doi: 10.1038/35081115
- Amann, M. et al. 2009. Antitumor activity of an EpCAM/CD3-bispecific BiTE antibody during long-term treatment of mice in the absence of T-cell anergy and sustained cytokine release. *J Immunother* 32(5), pp. 452-464. doi: 10.1097/CJI.0b013e3181a1c097
- Attaf, M. et al. 2015a.  $\alpha\beta$  T cell receptors as predictors of health and disease. *Cell Mol Immunol*. Vol. 12. pp. 391-399.
- Attaf, M. et al. 2015b. The T cell antigen receptor: the Swiss army knife of the immune system. *Clin Exp Immunol* 181(1), pp. 1-18. doi: 10.1111/cei.12622
- Bai, L. et al. 2012. The majority of CD1d-sulfatide-specific T cells in human blood use a semiinvariant V $\delta$ 1 TCR. *Eur J Immunol* 42(9), pp. 2505-2510. doi: 10.1002/eji.201242531
- Balakrishnan, A. et al. 2006. Metalloprotease inhibitors GM6001 and TAPI-0 inhibit the obligate intracellular human pathogen *Chlamydia trachomatis* by targeting peptide deformylase of the bacterium. *J Biol Chem* 281(24), pp. 16691-16699. doi: 10.1074/jbc.M513648200
- Benaud, C. et al. 2015. Annexin A2 is required for the early steps of cytokinesis. *EMBO Rep* 16(4), pp. 481-489. doi: 10.15252/embr.201440015
- Bendle, G. M. et al. 2010. Lethal graft-versus-host disease in mouse models of T cell receptor gene therapy. *Nat Med* 16(5), pp. 565-570, 561p following 570. doi: 10.1038/nm.2128
- Betts, M. R. et al. 2003. Sensitive and viable identification of antigen-specific CD8+ T cells by a flow cytometric assay for degranulation. *J Immunol Methods* 281(1-2), pp. 65-78.

- Bianchi, V. et al. 2016. A Molecular Switch Abrogates Glycoprotein 100 (gp100) T-cell Receptor (TCR) Targeting of a Human Melanoma Antigen. *J Biol Chem* 291(17), pp. 8951-8959. doi: 10.1074/jbc.M115.707414
- Birkinshaw, R. W. et al. 2015. alphabeta T cell antigen receptor recognition of CD1a presenting self lipid ligands. *Nat Immunol* 16(3), pp. 258-266. doi: 10.1038/ni.3098
- Blake, D. J. et al. 1998. beta-dystrobrevin, a member of the dystrophin-related protein family. *Proc Natl Acad Sci U S A* 95(1), pp. 241-246.
- Blank, C. and Mackensen, A. 2007. Contribution of the PD-L1/PD-1 pathway to T-cell exhaustion: an update on implications for chronic infections and tumor evasion. *Cancer Immunol Immunother* 56(5), pp. 739-745. doi: 10.1007/s00262-006-0272-1
- Bolotin, D. A. et al. 2015. MiXCR: software for comprehensive adaptive immunity profiling. *Nat Methods*. Vol. 12. United States, pp. 380-381.
- Bondarava, M. et al. 2009. alpha-ENaC is a functional element of the hypertonicity-induced cation channel in HepG2 cells and it mediates proliferation. *Pflugers Arch* 458(4), pp. 675-687. doi: 10.1007/s00424-009-0649-z
- Brandes, M. et al. 2009. Cross-presenting human gammadelta T cells induce robust CD8+ alphabeta T cell responses. *Proc Natl Acad Sci U S A* 106(7), pp. 2307-2312. doi: 10.1073/pnas.0810059106
- Brandes, M. et al. 2005. Professional antigen-presentation function by human gammadelta T Cells. *Science* 309(5732), pp. 264-268. doi: 10.1126/science.1110267
- Buccheri, S. et al. 2014. Efficacy and safety of gammadeltaT cell-based tumor immunotherapy: a meta-analysis. *J Biol Regul Homeost Agents* 28(1), pp. 81-90.
- Burtrum, D. B. et al. 1996. TCR gene recombination and alpha beta-gamma delta lineage divergence: productive TCR-beta rearrangement is neither exclusive nor preclusive of gamma delta cell development. *J Immunol* 157(10), pp. 4293-4296.
- Caccamo, N. et al. 2006. CXCR5 identifies a subset of Vgamma9Vdelta2 T cells which secrete IL-4 and IL-10 and help B cells for antibody production. *J Immunol* 177(8), pp. 5290-5295.
- Callahan, M. K. and Wolchok, J. D. 2013. At the bedside: CTLA-4- and PD-1-blocking antibodies in cancer immunotherapy. *J Leukoc Biol* 94(1), pp. 41-53. doi: 10.1189/jlb.1212631
- Canessa, C. M. et al. 1994. Amiloride-sensitive epithelial Na<sup>+</sup> channel is made of three homologous subunits. *Nature* 367(6462), pp. 463-467. doi: 10.1038/367463a0
- Caren, H. et al. 2011. Identification of epigenetically regulated genes that predict patient outcome in neuroblastoma. *BMC Cancer* 11, p. 66. doi: 10.1186/1471-2407-11-66

- Chang, M. H. et al. 2016. Long-term Effects of Hepatitis B Immunization of Infants in Preventing Liver Cancer. *Gastroenterology* 151(3), pp. 472-480.e471. doi: 10.1053/j.gastro.2016.05.048
- Chen, L. and Flies, D. B. 2013. Molecular mechanisms of T cell co-stimulation and co-inhibition. *Nat Rev Immunol* 13(4), pp. 227-242. doi: 10.1038/nri3405
- Chien, Y. H. and Konigshofer, Y. 2007. Antigen recognition by gammadelta T cells. *Immunol Rev* 215, pp. 46-58. doi: 10.1111/j.1600-065X.2006.00470.x
- Cho, S. W. et al. 2013. Targeted genome engineering in human cells with the Cas9 RNA-guided endonuclease. *Nat Biotechnol* 31(3), pp. 230-232. doi: 10.1038/nbt.2507
- Ciccone, E. et al. 1989. Specificity of human T lymphocytes expressing a gamma/delta T cell antigen receptor. Recognition of a polymorphic determinant of HLA class I molecules by a gamma/delta clone. *Eur J Immunol* 19(7), pp. 1267-1271. doi: 10.1002/eji.1830190718
- Cole, D. K. et al. 2016. Hotspot autoimmune T cell receptor binding underlies pathogen and insulin peptide cross-reactivity. *J Clin Invest* 126(6), pp. 2191-2204. doi: 10.1172/jci85679
- Cole, D. K. et al. 2012. Modification of the carboxy-terminal flanking region of a universal influenza epitope alters CD4(+) T-cell repertoire selection. *Nat Commun* 3, p. 665. doi: 10.1038/ncomms1665
- Cole, D. K. et al. 2014. T-cell Receptor (TCR)-Peptide Specificity Overrides Affinity-enhancing TCR-Major Histocompatibility Complex Interactions\*. *J Biol Chem*. Vol. 289. pp. 628-638.
- Cole, D. K. et al. 2007. Human TCR-binding affinity is governed by MHC class restriction. *J Immunol* 178(9), pp. 5727-5734.
- Cole, D. K. et al. 2009. Germ line-governed recognition of a cancer epitope by an immunodominant human T-cell receptor. *J Biol Chem* 284(40), pp. 27281-27289. doi: 10.1074/jbc.M109.022509
- Colf, L. A. et al. 2007. How a single T cell receptor recognizes both self and foreign MHC. *Cell* 129(1), pp. 135-146. doi: 10.1016/j.cell.2007.01.048
- Cong, L. et al. 2013. Multiplex genome engineering using CRISPR/Cas systems. *Science* 339(6121), pp. 819-823. doi: 10.1126/science.1231143
- Constant, P. et al. 1994. Stimulation of human gamma delta T cells by nonpeptidic mycobacterial ligands. *Science* 264(5156), pp. 267-270.
- Couzin-Frankel, J. 2013. Breakthrough of the year 2013. Cancer immunotherapy. *Science*. Vol. 342. United States, pp. 1432-1433.
- Cunningham, C. et al. 2010. Sequences of complete human cytomegalovirus genomes from infected cell cultures and clinical specimens. *J Gen Virol*. Vol. 91. pp. 605-615.

Dai, Y. et al. 2012. Ectopically expressed human tumor biomarker MutS homologue 2 is a novel endogenous ligand that is recognized by human gammadelta T cells to induce innate anti-tumor/virus immunity. *J Biol Chem* 287(20), pp. 16812-16819. doi: 10.1074/jbc.M111.327650

Dascher, C. C. 2007. Evolutionary biology of CD1. *Curr Top Microbiol Immunol* 314, pp. 3-26.

Davey, M. S. et al. 2017. Clonal selection in the human Vdelta1 T cell repertoire indicates gammadelta TCR-dependent adaptive immune surveillance. *Nat Commun* 8, p. 14760. doi: 10.1038/ncomms14760

Davis, H. E. et al. 2002. Polybrene increases retrovirus gene transfer efficiency by enhancing receptor-independent virus adsorption on target cell membranes. *Biophys Chem* 97(2-3), pp. 159-172.

Davis, M. and Bjorkman, P. 1988. T-cell antigen receptor genes and T-cell recognition. *Nature* 334, p. 395402

Davis, M. M. 2004. The evolutionary and structural 'logic' of antigen receptor diversity. *Semin Immunol* 16(4), pp. 239-243. doi: 10.1016/j.smim.2004.08.003

de Coo, R. F. et al. 1997. Molecular cloning and characterization of the human mitochondrial NADH:oxidoreductase 10-kDa gene (NDUFV3). *Genomics* 45(2), pp. 434-437. doi: 10.1006/geno.1997.4930

de la Salle, H. et al. 2005. Assistance of microbial glycolipid antigen processing by CD1e. *Science* 310(5752), pp. 1321-1324. doi: 10.1126/science.1115301

Del Monaco, S. M. et al. 2009. Cell migration in BeWo cells and the role of epithelial sodium channels. *J Membr Biol* 232(1-3), pp. 1-13. doi: 10.1007/s00232-009-9206-0

DeMars, R. et al. 1984. Homozygous deletions that simultaneously eliminate expressions of class I and class II antigens of EBV-transformed B-lymphoblastoid cells. I. Reduced proliferative responses of autologous and allogeneic T cells to mutant cells that have decreased expression of class II antigens. *Hum Immunol* 11(2), pp. 77-97.

Deng, Y. et al. 2015. Annexin A2 plays a critical role in epithelial ovarian cancer. *Arch Gynecol Obstet* 292(1), pp. 175-182. doi: 10.1007/s00404-014-3598-5

Dieli, F. et al. 2007. Targeting human {gamma}delta T cells with zoledronate and interleukin-2 for immunotherapy of hormone-refractory prostate cancer. *Cancer Res* 67(15), pp. 7450-7457. doi: 10.1158/0008-5472.can-07-0199

Dimova, T. et al. 2015. Effector Vgamma9Vdelta2 T cells dominate the human fetal gammadelta T-cell repertoire. *Proc Natl Acad Sci U S A* 112(6), pp. E556-565. doi: 10.1073/pnas.1412058112

Dolton, G. et al. 2015. More tricks with tetramers: a practical guide to staining T cells with peptide-MHC multimers. *Immunology* 146(1), pp. 11-22. doi: 10.1111/imm.12499

- Donia, M. et al. 2012. Analysis of V $\delta$ 1 T cells in clinical grade melanoma-infiltrating lymphocytes. *Oncoimmunology* 1(8), pp. 1297-1304. doi: 10.4161/onci.21659
- Drake, C. G. et al. 2006. Mechanisms of immune evasion by tumors. *Adv Immunol* 90, pp. 51-81. doi: 10.1016/S0065-2776(06)90002-9
- Drees, B. et al. 2000. Characterization of the interaction between zyxin and members of the Ena/vasodilator-stimulated phosphoprotein family of proteins. *J Biol Chem* 275(29), pp. 22503-22511. doi: 10.1074/jbc.M001698200
- Dressman, M. A. et al. 2001. Genes that co-cluster with estrogen receptor alpha in microarray analysis of breast biopsies. *Pharmacogenomics J* 1(2), pp. 135-141.
- Dudley, M. E. et al. 2008. Adoptive cell therapy for patients with metastatic melanoma: evaluation of intensive myeloablative chemoradiation preparative regimens. *J Clin Oncol* 26(32), pp. 5233-5239. doi: 10.1200/jco.2008.16.5449
- Dulberger, C. L. et al. 2017. Human Leukocyte Antigen F Presents Peptides and Regulates Immunity through Interactions with NK Cell Receptors. *Immunity* 46(6), pp. 1018-1029.e1017. doi: 10.1016/j.immuni.2017.06.002
- Déchanet, J. et al. 1999. Implication of gammadelta T cells in the human immune response to cytomegalovirus. *J Clin Invest* 103(10), pp. 1437-1449. doi: 10.1172/JCI5409
- Edinger, R. S. et al. 2012. The epithelial sodium channel (ENaC) establishes a trafficking vesicle pool responsible for its regulation. *PLoS One* 7(9), p. e46593. doi: 10.1371/journal.pone.0046593
- Eisenreich, W. et al. 2004. Biosynthesis of isoprenoids via the non-mevalonate pathway. *Cell Mol Life Sci* 61(12), pp. 1401-1426. doi: 10.1007/s00018-004-3381-z
- Ekeruche-Makinde, J. et al. 2013. Peptide length determines the outcome of TCR/peptide-MHCI engagement. *Blood* 121(7), pp. 1112-1123. doi: 10.1182/blood-2012-06-437202
- Erlich, H. et al. 1986. Molecular analysis of HLA class I and class II antigen loss mutants reveals a homozygous deletion of the DR, DQ, and part of the DP region: implications for class II gene order. *Hum Immunol* 16(2), pp. 205-219.
- Facciotti, F. et al. 2011. Fine tuning by human CD1e of lipid-specific immune responses. *Proc Natl Acad Sci U S A* 108(34), pp. 14228-14233. doi: 10.1073/pnas.1108809108
- Farnault, L. et al. 2013. Clinical evidence implicating gamma-delta T cells in EBV control following cord blood transplantation. *Bone Marrow Transplant* 48(11), pp. 1478-1479. doi: 10.1038/bmt.2013.75
- Farouk, S. E. et al. 2004. Gamma delta T cells inhibit in vitro growth of the asexual blood stages of *Plasmodium falciparum* by a granule exocytosis-dependent cytotoxic pathway that requires granulysin. *Eur J Immunol* 34(8), pp. 2248-2256. doi: 10.1002/eji.200424861

Felix, N. J. and Allen, P. M. 2007. Specificity of T-cell alloreactivity. *Nat Rev Immunol* 7(12), pp. 942-953. doi: 10.1038/nri2200

Ferrero, I. et al. 2006. TCRgamma silencing during alphabeta T cell development depends upon pre-TCR-induced proliferation. *J Immunol* 177(9), pp. 6038-6043.

Fesnak, A. D. et al. 2016. Engineered T Cells: The Promise and Challenges of Cancer Immunotherapy. *Nat Rev Cancer* 16(9), pp. 566-581. doi: 10.1038/nrc.2016.97

Figueiredo, C. et al. 2013. MHC Universal Cells Survive in an Allogeneic Environment after Incompatible Transplantation. *Biomed Res Int* 2013, doi: 10.1155/2013/796046

Flament, C. et al. 1994. Human TCR-gamma/delta alloreactive response to HLA-DR molecules. Comparison with response of TCR-alpha/beta. *J Immunol* 153(7), pp. 2890-2904.

Fujishima, N. et al. 2007. Skewed T cell receptor repertoire of Vdelta1(+) gammadelta T lymphocytes after human allogeneic haematopoietic stem cell transplantation and the potential role for Epstein-Barr virus-infected B cells in clonal restriction. *Clin Exp Immunol* 149(1), pp. 70-79. doi: 10.1111/j.1365-2249.2007.03388.x

Galon, J. et al. 2006. Type, density, and location of immune cells within human colorectal tumors predict clinical outcome. *Science* 313(5795), pp. 1960-1964. doi: 10.1126/science.1129139

Garcia, K. C. et al. 1997. Alphabeta T cell receptor interactions with syngeneic and allogeneic ligands: affinity measurements and crystallization. *Proc Natl Acad Sci U S A* 94(25), pp. 13838-13843.

Gargett, T. and Brown, M. P. 2014. The inducible caspase-9 suicide gene system as a "safety switch" to limit on-target, off-tumor toxicities of chimeric antigen receptor T cells. *Front Pharmacol* 5, doi: 10.3389/fphar.2014.00235

Gattinoni, L. et al. 2005. Removal of homeostatic cytokine sinks by lymphodepletion enhances the efficacy of adoptively transferred tumor-specific CD8+ T cells. *J Exp Med* 202(7), pp. 907-912. doi: 10.1084/jem.20050732

Gentles, A. J. et al. 2015. The prognostic landscape of genes and infiltrating immune cells across human cancers. *Nat Med* 21(8), pp. 938-945. doi: 10.1038/nm.3909

Gober, H. J. et al. 2003. Human T cell receptor gammadelta cells recognize endogenous mevalonate metabolites in tumor cells. *J Exp Med* 197(2), pp. 163-168.

Golden-Mason, L. et al. 2009. Negative immune regulator Tim-3 is overexpressed on T cells in hepatitis C virus infection and its blockade rescues dysfunctional CD4+ and CD8+ T cells. *J Virol* 83(18), pp. 9122-9130. doi: 10.1128/JVI.00639-09

Green, A. E. et al. 2004. Recognition of nonpeptide antigens by human V gamma 9V delta 2 T cells requires contact with cells of human origin. *Clin Exp Immunol* 136(3), pp. 472-482. doi: 10.1111/j.1365-2249.2004.02472.x

- Groh, V. et al. 1998. Recognition of stress-induced MHC molecules by intestinal epithelial gammadelta T cells. *Science* 279(5357), pp. 1737-1740.
- Gross, G. et al. 1989. Generation of effector T cells expressing chimeric T cell receptor with antibody type-specificity. *Transplant Proc* 21(1 Pt 1), pp. 127-130.
- Haks, M. C. et al. 2005. Attenuation of gammadeltaTCR signaling efficiently diverts thymocytes to the alphabeta lineage. *Immunity* 22(5), pp. 595-606. doi: 10.1016/j.immuni.2005.04.003
- Halary, F. et al. 2005. Shared reactivity of V{delta}2(neg) {gamma}{delta} T cells against cytomegalovirus-infected cells and tumor intestinal epithelial cells. *J Exp Med* 201(10), pp. 1567-1578. doi: 10.1084/jem.20041851
- Haney, D. et al. 2011. Isolation of viable antigen-specific CD8+ T cells based on membrane-bound tumor necrosis factor (TNF)-alpha expression. *J Immunol Methods* 369(1-2), pp. 33-41. doi: 10.1016/j.jim.2011.04.003
- Hanukoglu, I. 2017. ASIC and ENaC type sodium channels: conformational states and the structures of the ion selectivity filters. *Febs j* 284(4), pp. 525-545. doi: 10.1111/febs.13840
- Hanukoglu, I. and Hanukoglu, A. 2016. Epithelial sodium channel (ENaC) family: Phylogeny, structure-function, tissue distribution, and associated inherited diseases. *Gene* 579(2), pp. 95-132. doi: 10.1016/j.gene.2015.12.061
- Harly, C. et al. 2012. Key implication of CD277/butyrophilin-3 (BTN3A) in cellular stress sensing by a major human gammadelta T-cell subset. *Blood* 120(11), pp. 2269-2279. doi: 10.1182/blood-2012-05-430470
- Hassel, J. C. et al. 2017. Combined immune checkpoint blockade (anti-PD-1/anti-CTLA-4): Evaluation and management of adverse drug reactions. *Cancer Treat Rev* 57, pp. 36-49. doi: 10.1016/j.ctrv.2017.05.003
- Hayday, A. C. 2009. Gammadelta T cells and the lymphoid stress-surveillance response. *Immunity* 31(2), pp. 184-196. doi: 10.1016/j.immuni.2009.08.006
- Hayes, S. M. et al. 2005. TCR signal strength influences alphabeta/gammadelta lineage fate. *Immunity* 22(5), pp. 583-593. doi: 10.1016/j.immuni.2005.03.014
- Hidalgo, J. V. et al. 2014. Histological Analysis of gammadelta T Lymphocytes Infiltrating Human Triple-Negative Breast Carcinomas. *Front Immunol* 5, p. 632. doi: 10.3389/fimmu.2014.00632
- Himoudi, N. et al. 2012. Human gammadelta T lymphocytes are licensed for professional antigen presentation by interaction with opsonized target cells. *J Immunol* 188(4), pp. 1708-1716. doi: 10.4049/jimmunol.1102654
- Hintz, M. et al. 2001. Identification of (E)-4-hydroxy-3-methyl-but-2-enyl pyrophosphate as a major activator for human gammadelta T cells in Escherichia coli. *FEBS Lett* 509(2), pp. 317-322.

- Hinz, T. et al. 1997. Identification of the complete expressed human TCR V gamma repertoire by flow cytometry. *Int Immunol* 9(8), pp. 1065-1072.
- Hoare, H. L. et al. 2006. Structural basis for a major histocompatibility complex class Ib-restricted T cell response. *Nat Immunol* 7(3), pp. 256-264. doi: 10.1038/ni1312
- Holland, C. J. et al. 2013. Re-Directing CD4(+) T Cell Responses with the Flanking Residues of MHC Class II-Bound Peptides: The Core is Not Enough. *Front Immunol* 4, p. 172. doi: 10.3389/fimmu.2013.00172
- Holland, C. J. et al. 2015. Enhanced Detection of Antigen-Specific CD4+ T Cells Using Altered Peptide Flanking Residue Peptide-MHC Class II Multimers. *J Immunol* 195(12), pp. 5827-5836. doi: 10.4049/jimmunol.1402787
- Horvath, P. and Barrangou, R. 2010. CRISPR/Cas, the immune system of bacteria and archaea. *Science* 327(5962), pp. 167-170. doi: 10.1126/science.1179555
- Hui-Yuen, J. et al. 2011. Establishment of Epstein-Barr Virus Growth-transformed Lymphoblastoid Cell Lines. *J Vis Exp*.
- Hummler, E. and Beermann, F. 2000. Scnn1 sodium channel gene family in genetically engineered mice. *J Am Soc Nephrol* 11 Suppl 16, pp. S129-134.
- Iulucci, J. D. et al. 2001. Intravenous safety and pharmacokinetics of a novel dimerizer drug, AP1903, in healthy volunteers. *J Clin Pharmacol* 41(8), pp. 870-879.
- Jao, L. E. et al. 2013. Efficient multiplex biallelic zebrafish genome editing using a CRISPR nuclease system. *Proc Natl Acad Sci U S A* 110(34), pp. 13904-13909. doi: 10.1073/pnas.1308335110
- Jena, B. et al. 2013. Chimeric antigen receptor (CAR)-specific monoclonal antibody to detect CD19-specific T cells in clinical trials. *PLoS One* 8(3), p. e57838. doi: 10.1371/journal.pone.0057838
- Jinushi, M. et al. 2003. Expression and role of MICA and MICB in human hepatocellular carcinomas and their regulation by retinoic acid. *Int J Cancer* 104(3), pp. 354-361. doi: 10.1002/ijc.10966
- Jonasch, E. et al. 2008. Vaccination of metastatic renal cell carcinoma patients with autologous tumour-derived vitespen vaccine: clinical findings. *Br J Cancer* 98(8), pp. 1336-1341. doi: 10.1038/sj.bjc.6604266
- Jordan, M. and Wurm, F. 2004. Transfection of adherent and suspended cells by calcium phosphate. *Methods* 33(2), pp. 136-143. doi: 10.1016/j.ymeth.2003.11.011
- Kallemeijn, M. J. et al. 2017. Ageing and latent CMV infection impact on maturation, differentiation and exhaustion profiles of T-cell receptor gammadelta T-cells. *Sci Rep* 7(1), p. 5509. doi: 10.1038/s41598-017-05849-1
- Kalluri, R. 2003. Basement membranes: structure, assembly and role in tumour angiogenesis. *Nat Rev Cancer* 3(6), pp. 422-433. doi: 10.1038/nrc1094



- Kapoor, N. et al. 2009. Knockdown of ASIC1 and epithelial sodium channel subunits inhibits glioblastoma whole cell current and cell migration. *J Biol Chem* 284(36), pp. 24526-24541. doi: 10.1074/jbc.M109.037390
- Khan, M. W. et al. 2014. Potential Use of gammadelta T Cell-Based Vaccines in Cancer Immunotherapy. *Front Immunol* 5, p. 512. doi: 10.3389/fimmu.2014.00512
- Kiessling, M. K. et al. 2016. Identification of oncogenic driver mutations by genome-wide CRISPR-Cas9 dropout screening. *BMC Genomics* 17(1), p. 723. doi: 10.1186/s12864-016-3042-2
- Kim, H. S. et al. 2017. CRISPR/Cas9-mediated gene knockout screens and target identification via whole-genome sequencing uncover host genes required for picornavirus infection. *J Biol Chem* 292(25), pp. 10664-10671. doi: 10.1074/jbc.M117.782425
- Kim, J. M. et al. 2011. Graft-versus-host disease after kidney transplantation. *J Korean Surg Soc* 80(Suppl 1), pp. S36-39. doi: 10.4174/jkss.2011.80.Suppl1.S36
- Kirkwood, J. M. et al. 2001. High-dose interferon alfa-2b significantly prolongs relapse-free and overall survival compared with the GM2-KLH/QS-21 vaccine in patients with resected stage IIB-III melanoma: results of intergroup trial E1694/S9512/C509801. *J Clin Oncol* 19(9), pp. 2370-2380. doi: 10.1200/jco.2001.19.9.2370
- Kistowska, M. et al. 2008. Dysregulation of the host mevalonate pathway during early bacterial infection activates human TCR gamma delta cells. *Eur J Immunol* 38(8), pp. 2200-2209. doi: 10.1002/eji.200838366
- Kjer-Nielsen, L. et al. 2012. MR1 presents microbial vitamin B metabolites to MAIT cells. *Nature* 491(7426), pp. 717-723. doi: 10.1038/nature11605
- Kobayashi, H. et al. 2007. Safety profile and anti-tumor effects of adoptive immunotherapy using gamma-delta T cells against advanced renal cell carcinoma: a pilot study. *Cancer Immunol Immunother* 56(4), pp. 469-476. doi: 10.1007/s00262-006-0199-6
- Kobayashi, K. S. and van den Elsen, P. J. 2012. NLRC5: a key regulator of MHC class I-dependent immune responses. *Nat Rev Immunol* 12(12), pp. 813-820. doi: 10.1038/nri3339
- Kohn, K. W. et al. 2014. Gene expression correlations in human cancer cell lines define molecular interaction networks for epithelial phenotype. *PLoS One* 9(6), p. e99269. doi: 10.1371/journal.pone.0099269
- Kondo, M. et al. 2011. Expansion of human peripheral blood gammadelta T cells using zoledronate. *J Vis Exp* (55), doi: 10.3791/3182
- Kong, Y. et al. 2009. The NKG2D ligand ULBP4 binds to TCRgamma9/delta2 and induces cytotoxicity to tumor cells through both TCRgammadelta and NKG2D. *Blood* 114(2), pp. 310-317. doi: 10.1182/blood-2008-12-196287
- Kurioka, A. et al. 2015. MAIT cells are licensed through granzyme exchange to kill bacterially sensitized targets. *Mucosal Immunol* 8(2), pp. 429-440. doi: 10.1038/mi.2014.81

Lamers, C. H. et al. 2006. Treatment of metastatic renal cell carcinoma with autologous T-lymphocytes genetically retargeted against carbonic anhydrase IX: first clinical experience. *J Clin Oncol*. Vol. 24. United States, pp. e20-22.

Lanca, T. et al. 2010. The MHC class Ib protein ULBP1 is a nonredundant determinant of leukemia/lymphoma susceptibility to gammadelta T-cell cytotoxicity. *Blood* 115(12), pp. 2407-2411. doi: 10.1182/blood-2009-08-237123

Landais, E. et al. 2005. The human T cell immune response to Epstein-Barr virus. *Int J Dev Biol* 49(2-3), pp. 285-292. doi: 10.1387/ijdb.041947el

Lanier, L. L. 2015. NKG2D Receptor and Its Ligands in Host Defense. *Cancer Immunol Res* 3(6), pp. 575-582. doi: 10.1158/2326-6066.cir-15-0098

Laugel, B. et al. 2005. Design of soluble recombinant T cell receptors for antigen targeting and T cell inhibition. *J Biol Chem* 280(3), pp. 1882-1892. doi: 10.1074/jbc.M409427200

Le Nours, J. et al. 2016. Atypical natural killer T-cell receptor recognition of CD1d-lipid antigens. *Nat Commun* 7, p. 10570. doi: 10.1038/ncomms10570

Lefranc, M. P. 2001. Nomenclature of the human T cell receptor genes. *Curr Protoc Immunol* Appendix 1, p. Appendix 10. doi: 10.1002/0471142735.ima01os40

Legut, M. et al. 2015. The promise of  $\gamma\delta$  T cells and the  $\gamma\delta$  T cell receptor for cancer immunotherapy. *Cell Mol Immunol*, doi: 10.1038/cmi.2015.28

Legut, M. et al. 2017. CRISPR-mediated TCR replacement generates superior anticancer transgenic T-cells. *Blood*, doi: 10.1182/blood-2017-05-787598

Linette, G. P. et al. 2013. Cardiovascular toxicity and titin cross-reactivity of affinity-enhanced T cells in myeloma and melanoma. *Blood*. Vol. 122. pp. 863-871.

Lissina, A. et al. 2009. Protein kinase inhibitors substantially improve the physical detection of T-cells with peptide-MHC tetramers. *J Immunol Methods* 340(1), pp. 11-24. doi: 10.1016/j.jim.2008.09.014

Liu, C. et al. 2016. ENaC/DEG in Tumor Development and Progression. *J Cancer*. Vol. 7. pp. 1888-1891.

Luoma, A. M. et al. 2013. Crystal structure of V $\delta$ 1 T cell receptor in complex with CD1d-sulfatide shows MHC-like recognition of a self-lipid by human  $\gamma\delta$  T cells. *Immunity* 39(6), doi: 10.1016/j.immuni.2013.11.001

Maciocia, P. M. et al. 2017. Targeting the T cell receptor beta-chain constant region for immunotherapy of T cell malignancies. *Nat Med*, doi: 10.1038/nm.4444

Malhotra, V. and Perry, M. C. 2003. Classical chemotherapy: mechanisms, toxicities and the therapeutic window. *Cancer Biol Ther* 2(4 Suppl 1), pp. S2-4.

- Mali, P. et al. 2013. Cas9 as a versatile tool for engineering biology. *Nat Methods* 10(10), pp. 957-963. doi: 10.1038/nmeth.2649
- Mami-Chouaib, F. et al. 1996. TCR alpha/beta and TCR gamma/delta CD4-/CD8- HLA-DR alloreactive CTL clones do not use Fas/Fas ligand pathway to lyse their specific target cells. *Hum Immunol* 51(1), pp. 13-22.
- Mandelcorn-Monson, R. L. et al. 2003. Cytotoxic T lymphocyte reactivity to gp100, MelanA/MART-1, and tyrosinase, in HLA-A2-positive vitiligo patients. *J Invest Dermatol* 121(3), pp. 550-556. doi: 10.1046/j.1523-1747.2003.12413.x
- Mangan, B. A. et al. 2013. Cutting edge: CD1d restriction and Th1/Th2/Th17 cytokine secretion by human Vdelta3 T cells. *J Immunol* 191(1), pp. 30-34. doi: 10.4049/jimmunol.1300121
- Marin, V. et al. 2012. Comparison of different suicide-gene strategies for the safety improvement of genetically manipulated T cells. *Hum Gene Ther Methods* 23(6), pp. 376-386. doi: 10.1089/hgtb.2012.050
- Marlin, R. et al. 2017. Sensing of cell stress by human gammadelta TCR-dependent recognition of annexin A2. *Proc Natl Acad Sci U S A* 114(12), pp. 3163-3168. doi: 10.1073/pnas.1621052114
- Marx, S. et al. 1997. Activation of human gamma delta T cells by Mycobacterium tuberculosis and Daudi lymphoma cells: differential regulatory effect of IL-10 and IL-12. *J Immunol* 158(6), pp. 2842-2848.
- Matis, L. A. et al. 1989. Structure and specificity of a class II MHC alloreactive gamma delta T cell receptor heterodimer. *Science* 245(4919), pp. 746-749.
- McCormack, E. et al. 2013. Bi-specific TCR-anti CD3 redirected T-cell targeting of NY-ESO-1- and LAGE-1-positive tumors. *Cancer Immunol Immunother* 62(4), pp. 773-785. doi: 10.1007/s00262-012-1384-4
- Meissner, T. B. et al. 2010. NLR family member NLRC5 is a transcriptional regulator of MHC class I genes. *Proc Natl Acad Sci U S A* 107(31), pp. 13794-13799. doi: 10.1073/pnas.1008684107
- Menschikowski, M. et al. 2011. Expression and shedding of endothelial protein C receptor in prostate cancer cells. *Cancer Cell Int*. Vol. 11. p. 4.
- Miller, S. D. et al. 2007. Antigen-specific tolerance strategies for the prevention and treatment of autoimmune disease. *Nat Rev Immunol* 7(9), pp. 665-677. doi: 10.1038/nri2153
- Mohan Rao, L. V. et al. 2014. Endothelial cell protein C receptor: a multiliganded and multifunctional receptor. *Blood*. Vol. 124. pp. 1553-1562.
- Moody, D. B. et al. 1999. Uptake and processing of glycosylated mycolates for presentation to CD1b-restricted T cells. *Immunol Lett* 65(1-2), pp. 85-91.
- Moresco, E. M. Y. et al. 2013. Going Forward with Genetics: Recent Technological Advances and Forward Genetics in Mice. *Am J Pathol*. Vol. 182. pp. 1462-1473.

Morgan, R. A. et al. 2006. Cancer regression in patients after transfer of genetically engineered lymphocytes. *Science* 314(5796), pp. 126-129. doi: 10.1126/science.1129003

Munk, M. E. et al. 1990. Target cell lysis and IL-2 secretion by gamma/delta T lymphocytes after activation with bacteria. *J Immunol* 145(8), pp. 2434-2439.

Murray, R. J. et al. 1992. Identification of target antigens for the human cytotoxic T cell response to Epstein-Barr virus (EBV): implications for the immune control of EBV-positive malignancies. *J Exp Med* 176(1), pp. 157-168.

Nagai, M. et al. 1998. Suppression of alloreactivity with gamma delta T-cells: relevance to increased gamma delta T-cells following bone marrow transplantation. *Biomed Pharmacother* 52(3), pp. 137-142. doi: 10.1016/s0753-3322(98)80092-9

Nagorsen, D. et al. 2009. Immunotherapy of lymphoma and leukemia with T-cell engaging BiTE antibody blinatumomab. *Leuk Lymphoma* 50(6), pp. 886-891. doi: 10.1080/10428190902943077

Neurauter, A. A. et al. 2007. Cell isolation and expansion using Dynabeads. *Adv Biochem Eng Biotechnol* 106, pp. 41-73. doi: 10.1007/10\_2007\_072

Nielsen, M. M. et al. 2017. gammadelta T cells in homeostasis and host defence of epithelial barrier tissues. *Nat Rev Immunol*, doi: 10.1038/nri.2017.101

Nieto-Torres, J. L. et al. 2015. Relevance of Viroporin Ion Channel Activity on Viral Replication and Pathogenesis. *Viruses*. Vol. 7. pp. 3552-3573.

O'Brien, R. L. and Born, W. 1991. Heat shock proteins as antigens for gamma delta T cells. *Semin Immunol* 3(2), pp. 81-87.

O'Neil-Andersen, N. J. and Lawrence, D. A. 2002. Differential modulation of surface and intracellular protein expression by T cells after stimulation in the presence of monensin or brefeldin A. *Clin Diagn Lab Immunol* 9(2), pp. 243-250.

Oates, J. et al. 2015. ImmTACs for targeted cancer therapy: Why, what, how, and which. *Mol Immunol* 67(2 Pt A), pp. 67-74. doi: 10.1016/j.molimm.2015.01.024

Obst, R. 2015. The Timing of T Cell Priming and Cycling. *Front Immunol* 6, p. 563. doi: 10.3389/fimmu.2015.00563

Oganesyan, V. et al. 2002. The Crystal Structure of the Endothelial Protein C Receptor and a Bound Phospholipid. doi: 10.1074/jbc.C200163200

Omiya, R. et al. 2002. Inhibition of EBV-induced lymphoproliferation by CD4(+) T cells specific for an MHC class II promiscuous epitope. *J Immunol* 169(4), pp. 2172-2179.

- Onishi, M. et al. 2015. Annexin A2 regulates angiogenesis and invasion phenotypes of malignant glioma. *Brain Tumor Pathol* 32(3), pp. 184-194. doi: 10.1007/s10014-015-0216-6
- Paget, C. et al. 2012. Role of gammadelta T cells in alpha-galactosylceramide-mediated immunity. *J Immunol* 188(8), pp. 3928-3939. doi: 10.4049/jimmunol.1103582
- Pardoll, D. M. 2012. The blockade of immune checkpoints in cancer immunotherapy. *Nat Rev Cancer* 12(4), pp. 252-264. doi: 10.1038/nrc3239
- Patel, O. et al. 2013. Recognition of vitamin B metabolites by mucosal-associated invariant T cells. *Nat Commun* 4, p. 2142. doi: 10.1038/ncomms3142
- Patel, S. J. et al. 2017. Identification of essential genes for cancer immunotherapy. *Nature* 548(7669), pp. 537-542. doi: 10.1038/nature23477
- Paulos, C. M. et al. 2007. Microbial translocation augments the function of adoptively transferred self/tumor-specific CD8<sup>+</sup> T cells via TLR4 signaling. *J Clin Invest* 117(8), pp. 2197-2204. doi: 10.1172/jci32205
- Pellicci, D. G. et al. 2014. The molecular bases of delta/alphabeta T cell-mediated antigen recognition. *J Exp Med* 211(13), pp. 2599-2615. doi: 10.1084/jem.20141764
- Phan, G. Q. and Rosenberg, S. A. 2013. Adoptive cell transfer for patients with metastatic melanoma: the potential and promise of cancer immunotherapy. *Cancer Control* 20(4), pp. 289-297.
- Poccia, F. et al. 2002. Innate T-cell immunity in HIV infection: the role of Vgamma9Vdelta2 T lymphocytes. *Curr Mol Med* 2(8), pp. 769-781.
- Price, D. A. et al. 1999. Cytotoxic T lymphocytes, chemokines and antiviral immunity. *Immunol Today* 20(5), pp. 212-216.
- Prinz, I. et al. 2006. Visualization of the earliest steps of gammadelta T cell development in the adult thymus. *Nat Immunol* 7(9), pp. 995-1003. doi: 10.1038/ni1371
- Puig-Pey, I. et al. 2010. Characterization of  $\gamma\delta$  T cell subsets in organ transplantation. *Transplant International* 23(10), pp. 1045-1055. doi: 10.1111/j.1432-2277.2010.01095.x
- Pule, M. A. et al. 2008. Virus-specific T cells engineered to coexpress tumor-specific receptors: persistence and antitumor activity in individuals with neuroblastoma. *Nat Med* 14(11), pp. 1264-1270. doi: 10.1038/nm.1882
- Qi, Q. et al. 2014. Diversity and clonal selection in the human T-cell repertoire. *Proc Natl Acad Sci U S A* 111(36), pp. 13139-13144. doi: 10.1073/pnas.1409155111
- Ravens, S. et al. 2017. Human gammadelta T cells are quickly reconstituted after stem-cell transplantation and show adaptive clonal expansion in response to viral infection. *Nat Immunol* 18(4), pp. 393-401. doi: 10.1038/ni.3686

- Reck, M. et al. 2016. Pembrolizumab versus Chemotherapy for PD-L1-Positive Non-Small-Cell Lung Cancer. *N Engl J Med* 375(19), pp. 1823-1833. doi: 10.1056/NEJMoa1606774
- Rellahan, B. L. et al. 1991. Junctional sequences influence the specificity of gamma/delta T cell receptors. *J Exp Med* 173(2), pp. 503-506.
- Rhodes, D. A. et al. 2015. Activation of human gammadelta T cells by cytosolic interactions of BTN3A1 with soluble phosphoantigens and the cytoskeletal adaptor periplakin. *J Immunol* 194(5), pp. 2390-2398. doi: 10.4049/jimmunol.1401064
- Riano, F. et al. 2014. Vgamma9Vdelta2 TCR-activation by phosphorylated antigens requires butyrophilin 3 A1 (BTN3A1) and additional genes on human chromosome 6. *Eur J Immunol* 44(9), pp. 2571-2576. doi: 10.1002/eji.201444712
- Ribeiro, S. T. et al. 2015. Five Layers of Receptor Signaling in gammadelta T-Cell Differentiation and Activation. *Front Immunol* 6, p. 15. doi: 10.3389/fimmu.2015.00015
- Richter, H. et al. 2013. Exploiting CRISPR/Cas: interference mechanisms and applications. *Int J Mol Sci* 14(7), pp. 14518-14531. doi: 10.3390/ijms140714518
- Robins, H. S. et al. 2009. Comprehensive assessment of T-cell receptor beta-chain diversity in alphabeta T cells. *Blood* 114(19), pp. 4099-4107. doi: 10.1182/blood-2009-04-217604
- Robinson, J. et al. 2016. The IPD-IMGT/HLA Database - New developments in reporting HLA variation. *Hum Immunol* 77(3), pp. 233-237. doi: 10.1016/j.humimm.2016.01.020
- Rock, E. P. et al. 1994. CDR3 length in antigen-specific immune receptors. *J Exp Med* 179(1), pp. 323-328.
- Roelofs, A. J. et al. 2009. Peripheral blood monocytes are responsible for gammadelta T cell activation induced by zoledronic acid through accumulation of IPP/DMAPP. *Br J Haematol* 144(2), pp. 245-250. doi: 10.1111/j.1365-2141.2008.07435.x
- Roll, J. D. et al. 2008. DNMT3b overexpression contributes to a hypermethylator phenotype in human breast cancer cell lines. *Mol Cancer* 7, p. 15. doi: 10.1186/1476-4598-7-15
- Rosenberg, S. A. et al. 1988. Use of tumor-infiltrating lymphocytes and interleukin-2 in the immunotherapy of patients with metastatic melanoma. A preliminary report. *N Engl J Med* 319(25), pp. 1676-1680. doi: 10.1056/nejm198812223192527
- Roy, S. et al. 2016a. Molecular Analysis of Lipid-Reactive Vdelta1 gammadelta T Cells Identified by CD1c Tetramers. *J Immunol* 196(4), pp. 1933-1942. doi: 10.4049/jimmunol.1502202
- Roy, S. et al. 2016b. Molecular Analysis of Lipid-Reactive Vdelta1 gamma delta T Cells Identified by CD1c Tetramers. *J Immunol* 196(4), pp. 1933-1942. doi: 10.4049/jimmunol.1502202

- Roy, S. et al. 2014. Molecular basis of mycobacterial lipid antigen presentation by CD1c and its recognition by alphabeta T cells. *Proc Natl Acad Sci U S A* 111(43), pp. E4648-4657. doi: 10.1073/pnas.1408549111
- Ruf, W. and Schaffner, F. 2014. Role of the protein C receptor in cancer progression. *Thromb Res* 133 Suppl 2, pp. S85-89. doi: 10.1016/s0049-3848(14)50014-x
- Russano, A. M. et al. 2006. Recognition of pollen-derived phosphatidyl-ethanolamine by human CD1d-restricted gamma delta T cells. *J Allergy Clin Immunol* 117(5), pp. 1178-1184. doi: 10.1016/j.jaci.2006.01.001
- Salio, M. et al. 2014. Biology of CD1- and MR1-restricted T cells. *Annu Rev Immunol* 32, pp. 323-366. doi: 10.1146/annurev-immunol-032713-120243
- San Jose, E. et al. 2000. Triggering the TCR complex causes the downregulation of nonengaged receptors by a signal transduction-dependent mechanism. *Immunity* 12(2), pp. 161-170.
- Schietinger, A. and Greenberg, P. D. 2014. Tolerance and exhaustion: defining mechanisms of T cell dysfunction. *Trends Immunol* 35(2), pp. 51-60. doi: 10.1016/j.it.2013.10.001
- Schossere, M. et al. 2015. Methylation of ribosomal RNA by NSUN5 is a conserved mechanism modulating organismal lifespan. *Nat Commun* 6, p. 6158. doi: 10.1038/ncomms7158
- Sebestyen, Z. et al. 2016. RhoB Mediates Phosphoantigen Recognition by Vgamma9Vdelta2 T Cell Receptor. *Cell Rep* 15(9), pp. 1973-1985. doi: 10.1016/j.celrep.2016.04.081
- Serrat, N. et al. 2010. The locus control region of the MHC class II promoter acts as a repressor element, the activity of which is inhibited by CIITA. *Mol Immunol* 47(4), pp. 825-832. doi: 10.1016/j.molimm.2009.09.040
- Sewell, A. K. 2012. Why must T cells be cross-reactive? *Nat Rev Immunol* 12(9), pp. 669-677. doi: 10.1038/nri3279
- Shafi, S. et al. 2011. An NKG2D-mediated human lymphoid stress surveillance response with high interindividual variation. *Sci Transl Med* 3(113), p. 113ra124. doi: 10.1126/scitranslmed.3002922
- Shalem, O. et al. 2014. Genome-scale CRISPR-Cas9 knockout screening in human cells. *Science* 343(6166), pp. 84-87. doi: 10.1126/science.1247005
- Shehata, M. F. 2009. Regulation of the epithelial sodium channel [ENaC] in kidneys of salt-sensitive Dahl rats: insights on alternative splicing. *Int Arch Med* 2(1), p. 28. doi: 10.1186/1755-7682-2-28
- Shi, C. X. et al. 2017a. CRISPR genome-wide screening identifies dependence on the proteasome subunit PSMC6 for Bortezomib sensitivity in multiple myeloma. *Mol Cancer Ther*, doi: 10.1158/1535-7163.mct-17-0130
- Shi, L. et al. 2017b. CRISPR knock out CTLA-4 enhances the anti-tumor activity of cytotoxic T lymphocytes. *Gene* 636, pp. 36-41. doi: 10.1016/j.gene.2017.09.010

Shi, P. et al. 2014. Valproic acid sensitizes pancreatic cancer cells to natural killer cell-mediated lysis by upregulating MICA and MICB via the PI3K/Akt signaling pathway. *BMC Cancer*. Vol. 14. p. 370.

Siegel, R. et al. 2014. Cancer statistics, 2014. *CA Cancer J Clin* 64(1), pp. 9-29. doi: 10.3322/caac.21208

Sinzger, C. et al. 2008. Cloning and sequencing of a highly productive, endotheliotropic virus strain derived from human cytomegalovirus TB40/E. *J Gen Virol* 89(Pt 2), pp. 359-368. doi: 10.1099/vir.0.83286-0

Skinner, S. R. et al. 2016. Human papillomavirus (HPV)-16/18 AS04-adjuvanted vaccine for the prevention of cervical cancer and HPV-related diseases. *Expert Rev Vaccines* 15(3), pp. 367-387. doi: 10.1586/14760584.2016.1124763

Smith-Garvin, J. E. et al. 2009. T cell activation. *Annu Rev Immunol* 27, pp. 591-619. doi: 10.1146/annurev.immunol.021908.132706

Spada, F. M. et al. 2000. Self-recognition of CD1 by gamma/delta T cells: implications for innate immunity. *J Exp Med* 191(6), pp. 937-948.

Stadinski, B. D. et al. 2016. Hydrophobic CDR3 residues promote the development of self-reactive T cells. *Nat Immunol* 17(8), pp. 946-955. doi: 10.1038/ni.3491

Steinmann, E. and Pietschmann, T. 2010. Hepatitis C virus p7-a viroporin crucial for virus assembly and an emerging target for antiviral therapy. *Viruses* 2(9), pp. 2078-2095. doi: 10.3390/v2092078

Straathof, K. C. et al. 2005. An inducible caspase 9 safety switch for T-cell therapy. *Blood* 105(11), pp. 4247-4254. doi: 10.1182/blood-2004-11-4564

Su, S. et al. 2016. CRISPR-Cas9 mediated efficient PD-1 disruption on human primary T cells from cancer patients. *Sci Rep* 6, p. 20070. doi: 10.1038/srep20070

Sznol, M. et al. 2017. Pooled Analysis Safety Profile of Nivolumab and Ipilimumab Combination Therapy in Patients With Advanced Melanoma. *J Clin Oncol*, p. Jco2016721167. doi: 10.1200/jco.2016.72.1167

Tan, M. P. et al. 2017. Human leucocyte antigen class I-redirected anti-tumour CD4+ T cells require a higher T cell receptor binding affinity for optimal activity than CD8+ T cells. *Clin Exp Immunol* 187(1), pp. 124-137. doi: 10.1111/cei.12828

Tan, M. P. et al. 2015. T cell receptor binding affinity governs the functional profile of cancer-specific CD8+ T cells. *Clin Exp Immunol* 180(2), pp. 255-270. doi: 10.1111/cei.12570

Tanaka, Y. et al. 1994. Nonpeptide ligands for human gamma delta T cells. *Proc Natl Acad Sci U S A* 91(17), pp. 8175-8179.

Tanyi, J. L. et al. 2017. Possible Compartmental Cytokine Release Syndrome in a Patient With Recurrent Ovarian Cancer After Treatment With Mesothelin-targeted CAR-T Cells. *J Immunother* 40(3), pp. 104-107. doi: 10.1097/cji.0000000000000160



- Tchagang, A. B. et al. 2008. Early detection of ovarian cancer using group biomarkers. *Mol Cancer Ther* 7(1), pp. 27-37. doi: 10.1158/1535-7163.mct-07-0565
- Theirez, A. et al. 2007. Self/non-self discrimination by human gammadelta T cells: simple solutions for a complex issue? *Immunol Rev* 215, pp. 123-135. doi: 10.1111/j.1600-065X.2006.00468.x
- Turchinovich, G. and Hayday, A. C. 2011. Skint-1 identifies a common molecular mechanism for the development of interferon-gamma-secreting versus interleukin-17-secreting gammadelta T cells. *Immunity* 35(1), pp. 59-68. doi: 10.1016/j.immuni.2011.04.018
- Tyler, C. J. et al. 2015. Human Vgamma9/Vdelta2 T cells: Innate adaptors of the immune system. *Cell Immunol* 296(1), pp. 10-21. doi: 10.1016/j.cellimm.2015.01.008
- Tyler, C. J. et al. 2017. Antigen-Presenting Human gammadelta T Cells Promote Intestinal CD4+ T Cell Expression of IL-22 and Mucosal Release of Calprotectin. *J Immunol* 198(9), pp. 3417-3425. doi: 10.4049/jimmunol.1700003
- Uldrich, A. P. et al. 2013. CD1d-lipid antigen recognition by the gammadelta TCR. *Nat Immunol* 14(11), pp. 1137-1145. doi: 10.1038/ni.2713
- Van de Walle, I. et al. 2013. Specific Notch receptor–ligand interactions control human TCR- $\alpha\beta/\gamma\delta$  development by inducing differential Notch signal strength. *J Exp Med*. Vol. 210. pp. 683-697.
- van den Elsen, P. J. et al. 2011. Expression Regulation of Major Histocompatibility Complex Class I and Class II Encoding Genes. *Frontiers in Immunology* 2, doi: 10.3389/fimmu.2011.00048
- van der Gaag, E. J. et al. 2002. Role of zyxin in differential cell spreading and proliferation of melanoma cells and melanocytes. *J Invest Dermatol* 118(2), pp. 246-254. doi: 10.1046/j.0022-202x.2001.01657.x
- van der Harst, D. et al. 1991. Selective outgrowth of CD45RO+ V gamma 9+/V delta 2+ T-cell receptor gamma/delta T cells early after bone marrow transplantation. *Blood* 78(7), pp. 1875-1881.
- van Loenen, M. M. et al. 2010. Mixed T cell receptor dimers harbor potentially harmful neoreactivity. *Proc Natl Acad Sci U S A*. Vol. 107. pp. 10972-10977.
- Vander Heiden, M. G. et al. 2009. Understanding the Warburg Effect: The Metabolic Requirements of Cell Proliferation. *Science* 324(5930), pp. 1029-1033. doi: 10.1126/science.1160809
- Vantourout, P. and Hayday, A. 2013. Six-of-the-best: unique contributions of  $\gamma\delta$  T cells to immunology. *Nat Rev Immunol* 13(2), pp. 88-100. doi: 10.1038/nri3384
- Varley, K. E. et al. 2014. Recurrent read-through fusion transcripts in breast cancer. *Breast Cancer Res Treat* 146(2), pp. 287-297. doi: 10.1007/s10549-014-3019-2
- Vavassori, S. et al. 2013. Butyrophilin 3A1 binds phosphorylated antigens and stimulates human gammadelta T cells. *Nat Immunol* 14(9), pp. 908-916. doi: 10.1038/ni.2665

- Vermijlen, D. et al. 2010. Human cytomegalovirus elicits fetal gammadelta T cell responses in utero. *J Exp Med* 207(4), pp. 807-821. doi: 10.1084/jem.20090348
- Vilmer, E. et al. 1988. Prominent expansion of circulating lymphocytes bearing gamma T-cell receptors, with preferential expression of variable gamma genes after allogeneic bone marrow transplantation. *Blood* 72(3), pp. 841-849.
- Wang, J. et al. 2012. MicroRNA-610 inhibits the migration and invasion of gastric cancer cells by suppressing the expression of vasodilator-stimulated phosphoprotein. *Eur J Cancer* 48(12), pp. 1904-1913. doi: 10.1016/j.ejca.2011.11.026
- Wang, L. X. et al. 2005. Host lymphodepletion augments T cell adoptive immunotherapy through enhanced intratumoral proliferation of effector cells. *Cancer Res* 65(20), pp. 9547-9554. doi: 10.1158/0008-5472.can-05-1175
- Watanabe, T. et al. 2014. Prediction of response to preoperative chemoradiotherapy in rectal cancer by using reverse transcriptase polymerase chain reaction analysis of four genes. *Dis Colon Rectum* 57(1), pp. 23-31. doi: 10.1097/01.dcr.0000437688.33795.9d
- Weekes, M. P. et al. 2014. Quantitative temporal viromics: an approach to investigate host-pathogen interaction. *Cell* 157(6), pp. 1460-1472. doi: 10.1016/j.cell.2014.04.028
- Weiner, L. M. et al. 2009. Monoclonal Antibodies for Cancer Immunotherapy. *Lancet* 373(9668), pp. 1033-1040. doi: 10.1016/s0140-6736(09)60251-8
- Wilkinson, G. W. et al. 2015. Human cytomegalovirus: taking the strain. *Med Microbiol Immunol* 204(3), pp. 273-284. doi: 10.1007/s00430-015-0411-4
- Willcox, C. R. et al. 2012. Cytomegalovirus and tumor stress surveillance by binding of a human  $\gamma\delta$  T cell antigen receptor to endothelial protein C receptor. *Nat Immunol* 13(9), pp. 872-879. doi: 10.1038/ni.2394
- Wrobel, P. et al. 2007. Lysis of a broad range of epithelial tumour cells by human gamma delta T cells: involvement of NKG2D ligands and T-cell receptor- versus NKG2D-dependent recognition. *Scand J Immunol* 66(2-3), pp. 320-328. doi: 10.1111/j.1365-3083.2007.01963.x
- Wu, R. et al. 2012a. Adoptive T-cell therapy using autologous tumor-infiltrating lymphocytes for metastatic melanoma: current status and future outlook. *Cancer J* 18(2), pp. 160-175. doi: 10.1097/PPO.0b013e31824d4465
- Wu, X. et al. 2012b. Valproic acid upregulates NKG2D ligand expression through an ERK-dependent mechanism and potentially enhances NK cell-mediated lysis of myeloma. *Neoplasia* 14(12), pp. 1178-1189.
- Wu, Y. and Kang, T. 2016. Protein stability regulators screening assay (Pro-SRSA): protein degradation meets the CRISPR-Cas9 library. *Chin J Cancer* 35(1), p. 60. doi: 10.1186/s40880-016-0125-z

- Wu, Y. et al. 2009. Human  $\gamma\delta$  T Cells: A Lymphoid Lineage Cell Capable of Professional Phagocytosis. doi: 10.4049/jimmunol.0901772
- Wucherpfennig, K. W. et al. 2010. Structural Biology of the T-cell Receptor: Insights into Receptor Assembly, Ligand Recognition, and Initiation of Signaling. *Cold Spring Harb Perspect Biol.* Vol. 2.
- Xu, B. et al. 2011. Crystal structure of a gammadelta T-cell receptor specific for the human MHC class I homolog MICA. *Proc Natl Acad Sci U S A* 108(6), pp. 2414-2419. doi: 10.1073/pnas.1015433108
- Xu, S. et al. 2016. Potential Roles of Amiloride-Sensitive Sodium Channels in Cancer Development. *Biomed Res Int* 2016, doi: 10.1155/2016/2190216
- Yuan, P. et al. 2015. Chondroitin sulfate proteoglycan 4 functions as the cellular receptor for Clostridium difficile toxin B. *Cell Res* 25(2), pp. 157-168. doi: 10.1038/cr.2014.169
- Zarin, P. et al. 2014. Enforcement of gammadelta-lineage commitment by the pre-T-cell receptor in precursors with weak gammadelta-TCR signals. *Proc Natl Acad Sci U S A* 111(15), pp. 5658-5663. doi: 10.1073/pnas.1312872111
- Zaritskaya, L. et al. 2010. New flow cytometric assays for monitoring cell-mediated cytotoxicity. *Expert Rev Vaccines* 9(6), pp. 601-616. doi: 10.1586/erv.10.49
- Zhang, Z. et al. 2014. miR-125b inhibits hepatitis B virus expression in vitro through targeting of the SCNN1A gene. *Arch Virol* 159(12), pp. 3335-3343. doi: 10.1007/s00705-014-2208-y
- Ziegler, H. et al. 2014. Human Peripheral CD4(+) Vdelta1(+) gammadeltaT Cells Can Develop into alphabetaT Cells. *Front Immunol* 5, p. 645. doi: 10.3389/fimmu.2014.00645
- Zotova, A. et al. 2016. Determining antigen specificity of a monoclonal antibody using genome-scale CRISPR-Cas9 knockout library. *J Immunol Methods* 439, pp. 8-14. doi: 10.1016/j.jim.2016.09.006



## 8 Appendix

**Table 8.1: Primers used for sequencing and PCR**

<b>Primer name</b>	<b>Sequence (5'-3')</b>	<b>Application</b>
TRD R1	CAGTCTTTGCAAACAGCATTC	trd PCR
TRD R2	ATGGTTTGGTATGAGGCTGAC	trd PCR
TRG R1	CATGTCTGACGATACATCTGTG	trg PCR
TRG R2	ACATCTGCATCAAGTTGTTTAT	trg PCR
UPM F	CTAATACGACTCACTATAGGGC AAGCAGTGGTATCAACGCAGAGT	trd/trg PCR
Short UPM F	CTAATACGACTCACTATAGGGC	trd/trg PCR
M13 F	GTAAAACGACGGCCAG	TOPO PCR and sequencing
M13 R	CAGGAAACAGCTATGAC	TOPO PCR and sequencing
pELNS F1	GAGTTTGGATCTTGGTTCATTC	pELNS PCR
pELNS F2	CTTCCATTTCAAGGTGTCGTG	pELNS sequencing
pELNS R1	GCATTAAAGCAGCGTATCCAC	pELNS PCR
pELNS R2	CCAGAGGTTGATTGTGCGAC	pELNS sequencing
pELNS R3	AGAAACTTGCACCGCATATG	pELNS sequencing
GeCKO F1	AATGGACTATCATATGCTTACCGTAACTTGAAAGT ATTTCG	pLentiCRISPR PCR and sequencing
GeCKO R1	TGTGGGCGATGTGCGCTCTG	pLentiCRISPR PCR
GeCKO F2	TCTTGTGGAAAGGACGAAACACCG	pLentiCRISPR PCR
GeCKO R2	ACCGGAGCCAATTCCCACTCCTTTC	pLentiCRISPR PCR
GeCKO seq	AAAAGCACCGACTCGGTGCCAC	pLentiCRISPR PCR and sequencing
Adaptor F	AATGGACTATCATATGCTTACCGTAACTTGAAAGT ATTTCG	GeCKO library PCR
Adaptor R	TCTACTATTCTTTCCCCTGCACTGTTGTGGGCGATG TGCGCTCTG	GeCKO library PCR

T7 F	TAATACGACTCACTATAGGG	pGMT7 PCR and sequencing
T7 R	GCTAGTTATTGCTCAGCGG	pGMT7 PCR and sequencing

**Table 8.2: Amino acid sequence of  $\gamma\delta$  TCRs synthesised and cloned into the lentiviral vector pELNS.** CDR3 sequences are underlined while the constant domains are shown in colour (blue – TRGC1, red – TRDC), and the 2A sequence with linker is shown in grey.

### SW.3G1 TCR

MRWALAVLLAFLSPASQKSSNLEGRTKSVTRQTGSSAEITCDLTVNTFYIHWYHQQEGKAPQRLLYYDVST  
 ARDVLESGLSPGKYYHTPRRWSWILRLQNLIENTSGVYYCATWDRRD**CATWDRRDYKKLFG**SGTTLVVT  
**DKQLDADVSPKPTIFLPSIAETKLQKAGTYLCLLEKFFPDV**IKIHWQEKKSN**TILGSQEGNTMKTNDTYMKFS**  
**WLTVPKSLDKEHRCIVRHENNKNGVDQE**IFPIKTDVITMDPKDNCSKDANDTLLQLTNTSAYMYLLLL  
**LKSVVYFAITCCLLRRTAFCCNGEKS**GGSGGEGRGSLLTCGDVEENPGPMLFSSLLCVFAFSYSGSSVAQKV  
 TQAQSSVSMPVRKAVTLNCLYETSWWSYIFWYKQLPSKEMIFLIRQGSDEQNAKSGRYSVNFKKAASVA  
 LTISALQLEDSAKYF**CALGVLP****TVTGGGLIF**GKGTRVTV**ERSQPHTKPSVFVMKNGTNVACLVKEFY**PKDIRI  
**NLVSSKKITEFDPAIVISPSGKYNAVKLGKYEDSNSVTCSVQHDNKT**VHSTDFEVKTDSTDHVKPKETENTKQ  
**PSKSCHKPKAIVHTEKVNMMSLTVLGLRMLFAKT**VAVNFLLTAKLFFL

### SW.6B10 TCR

MLLALALLAFLPPASQKSSNLEGRTKSVTRPTGSSAVITCDLPVENAVYTHWYHQQEGKAPQRLLYYDSYNS  
 RVVLESGISREKYHTYASTGKSLKFILENLIERDSGVYY**CATWVPATYYKKLFG**SGTTLVVT**DKQLDADVSPK**  
**TIFLPSIAETKLQKAGTYLCLLEKFFPDV**IKIHWQEKKSN**TILGSQEGNTMKTNDTYMKFSWLTVPKSLDKEH**  
**RCIVRHENNKNGVDQE**IFPIKTDVITMDPKDNCSKDANDTLLQLTNTSAYMYLLLLLKSVVYFAITCCL  
**RRRTAFCCNGEKS**GGSGGEGRGSLLTCGDVEENPGPMLFSSLLCVFAFSYSGSSVAQKV**TQAQSSVSMPVR**  
 KAVTLNCLYETSWWSYIFWYKQLPSKEMIFLIRQGSDEQNAKSGRYSVNFKKAASVALTISALQLEDSAKY  
**FCALGEPRPSYVLGDTGEYTDK**LIFGKGTRVTV**ERSQPHTKPSVFVMKNGTNVACLVKEFY**PKDIRINLV  
**SSKKITEFDPAIVISPSGKYNAVKLGKYEDSNSVTCSVQHDNKT**VHSTDFEVKTDSTDHVKPKETENTKQPSKS  
**CHKPKAIVHTEKVNMMSLTVLGLRMLFAKT**VAVNFLLTAKLFFL

### SW.11H7 TCR

MQWALAVLLAFLSPASQKSSNLEGRTKSVIRQTGSSAEITCDLAEGSTGYIHWYHQQEGKAPQRLLYYDSYTS  
 SVVLESGISPGKYDTYGSTRKNLRMILRNLIENDSGVYY**CATWDGHYYKKLFG**SGTTLVVT**DKQLDADVSPK**  
**PTIFLPSIAETKLQKAGTYLCLLEKFFPDV**IKIHWQEKKSN**TILGSQEGNTMKTNDTYMKFSWLTVPKSLDKE**  
**HRCIVRHENNKNGVDQE**IFPIKTDVITMDPKDNCSKDANDTLLQLTNTSAYMYLLLLLKSVVYFAITCCL  
**LRRTAFCCNGEKS**GGSGGEGRGSLLTCGDVEENPGPMLFSSLLCVFAFSYSGSSVAQKV**TQAQSSVSMPV**  
 RKAVTLNCLYETSWWSYIFWYKQLPSKEMIFLIRQGSDEQNAKSGRYSVNFKKAASVALTISALQLEDSAKY  
**YFCALGVPAYVVTGDSWDTRQM**FFGTGIKLFVEP**ERSQPHTKPSVFVMKNGTNVACLVKEFY**PKDIRINLV  
**SSKKITEFDPAIVISPSGKYNAVKLGKYEDSNSVTCSVQHDNKT**VHSTDFEVKTDSTDHVKPKETENTKQPSKS  
**CHKPKAIVHTEKVNMMSLTVLGLRMLFAKT**VAVNFLLTAKLFFL

**Table 8.3: Amino acid sequences synthesized and cloned into the lentiviral pELNS.**

**HLA-DRB1\*0701**

AATMAISGVPVLGFFIIAVLMSAQESWAIKEEHVIIQAEFYLNPDQSGEFMFDFDGDGEIFHVDMAKKETVW  
RLEEFGRFASF EAQGALANIAVDKANLEIMTKRSNYTPITNVPPEVTVLTNSPVELREPNVLICFIDKFTPPVV  
NVTWLRNGKPVTTGVSETVFLPREDHLFRKFHYLPFLPSTEDVYDCRVEHWGLDEPLLKHWEFDAPSPLPET  
TENNVV CALGLTVGLVGIIIGTIFIHKGVRSNAAERRGPLGSGEGRGSLLTCGDVEENPGPMVCLKLPGGSCM  
AALTVTLMVLSSPLALAGDTQPRFLWQGYKCHFFNGTERVQFLERLFYNQEEFVRFSDVGEYRAVTELG  
RPVAESWNSQKDILEDRRGQVDTVCRHNYGVGESFTVQRRVHPEVTVYPAKTQPLQHHNLLVCSVSGFYF  
GSIEVRWFRNGQEEKAGVVSTGLIQNGDWTFQTLVMELETVPRSGEVYTCQVEHPSVMSPLTVEWRARSES  
AQSKMLSGVGGFVLGLLFLGAGLFIYFRNQKGHSGLQPTGFLS

**HLA-DRB1\*1501**

ATMQWALAVLLAFLSPASQKSSNLEGRKTSVIRQTGSSAEITCDLAEGSTGYIHWYHQQEGKAPQRLLYDS  
YTSSVVLSESGISPGKYDTYGSTRKNLRMLRNLIENDSGVYYCATWDGHYYKKLFGSGTTLVVTDKQLDADVS  
PKPTIFLPSIAETKLQKAGTYLCLLEKFFPDVIKIHWQEKKSNTILGSQEGNTMKTNDTYMKFSWLTVPKSLD  
KEHRCIVRHENNKNGVDQEIIFFPIKTDVITMDPKDNCSKDANDTLLLQLTNTSAYMYLLLLLSVVYFAITC  
CLLRRTAFCCNGEKGSGSGSGEGRGSLLTCGDVEENPGPMLFSSLLCVFAFSYSGSSVAQKVTQAQSSVSMP  
VRKAVTLNCLYETSWWSYYIFWYKQLPSKEMIFLIRQGSDEQNAKSGRYSVNFKKAASVALTISALQLEDSA  
KYFCALGVPAYVVTGDSWDTRQMFFGTGIKLFVEPRSQPHTKPSVFVMKNGTNVACLKVEFYPKDIRINLVS  
SKKITEFDPAIVISPSGKYNAVKLGKYEDSNSVTCVQHDNKT VHSTDFEVKTDSTDHVKPKETENTKQPSKS  
CHKPKAIVHTEKVNMMSLTVLGLRMLFAKTVAVNFLLTAKLFFL

**SCNN1A Isoform 1**

MEGNKLEEQDSSPPQSTPGLMKGNKREEQGLGPEPAAPQQPTAEELIEFHRSYRELFEFFCNNTTIHGAI  
RLVCSQHNRMKTAFAWVWLCTFGMMYWQFGLLFGEYFSYPVSLNINLNSDKLVFPAVTICTLNPYRYPEI  
KEELEELDRITEQTLFDLYKYSSFTTLVAGSRSRDLRGTLPHPLQRLRVPPPHGARRARSVASSLRDNNPQV  
DWKDWKIGFQLCNQNKSDCFYQTYSSGVDAREWYRFHYINILSRLPETLPSLEEDTLGNFIFACRFNQVSC  
NQANYSHFHHPMYGNCYTFNDKNNNLWMSSMPGINNGLSLMLRAEQNDFIPLLSTVTGARVMVHGQ  
DEPAFMDDGGFNLRPGVETSISMRKETLDRLGGDYGDCTKNGSDVPVENLYPSKYTQQVCIHSCFQESMIK  
ECGCAYIFYPRPQNVEYCDYRKHSSWGYYKLQVDFSSDHLGCFTKCRKPCSVTSYQLSAGYSRWPSVTSQ  
EWWFQMLSRQNNYTVNNKRNGVAKVNIFFKELNYKTNSESPSVTMVTLNLGSQWSLWFGSSVLSVVE  
MAELVFDLLVIMFLMLLRRFRSRYWSPGRGGRGAQEVASTLASSPPSHFCPHPMSLSLSQPGPAPSPALTA  
PPPAYATLGRPSPGGSGAGASSSTCPLGGP

**Table 8.4: Primer sequences for HiSeq (Illumina) sequencing of GeCKO libraries.**

Primer name	Illumina P5 and seq F	stagger	barcode F	priming site
Illumina F01		T	AAGTAGAG	
Illumina F02	AATGATACGGCGACCACCGAGAT	AT	CATGCTTA	TCTTGTGGAAAGGA
	CTAACTCTTTCCCTACACGACGC			CGAAACACC
Illumina F03	TCTTCCGATCT	GAT	GCACATCT	
Illumina F04		CGAT	TGCTCGAC	
Primer name	Illumina P7	barcode R	Illuminaseq R	priming site
Illumina R01		TCGCCTTG	GTGACTGGA	
	CAAGCAGAAGACGGCATACGAG		GTTTCAGACG	CCGACTCGGTGCCA
Illumina R02	AT	ATAGCGTC	TGTGCTCTT	CTTTTCAA
			CCGATCT	

**Table 8.5: Amino acid sequences synthesized and cloned into the expression vector pGMT7**

**HLA-A2 heavy chain (biotin tag underlined)**

MGSHSMRYFFTSVSRPGRGEPRIAVGYVDDTQFVRFDSDAASQRMEPRAPWIEQEGPEYWDGETRQVK  
 AHSQTHRVDLGLTRGYNQSEAGSHTVQRMYGCDVGSWDRFLRGYHQYAYDGKDYIALKEDLRSWTAAD  
 MAAQTTHKHWEAAHVAEQLRAYLEGTCVEWLRRLRYLENGKETLQRTDAPKTHMTHHAVSDHEATLRCWA  
 LSFYPAEITLTWQRDGEDQTQDTELVETRPAGDGTQKWAQVVPVPSGQE  
 QRYTCHVQHEGLPKPLTLRWEPLNDIFEAQKIEWHE

**β2-microglobulin**

MIQRTPKIQVYSRHPAENGKSNFLNCYVSGFHPSDIEVDLLKNGERIEKVEHSDLSFSKDWFSYLLYYTEFTPT  
 EKDEYACRVNH VTLSQPKIVKWDRDM

**HLA-DRA1\*0101 soluble α chain (biotintag underlined)**

IKEEHVIIQAEFYLNPDQSGEFMFDFDGDEIFHVDMAKKETVWRLEEFGRFASFEAQGALANIAVDKANLEI  
 MTKRSNYTPITNVPPEVTVLNTPVELREPNVLCFIDKFTPPVVNVTLRNGKPVTTGVSETVFLPREDHLF  
 RKFHYLPFLPSTEDVYDCRVEHWGLDEPLLKHWEFDAGLNDIFEAQKIEWHE



## HLA-DRB1\*0701 soluble $\beta$ chain

GDTQPRFLWQGKYKCHFFNGTERVQFLERLFYNQEEFVRFDSDVGEYRAVTELGRPVAESWNSQKDILED  
RGQVDTVCRHNYGVGESFTVQRRVHPEVTVPYPAKTRPLQHHNLLVCSVSGFYPAEVRWFRNGQEEKAG  
VVSTGLIQNGDWTFQTLVMLETVPRSGEVYTCQVEHPSVMSPLTVEWRA

**Table 8.6: Culture media and buffers used for protein expression, refolding and purification**

<b>Buffer</b>	<b>Composition</b>
Lysogeny broth (LB) Medium	10 g/L tryptone, 5 g/L yeast extract, 5 g/L NaCl (all Fisher Scientific), supplemented with 50 mg/L carbenecillin (Carbenecillin Direct)
LB agar plate medium	15 g/L agar bacteriological agar (Oxoid), 10 g/L tryptone, 5 g/L yeast extract, 5 g/L NaCl (all Fisher Scientific) and supplemented with 50 mg/L carbenecillin (Carbenecillin Direct)
TYP medium	16 g/L tryptone, 16 g/L yeast extract (both Fisher Scientific), 5 g/L potassium phosphate dibasic (Acros Organics) with 50 mg/L carbenecillin
Lysis buffer	10 mM Tris pH 8.1, 10 mM MgCl <sub>2</sub> , 150 mM NaCl, 10 % glycerol (all Fisher Scientific)
Triton wash buffer	0.5 % w/w Triton X, 50 mM Tris pH 8.1, 100mM NaCl, 2 mM EDTA (all Fisher Scientific)
Resuspension Buffer	50 mM Tris pH 8.1, 100 mM NaCl, 2 mM EDTA
Guanidine Buffer	6 M guanidine, 50 mM Tris pH8.1, 100 mM NaCl, 2 mM EDTA
pMHC I refold buffer	50 mM Tris pH 8, 2mM EDTA pH 8, 400 mM L-arginine (SAFC), 0.74 g/L cysteamine and 0.83 g/L cystamine
TCR refold buffer	50 mM Tris pH 8, 2 mM EDTA pH 8, 2.5 M Urea (Fisher Scientific), 0.74 g/L cysteamine and 0.83 g/L cystamine

Ion exchange buffer A	10 mM Tris
Ion exchange buffer B	10 mM Tris, 1 M NaCl
Biomix A	0.5 M Bicine buffer pH 8.3
Biomix B	100 mM ATP, 100 mM MgO (Ac) <sub>2</sub> , 500 µL Biotin
Biacore buffer-HPS	10 mM HEPES pH 7.4, 150 mM NaCl, 3 mM EDTA and 0.005 % (v/v) Surfactant P20 (GE Healthcare)
Crystal Buffer	10 mM Tris pH 8.1 and 10 mM NaCl
ITC buffer	20 mM Hepes pH 7.4 and 150 mM NaCl
Reducing sample buffer	125 mM Tris pH 6.8, 4 % SDS, 20 % glycerol, 20 µg/mL bromophenol blue, 10 % DTT
Non-reducing sample buffer	125 mM Tris pH 6.8, 4 % SDS, 20 % glycerol, 20 µg/mL bromophenol blue
Urea Buffer A	8M Urea, 20mM Tris pH 8.1 and 0.5 mM EDTA; pH8.1
Urea Buffer B	8M Urea, 1 M NaCl, 20mM Tris pH 8.1 and 0.5 mM EDTA; pH8.1
HLA Class-II Refold Buffer	25 % v/v glycerol, 20 mM Tris, 1mM EDTA, 20 mM NaCl, 1.48 g/L (13 mM) cysteamine hydrochloride and 0.83 g/L (3.7 mM) cystamine hydrochloride
CAPS elution buffer	50 mM 3-(Cyclohexylamino)-1-propanesulfonic acid (CAPS); pH 11.5
Neutralisation buffer	300 mM sodium phosphate; pH 6
Sample loading buffer (4X)	4 M dithiothreitol (DTT), 1 M Tris, 0.008 % bromophenol blue, 10 % SDS, 40 % v/v glycerol; pH 6.8

---

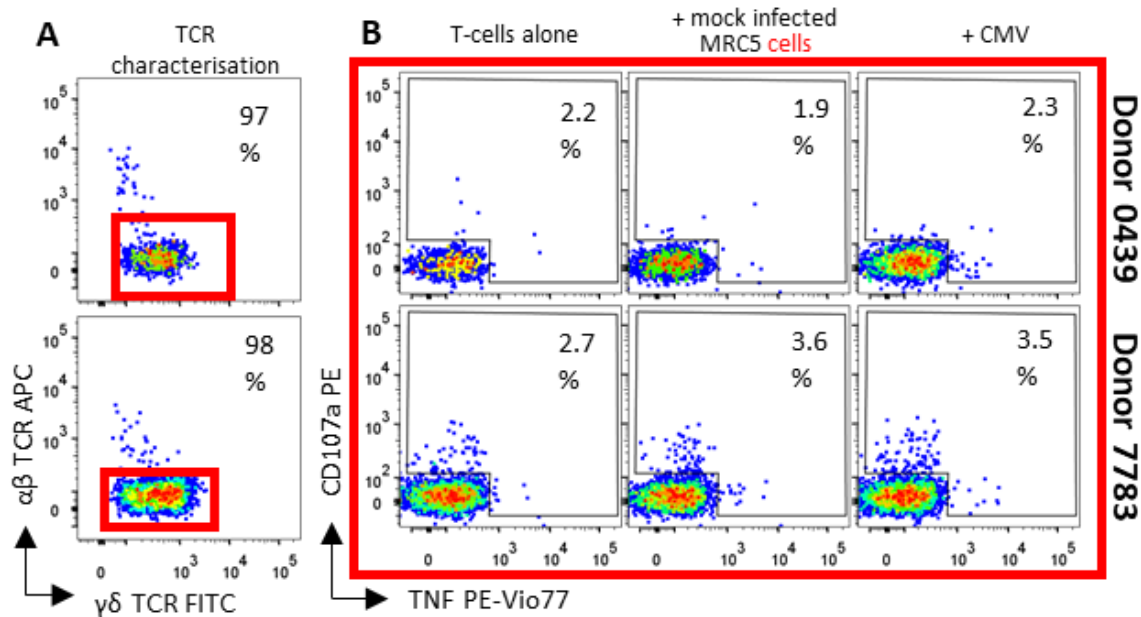
All buffers filtered using a 0.45 µm filter and vacuum pump system prior to use or application on AKTA FPLC

Chemicals obtained from Sigma or Fisher scientific unless stated

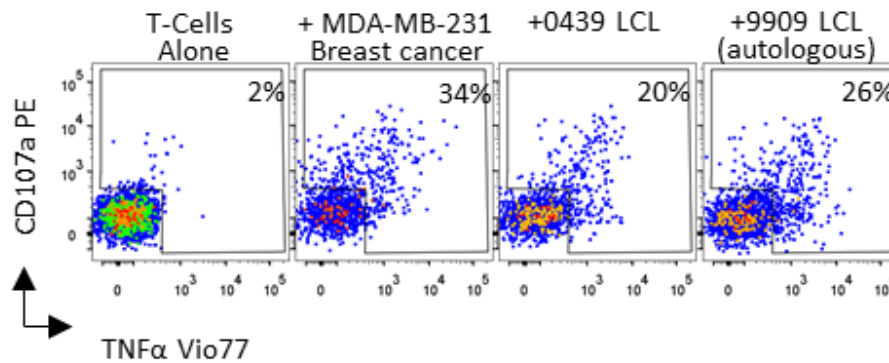
---

Table 8.7: HLA-typing information for LCL used in the thesis for  $\gamma\delta$  T-cell donors and priming donors

LCL	HLA-A	HLA-B	HLA-C	HLA-DR	HLA-DQ	HLA-DP
9909	2301 2402	2705 4901	0202 0701	B1: 1104 1501	B1:0301 0602	B1:0401G 0401G
				B3:0202 B5:0101	A1:0102 0505	A1:0103 0103
				B1:0301 0701	B1:0201 0202	B1:0101G 0301G
0439	0101 0201	0801 4403	0701 1601	B3:0101 B4:0101	A1:0201 0501	A1:0103 0201
				B1:0101 1454	B1:0501 0503	B1:0401G 0401G
				B3:0202	A1:0101 0104	A1:0103 0103
BB67	0301 1101	3501 3501	0401 0401	A:0101		
				B1:0501	A1:0101	
				B6:0101	B1:0501	B1: 0401
HOM-2	3001 3001	2701 0502	0102 0102			
Pt146	0201 3101	1501 4001	3001 0401	B1:0401	A1:0301	A1:0103
				B1:0404	B1:0302	B1:0301
				B4:0103		B1:0401



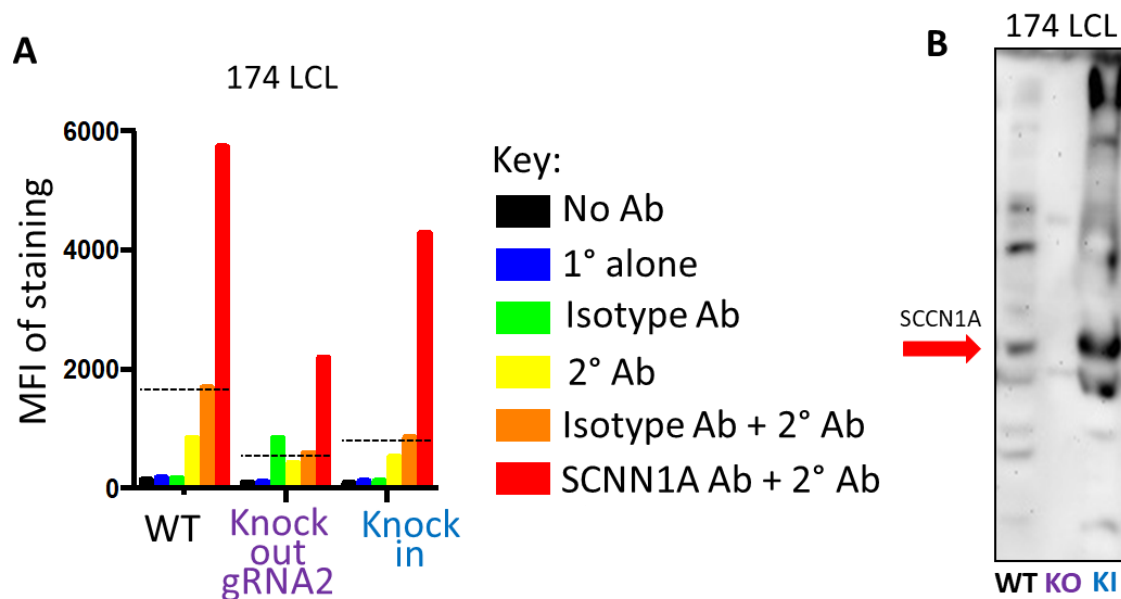
**Figure 8.1: Cytomegalovirus infected fibroblasts failed to prime  $\gamma\delta$  T-cells from PBMC.** Magnetically-enriched  $\delta\gamma$  T-cell lines from PBMCs of donors 0439 and 7783 were co-incubated with cytomegalovirus virus (CMV) infected MRC5 fibroblast cells at an E:T of 1:4 for 14 days followed by a restimulation for another 14 days. Following the co-incubation period ICS was performed by incubating 100,000 of the lines alone, with mock infected MRC5 cells or CMV infected MRC cells 6 h at an effector (E) to target (T) of 1:1. (A) Live CD3<sup>+</sup> cells stained for  $\gamma\delta$  and  $\alpha\beta$  TCRs. The percentage of  $\gamma\delta$  TCR<sup>+</sup> cells is shown. (B)  $\gamma\delta$  T-cells from A stained for CD107a and TNF to assess function following indicated incubation conditions. The percentage of cells in the activated cell gate is shown.



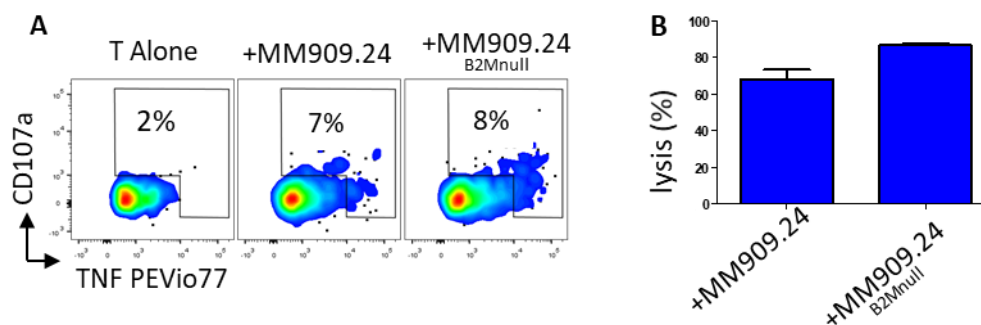
**Figure 8.2: EBV transformed B cell lines prime  $\gamma\delta$  T-cell lines that exhibit cancer reactivity.** Magnetic sorting techniques were used to enrich a  $\gamma\delta$  T-cell line from donor 9909, which was primed with non-autologous LCL from donors 0439, Pt-146 and HOM-2. In a 6 h intracellular cytokine staining (ICS) assay the T-cell line was co-incubated with indicated LCLs and the breast cancer cell line MDA-MB-231 at an E:T of 1:1. Viable CD3<sup>+</sup> cells were stained for TNF and CD107a. The percentage of cells in each gate is shown.

**Table 8.8: Sequence alignment of SCCN1A splice isoforms.** Isoform 1 is the canonical sequence. Highlighted amino acids in BLACK: region used to generate the polyclonal Ab used in this study. RED: Sites of protein variants. BLUE: amino acid differences between splice isoforms.

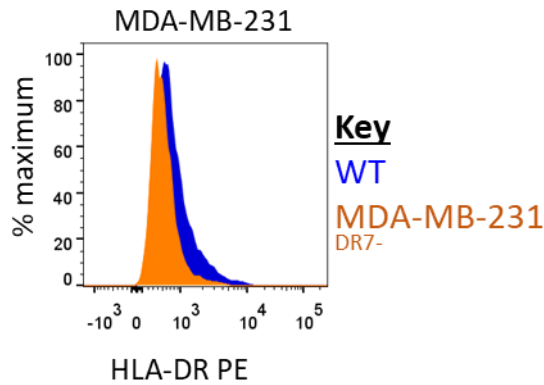
Isoform 11	-----M	1
Isoform 21	MGMARGLTRVPGVMGEGTQGPESLDPCSPQSTPGLMKGNKLEEQDPRLPQIPGLM	60
Isoform 31	-----M	1
Isoform 41	-----M	1
Isoform 51	-----M	1
Isoform 61	-----MSSIKGNKLEEQDPRLPQIPGLM	24
2	EGNKLEEQDSSPPQSTPGLMKGNKREEQGLGPEPAAPQOPTAEEALIEFHRSYRELFEF	61
61	EGNKLEEQDSSPPQSTPGLMKGNKREEQGLGPEPAAPQOPTAEEALIEFHRSYRELFEF	120
2	EGNKLEEQDSSPPQSTPGLMKGNKREEQGLGPEPAAPQOPTAEEALIEFHRSYRELFEF	61
2	EGNKLEEQDSSPPQSTPGLMKGNKREEQGLGPEPAAPQOPTAEEALIEFHRSYRELFEF	61
2	EGNKLEEQDSSPPQSTPGLMKGNKREEQGLGPEPAAPQOPTAEEALIEFHRSYRELFEF	61
25	EGNKLEEQDSSPPQSTPGLMKGNKREEQGLGPEPAAPQOPTAEEALIEFHRSYRELFEF	84
62	FCNNTTIHGAILRVCSQHNRMKTAFAVWLWLCFTFGMMYQFGLLFGEYFSYPVSLNINLN	121
121	FCNNTTIHGAILRVCSQHNRMKTAFAVWLWLCFTFGMMYQFGLLFGEYFSYPVSLNINLN	180
62	FCNNTTIHGAILRVCSQHNRMKTAFAVWLWLCFTFGMMYQFGLLFGEYFSYPVSLNINLN	121
62	FCNNTTIHGAILRVCSQHNRMKTAFAVWLWLCFTFGMMYQFGLLFGEYFSYPVSLNINLN	121
62	FCNNTTIHGAILRVCSQHNRMKTAFAVWLWLCFTFGMMYQFGLLFGEYFSYPVSLNINLN	121
85	FCNNTTIHGAILRVCSQHNRMKTAFAVWLWLCFTFGMMYQFGLLFGEYFSYPVSLNINLN	144
122	SDKLVPVAVTICTLNPYRYPEIKEELEELDRITEQTLFDLYKYSSFTTLVAGSRSRDRL	181
181	SDKLVPVAVTICTLNPYRYPEIKEELEELDRITEQTLFDLYKYSSFTTLVAGSRSRDRL	240
122	SDKLVPVAVTICTLNPYRYPEIKEELEELDRITEQTLFDLYKYSSFTTLVAGSRSRDRL	181
122	SDKLVPVAVTICTLNPYRYPEIKEELEELDRITEQTLFDLYKYSSFTTLVAGSRSRDRL	181
122	SDKLVPVAVTICTLNPYRYPEIKEELEELDRITEQTLFDLYKYSSFTTLVAGSRSRDRL	181
145	SDKLVPVAVTICTLNPYRYPEIKEELEELDRITEQTLFDLYKYSSFTTLVAGSRSRDRL	204
182	GTLPHPLQRLRVPPPPHGARRARSVASSLRDNNPQVDWKDWKIGFQICNQNKSS--DCFYC	239
241	GTLPHPLQRLRVPPPPHGARRARSVASSLRDNNPQVDWKDWKIGFQICNQNKSS--DCFYC	298
182	GTLPHPLQRLRVPPPPHGARRARSVASSLRDNNPQVDWKDWKIGFQICNQNKSS--DCFYC	241
182	GTLPHPLQRLRVPPPPHGARRARSVASSLRDNNPQVDWKDWKIGFQICNQNKSS--DCFYC	239
182	GTLPHPLQRLRVPPPPHGARRARSVASSLRDNNPQVDWKDWKIGFQICNQNKSS--DCFYC	239
205	GTLPHPLQRLRVPPPPHGARRARSVASSLRDNNPQVDWKDWKIGFQICNQNKSS--DCFYC	262
240	TYSSVDAVREWYRFHYINILSRPETLPSLEEDTLGNFIFACRFNQVSCNQANYSHFHH	299
299	TYSSVDAVREWYRFHYINILSRPETLPSLEEDTLGNFIFACRFNQVSCNQANYSHFHH	358
242	LYFG-----	245
240	TYSSVDAVREWYRFHYINILSRPETLPSLEEDTLGNFIFACRFNQVSCNQANYSHFHH	299
240	TYSSVDAVREWYRFHYINILSRPETLPSLEEDTLGNFIFACRFNQVSCNQANYSHFHH	299
263	TYSSVDAVREWYRFHYINILSRPETLPSLEEDTLGNFIFACRFNQVSCNQANYSHFHH	322
300	PMYGNCYTFNDKNNNLWMSSMPGINNGLSLMLRAEQNDFIPLLSTVTGARVMVHGQDEP	359
359	PMYGNCYTFNDKNNNLWMSSMPGINNGLSLMLRAEQNDFIPLLSTVTGARVMVHGQDEP	418
246	-----	245
300	PMYGNCYTFNDKNNNLWMSSMPGINN-----VTGARVMVHGQDEP	340
300	PMYGNCYTFNDKNNNLWMSSMPGINNGLSLMLRAEQNDFIPLLSTVTGARVMVHGQDEP	359
323	PMYGNCYTFNDKNNNLWMSSMPGINNGLSLMLRAEQNDFIPLLSTVTGARVMVHGQDEP	382
360	AFMDDGGFNLRPGVETSISMRKETLDRLGDDYGDCTKNGSDVPEVENLYPSKYTQQVCIH	419
419	AFMDDGGFNLRPGVETSISMRKETLDRLGDDYGDCTKNGSDVPEVENLYPSKYTQQVCIH	478
246	-----	245
341	AFMDDGGFNLRPGVETSISMRKETLDRLGDDYGDCTKNGSDVPEVENLYPSKYTQQVCIH	400
360	AFMDDGGFNLRPGVETSISMRKETLDRLGDDYGDCTKNGSDVPEVENLYPSKYTQQVCIH	419
383	AFMDDGGFNLRPGVETSISMRKETLDRLGDDYGDCTKNGSDVPEVENLYPSKYTQQVCIH	442
420	CFQESMIKECGCAYIFYPRPQNVYCDYRKHSWG-----YCY	457
479	CFQESMIKECGCAYIFYPRPQNVYCDYRKHSWG-----YCY	516
246	-----	245
401	CFQESMIKECGCAYIFYPRPQNVYCDYRKHSWG-----YCY	438
420	CFQESMIKECGCAYIFYPRPQNVYCDYRKHSWGQVRSITPVI PALWEAEAGSGRGYCY	479
443	CFQESMIKECGCAYIFYPRPQNVYCDYRKHSWG-----YCY	480
458	YKLQVDFSSDHLGCFTKCRKPCSVTSYQLSAGYSRAPSVTQSQEWVFQMLSRQNNYTVNNK	517
517	YKLQVDFSSDHLGCFTKCRKPCSVTSYQLSAGYSRAPSVTQSQEWVFQMLSRQNNYTVNNK	576
246	-----	245
439	YKLQVDFSSDHLGCFTKCRKPCSVTSYQLSAGYSRAPSVTQSQEWVFQMLSRQNNYTVNNK	498
480	YKLQVDFSSDHLGCFTKCRKPCSVTSYQLSAGYSRAPSVTQSQEWVFQMLSRQNNYTVNNK	539
481	YKLQVDFSSDHLGCFTKCRKPCSVTSYQLSAGYSRAPSVTQSQEWVFQMLSRQNNYTVNNK	540
518	RNGVAKVNIFFKELNYKTNSPSPVMTVLLSNLGSQWSLWFGSSVLSVVMEMAEIVFDLL	577
577	RNGVAKVNIFFKELNYKTNSPSPVMTVLLSNLGSQWSLWFGSSVLSVVMEMAEIVFDLL	636
246	-----	245
499	RNGVAKVNIFFKELNYKTNSPSPVMTVLLSNLGSQWSLWFGSSVLSVVMEMAEIVFDLL	558
540	RNGVAKVNIFFKELNYKTNSPSPVMTVLLSNLGSQWSLWFGSSVLSVVMEMAEIVFDLL	599
541	RNGVAKVNIFFKELNYKTNSPSPVMTVLLSNLGSQWSLWFGSSVLSVVMEMAEIVFDLL	600
578	VIMFLMLLRRFRSRYWSPGRGGRGAQEVASTLASSPPSHFCPPHMSLSLSQPGPAPSPAL	637
637	VIMFLMLLRRFRSRYWSPGRGGRGAQEVASTLASSPPSHFCPPHMSLSLSQPGPAPSPAL	696
246	-----	245
559	VIMFLMLLRRFRSRYWSPGRGGRGAQEVASTLASSPPSHFCPPHMSLSLSQPGPAPSPAL	618
600	VIMFLMLLRRFRSRYWSPGRGGRGAQEVASTLASSPPSHFCPPHMSLSLSQPGPAPSPAL	659
601	VIMFLMLLRRFRSRYWSPGRGGRGAQEVASTLASSPPSHFCPPHMSLSLSQPGPAPSPAL	660
638	TAPPPAYATLGPRPSPGGSAGASSSTCPLGGP	669
697	TAPPPAYATLGPRPSPGGSAGASSSTCPLGGP	728
246	-----	245
619	TAPPPAYATLGPRPSPGGSAGASSSTCPLGGP	650
660	TAPPPAYATLGPRPSPGGSAGASSSTCPLGGP	691
661	TAPPPAYATLGPRPSPGGSAGASSSTCPLGGP	692



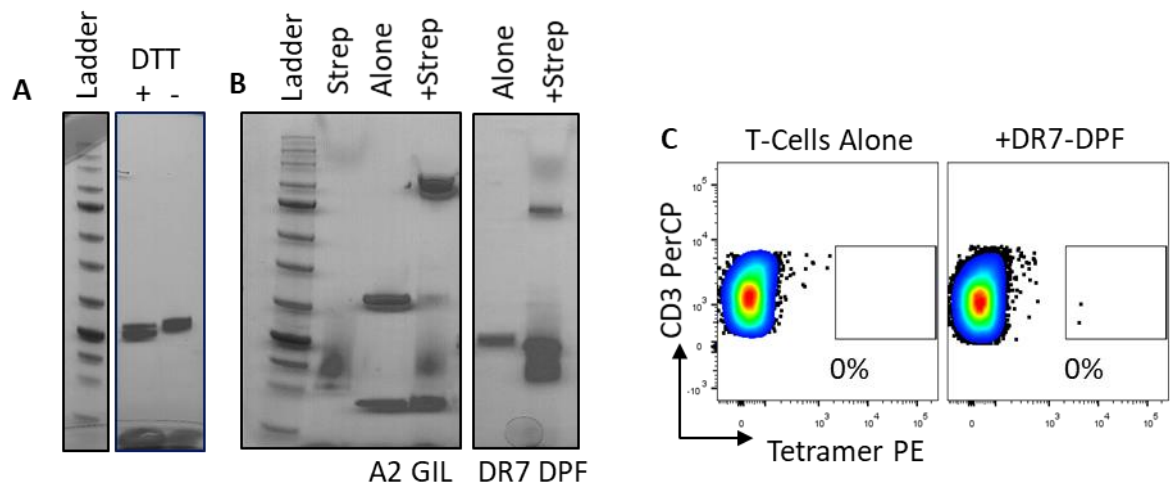
**Figure 8.3: SCCN1A expression in knockout and knockin .174 cell lines.** (A) Unconjugated anti-SCCN1A antibody (Ab) staining of .174 LCL: WT, *SCCN1A* knock-out gRNA2, and gRNA2 cells that had also received a codon optimized SCCN1A transgene by lentivirus transduction (*knock-in*). Fluorescence shown graphically (y-axis). An isotype control Ab was used with the dotted line set at the fluorescence seen for isotype Ab + PE conjugated 2° Ab for each cell line. Transduced 174s for gRNAs or the full length SCCN1A gene were maintained as lines and not cloned. (B) Confirmation of SCCN1A protein expression in 174 WT, gRNA2 knockout, and knock in cells by western blot analysis.



**Figure 8.4: The recognition of tumour cell line MM909.24 by clone SW.6B10 does not require  $\beta$ 2M.** Melanoma cell line MM909.24 was transduced with a CRISPR/Cas9 gRNA targeting  $\beta$ 2-macroglobulin ( $\beta$ 2M). (A) In a 4 h TAPi activation assay clone SW.6B10 was co-incubated with wild type and  $\beta$ 2M knockout MM909.24 cells at an E:T of 1:1. (B) In a 6.5 h cytotoxicity chromium assay SW.6B10 was co-incubated with target cells as in (A).

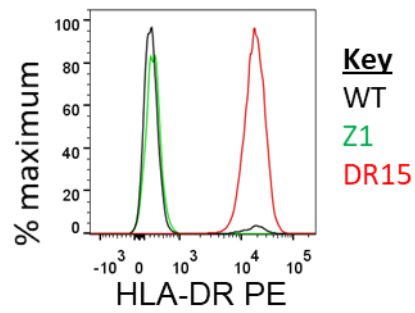


**Figure 8.5: CRISPR/Cas9 targeted knockout of HLA-DR7 in tumour cell line MDA-MB-231.** Cell line MDA-MB-231 was transduced with a CRISPR/Cas9 gRNA targeting HLA-DR7, generating **MDA-MB-231<sup>DR7-</sup>**. MDA-MB-231 wild type (**WT**) and **MDA-MB-231<sup>DR7-</sup>** cells were stained with a pan HLA-DR antibody and displayed following exclusion of dead (Vivid<sup>+</sup>) cells.



**Figure 8.6: SW.6B10 recognizes a specific peptide bound with HLA-DRB1\*0701.** (A) HLA-DR7 was refolded with an irrelevant peptide (DPF): HLA-DR7/DPF. SDS-PAGE was carried out to show purity of refolded monomer, + and – DTT. (B) A streptavidin shift assay was performed on refolded monomer to validate correct biotinylation, using HLA-A2/GIL monomer (used successfully for tetramer staining previously) as a positive control. (C) The HLA-DR7/DPF monomer was tetramerised according to the boosted protocol and used to staining SW.6B10 T-cells. Viable cells were gated and displayed as CD3 versus tetramer.





**Figure 8.7: HLA-DR staining of .174 LCL transduced with HLA-DR15.** .174 LCL were transduced with a construct co-expressing HLA-DR15 and rCD2. As a control .174 LCL were also transduced with a construct co-expressing zeiker 1 (Z1) protein and rCD2, as a control. Wild type (WT), DR15, and Z1 transduced .174 cells were stained for HLA-DR and displayed following the exclusion of dead (Vivd<sup>+</sup>) cells.